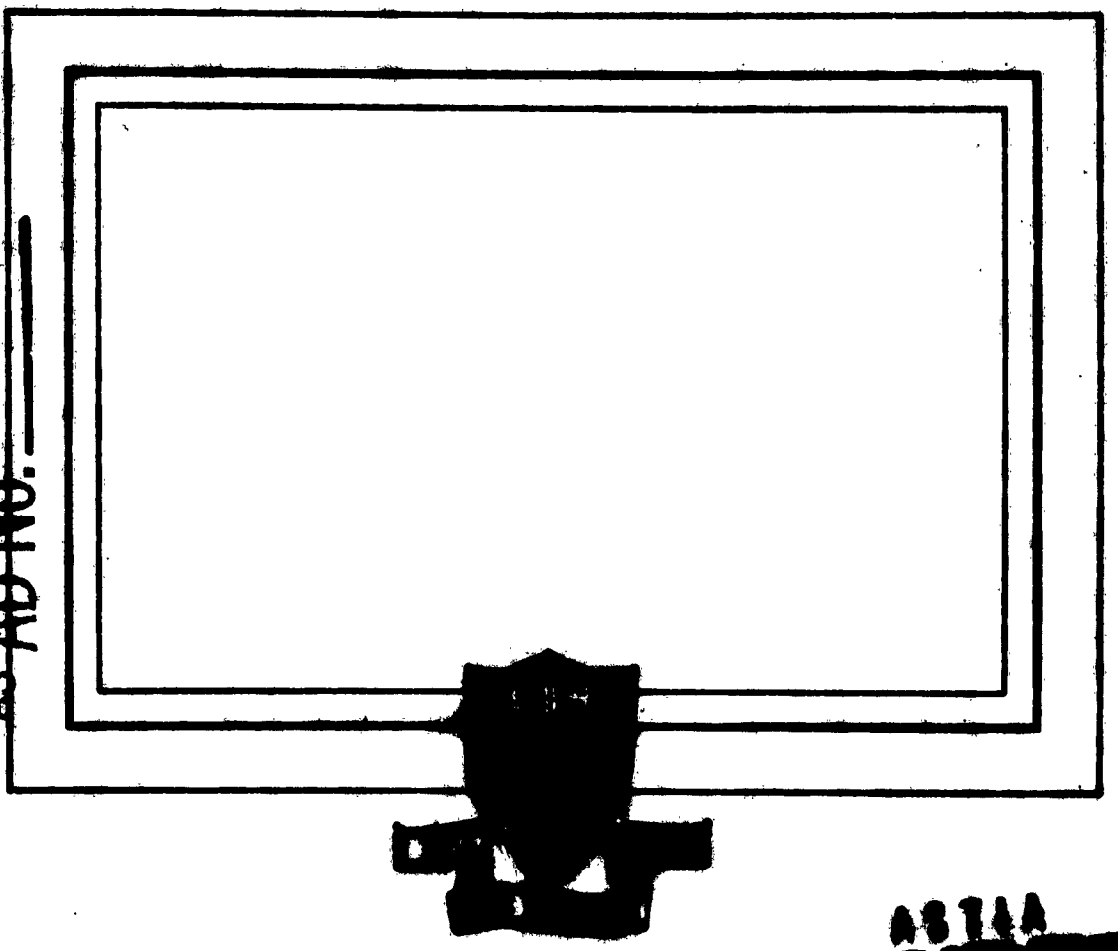

PRINCETON UNIVERSITY

INVESTIGATIONS OF THE EFFECT OF GAS COLLISIONS AND OPTICAL PUMPING ON THE BREADTH OF SPECTRAL LINES

Microwave Atomic Oscillator Using the Hyperfine Transition of Rb^{87}

Final Report on Optical Detection Phase
(October 1, 1957 - September 30, 1960)

Palmer Physical Laboratory
Princeton University
Princeton, New Jersey

Prepared by C. O. Alley

Approved: R. H. Dicke

R. H. Dicke, Project Leader
Professor of Physics

Contract No. DA-36-039 SC-70147

File No. 229-PH-56-91 (3501)

Contract placed by

U. S. Army Signal Corps Engineering Laboratory
Fort Monmouth, New Jersey

GENERAL CONTENTS

A list of some typographical errata is included at the end of the report.

I. PURPOSE.

The purpose of this investigation is to study the effects of gas collisions on the Doppler width of microwave spectral lines and to utilize optical pumping to reduce exchange collision broadening and to increase signal power for use in atomic frequency standards. The possibility of the use of an atomic oscillator employing atomic amplification is also to be investigated.

II. ABSTRACT.

A new method of optical detection of the $m_F = 0 \leftrightarrow m_F = 0$, $\Delta F = 1$ ground state magnetic hyperfine transition in alkali atoms, which is important for atomic frequency standards because of its first order independence of an external magnetic field, has been investigated theoretically and experimentally demonstrated for rubidium 87. After orientation by optical pumping, a quantum mechanical superposition state is produced by a 90° rf pulse. A phase change between $m_F = 0$ state and its partner states of the same F value is caused by a microwave field at ~ 6835 Mc/sec coupling the two $m_F = 0$ states. This phase change is converted into a population change by a second rf pulse to yield a large change in the resonance scattering of the optical pumping light, on the order of that obtained by reversal of the orientation of the vapor.

Other methods of optical detection of this resonance were studied theoretically and are discussed: selective hyperfine absorption within the gas cell; a rubidium 85 gas cell hyperfine filter; and a polarization bridge.

Wall coatings for the inhibition of spin relaxation in confined oriented vapors were studied experimentally. It was demonstrated that treatment of glass surfaces with alkylchlorosilane vapors provides coatings at least as effective as long chain saturated hydrocarbon waxes with the

added advantages of ease of application and the ability to withstand baking under vacuum at $\sim 350^{\circ}$ C without deterioration. The $0 \leftrightarrow 0$ hyperfine resonance in such coated cells exhibited a reduced Doppler width (because of the confinement of the atoms) of the same order as that produced by a buffer gas, and displayed a negative frequency shift of a few kc/sec.

Other subjects investigated included spin echo methods applied to oriented vapors; optical pumping with pulsed light sources; the general theory of optical pumping and detection; and digital computer solutions of the optical pumping equations for σ^{+} D_2 light and partial excited state relaxation.

III. PUBLICATIONS, LECTURES, REPORTS, AND CONFERENCES.

The final report on the microwave detection phase of this contract was distributed in 1957 (see reference 1 of the present report). Publications and talks associated with that phase of the contract are included in the following list.

Publications

T. R. Carver, "Rubidium Oscillator Experiments", Proceedings of the 11th Annual Symposium on Frequency Control, May, 1957.

_____, "Theoretical Limits of Atomic Frequency Control", Proceedings of the 12th Annual Symposium on Frequency Control, May, 1958.

_____, "The Use of Optical Pumping to Enhance Microwave Detection of Doppler Reduced Hyperfine Lines in Rb^{87}", Proceedings of the Ann Arbpr Conferences on Optical Pumping, June, 1959.

R. H. Dicke, "Time Scales in the Structure of the Universe", Proceedings of the 13th Annual Symposium on Frequency Control, May, 1959.

C. O. Alley, "Triple Resonance Method to Achieve Narrow and Strong Spectral Lines", Proceedings of the 13th Annual Symposium on Frequency Control, May, 1959.

_____, "Pulse Techniques in the Optical Detection of Ground State Resonances in Rubidium 87", Proceedings of the Ann Arbor Conference on Optical Pumping, June, 1959.

R. H. Dicke, "New Possibilities for Fundamental Experiments and Techniques", Quantum Electronics, Edited by C. H. Townes (Columbia University Press, New York, 1960).

C. O. Alley, "Coherent Pulse Techniques in the Optical Detection of the $0 \leftrightarrow 0$ Ground State Hyperfine Resonance in Rubidium 87", Quantum Electronics, edited by C. H. Townes (Columbia University Press, New York, 1960).

R. H. Dicke, "Is the Fine Structure Constant Invariant?", Proceedings of the 14th Annual Symposium on Frequency Control, May, 1960.

C. O. Alley, "Wall Coatings of Alkylchlorosilanes for the Inhibition of Spin Relaxation", Advances in Quantum Electronics, edited by J. R. Singer (Columbia University Press, New York, 1961).

Publication of the material in this report as several separate papers is anticipated.

Lectures

All of the above papers were first given as talks at the symposia, and conferences cited.

Additional talks which were not published are given below.

T. R. Carver, "Rubidium Gas Cell Experiments", Proceedings of the 10th Annual Symposium on Frequency Control, May, 1957.

T, R. Carver, "Use of Optical Orientation in Gas Cell Atomic Standards", invited paper at the Winter Meeting on the West Coast of The American Physical Society, December, 1957 (Bull. Am. Phys. Soc. 2, No. 8, 1957).

R. H. Dicke, "Optical Pumping", invited talk at the meeting of the National Academy of Sciences, April, 1958.

T. R. Carver, "Use of Optical Orientation for Atomic Clocks and Frequency Standards", Colloque Internationaux de C.N.R.S. Sur la Resonance Magnetique, Paris, July, 1958.

C. O. Alley, "Optical Pumping, Atomic Clocks, and Coherent Pulse Techniques", Physics Colloquium of the University of Pennsylvania, November, 1959.

_____, lectures on optical pumping in Physics 572, Princeton University, Selected Topics in Experimental Physics, March, 1960.

_____, "Optical Pumping, Atomic Clocks, and Coherent Pulse Techniques", Raytheon Research Laboratory, March, 1960.

_____, "Optical Pumping, Atomic Clocks, and Coherent Pulse Techniques", Talk given to Physics Colloquium at the University of Maryland, May, 1960.

_____, "Optical Pumping and Atomic Clocks", special Physics Colloquium at the University of Michigan, May, 1960.

_____, "Optical Pumping" seminar at the Institute of Optics, University of Rochester, May, 1960.

Reports

R. H. Dicke, T. R. Carver, C. O. Alley, and N. S. Vander Ven, Final Report on the Microwave Detection Phase of the present contract, December, 1957 (see reference 1 of this report).

Conferences

In addition to the conferences represented by the above papers and talks the Conference on Microwave Spectroscopy at Duke University in November, 1957 was attended by C. O. Alley who gave a brief report on the microwave detection phase of this contract.

IV. FACTUAL DATA
(Sections I through IV of the following part of the report)

V. OVERALL CONCLUSIONS
(Sections V A through V E of the following part of the report)

VI. RECOMMENDATIONS
(Section V F of the following part of the report)

TABLE OF CONTENTS

LIST OF ILLUSTRATIONS

Figures

Tables

I. INTRODUCTION

Optical detection of resonances among magnetic substates of the ground states of atoms whose thermal equilibrium populations have been altered by the transfer of angular momentum from a polarized beam of light--optical pumping--yields strong signals for transitions among Zeeman states and for all hyperfine transitions except for the magnetic field independent one ($m_F = 0 \leftrightarrow m_F = 0$) which is important for atomic clocks. A new method of optically detecting this transition with signals comparable to the others has been developed.

After orientation of the atoms by optical pumping, an oscillatory radio frequency magnetic field pulse at the Larmor frequency is used to introduce phase relations among the magnetic substates. A phase change between the $m_F = 0$ states and the partner states of the same F value is produced by coupling the $m_F = 0$ states by a microwave field. This phase change is converted into a population change by a second rf pulse, coherent with the first but of opposite phase, yielding a large change in optical absorption.

This is the main result of the research to be described. However as by products of this research was done on spin echo methods in an oriented vapor, including Carr-Purcell Techniques; on wall coatings for the inhibition of spin relaxation; on optical pumping with pulsed light sources; and on the theory of optical pumping and optical detection.

A. Motivation of the Investigation

Successful detection of the collision narrowed field independent $(2,0) \leftrightarrow (1,0)$ hyperfine transition in the ground state of rubidium 87 by T.R. Carver [1] using sensitive microwave techniques combined with optical pumping of rubidium vapor in a buffer gas cell provided the immediate basis for this investigation. These researches were based in turn on earlier measurements of the ground state hyperfine splitting in atomic hydrogen by J.P. Wittke [2] which first demonstrated experimentally the technique of reduction of Doppler width by collisions with buffer gas atoms proposed by Prof. R.H. Dicke.[3] The work on microwave detection in rubidium also profited from work on the detection of microwave molecular resonances using coherent plus techniques by R.H. Romer,[4] from studies of optical pumping by W.B. Hawkins, [5] and from an investigation of the effect of a buffer gas on optical pumping by P.L. Bender. [6] Related work done at locations other than Princeton will be discussed below.

Optical detection seemed to afford a simpler means of monitoring the frequency dependence of microwave absorption in rubidium vapor and had indeed been considered briefly by Dicke and Carver before the microwave work was started. An advantage beyond that of experimental simplicity is that one detects a transition involving microwave photons of $\sim 3 \times 10^{-5}$ ev energy by the use of optical photons of ~ 1 ev energy, with a consequent improvement in signal to noise considerations.

A more general underlying motivation for research on atomic frequency standards has been the desire to develop them to a precision that will enable their use in experimental investigations of gravitational and cosmological questions.

B. Survey of Important Developments in Optical Pumping and Optical Detection of Resonances

There were two independent paths leading to the orientation or alignment of atoms in their ground states by the absorption and subsequent emission of polarized optical resonance radiation--the technique that has become known as "optical pumping". One approach originated with the attempts of Prof. R.H. Dicke at Princeton to obtain polarized free electrons.(7) A polarized first excited state in sodium was obtained by irradiating the sodium vapor with circularly polarized resonance radiation. While in the excited state the polarized electron was detached from the sodium atom by ultra-violet ionizing radiation in a manner preserving the spin state. Although the measurement of the magnetic moment of these oriented free electrons was not successful, the idea of obtaining ground state orientation was suggested by the work. Experiments to demonstrate this were carried out by W.B. Hawkins(5) using a sodium beam. The degree of orientation was determined by studying the change in the ratio of σ to π linear polarizations in the resonance radiation scattered at 90°. The use of an inert buffer gas to keep the sodium atoms in the illuminated region for longer times, allowing the absorption of more photons, and thereby enhancing considerably the degree of orientation achieved, was explored by P.L. Bender.(6)

The other route to optical pumping began with the suggestion[8a] by Prof. F.L. Bitter of MIT and discussion[8b] by Prof. A. Kastler and J. Brossel of The University of Paris that magnetic resonances in optically excited states of gases could be observed by selectively populating the magnetic substates by the absorption of polarized radiation and observing the change in the polarization of the light emitted when the magnetic substates are mixed by the action of an oscillating magnetic field. This technique, which was christened "double resonance," suggested to Prof. Kastler the possibility of orienting atoms in their ground states by the method described above.[8c] It was he who named the technique "Le pompage optique." An unsuccessful first attempt to demonstrate this orientation was made by J. Brossel when visiting at MIT. A successful demonstration was carried out in Paris by J. Winter and B. Cagnac [9] using a long beam of sodium atoms, illuminated along their path by several sodium lamps, about the same time as Hawkins' demonstration, the orientation being observed by the change in the ratio of orthogonal polarizations in the scattered light from a probing polarized beam. Studies of the use of buffer gases to enhance the orientation and to enable the production of orientation in sealed cells were explored at Paris by C. Cohen-Tannoudji.[10] The observation of Zeeman resonances in the ground state of oriented or aligned vapors by monitoring the change of the ratio of polarizations of scattered light was accomplished by J. Blamont, J.P. Barrat, J. Winter and others of the Paris group,[11] and included multiple quantum transitions.

An important advance was made by Prof. H.G. Dehmelt [12] of the University of Washington who pointed out that ground state resonances in oriented alkali vapor could be observed by the change in the

intensity of transmitted or scattered circularly polarized resonance radiation if the peak intensities of the D_1: ($^2S_{\frac{1}{2}} \rightarrow {}^2P_{\frac{1}{2}}$) and D_2: ($^2S_{\frac{1}{2}} \rightarrow {}^2P_{3/2}$) lines were different. The ratio of these peak intensities is very nearly unity, as had been measured by Hawkins [13] for typical discharge conditions, and most workers had assumed the ratio to be unity when computing orientations from observations on scattering. It was experimentally demonstrated by Dehmelt that large signals could be obtained for only small departures from unity of the D_1/D_2 peak intensity ratio, and that such departures could be achieved by the passage of the radiation through the vapor, since the absorption cross-section for D_2 is twice that for D_1. The use of filters to suppress one of the D lines is thus desirable, as was emphasized by W. Franzen and A.G. Emslie.[14] Another consequence of unequal peak intensities of the two D lines is that an assemblage of oriented atoms precessing at the Larmor frequency in a magnetic field will modulate a beam of circularly polarized light at this frequency. This was also pointed out by Dehmelt and the idea as experimentally developed by W.E. Bell and Arnold Bloom [15] forms the basis of an excellent magnetometer.

C. Problems Associated with the Optical Detection of the (2,0)↔(1,0) Hyperfine Transition

An examination of the theoretical transition probabilities associated with electronic dipole transitions between the (F, m_F) hyperfine states of the $^2S_{\frac{1}{2}}$ ground state and those of the $^2P_{\frac{1}{2}}$ and $^2P_{3/2}$ first excited states in an alkali atom, neglecting such small effects as configuration mixing (see Section II A 3 and Appendix D, for details, and also Figures 1 and 2) reveals that the absorption

cross section is the same for the (2,0) as for the(1,0) hyperfine state. (It is assumed here that the nucleus has spin 3/2 as is the case for rubidium 87. Similar conclusions hold for any alkali nucleus having half integral spin.) If the peak intensities of the corresponding hyperfine lines in the incident optical radiation are equal, as is the case for the radiation from broadened electrical discharge light sources, (see Section III, paragraph A) there will be no observable light scattering effects if the relative populations of the two states are altered by an appropriate microwave electromagnetic field coupling the two states. This uniform absorption probability exists for the D_1 and D_2 fine structure components individually and for any type of polarization. It results from the symmetry properties peculiar to $m_F = 0$ states.

If one can alter the spectral composition of the incident radiation by suppressing one of the hyperfine components associated with the ground state splitting, then clearly there will be a change in the light transmission or scattering when the (2,0) and (1,0) states are mixed by the microwave field and this will afford a means of optical detection.

The use of optical interferometry to accomplish the filtering of the incident light will necessarily be associated with a very small solid angle in the optical system--too small to give adequate light flux for optical pumping. It should be remarked that the simplest configuration would use the same beam of light for both the establishment of a non-thermal equilibrium population distribution between the states in question and for the detection of the alteration of this distribution by the microwave radiation. If one wished to

use separate beams of light perhaps this filtering method could be used. Another possibility would be to filter the optical radiation after it had passed through the gas cell. This would also require collimation and resulting rigid mechanical tolerances and yield only small fluxes for detection.

Better optical filters can be made from the selective absorption in a cell of rubidium vapor. The hyperfine components have different scattering cross sections and there will thus be filtering action as the radiation passes through the cell. After the initial suggestion by R. H. Dicke, detailed calculations were made on this effect (See Appendix A). These showed that quite good signal to noise ratios could be obtained. Experimental demonstration of this selective hyperfine method of optical detection was carried out for sodium vapor by M. Arditi at the suggestion of T.R. Carver[16], by W.E. Bell and A. Bloom,[17] and soon thereafter for other alkalis.[18]

An even better gas cell hyperfine filter relies on the selective hyperfine absorption in rubidium 85 which has a nuclear spin of 5/2. The resulting shift in the energy levels of the ground state compared to rubidium 87 resulting from the different multiplicities is very favorable for providing an unequal ratio for the intensities of rubidium 87 hyperfine components. Figure 24 in Appendix A shows this effect and further discussion is given there. This method was independently conceived by T. R. Carver and C. O. Alley, by A. Kastler (private communication to M. Arditi), and by P. L. Bender[19]. The technique has been used in the optically pumped, optically detected gas cell atomic clocks studied by several groups.[20]

The coincidence of one of the optical hyperfine transitions in rubidium with an intense spectral line in the radiation from a discharge in another gas could be used for altering the thermal population difference of the two hyperfine states and optical detection of the $(2,0) \leftrightarrow (1,0)$ transition. Such a source for cesium was found in a line from an argon discharge, slightly shifted by an external magnetic field, by P.L. Bender and E.C. Beaty [21]. A convenient similar source has not been found for rubidium.

An optical polarization bridge for the sensitive detection of the $0 \leftrightarrow 0$ resonance was explored theoretically and partially constructed. This allows the signal to appear on a null background and utilizes the selective hyperfine filtering. It was not pursued further in view of the more interesting approach discussed in the next paragraph. The polarization bridge is described in Appendix B.

D. A New Method of Optical Detection: Phase Destruction Using Coherent Pulse Techniques

Although the methods discussed above work adequately well the signals are much weaker than the optical detection signals obtainable from Zeeman resonances. As a general principle regarding atomic frequency stabilization, it is often experimentally desirable to obtain as narrow a line as possible (See Appendix C). As lines are narrowed by changing the experimental conditions this usually involves a sacrifice of signal strength. Thus it is desirable to have a detection method yielding as large a signal as possible in order that this may be sacrificed in favor of a narrower line.

In addition to this type of line narrowing it is also possible to narrow a line artificially by using two coherently phased pulses to select only the longer lived atoms from among those undergoing relaxation, as has been proposed by Prof. R.H. Dicke.[22] This technique is briefly analyzed in Appendix C.

The phase destruction method will be fully described in Section II E, but the basic idea is as follows (See Figure 4). A coherent quantum mechanical superposition state of the 2F + 1 magnetic substates of angular momentum F can be formed by allowing an rf pulse at the Larmor precession frequency to act on an oriented system in a weak magnetic field. Such a state is provided, for example, by a 90° pulse which changes a system previously oriented by optical pumping along the z-direction into a free precession state in the x-y plane. The $m_F = 0$ state can have its phase with respect to its partner states altered if it is coupled to the other $m_F = 0$ hyperfine state by a microwave field of the appropriate polarization and frequency. The original superposition state is now altered and if an inverse 90° pulse is applied the result will not be the original oriented state but something quite different. If the phase alteration had not occurred, an inverse 90° pulse would exactly reproduce the original oriented state (neglecting relaxation effects). The populations in this final state are quite different from those in the original oriented state and this leads to a markedly different optical absorption. The change is large and of the same order as that obtained from Zeeman resonances. This change will be calculated in Section II E using density matrix techniques.

E. Investigations of Other Topics

One of the major problems associated with the phase destruction method is the influence of magnetic field inhomogeneities on the free precession. Since atoms in different parts of the cell precess at different frequencies they can get out of phase, if the inhomogeneities are large, in a time less than the time interval one would like to have between the two 90° pulses. The line width of the hyperfine resonance detected by this means should be essentially the reciprocal of this time interval. This type of dephasing can be avoided by the use of spin echo techniques, first developed by Hahn.[23] These techniques were first applied to optically oriented vapors in the course of this investigation. A means of preserving phase relations when precessing spins diffuse in an inhomogeneous magnetic field by the use of repeated 180° pulses was developed by Carr and Purcell.[24] This technique was also applied to precessing rubidium atoms in a buffer gas during the course of this work.

One way of avoiding the detrimental effects of inhomogeneous fields is to average out the effects by allowing the precessing atoms to move rapidly around in a gas cell whose walls are non-relaxing. If the spread of precession frequencies is small compared to the reciprocal of the average transit time between collisions the dephasing effect will be reduced. Several wall coating materials were studied. The most useful result was the demonstration that coatings obtained by treatment with alkylchlorosilanes are as effective as long chain hydrocarbon waxes. They possess the advantages of forming a chemical bond with the walls and therefore of being bakeable without deterioration and of being relatively easy to apply.

The optical pumping process itself contributes to the broadening of the hyperfine resonance line and to destroying the phase relations that one must preserve during the interval between the 90° pulses. It is therefore desirable to cut the lights off during this interval. Several methods of doing this were explored experimentally. An additional advantage of doing this is to remove the small shifts in the hyperfine resonance frequency caused by an unsymmetrical spectral distribution of the optical radiation.

A reformulation of the theory of optical pumping was carried out and some digital computer solutions obtained for several conditions of relaxation and pumping with D_2 radiation not previously available.

II. THEORY

In this section some theoretical considerations will be presented on optical pumping and on the optical detection of resonances which have been found useful in devising possible types of detection systems for the $(F, m_F = 0) \longleftrightarrow (F-1, m_{F-1} = 0)$ ground state hyperfine resonance in alkalis. The differential equations governing the optical pumping dynamics including relaxation phenomena are given an explicit matrix formulation and the relation of this to a stochastic approach of the Markov type is shown. A convenient way of describing the behavior of assemblages of atomic systems is in terms of the density matrix and appropriate operators to describe the absorption of light in this formalism are presented in connection with the notion of an effective oscillator strength. Weak field Zeeman resonances are nicely described in terms of rotations of higher spin systems using irreducible representations of the rotation group and an application of this approach is made to describe the effect of rf pulses. Using these techniques a calculation of the performance of the phase destructive method of detection of the hyperfine resonance is given.

A. Optical Pumping

1. Other Theoretical Descriptions

A calculation of the transition probabilities for optical pumping was carried out by W.B. Hawkins and R.H. Dicke[5] based on the treatment of the absorption and emission of resonance radiation given by Heitler.[25] The contribution of interference terms among the hyperfine components of the ^2P excited states of sodium 23 whose separations are on the order of ten times the

natural line width was shown to be only a few percent and was therefore neglected. In the case of rubidium 87, for which the present calculations were done, the excited state hyperfine splittings are about a factor of 4 greater than those for sodium so that the contribution of these interference terms can be neglected with even less error. (In the case of atomic hydrogen, for which no direct optical pumping has yet been done, the hyperfine splittings of the $^2P_{\frac{1}{2}}$ and $^2P_{3/2}$ states are much less than the natural line width, so that such interference contributions will be quite important). Using these probabilities the stochastic approach (valid if the absorption probability out of each magnetic substate of the ground state is the same) was used to compute expected orientations and alignments for various experimental situations by W. B. Hawkins[5] and also by P. L. Bender[6] who considered the question of the mixing of the excited hyperfine states by buffer gas collisions.

A matrix formulation somewhat similar to that described below has been given by C. Cohen-Tannoudji.[26] Differential equations adapted from the Bloch theory of magnetic resonance have been used by Bloom and Bell.[15] A set of equations for optical orientation using circularly polarized D_1 radiation has been given by Franzen and Emslie[27] who present also the results of some numeral integrations on the time development of the populations.

2. Notation in Relation to the Density Matrix[28]

Although the notationally consistent way of proceeding would be to work always with the density matrix describing the assemblage of atoms, some departure from this will simplify the writing of the equations describing the dynamics of optical pumping.

In particular the diagonal elements of the 8 by 8 density matrix for the magnetic substates of the ground state of the alkali atom represent the fractional populations of atoms in these states. They will be designated by N_i rather than by ρ_{ii} and formed into a population column vector $\underline{N}$. The subscript refers to the (F, m_F) state in the following correspondence:

(F, m_F)	(1,-1)	(1,0)	(1,1)	(2,-2)	(2,-1)	(2,0)	(2,1)	(2,2)
i	1	2	3	4	5	6	7	8

If one considers only incoherent optical pumping, in which it is assumed that the absorption of optical radiation destroys phase relations among the substates, it is perfectly legitimate to deal only with the diagonal elements of the density matrix as is generally done in describing rate processes by the "master equation."[29] However a more careful treatment containing the off-diagonal elements is really called for, particularly since the recent advent of coherent optical radiation from optical masers.[30] Techniques such as those of the present experiments should be able to detect the preservation of coherence during the resonance fluorescence process.

3. Calculation of Transition Probabilities

When one treats the incident optical radiation as incoherent (or better stated, when the coherence time of the radiation is much less than the excited state lifetime) the treatment of Hawkins and Dicke [5] leads to transition probabilities which are proportional

to the square of the matrix elements of the operator $\vec{p}\cdot\vec{A}$ between the states in question, where $\vec{p}$ in the linear momentum operator and $\vec{A}$ the vector potential of the incident radiation. (It is not necessary to quantize the field oscillators for this calculation). One needs then the matrix elements

$$\left(\psi^{F}_{m_F} , \vec{p}\, \psi^{F'}_{m_{F'}} \right)$$

which can be shown to be equal to $i m \omega \left(\psi^{F}_{m_F} , \vec{r}\, \psi^{F'}_{m_{F'}} \right)$

where $\omega = \frac{E'-E}{\hbar}$ and $\vec{r}$ is the vector operator for position. Such matrix elements of a vector operator between states of definite total angular momentum and z-component of angular momentum are well known.[31,32] By means of the Wigner-Eckart theorem [32] they can be expressed as a product of a Wigner 3-j symbol (essentially a Clebsch-Gordon coefficient, see Appendix D) $\left(F\, m_F \,/\, \sigma \,/\, F'\, m_{F'} \right)$ giving the $m_F, m_{F'}$ dependence and a reduced matrix element $\mathcal{J}_{FF'}$ giving the dependence on F and F'

$$\left(\psi^{F}_{m_F} , p^{(\sigma)} \psi^{F'}_{m_{F'}} \right) = \left(F\, m_F \,/\, \sigma \,/\, F'\, m_{F'} \right) \mathcal{J}_{FF'} \qquad (1)$$

$p^{(\sigma)}$ represents

$$(p_x + i p_y)/\sqrt{2} \quad , \quad p_z \quad , \quad \text{or} \quad -(p_x - i p_y)/\sqrt{2}$$

accordingly as $(\sigma) = -1, 0,$ or 1

$\mathcal{J}_{FF'}$ can be expressed in terms of the nuclear spin I and the electronic angular momentum J by means of a Wigner 6-j symbol (explained in Appendix D) and another quantity $\mathcal{J}_{JJ'}$

$$\mathcal{J}_{FF'} = (-1)^{2F - J + I + F' + 1} \begin{Bmatrix} F & I & F' \\ J' & I & J \end{Bmatrix} \sqrt{2F+1}\,\sqrt{2F'+1}\, \mathcal{J}_{JJ'} \qquad (2)$$

The quantity $\mathcal{J}_{J J'}$ depends on the orbital angular momentum L and the electron spin angular momentum S and can be expressed in terms of a similar equation involving a 6-j symbol. For the two D lines in question

$$D_1 : \; ^2S_{\frac{1}{2}} \longrightarrow \; ^2P_{\frac{1}{2}} \qquad (7947.6\text{Å})$$

$$D_{2'} : \; ^2S_{\frac{1}{2}} \longrightarrow \; ^2P_{3/2} \qquad (7800.2\text{Å})$$

one finds that

$$\mathcal{J}_{\frac{1}{2}\frac{1}{2}} = \frac{1}{\sqrt{2}} \mathcal{J}_{\frac{1}{2}\frac{3}{2}} \qquad (3)$$

expressing the fact that absorption cross-sections for D_2 radiation are twice those for D_1 radiation.

These expressions are just those which lead to the Hönl-Kronig intensity ratios[32] for fine structure multiplets in the case of Russell-Saunders coupling. They are equally valid for hyperfine structure multiplets since the angular momentum relation $F = I + J$ involves the same type of coupling as $J = S + L$ in terms of direct product wave functions.

Let us denote the absolute square of these matrix elements by

$$T_{ik}^{(r)} = |(i|\rho^{(r)}|k)|^2 = T_{ki}^{(r)} \qquad (4)$$

(4)

For a particular type of incident polarization one will have a particular $\rho^{(\sigma)}$ or a linear combination of $\rho^{(\sigma)}$'s corresponding to certain changes in m_F:

Denote by $\vec{\epsilon}$ the unit vector describing the polarization of $\vec{A}$: $\vec{A} = A\vec{\epsilon}$; by $\vec{k}$ the unit vector along the z-axis, taken as the axis of quantization; and by $\vec{i}$ and $\vec{j}$ the unit vectors along the x and y axes, respectively. Then one has:

σ^- radiation $(\Delta m_F = -1)$

$\vec{\epsilon} = (\vec{i} + i\vec{j})/\sqrt{2} \Longrightarrow \vec{\rho}\cdot\vec{\epsilon} = (\rho_x + i\rho_y)/\sqrt{2} = \rho^{(-1)}$

σ^+ radiation $(\Delta m_F = +1)$

$\vec{\epsilon} = (\vec{i} - i\vec{j})/\sqrt{2} \Longrightarrow \vec{\rho}\cdot\vec{\epsilon} = (\rho_x - i\rho_y)/\sqrt{2} = -\rho^{(+1)}$

σ radiation $(\Delta m_F = +1 \text{ and } -1)$

$\vec{\epsilon} = \sqrt{\alpha}\,\vec{i} + \sqrt{1-\alpha}\,\vec{j} \Longrightarrow \vec{\rho}\cdot\vec{\epsilon} = \sqrt{\alpha}\,\rho_x + \sqrt{1-\alpha}\,\rho_y$

$= \frac{1}{\sqrt{2}}\left[(\sqrt{\alpha} - \sqrt{1-\alpha})\rho^{(+1)} - (\sqrt{\alpha} + \sqrt{1-\alpha})\rho^{(-1)}\right.$

π radiation $(\Delta m_F = 0)$

$\vec{\epsilon} = \vec{k} \Longrightarrow \vec{\rho}\cdot\vec{\epsilon} = \rho_z$

The symbol (σ) will frequently be used in subsequent expressions to indicate the type of polarizations, (-1), (0), (+1) standing for σ^-, π, and σ^+ polarizations, respectively. It is not to be confused with σ polarization, which is described as a linear combination of σ^+ and σ^- polarizations.

There is no constraint on the change in m_F for the emission of light by an excited (F, m_F) state and Δm_F can be ± 1 or 0 for electric dipole transitions. The radiation emitted by such transitions is best described in terms of a density matrix which includes both the angular distribution and the polarization state.(33)

$$\Delta m = 0: \quad \hat{\rho}^{(0)} = \sin^2\theta \left(\underline{1} + \underline{\sigma}_3\right) \tag{5a}$$

$$\Delta m = \pm 1 \quad \hat{\rho}^{(\pm 1)} = \frac{1}{2}(1+\cos^2\theta)\left(\underline{1} - \frac{\sin^2\theta\,\underline{\sigma}_3 \pm 2\cos\theta\,\underline{\sigma}_2}{1+\cos^2\theta}\right)$$

where $$\underline{\sigma}_1 = \begin{pmatrix} 0 & 1 \\ 1 & 0 \end{pmatrix}; \quad \underline{\sigma}_2 = \begin{pmatrix} 0 & i \\ -i & 0 \end{pmatrix}; \quad \underline{\sigma}_3 = \begin{pmatrix} 1 & 0 \\ 0 & -1 \end{pmatrix} \tag{5b}$$

and θ is measured with respect to the axis of quantization. In these expressions, a linear polarization basis is used with one direction in the plane containing the propagation vector and the z-axis and the other perpendicular to it.

The conditional probabilities describing the transfer of population among the ground states may be expressed as

$$P_{ij}^{(\sigma)} \propto \sum_k |(i|\vec{A}^{(\sigma)}\cdot\vec{p}|k)|^2\,|(k|\vec{A}^{\varepsilon_{emiss.}}\cdot\vec{p}|j)|^2$$

$$\propto \sum_k T_{ik}^{(\sigma)}\,T_{kj}^{\varepsilon_{emiss.}} \tag{6}$$

$$\propto \left(\underline{T}^{(\sigma)}\,\underline{T}^{\varepsilon_{emiss}}\right)_{ij}$$

where $P_{ij}^{(\sigma)}$ means the probability that if the atom is in state i it goes to state j by absorption of radiation with polarization (σ) and emission of radiation. The sum is over the various accessible intermediate excited states. Since the selection rules are included in the calculation of the matrix elements, one can write this sum as a matrix product. Since all types of polarization are possible in emission, one has

$$\underline{T}^{\varepsilon_{emiss}} = \sum_\sigma \underline{T}^{(\sigma)} \tag{7}$$

One must normalize the row sums of $P_{ij}^{(\sigma)}$ so that $\sum_j P_{ij}^{(\sigma)} = 1$ expressing the requirement that an atom is certain to find itself in some state. Such matrices are called <u>stochastic</u> by mathematicians, and play a large role in Markov processes.[34] For absorption of circularly polarized D_1 or D_2 radiation alone, it is not equally probable that each of the eight substates absorb a photon. This is shown by the sum over j being dependent on i. However, one can incorporate this varying absorption probability into the discussion of the time rate of absorption to be given below and still talk of stochastic pumping matrices.

In Appendix D the transition probabilities are tabulated for both D_1 and D_2 transitions for rubidium 87, along with the stochastic matrices for several kinds of optical pumping.

It is worth stating certain sum rules[35] which hold for electronic dipole transitions, for these are helpful in visualizing the pumping process and as a double check on calculations. Also, in some cases, one can compute the transition probabilities directly from the resulting simultaneous equations.

The sum of all transition probabilities ($\Delta m_F = \pm 1$ and 0) from an (F, M_F) state is the same for each particular m_F state of total angular momentum F. This holds both for absorption and emission. That this must be so can be seen physically by symmetry arguments. An isotropically excited state will have equal populations in each m_F state. There is no reason for the isotropy to change as the atoms emit radiation (assuming no preferential selection of modes by a resonant cavity structure) so that the populations must remain equal as the atoms radiate. This gives the following rule:

(1) $\sum_\sigma \sum_j T_{ij}^{(\sigma)}$ is independent of i

Another sum rule is that the sum over initial and final states for each type of Δm_F transition is independent of the type:

$$(2) \qquad \sum_i \sum_j T_{ij}^{(\sigma)} \qquad \text{is independent of } \sigma$$

See Figure 1 for an illustration of these rules. They are derived in Appendix D.

The second sum rule in connection with the density matrices for radiation given above in equation (5) shows that an initially isotropically excited state emits unpolarized radiation with no preferred direction. More details are given in Appendix E for an oriented or aligned excited state.

4. Effect of Collisions in the Excited State on the Optical Pumping Stochastic Matrices

If one knows the appropriate stochastic matrix describing the transfer of populations during a collision one can easily modify the matrices given above. If R_{kl} is the relaxation stochastic matrix, the appropriate pumping matrix is

$$\hat{P}_{ij}^{(\sigma)} = \sum_k \sum_l T_{ik}^{(\sigma)} R_{kl} I_{lj}^{(\sigma)} \qquad (8)$$

There is no accurate knowledge of R_{kl} but as a first approximation one may assume it to be uniform: $R_{kl} = C$ for each pair kl. The first of the above sum rules then shows that

$$P_{ij} = A + B\,C \sum_k T_{ik}^{(\sigma)}$$

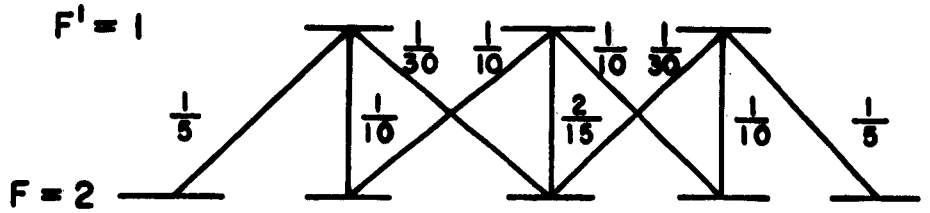

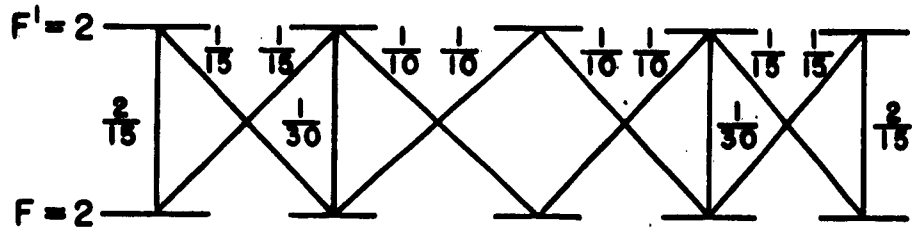

$$T_{ik}^{(\sigma)} = (F, m \; 1 \, \sigma, F'_{m'})^2 \begin{Bmatrix} F & 1 & F' \\ J' & I & J \end{Bmatrix}^2 (2F+1)(2F'+1) T^2_{JJ'}$$

$$\sum_{m,m'} (F, m \; 1 \, \sigma, F'_{m'})^2 = \frac{1}{3}$$

$$\sum_{m',\sigma} (F, m \; 1 \, \sigma \; F'_{m'})^2 = \frac{1}{2F+1}$$

$$\sum_{F'} \begin{Bmatrix} F & 1 & F' \\ J' & I & J \end{Bmatrix}^2 (2F+1)(2F'+1) T^2_{JJ'} = \frac{2F+1}{2J+1} T^2_{JJ'}$$

ILLUSTRATING SUM RULES

FIG. 1

where one has put $\sum_i T_{ij}^{(mix)} = \sum_i \sum_\sigma T_{ij}^{(\sigma)} = B$

If $\sum_k T_{jk}^{(\sigma)} = A^{(\sigma)}$, independent of i, then

$$\hat{P}_{ij}^{(\sigma)} \propto B\, C\, A^{(\sigma)}$$

and

$$\hat{P}_{ij}^{(\sigma)} = \frac{1}{S} = R_{ij}$$

by definition of the stochastic matrix: $\sum_j \hat{P}_{ij}^{(\sigma)} = 1.$

If $\sum_k T_{ik}^{(\sigma)} = A_i^{(\sigma)}$, different for each i as in the case for σ^+ (or σ^-) D_1 or D_2 pumping, one may still define a stochastic matrix $R_{ij} = \frac{1}{S}$ provided a diagonal matrix having elements $A_i^{(\sigma)}$ is introduced as described in Section II A 6 below.

It is just this existance of different absorption cross-sections for the magnetic substates of the ground state that allows orientation to be achieved in the presence of large buffer gas pressures that result in nearly complete mixing in the excited state.[12] A method of dealing with partial mixing is briefly described in Section II A 8 and in Appendix E.

A more realistic assumption regarding this type of relaxation is that the electron and nucleus are decoupled during the collision which randomizes the electron's angular momentum, leaving the spin of the nucleus unaffected. Such relaxation stochastic matrices can be constructed from a knowledge of the Wigner coupling coefficients.[36] They are presented for rubidium 87 in Appendix D.

5. Rate of Absorption of Photons

If the beam of incident radiation is characterized by a spectral distribution of intensity I_ν photons/sec -cm^2-cycle, and the cross-section for absorption by an atom is σ_ν cm^2 at the frequency ν, then the rate of absorption of photons is given by

$$\Gamma = \int_0^\infty I_\nu \, \sigma_\nu \, d\nu \qquad \text{photons per sec per atom} \quad (9)$$

When the spectral width of the light source $\Delta\nu_L$ is several times greater than the Doppler width of the absorbing atoms $\Delta\nu_D$ (This is much greater than the natural line width $\Delta\nu_N$) it is a good approximation to regard I_ν as constant over the interval where σ_ν is appreciable, equal to its value at the center frequency ν_0, and the expression for Γ becomes

$$\Gamma = I_{\nu_0} \int_0^\infty \sigma_\nu \, d\nu \qquad (10)$$

Now it is a result of the theory of the interaction of electromagnetic radiation with matter,[37] that

$$\int_0^\infty \sigma_\nu \, d\nu = 2\pi \frac{e^2}{\hbar c} \, \omega_{ki} \, |(i|\vec{r}\cdot\vec{\epsilon}|k)|^2 \qquad (11)$$

where

$$\omega_{ki} = \frac{E_k - E_i}{\hbar}$$

and i and k characterize the initial and excited states respectively.

It is convenient to define an oscillator strength which characterizes the strength of the absorption by the definition

$$f_{ik} = \frac{2\pi}{\hbar} \omega_{ki} |(k|\vec{F}\cdot\vec{\epsilon}|i)|^2 \tag{12}$$

so that we obtain

$$\int_{\text{line}} \sigma_\nu \, d\nu = \pi c r_0 f_{ik} \tag{13}$$

where r_0 is the classical radius of the electron. When the natural line width $\Delta\nu_N$ is much less than $\Delta\nu_D$, the Doppler width of the absorbing line, the convolution of the two yields for the actual value of σ_ν the approximate expression

$$\sigma_\nu = (\pi c r_0 f_{ik}) \frac{2}{\Delta\nu_D}\sqrt{\frac{\ln 2}{\pi}} \exp\left\{-\left[\frac{2(\nu-\nu_0)\sqrt{\ln 2}}{\Delta\nu_D}\right]^2\right\} \tag{14}$$

The oscillator strengths are proportional to the transition probabilities defined earlier, since the hyperfine splittings are completely negligible when compared to the optical transition frequency, so that ω_{ki} has essentially the same value for all the f_{ik}.

There will thus be a $\Gamma_i^{(\sigma)}$ for each of the eight ground substates which will depend on the polarization of the incident radiation. It is non-uniform for example for $\sigma^{\pm}$ radiation if the peak intensities of the D_1 and D_2 lines are different. (See Figure 2)

6. Formulation of the Differential Equations for Optical Pumping (An alternative and more detailed discussion is given in Appendix E)

The time rate of change of the population of one of the ground substates will be the difference of two terms: the rate of increase due to the pumping process minus the rate of decrease due to absorption by the state itself. The first term for state j is

$$\sum_i \Gamma_i N_i P_{ij}$$

where P_{ij} is the conditional probability that if an atom in state i absorbs a photon, it ends up in state j . The second term is simply $\Gamma_j N_j$.

Thus $$\dot{N}_j = \sum_i \Gamma_i N_i P_{ij} - \Gamma_j N_j \qquad (15)$$

If one defines a diagonal matrix $\underline{\underline{A}}$ having elements A_i given by

$$\Gamma_i = \Gamma A_i \qquad (16)$$

and having $Tr\, \underline{\underline{A}} = 8$, so that $\Gamma = \frac{1}{8} \sum_i \Gamma_i$ then the equation becomes in matrix form, using the transposed matrix $\underline{\underline{P}}^T$

$$\underline{\dot{N}} = \Gamma \left(\underline{\underline{P}}^T - \underline{\underline{\mathbb{I}}} \right) \underline{\underline{A}}\, \underline{N} \qquad (17)$$

This is the basic equation. If there are several kinds of pumping proceeding simultaneously, for example, non uniform spectral distribution among hyperfine lines, unequal peak intensities of D_1 and D_2, partial polarizations, etc. one can add several expressions of this sort. Similar terms can be added to describe relaxation effects of alkali-alkali collisions or wall collisions:

$$\frac{1}{T} \left(\underline{\underline{R}}^T - \underline{\underline{1}} \right) \underline{\underline{B}}\, \underline{N}$$

Here $\underline{\underline{R}}$ is the type of relaxation matrix discussed earlier, $\underline{\underline{B}}$ is diagonal with trace 8 and T is an average time between collisions for the atom.

The combination of two types of pumping affords a particularly simple demonstration that pumping with a narrowly directed beam of unpolarized light results in <u>alignment</u> of the atoms along the axis defined by the beam.[5] One may regard the unpolarized light as an equal mixture of σ^+ and σ^- light so that the pumping equation becomes

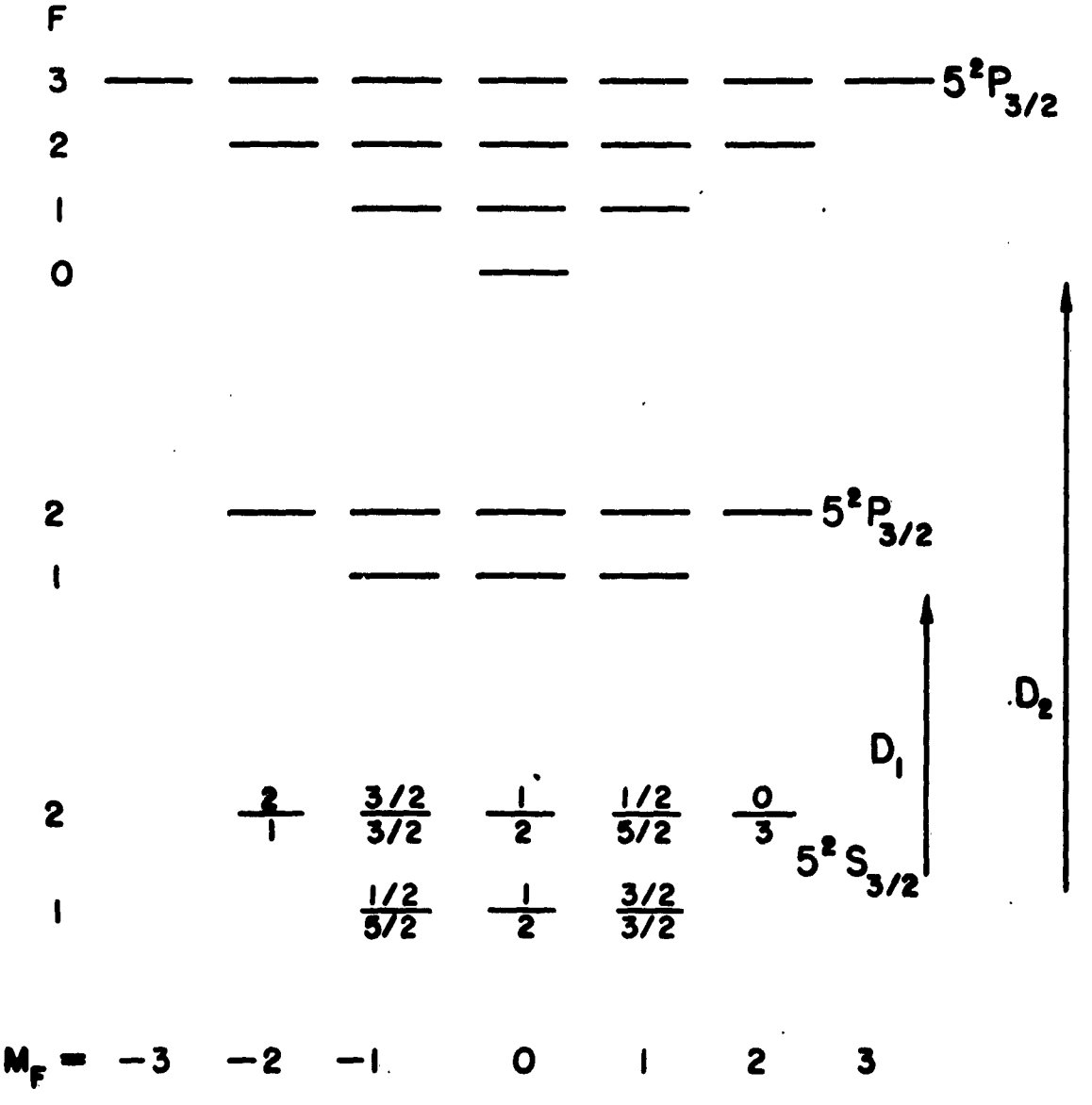

HYPERFINE SUBSTATES INVOLVED IN OPTICAL PUMPING.
RELATIVE ABSORPTION PROBABILITIES FOR σ^+ RADIATION

D_1 RADIATION: ABOVE THE SUBSTATE

D_2 RADIATION: BELOW THE SUBSTATE

FIG. 2

$$\dot{\underline{N}} = \left[\Gamma^{(+1)}\underline{P}^{(+1)T}\underline{A}^{(+1)} + \Gamma^{(-)}\underline{P}^{(-)T}\underline{A}^{(-)} - \left(\Gamma^{(+1)}\underline{A}^{(+1)} + \Gamma^{(-)}\underline{A}^{(-)}\right)\right]\underline{N}$$

$$= \frac{1}{2}\Gamma\left[\frac{\left(\underline{P}^{(+1)T}\underline{A}^{(+1)} + \underline{P}^{(-)T}\underline{A}^{(-)}\right)}{2} - \underline{\underline{\Pi}}\right] 2\,\underline{\underline{\Pi}}\,\underline{N} \qquad (18)$$

since $\Gamma^{(+1)} = \Gamma^{(-)} = \frac{1}{2}\Gamma$ for unpolarized light and where the relation $\underline{A}^{(+1)} + \underline{A}^{(-)} = 2\,\underline{\underline{\Pi}}$ follows from the sum rules (See Appendix D).

The effective pumping matrix is then

$$\underline{P}^{T}(\text{unpolarized}) = \frac{1}{2}\left(\underline{P}^{(+1)T}\underline{A}^{(+1)} + \underline{P}^{(-)T}\underline{A}^{(-)}\right) \qquad (19)$$

From the matrix elements of $\vec{P}\cdot\vec{A}$ for σ pumping given in Section II A 3

$$\vec{P}\cdot\vec{A} \propto \frac{1}{\sqrt{2}}\left[\left(\sqrt{\alpha} - i\sqrt{1-\alpha}\right)P^{(-1)} - \left(\sqrt{\alpha} + i\sqrt{1-\alpha}\right)P^{(+1)}\right]$$

one notes that for a possible transition either the matrix elements of $p^{(-1)}$ or those of $p^{(+1)}$ will vanish and that the square of the coefficient for either of these terms is $\frac{1}{2}$. Thus the pumping matrix for σ radiation, directed necessarily at 90° to the axis of quantization, is

$$\underline{P}^{T}(\sigma) = \frac{1}{2}\underline{P}^{(+1)T}\underline{A}^{(+1)} + \frac{1}{2}\underline{P}^{(-1)T}\underline{A}^{(-)} \qquad (20)$$

which is the same as that for the unpolarized light given in equation (19). It is known that σ pumping results in alignment, redistributing the population towards $+m_F$ and $-m_F$ equally.

It is worth emphasizing that the pumping matrices for π or σ radiation for $^1\Sigma$ transitions are <u>doubly stochastic</u>, column

sums as well as row sums equalling unity. From the form of the equation for pumping it is clear that for a uniform initial population distribution the time rate of change will be identically zero and no redistribution of population will result. The basic reason is that no electronic alignment in states of electronic angular momentum $\frac{1}{2}$ is possible and both the $^2S_{\frac{1}{2}}$ and $^2P_{\frac{1}{2}}$ states are of this type. Greater efficiency in the use of photons is thus possible for π or σ pumping by suppressing the D_1 radiation.

7. Derivation of the Stochastic Equations from the Differential Equations

The solutions of the matrix equation--

$$\dot{\underline{N}} = \Gamma \left(\underline{\underline{P}}^T - \underline{\underline{1}} \right) \underline{\underline{A}}\, \underline{N} \tag{21}$$

can be written formally [38]

$$\underline{N}(t) = e^{\Gamma \left(\underline{\underline{P}}^T - \underline{\underline{1}} \right) \underline{\underline{A}}\, t}\, \underline{N}(0) \tag{22}$$

If $\underline{\underline{A}}$ is the unit matrix, one may rewrite the equation by expanding the exponential to yield

$$\begin{aligned} \underline{N}(t) &= e^{-\Gamma t}\, e^{\Gamma \underline{\underline{P}}^T t}\, \underline{N}(0) \\ &= \left[\sum_{n=0}^{\infty} \frac{(\Gamma t)^n}{n!}\, e^{-\Gamma t} \left(\underline{\underline{P}}^T \right)^n \right] \underline{N}(0) \end{aligned} \tag{23}$$

which is just a sum of Poisson distributions for the probability of absorbing n photons in time t, each photon absorbed corresponding to one action of the matrix $\underline{\underline{P}}^T$ on the population vector $\underline{N}$. This is the equation used in earlier work at Princeton to compute population distributions. The relation to Markov processes [39] is evident. If $\underline{\underline{A}}$ is

not $\underline{\underline{1}}$ then it will not in general commute with $\underline{\underline{P}}^T$ and such an approach is not possible.

8. Computer Solutions of the Equations

To allow for arbitrary ratios of D_1 to D_2 light, different amounts of mixing of excited states, and different relaxation times for ground state relaxation the equations have been put into a form in which a few numerical parameters can specify these conditions. They are given for σ^+ pumping and the subscript i refers to D_1 or D_2.

$$\frac{d}{dt}\underline{N} = \left[\sum_{i=1}^{2} \Gamma_i \left(\underline{\underline{P}}'^T - \underline{\underline{1}}\right)\underline{\underline{A}}_i + \frac{1}{T}\left(\underline{\underline{R}}^T - \underline{\underline{1}}\right)\right]\underline{N} \qquad (24)$$

where

$$\underline{\underline{P}}'^T = (1 - q_i)\underline{\underline{P}}_i^T + q_i \underline{\underline{\hat{P}}}^T \qquad (25)$$

$\underline{\underline{P}}$ is the stochastic pumping matrix for no mixing and $\underline{\underline{\hat{P}}}$ is the matrix for complete mixing as described in Section II A 4.

It is shown in Appendix E that this is the appropriate form taken when uniform relaxation occurs in the excited state, so that $\underline{\underline{\hat{P}}} = \underline{\underline{R}}$. The analysis there shows that

$$q = \frac{\tau'}{\tau' + T'},$$

where τ' is the optical decay time and T' is the characteristic time between relaxing collisions in the excited state.

If one introduces

$$\Gamma = \Gamma_1 + \Gamma_2$$

$$\tau = \Gamma t$$

$$\chi = \frac{\Gamma_1}{\Gamma}$$

$$\underline{\underline{M}}_i = \left(\underline{\underline{P}}_i^T - \underline{\underline{\mathbb{1}}}\right) \underline{\underline{A}}_i \tag{26}$$

$$\underline{\underline{N}}_i = \left(\underline{\underline{\hat{P}}}_i^T - \underline{\underline{P}}_i^T\right) \underline{\underline{A}}_i$$

$$\rho = \frac{1}{\Gamma T}$$

the equation becomes

$$\frac{d\underline{N}}{d\tau} = \left[\chi\left(\underline{\underline{M}}_1 + q_1 \underline{\underline{N}}_1\right) + (1-\chi)\left(\underline{\underline{M}}_2 + \underline{\underline{N}}_2\right) + \rho\left(\underline{\underline{R}} - \underline{\underline{\mathbb{1}}}\right)\right] \underline{N} \tag{27}$$

A program for an IBM 650 computer was prepared to yield integral curves for the time development of the N_i (t) for a set of the parameters (χ, q_1, q_2, ρ). Some of this data is given in Appendix E, along with a discussion of the results.

The final equilibrium distribution of the N_i can be obtained by solving the equations

$$\frac{d}{d\tau} \underline{N} = 0 \tag{28}$$

for N_i (∞).

B. Optical Detection by Intensity Changes

1. Absorption Equations and Effective Oscillator Strengths

One does not have true absorption in the attenuation of a beam of resonance radiation as it travels through the vapor for it is re-radiated in all directions. However, one can neglect the small amount re-radiated in the forward direction and deal with the situation by the equation (assuming axial symmetry)

$$-\frac{dI_\nu}{dx} = n\,\sigma_\nu^{(i)} I_\nu \qquad (1)$$

for each component of the spectral intensity distribution I_ν. n is the density of atoms in the particular ground substate for which the cross section $\sigma_\nu^{(i)}$ is defined according to equation (14) in Section II A 5.

$$\sigma_\nu^{(i)} = \pi c r_e f_i \left(\frac{2}{\Delta\nu_D} \sqrt{\frac{\ln 2}{\pi}}\; e^{-\left[2\frac{\sqrt{\ln 2}}{\Delta\nu_D}(\nu-\nu_i)\right]^2} \right) \qquad (2)$$

which is valid if the natural width is small compared with the Doppler width $\Delta\nu_D$.

Under the conditions of a weak magnetic field there will be several ground substates which contribute to the cross section for a particular spectral component with oscillator strengths f_i which will in general be different for each substate. Under conditions where optical pumping is effective the populations of each of these substates will be different. It is then convenient to describe the situation by an effective cross section which is characterized by an <u>effective oscillator strength</u> f_{eff} defined by

$$\sum_i N_i \sigma_\nu^{(i)} = \left(\sum_i N_i f_i\right) \pi c r_e \cdot \begin{pmatrix}\text{Doppler}\\ \text{factor}\end{pmatrix} \qquad (3)$$

Since the diagonal elements of the absorption matrix $\underline{A}$ defined in Section II A 6 are proportional to the f_i one may write

$$f_{eff} = \sum_i N_i f_i = \sum_i \rho_{ii} f_i = f_o \, Tr \, \underline{\rho} \, \underline{A} \qquad (4)$$

where f_o is an appropriate constant. For the heavier alkali atoms, from sodium on, the oscillator strength for the principal resonance line $^2S \longleftrightarrow {}^2P$ is approximately unity. The small values of the oscillator strengths for transitions to higher states are compensated by the negative contributions from lower states, although these transitions do not occur since the lower states are occupied, so that the Thomas-Reiche-Kuhn sum rule is satisfied:

$$\sum_k f_{ik} = 1 \qquad (5)$$

The oscillator strengths satisfying this rule are defined in terms of electronic states. When one considers the hyperfine states and substates, the Wigner-Eckart decomposition for vector operators given in Section II A 3 enables one to assign appropriate oscillator strengths to the transitions between such states. It should be noted that equation (5) is usually derived from the commutation relation $[p_x, x] = \hbar/i$ and involves matrix elements of x. Clearly, the same argument holds for y and z, so that the Thomas-Reiche-Kuhn sum rule holds separately for each type of polarization: $\sigma^+, \sigma^-, \pi,$ or σ. This is related to the second sum rule discussed in Section II A 3.

Sometimes an <u>average oscillator strength</u> is defined by averaging over the initial magnetic substates and summing over the

final m-states.[35] Such average oscillator strengths obey "partial f-sum rules" which are stronger than the Thomas-Reiche-Kuhn sum rule.[40, 41]

2. Optical Pumping and Absorption as a Function of Distance of Penetration

There is selective filtering of the various spectral components of the radiation as it proceeds through the vapor cell. This in turn affects the pumping process at each distance into the cell so that the density matrix and therefore f_{eff} is a function of the distance x. This will be the situation if the alkali atoms are in a buffer gas which restricts their motion so that one can have a steady-state population distribution depending on x. However, if one uses a wall coated cell (to be discussed in Section III) which allows the atoms to move about freely in times short compared to the optical pumping time Γ^{-1}, complete spatial mixing can occur, resulting in the density matrix being independent of distance. However, there will still be a selective filtering effect.

To solve equation (1) one must first integrate with respect to x, noticing that σ_ν can be a function of x and then integrate the resulting expression for $I_\nu(x)$ with respect to ν to get the total intensity

$$I(x) = \int_0^\infty I_\nu(0) \exp\left\{ -\int_0^x f_{eff}(x)\,dx \cdot \pi c_1 \left(\frac{2}{\Delta\nu_D}\sqrt{\frac{\ln 2}{\pi}}\, e^{-\left[\frac{2\sqrt{\ln 2}}{\Delta\nu_D}(\nu-\nu_0)\right]^2} \right) \right\} d\nu \qquad (6)$$

where $I_\nu(0)$ is a Gaussian distribution. The integrand $I_\nu(x)$ in the above integral must be used in computing the value of photon absorption defined in Section II A 5 and the approximation made there is no longer appropriate. The types of integrals involving Gaussian distributions arising in this procedure were encountered by earlier researchers on resonance radiation and useful tabulations of numerical solutions are given in the book by Mitchell and Zemansky.[42] An approximate solution of the problem of selective hyperfine absorption using this approach is given in Appendix A.

A simpler approximate approach is to assume all spectral distributions to be rectangular with appropriate widths to account for the total area using the peak intensity at the center of the line. Then $I_\nu(x)$ will retain the same shape in the region of absorption. Under this assumption one can integrate equation (1) with respect to frequency before integrating with respect to x , and use the theorem on integrated cross-sections

$$-\frac{d}{dx}\int I_\nu(x)\,d\nu = n\,I_{\nu_c}(x)\int_0^\infty \sigma_\nu\,d\nu \qquad (7)$$

where $I_{\nu_c}(x)$ in the intensity per unit frequency at the center of the absorption line at position x . It is given by

$$I_{\nu_c}(x) = \frac{I(x)}{\Delta\nu_D} - I_{\nu_c}(0)\left[\frac{\Delta\nu_L}{\Delta\nu_D} - 1\right] \qquad (8)$$

After integration, one has

$$I_{\nu_c}(x) = I_{\nu_c}(0)\,(\Delta\nu_L - \Delta\nu_D) + \left[I(0) - I_{\nu_c}(0)\,(\Delta\nu_L - \Delta\nu_D)\right] e^{-\frac{\pi c\,\tau}{\Delta\nu_D}\int_0^x f_{eff}(x)\,dx} \qquad (9)$$

One can then proceed to calculate $\Gamma(x)$ and obtain a set of coupled non-linear equations, when one includes equation (17) of Section II A 6 and equation (4) of Section II B 1, to describe the diagonal density matrix ρ^{D} as a function of position.

The general solution of the position dependence of optical pumping has not been obtained, but this could be accomplished numerically with the aid of a digital computer.

3. The Absorption Operators

The fact that one can express the effective cross section for absorption by means of an effective oscillator strength

$$f_{eff} = f_0 \, Tr \, \rho \, A \tag{10}$$

leads one to search for a general non-diagonal operator A which could be used to express the absorption when phase relations among substates are established in the vapor so that the off-diagonal elements of the density matrix need to be considered.

One way of constructing the desired operator is to observe that the diagonal absorption matrixes given in Section A and Appendix D (See also Figure 2) may be written for D_1 with similar expressions for D_2.

$$A^{\sigma\pm} = I \mp \frac{(-1)^F}{2} m_F = I \mp \frac{(-1)^F}{2F} F_z$$

$$A^{\pi} = A^{\sigma} = I \tag{11}$$

The axis of quantization for defining the states is the z-axis. Consider now a density matrix for the states describing an incoherent situation and therefore having off-diagonal elements equal to zero.

Let a beam of radiation of some polarization be incident along a direction $\vec{n}$ not coinciding with the z-axis. The appropriate absorption operator is just the diagonal $\underline{A}$ when used with the density matrix defined in terms of states for which $\vec{n}$ is the z-axis. This density matrix is

$$\underline{\rho}(\vec{n}) = \underline{U}(\vec{n})\,\underline{\rho}(z)\,\underline{U}(\vec{n}) \tag{12}$$

where $\underline{U}(\vec{n})$ is the unitary transformation of the states corresponding to the change in the axis of quantization (This is discussed more fully in the next section). The effective oscillator strength f_{eff} for this beam will then be

$$\begin{aligned} f_{eff}(\vec{n}) &= f_0\, Tr\, \underline{\rho}(\vec{n})\,\underline{A} \\ &= f_0\, Tr\, \underline{U}(\vec{n})\,\underline{\rho}(z)\,\underline{U}^{-1}(\vec{n})\,\underline{A} \\ &= f_0\, Tr\, \underline{\rho}(z)\,\underline{U}^{-1}(\vec{n})\,\underline{A}\,\underline{U}(\vec{n}) \end{aligned} \tag{13}$$

Now

$$\underline{U}^{-1}(\vec{n})\,\underline{F}_z\,\underline{U}(\vec{n}) = \underline{\vec{F}}\cdot\vec{n} \tag{14}$$

for a vector operator[43] so we obtain the following general expressions for absorption operators for a beam of light of specified polarization and direction when the states are defined with respect to the z-axis

$$D_1: \quad \underline{A}^{\sigma\pm} = \underline{\mathbb{1}} \mp \frac{(-1)^F}{2t}\,\underline{\vec{F}}\cdot\vec{n}$$

$$\underline{A}^{\pi} = \underline{A}^{\sigma} = \underline{\mathbb{1}} \tag{15}$$

$$D_2: \quad \underline{A}^{\sigma\pm} = 2\,\underline{\mathbb{1}} \mp \frac{(-1)^F}{2t}\,\underline{\vec{F}}\cdot\vec{n}$$

$$\underline{A}^{\pi} = \underline{A}^{\sigma} = 2\,\underline{\mathbb{1}}$$

4. Modulation of Light Intensity by Larmor Precession

The effect of a 90° pulse on an assemblage of atoms possessing orientation in the z-direction is to rotate the net magnetic moment into the x-y plane where it undergoes precession at the Larmor frequency about the z-axis if this is also the direction of the magnetic field. The density matrix will possess off-diagonal elements, and a beam of light with σ^+ polarization having a direction $\vec{n}$ in the x-y plane, say x for convenience, will be modulated. This is easily calculated in the formalism that has been developed. The appropriate operator is

$$\underline{\underline{A}}^{\sigma^+} = \underline{\underline{1\!\!1}} \mp \frac{(-1)^F}{2\hbar} F_x \tag{16}$$

where

$$F_x = \frac{\hbar}{2}\begin{pmatrix} 0 & 2 & 0 & 0 & 0 \\ 2 & 0 & \sqrt{6} & 0 & 0 \\ 0 & \sqrt{6} & 0 & \sqrt{6} & 0 \\ 0 & 0 & \sqrt{6} & 0 & 2 \\ 0 & 0 & 0 & 2 & 0 \end{pmatrix} \quad \text{for } F = 2$$

$$= \hbar \begin{pmatrix} 0 & 1 & 0 \\ 1 & 0 & 1 \\ 0 & 1 & 0 \end{pmatrix} \quad \text{for } F = 1 \tag{17}$$

If one considers the initial state to be (2,2), then by methods involving rotation operators to be developed in the next section, the resulting wave function, containing only states for F = 2,

and density matrix can be computed. Then using the expression

$$f_{eff} = f_c \, Tr \, f \, A$$

one finds

$$f_{eff} = f_c \, (1 + \cos \omega t) \quad \text{for } D_1$$

$$f_{eff} = f_c \, (2 - \cos \omega t) \quad \text{for } D_2 \tag{18}$$

It is worth pointing out that the phases are opposite for D_1 and D_2 and that, for this case, there is 100% modulation for the D_1 radiation. One can use the methods described in the next several sections to compute the modulation for an actual initial density matrix to which all the states contribute. This yields

D_1 :

$$f_{eff} = f_c \left\{ 1 + \left[(\rho_{88} - \rho_{44}) + \tfrac{1}{2} (\rho_{77} - \rho_{55}) \right] \cos \omega t \right\} \quad (F = 2)$$

$$f_{eff} = f_c \left\{ 1 + \tfrac{1}{2} (\rho_{33} - \rho_{11}) \cos \omega t \right\} \quad (F = 1)$$

(19)

D_2 :

$$f_{eff} = f_c \left\{ 2 - \left[(\rho_{88} - \rho_{44}) + \tfrac{1}{2} (\rho_{77} - \rho_{55}) \right] \cos \omega t \right\} \quad (F = 2)$$

$$f_{eff} = f_c \left\{ 2 - \tfrac{1}{2} (\rho_{33} - \rho_{11}) \cos \omega t \right\} \quad (F = 1)$$

where the ρ_{ii} are the diagonal elements of the initial density matrix.

Although the states F = 1 and F = 2 precess in opposite directions as shown in Section II C 1, the absorption coefficients for the m_F states vary in the opposite sense with increasing m_F, as shown in Figure 2.

C. Description of Weak Field Zeeman Resonances as Rotations of Higher Spin Systems

1. Larmor Precession Frequency

The gyromagnetic ratio γ for the ground states corresponding to F = 1 and F = 2 can be expressed in terms of the ordinary Landé g-factor which describes the first order Zeeman splitting in a weak magnetic field B_o. It is given by[44]

$$\gamma = \frac{g_F \mu_o}{\hbar} \tag{1}$$

with μ_o being the Bohr magnetron $\frac{e\hbar}{2mc}$. g_F is given by[45]

$$g_F = g_J \left[\frac{F(F+1) + J(J+1) - I(I+1)}{2F(F+1)} \right] \tag{2}$$

where

$$g_J = 1 + \frac{J(J+1) + S(S+1) - L(L+1)}{2J(J+1)} \tag{3}$$

The ground state of an alkali atom has $J = \frac{1}{2}$, L = 0, $S = \frac{1}{2}$ so $g_J = 2$. For rubidium 87, I = 3/2, so one obtains

$$g_{F=1} = -\frac{1}{2}$$
$$g_{F=2} = +\frac{1}{2} \tag{4}$$

For electrons, which have a g-factor of approximately 2, the precession frequency is about 2.8 Mc/gauss, so that the precession frequency $\gamma B_o / 2\pi$ will be about 700 kc/gauss.

It should be noted that the sign of the g-factor is opposite for the two F states, hence the precession of these states will be in opposite directions at the same frequency. When one includes the higher order terms the several states will split differently and there will be several different Zeeman frequencies, so that these conclusions are not strictly correct. Only the weak field case, defined by the neglect of these higher terms, is considered here.(46)

2. Magnetic Resonance; Rabi-Ramsey-Schwinger Theorem(47)

An approximation frequently used in magnetic resonance calculations is to consider a rotating magnetic field of constant amplitude $\vec{B}_1$ in a plane perpendicular to the field $\vec{B}_0$, rather than a linearly oscillating field in this plane. Although this latter type of field is generally used in practice because of its convenience, it can be regarded as a superposition of oppositely rotating fields. The component rotating in the same direction as that of the Larmor precession of the magnetic moments is chiefly effective in tipping the moments when its frequency coincides with the Larmor frequency. The oppositely rotating component contributes very little to the motion and can be neglected. The equations can now be solved by an elegant method using rotation operators, which will be described. It should be noted that if one actually uses a rotating field, it can be made to affect either the F = 1 or the F = 2 states, depending on the sense of rotation.

It may be shown both in classical and in quantum mechanical terms that if one transforms to a coordinate system rotating with angular velocity $\vec{\omega}$ there appears in this system

an additional magnetic field γ [illegible]. [44] If [illegible] is chosen to be equal to $-\gamma \vec{B}_0$ the static field can be transformed away. When the rotating magnetic field B_1 is applied it appears as a constant field in this frame of reference and one may transform to another system rotating with angular velocity $-\gamma \vec{B}_1$ to transform it away also. In this system the interaction Hamiltonian vanishes and the states do not change in time. The actual development in time may be obtained by transforming back to the original laboratory coordinate system. This is known as the Rabi-Ramsey-Schwinger Theorem.

3. Irreducible Representations of the Rotation Group

The rotation of the coordinate system from coordinates $\vec{r}$ to coordinates $\vec{r}' = \underline{R}\,\vec{r}$ induces a transformation $\underline{U}(\underline{R})$ of the quantum mechanical state $\underline{\Psi}$ according to the definition [48]

$$\underline{U}(\underline{R})\,\underline{\Psi}(\vec{r}) = \underline{\Psi}(\underline{R}^{-1}\vec{r}) \tag{5}$$

from which $\underline{U}(\underline{R})$ is readily shown to be unitary. One best defines angular momentum operators in terms of the infinitesimal operators of the rotation group [49] and by iterating these one arrives at the following expression for $\underline{U}(\underline{R})$ for a rotation described by the Euler angles (α, β, γ) [50]

$$\underline{U}(\underline{R}) = \exp\left(\frac{i}{\hbar}\alpha \underline{F}_z\right) \exp\left(\frac{i}{\hbar}\beta \underline{F}_y\right) \exp\left(\frac{i}{\hbar}\gamma \underline{F}_z\right) \tag{6}$$

when the y-axis is chosen as the line of nodes.

The functions we are concerned with are the eigenfunctions of the operator for the square of the angular momentum, $\underline{F}^2$, which commutes with the rotation operator. Thus one must be

able to write the rotated state as a linear combination of the eigenfunctions of $\underline{F}^2$

$$\underline{U}(\underline{R})\,\psi^{F}_{m_F} = \sum_{m_F'=-F}^{F} \mathcal{D}^{(F)}(\underline{R})_{m_F' m_F}\,\psi^{F}_{m_F'} \qquad (7)$$

The matrices $\underline{\mathcal{D}}^{(F)}$ are representations of the rotation group and they may be shown to be irreducible--that is, that there is no submanifold among the functions that remains invariant under all rotations. The matrix elements $\mathcal{D}^{(F)}_{m_F' m_F}$ are expressable as

$$\mathcal{D}^{(F)}_{m_F' m_F} = \left(\psi^{F}_{m_F'},\ \underline{U}(\underline{K})\,\psi^{F}_{m_F}\right) \qquad (8)$$

For the representation in which $\underline{F}_z$ is diagonal

$$\mathcal{D}^{(F)}_{m_F' m_F} = e^{i m_F' \alpha}\left(\psi^{F}_{m_F'},\ \exp\left(\frac{i}{\hbar}\beta F_y\right)\psi^{F}_{m_F}\right) e^{i m_F \gamma} \qquad (9)$$

4. Construction of $\underline{\mathcal{D}}(\underline{R})$ using the Spectral Decomposition Theorem[52]

There are various methods for getting explicit expressions for the elements $\mathcal{D}^{(F)}_{m_F' m_F}$ described in the standard works on group theory.[51] These are very valuable for establishing relations but are a bit tedious for explicit numerical evaluation. A simple method for obtaining the matrix $\underline{\mathcal{D}}^{(F)}$ for a particular F was found to be use of the spectral decomposition theorem for operators,[52] which enables a function of an operator to be expressed as a sum over the eigenvalues of the function with the eigenvalue as argument multiplied by the projection operator onto the manifold characterized

m′ \ m	1	0	−1
1	$\frac{1}{2}(1+\cos\beta)$	$\frac{1}{\sqrt{2}}\sin\beta$	$\frac{1}{2}(1-\cos\beta)$
0	$\frac{-1}{\sqrt{2}}\sin\beta$	$\cos\beta$	$\frac{1}{\sqrt{2}}\sin\beta$
−1	$\frac{1}{2}(1-\cos\beta)$	$\frac{-1}{\sqrt{2}}\sin\beta$	$\frac{1}{2}(1+\cos\beta)$

TABLE 1 $\underline{\underline{\mathcal{D}}}^{(1)}_{(0\beta 0)}$ (Y−AXIS AS LINE OF NODES)

m′ \ m	2	1	0	−1	−2
2	$\frac{3}{8}+\frac{1}{8}\cos 2\beta+\frac{1}{2}\cos\beta$	$\frac{1}{4}\sin 2\beta+\frac{1}{2}\sin\beta$	$\frac{\sqrt{3}}{4\sqrt{2}}(1-\cos 2\beta)$	$-\frac{1}{4}\sin 2\beta+\frac{1}{2}\sin\beta$	$\frac{3}{8}+\frac{1}{8}\cos 2\beta-\frac{1}{2}\cos\beta$
1	$-\frac{1}{4}\sin 2\beta-\frac{1}{2}\sin\beta$	$\frac{1}{2}\cos 2\beta+\frac{1}{2}\cos\beta$	$\frac{\sqrt{3}}{2\sqrt{2}}\sin 2\beta$	$-\frac{1}{2}\cos 2\beta+\frac{1}{2}\cos\beta$	$-\frac{1}{4}\sin 2\beta+\frac{1}{2}\sin\beta$
0	$\frac{\sqrt{3}}{4\sqrt{2}}(1-\cos 2\beta)$	$\frac{-\sqrt{3}}{2\sqrt{2}}\sin 2\beta$	$\frac{1}{4}(1+3\cos 2\beta)$	$\frac{\sqrt{3}}{2\sqrt{2}}\sin 2\beta$	$\frac{\sqrt{3}}{4\sqrt{2}}(1-\cos 2\beta)$
−1	$\frac{1}{4}\sin 2\beta-\frac{1}{2}\sin\beta$	$-\frac{1}{2}\cos 2\beta+\frac{1}{2}\cos\beta$	$\frac{-\sqrt{3}}{2\sqrt{2}}\sin 2\beta$	$\frac{1}{2}\cos 2\beta+\frac{1}{2}\cos\beta$	$\frac{1}{4}\sin 2\beta+\frac{1}{2}\sin\beta$
−2	$\frac{3}{8}+\frac{1}{8}\cos 2\beta-\frac{1}{2}\cos\beta$	$\frac{1}{4}\sin 2\beta-\frac{1}{2}\sin\beta$	$\frac{\sqrt{3}}{4\sqrt{2}}(1-\cos 2\beta)$	$-\frac{1}{4}\sin 2\beta-\frac{1}{2}\sin\beta$	$\frac{3}{8}+\frac{1}{8}\cos 2\beta+\frac{1}{2}\cos\beta$

TABLE 2 $\underline{\underline{\mathcal{D}}}^{(2)}_{(0\beta 0)}$ (Y−AXIS AS LINE OF NODES)

m′ \ m	1	0	−1
1	$\frac{1}{2}e^{i\omega(t-t_0)}$	$\frac{\pm 1}{\sqrt{2}}e^{i\omega t}$	$\frac{1}{2}e^{i\omega(t+t_0)}$
0	$\frac{\mp 1}{\sqrt{2}}e^{-i\omega t_0}$	0	$\frac{\pm 1}{\sqrt{2}}e^{i\omega t_0}$
−1	$\frac{1}{2}e^{-i\omega(t+t_0)}$	$\frac{\mp 1}{\sqrt{2}}e^{-i\omega t}$	$\frac{1}{2}e^{-i\omega(t-t_0)}$

$\times e^{\frac{i}{t}E(t-t_0)}$

TABLE 3 $\underline{U}(\pm 90°)$ FOR F=1

m′ \ m	2	1	0	−1	−2
2	$\frac{1}{4}e^{-i2\omega(t-t_0)}$	$\frac{\mp 1}{\sqrt{2}}e^{-i\omega(t-t_0)}$	$\frac{\sqrt{3}}{2\sqrt{2}}e^{-i\omega 2t}$	$\frac{\mp 1}{2}e^{-i\omega(2t+t_0)}$	$\frac{1}{4}e^{-i2\omega(t+t_0)}$
1	$\frac{\pm 1}{2}e^{-i\omega(t-2t_0)}$	$\frac{-1}{2}e^{-i\omega(t-t_0)}$	0	$\frac{1}{2}e^{-i\omega(t_1+t_0)}$	$\frac{\mp 1}{2}e^{-i\omega(t+2t_0)}$
0	$\frac{\sqrt{3}}{2\sqrt{2}}e^{i\omega 2t_0}$	0	$-\frac{1}{2}$	0	$\frac{\sqrt{3}}{2\sqrt{2}}e^{-i\omega 2t_0}$
−1	$\frac{\pm 1}{2}e^{i\omega(t+2t_0)}$	$\frac{1}{2}e^{i\omega(t+t_0)}$	0	$\frac{-1}{2}e^{i\omega(t-t_0)}$	$\frac{\mp 1}{2}e^{i\omega(t-2t_0)}$
−2	$\frac{1}{4}e^{i2\omega(t+t_0)}$	$\frac{\pm 1}{2}e^{i\omega(2t+t_0)}$	$\frac{\sqrt{3}}{2\sqrt{2}}e^{i\omega 2t}$	$\frac{\pm 1}{2}e^{i\omega(2t-t_0)}$	$\frac{1}{4}e^{i2\omega(t-t_0)}$

$\times e^{\frac{-i}{t_0}E(t-t_0)}$

TABLE 4 $\underline{U}(\pm 90°)$ FOR F=2

by the eigenvalue. This yields for rotations about the y-axis

$$\underline{\underline{\mathcal{D}}}^{(F)}(0,\beta,0) = \exp\left(\frac{i}{\hbar}\beta \underline{F}_y\right) = \sum_{m_F=-F}^{F} e^{i\beta m_F} \underline{\underline{E}}_{m_F} \qquad (10)$$

where the $\underline{\underline{E}}_{m_F}$ are projection operators onto the manifold characterized by the eigenvalue m_F. The $\underline{\underline{E}}_{m_F}$ may easily be constructed by calculating the normalized eigenvectors of $\underline{\underline{F}}_y$ in a representation with $\underline{\underline{F}}_z$ diagonal

$$\underline{\underline{F}}_y \underline{\psi}^{(y)}_{m_F} = m_F \hbar \underline{\psi}^{(y)}_{m_F} \qquad (11)$$

Then the $\underline{\underline{E}}_{m_F}$ are the outer product operators formed with these $\underline{\psi}^{(y)}_{m_F}$

$$\underline{\underline{E}}_{m_F} = \underline{\psi}^{(y)}_{m_F} \underline{\psi}^{(y)*}_{m_F} \qquad (12)$$

One should remark that the wave functions $\underline{\psi}$ are written in column vector form whose elements are the coefficients in an expansion in terms of eigenstates of $\underline{\underline{F}}_z$

$$\underline{\psi} = \sum_{F=1}^{k} \sum_{m_F=-F}^{F} a^F_{m_F} \underline{\psi}^F_{m_F} = \begin{bmatrix} a'_1 \\ \vdots \\ a'_k \end{bmatrix} \qquad (13)$$

It is to be noted that when one represents a state in this way by a column vector of coefficients the rotation operator $\underline{\underline{U}}(R)$ applied to the state is just the ordinary matrix product $\underline{\underline{\mathcal{D}}}(R)\,\underline{\psi}$ rather than the product with the transpose of $\underline{\underline{\mathcal{D}}}$ as equation(7) gives for the transformation of the states themselves.

The irreducible representations $\underline{\underline{\mathcal{D}}}^{(1)}$ and $\underline{\underline{\mathcal{D}}}^{(2)}$ constructed in this way are presented in Tables 1 and 2.

5. Unitary Transformations Induced by Pulses

Using the Rabi-Ramsey-Schwinger Theorem, and explicitly neglecting the oppositely rotating term, the unitary transformation $\underset{\sim}{U}(t-t_0)$ giving the way in which a state changes under the action of an oscillating magnetic field $2 B_1 \cos\omega t$ at right angles to B_0 applied at t_0 and removed at t can now be given

$$\underset{\sim}{U}(t-t_1) = \exp\left(\frac{i}{\hbar}\underset{\sim}{F_z}\gamma B_0 t\right)\exp\left(\frac{i}{\hbar}\underset{\sim}{F_y}\gamma B_1(t-t_1)\right)\exp\left(\frac{-i}{\hbar}\underset{\sim}{F_z}\gamma B_0 t_0\right) \qquad (14)$$

where the direction of the rotating field B_1 has been taken to be along the y-axis in the rotating system. The matrix representations of the operator $\underset{\sim}{U}$ for $\pm 90°$ pulses ($\gamma B_1 \times (t_1-t_0) = \pm\frac{\pi}{2}$) are given in Tables 3 and 4.

For 180° pulses the unitary matrices are "skew-diagonal" beginning with + 1 in the upper right corner and alternating with - 1 until + 1 is reached in the lower left corner.

6. Effect of Magnetic Field Inhomogeneities

The detection of the $0 \leftrightarrow 0$ resonance by the phase destruction method, to be more fully described in Section II E, requires that the phase relations among the partner states set up by an initial 90° pulse be preserved among all atoms of the assemblage until the second - 90° pulse. These phase relations correspond to free precession in the x-y plane at the Larmor frequency. It is apparent that if the static magnetic field B_0 is not uniform over the volume of the cell containing the vapor, the atoms will precess at different rates and get out of phase with one another. One can easily obtain a relation between the fractional inhomogeneity $\Delta B/B_0$ and the

phase spread δ after a time τ:

$$\delta = \Delta\omega_0 \tau = \gamma \Delta B_0 \tau$$

$$\frac{\delta}{\omega_0 \tau} = \frac{\Delta B_0}{B_0} \qquad (15)$$

An allowable value of δ might be one radian. It is clear from equation (15) that for a fixed value of τ the required degree of homogeneity lessens as the field B_0, and hence the frequency ω_0, is reduced. At low fields, however, the contribution from small pieces of ferromagnetic material in the laboratory or from irregularities in shielding devices becomes relatively greater. If one wishes to have $\tau = 10^{-1}$ sec and $\omega_0 = 2\pi \times 10^5$ radians/sec, the requirement on $\Delta B_0/B_0$ for a one radian spread is $\Delta B_0/B_0 < 10^{-4}/2\pi$

The inhomogeneity would cause some of the atoms to be slightly off resonance in response to the pulse of rf and therefore to be tipped by slightly different angles, but this would not be serious. More deleterious would be a large inhomogeneity in the rf field B_1 over the volume of the cell, but even a few per cent spread in the angle of tipping would not be harmful.

7. Methods of Alleviating Magnetic Field Inhomogeneities: Spin Echo Techniques and Wall Coated Bulbs

If it is not possible to obtain the desired homogeneity by shielding the gas cell from external laboratory fields and creating the desired field by appropriate coils (See Section III C for details) one can still utilize pulse techniques of the spin-echo type devised by Hahn[53] to preserve the phase relations among the freely precessing atoms at the end of the time τ. This can be accomplished by inserting a 180° pulse midway between the two 90° pulses, as illustrated in Figure 3. Assuming that the atoms remain fixed in

space, precessing at a rate determined by the local magnetic field, some will go too fast and advance in phase while others will go too slowly and be retarded in phase. The effect of the 180° pulse is to reverse the phases of the atoms with respect to the average phase, or ideal phase, as illustrated. Now the more rapidly precessing atoms are retarded in phase, but will catch up with the others, while the more slowly precessing atoms are moved ahead in phase, but will fall back. The result is that they are all in phase at the end of a time equal to twice that between the first 90° pulse and the 180° pulse.

In a cell containing a buffer gas, the alkali atoms will not be fixed in position but will be diffusing among the buffer gas atoms. Under these circumstances it is still possible to preserve phases during a time interval by applying a succession of 180° pulses, spaced as shown in Figure 3, as was first demonstrated by Carr and Purcell.(54)

These techniques have been used successfully and experimental details will be given in Section III C.

Another method of reducing the effect of field inhomogeneities is to use a bulb whose walls have been coated with a material which bounces the oriented atoms off but affects the spin state only very slightly. The averaging effect of the motion of the precessing atoms in the inhomogenous field can lead to an increase in the effective time for dephasing. Some estimates can be obtained by using the notion of a random walk in phase. If $\Delta\omega$ is the spread in angular frequencies due to the inhomogeneities and τ_0 is the transit time across the cell, the basic step in phase will be $\Delta\omega\tau_0$. The number of such steps in a time τ is τ/τ_0 and the

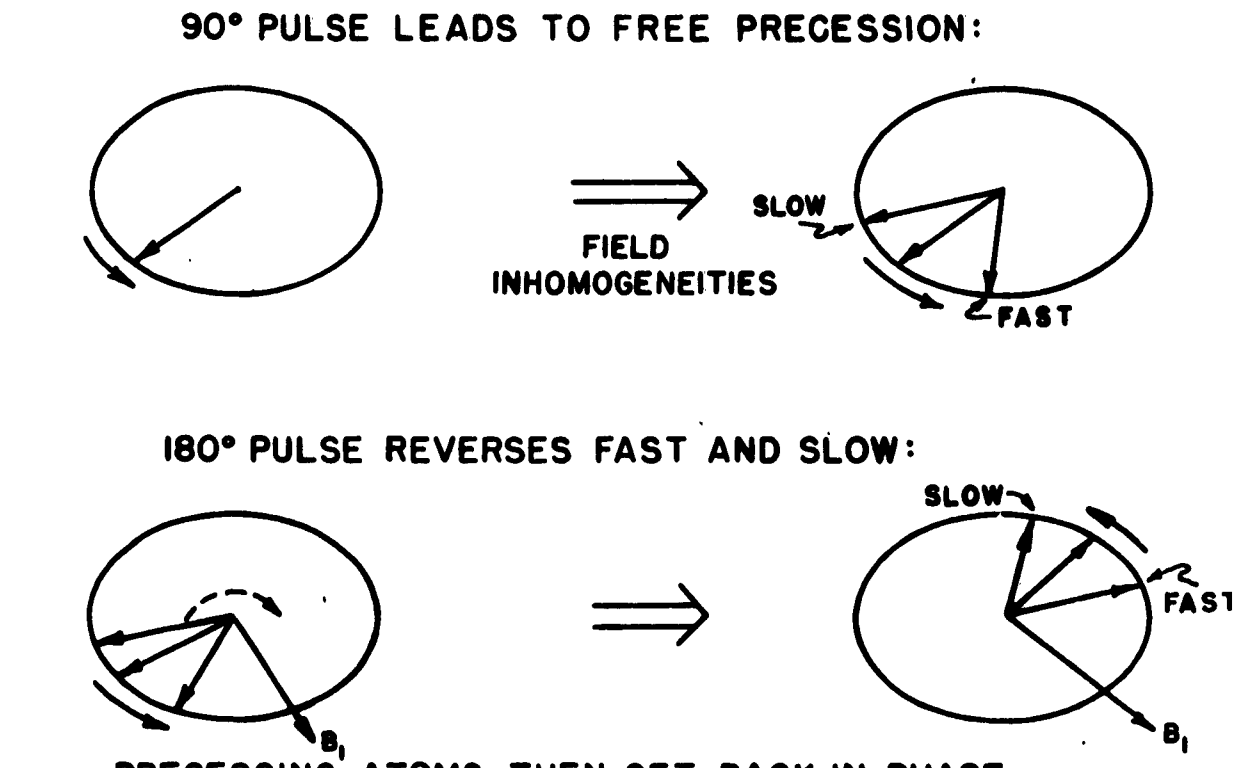

SPIN ECHO (HAHN)

FIG. 3

average phase spread developed in this time is

$$\Delta \varphi = \Delta \omega \tau_0 \sqrt{\frac{\tau}{\tau_0}} \tag{16}$$

Defining τ by putting $\Delta\varphi = 1$, we obtain

$$\tau = \frac{1}{\Delta\omega}\left(\frac{1}{\Delta\omega\tau_0}\right) \tag{17}$$

An improvement will be achieved if $\Delta\omega\tau_0 < 1$. If ΔB_0 is proportional to B_0, we can gain by going to lower field strengths for a fixed size bulb. If ΔB_0 is independent of B_0, one can only gain by reducing the size the cell and thereby reducing τ_0. This would also reduce the value of ΔB_0 and thereby $\Delta\omega$ under most circumstances. Wall coatings to achieve such effects were investigated and are described in Section II B.

8. Effect of a Sinusoidally-Varying Magnetic Field

If the magnetic field B_0 is not constant but has a small time varying part the Larmor frequency will not be constant during an interval of free precession and departures from the "equilibrium angle", defined for the constant field B_0, will develop. The case where the time variation of B_0 is slow compared to the Larmor period will be treated, having in mind a 60 cycle magnetic field, so a sinusoidal variation will be assumed. The effect of such a field was difficult to suppress experimentally and was therefore used as a method of detection as described in Section IV A.

The angle of rotation swept out by the oriented atoms freely precessing in the x-y plane during a time interval τ following a 90° pulse at time t_0 is given by

$$\varphi = \gamma B_0 \tau + \gamma \int_{t_0}^{t_0+\tau} \Delta B \cos \frac{2\pi t}{T_e} \, dt \qquad (17)$$

when the time varying point of the field is $\Delta B \cos(2\pi t/T_e)$. The angle of departure from the equilibrium angle, as shown in Figure 4 is then

$$\Delta \varphi = \gamma \frac{\Delta B T_e}{2\pi} \sin \frac{2\pi t}{T_e} \Big|_{t_0}^{t_0+\tau} \qquad (18)$$

$$= \gamma \frac{\Delta B T_e}{2\pi} 2 \sin \frac{\pi \tau}{T_e} \cos \frac{2\pi}{T_e}\left(t_0 + \frac{\tau}{2}\right)$$

It is convenient to define

$$\left.\begin{aligned} \alpha &= \frac{\pi \tau}{T_e} \\ \theta &= \frac{2\pi t_0}{T_e} \\ A &= \gamma \frac{\Delta B T_e}{\pi} \sin \alpha \end{aligned}\right\} \qquad (19)$$

When a -90° pulse is applied after the interval τ, it will rotate spins having the equilibrium angle back into the original vertical position they had before the first 90° pulse. However, if there has been a departure $\Delta\varphi$ from this equilibrium angle, the spins after the -90° pulse will make an angle $\Delta\varphi$ with the vertical axis.

It is shown in Section II B 4 that the optical absorption of a σ^+ beam of light directed along the z-axis by an oriented assemblage of atoms is proportional to the cosine of the angle between the direction of orientation and the z-axis. Thus the light transmission of a σ^+ beam following the -90° pulse will be given by

$$f_{eff} \propto \cos[A \cos(\theta + \alpha)] \qquad (20)$$

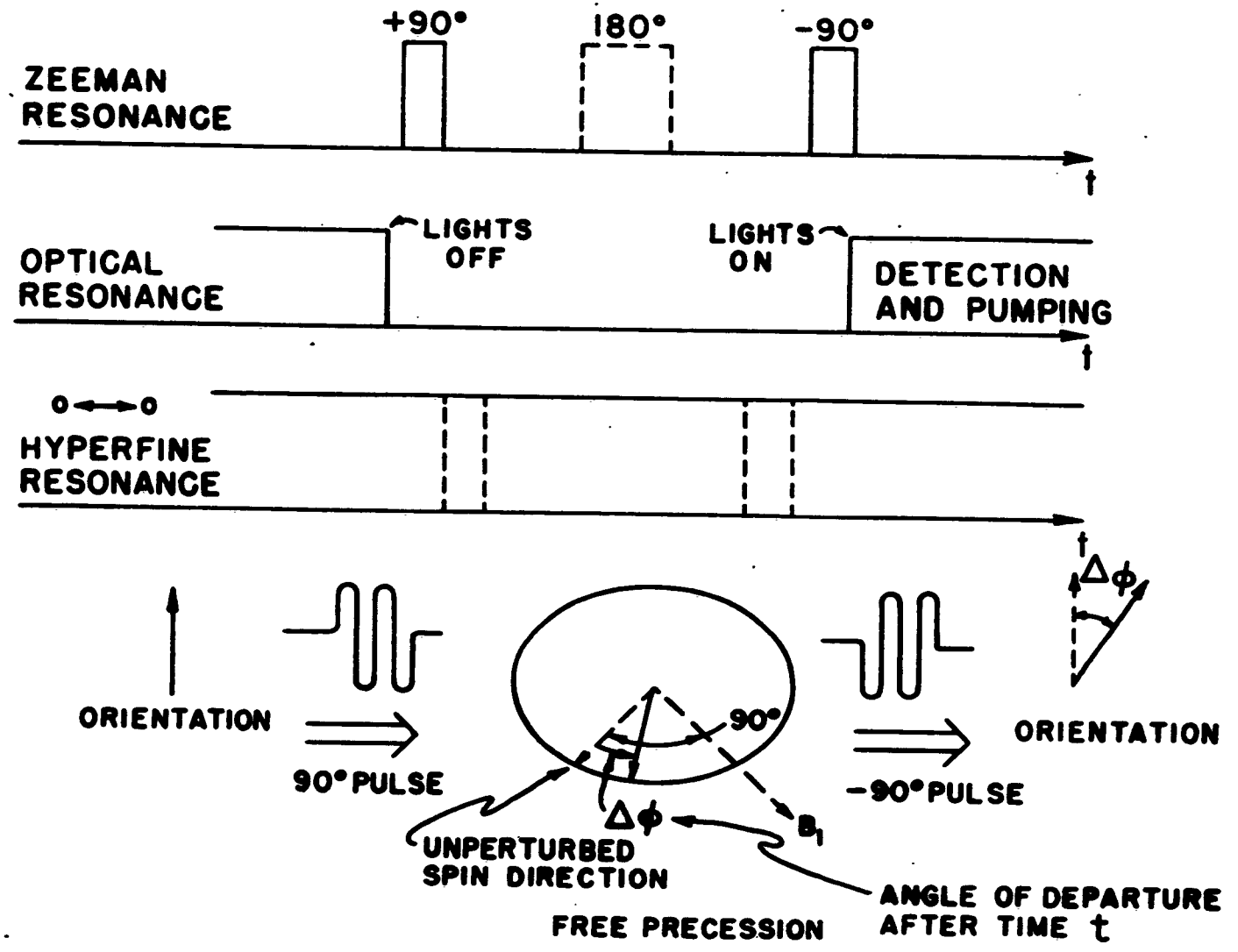

PULSE SEQUENCE FOR PHASE DESTRUCTIVE DETECTION

FIG. 4

The phase angle θ at which the first 90° pulse occurs will change from repetition to repetition of the double pulse sequence unless there is a definite harmonic relation between the period T_e of the external disturbance and the repetition period T_r. If $T_r = a T_e$ then the phase advance $\Delta\theta$ per repetition time is

$$\Delta\theta = 2\pi \{a - [a]\} \tag{21}$$

where $[a]$ denotes the greatest integer less than a. Regarded as a function of time, to be sampled every T_r seconds, one has

$$\theta = \frac{a - [a]}{T_r} 2\pi t = \omega' t \tag{22}$$

which defines a "reduced beat frequency," ω', between the magnetic field frequency T_e^{-1} and the repetition frequency T_r^{-1}.

The time variation of the optical transmission then represents a situation similar to that of frequency modulation. The frequencies which appear are given by taking the real part of[55]

$$e^{iA\cos(\theta+\alpha)} = \sum_{n=-\infty}^{\infty} (i)^n J_n(A)\, e^{in(\theta+\alpha)}$$

$$= J_0(A) + 2\sum_{n=1}^{\infty} (i)^n J_n(A) \cos n(\theta+\alpha) \tag{23}$$

where the $J_n(A)$ are the Bessel functions of the first kind of order n and use has been made of the relation

$$J_{-n}(A) = (-1)^n J_n(A)$$

Thus one obtains

$$f_{(t)} \propto J_0(A) + 2\sum_{n=1}^{\infty} (-1)^n J_{2n}(A) \cos 2n(\omega' t + \alpha) \qquad (24)$$

As the amplitude A, which depends on the strength of the time varying magnetic field and on the interval τ between 90° pulses, is increased, many frequencies can contribute, giving a very complicated response. It should be noted that only even harmonics of the reduced beat frequency ω' occur.

Experimental evidence for this complicated behavior as a function of τ is given in Section IV A.

D. Hyperfine Resonance Between $m_F = 0$ States

1. Contact Interaction Term

Because of the spherical symmetry of S-states one would not at first expect to see any splitting produced by the interaction between the magnetic moments of the electron and the nucleus, for which the interaction Hamiltonian is

$$\underline{H} = \frac{1}{r^3}\left(\vec{\mu}_e \cdot \vec{\mu}_N - 3\vec{\mu}_e \cdot \vec{r}\, \vec{\mu}_N \cdot \vec{r}\right) \qquad (1)$$

However, an additional term must be added to this Hamiltonian, the so-called contact interaction term,

$$\underline{H}_{Contact} = -\frac{8\pi}{3} \vec{\mu}_e \cdot \vec{\mu}_N\, \delta^{(3)}(\vec{r}) \qquad (2)$$

and it is this which contributes the magnetic hyperfine splitting in S states, for which the wave function does not vanish at the origin:

$$(\Delta E)_{HF} = -\frac{8\pi}{3} \vec{\mu}_e \cdot \vec{\mu}_N\, |\psi(0)|^2 \qquad (3)$$

This term was derived by Fermi[56] from the Dirac equation and was long thought to be of relativistic origin although approximate semi-classical arguments could be used to derive its value.[57] Recently Ferrell[58] has given completely classical arguments to show that it must appear whenever there is a discrete magnetic moment embedded in a continuous distribution of magnetization.

The dependence of the ground state hyperfine energy levels of rubidium 87 on an external magnetic field is linear except for the $m_F = 0$ substates, for which it is quadratic. The $0 \leftrightarrow 0$ transition is thus of particular interest since the frequency is given by

$$\frac{\nu - \nu_0}{\nu_0} = 0.84 \times 10^{-7} B_0^2 \qquad (4)$$

making it very insensitive to field inhomogeneities.

2. Coupled Equations and Approximate Solution in Terms of a Unitary Transformation

The interaction Hamiltonian $\underset{\sim}{H_{int}}$ is

$$\underset{\sim}{H_{int}} = -(\gamma_J \underset{\sim}{\vec{J}} + \gamma_I \underset{\sim}{I}) \cdot \vec{B} \cos \omega_0 (t - \tfrac{z}{c}) \qquad (5)$$

where

$\underset{\sim}{J}$ = electron angular momentum operator

γ_I = nuclear gyromagnetic ratio = $g_I \mu_N / \hbar$

μ_N = nuclear magneton

$\underset{\sim}{\vec{I}}$ = nuclear spin angular momentum operator

$\vec{B}$ = amplitude of magnetic field in the incident plane wave

ω_0 = hyperfine resonant angular frequency

In order for this to connect (2,0) and (1,0) $\vec{B}$ must be along the axis of quantization, which is chosen to be the z-axis. Then the interaction matrix element is

$$\left(2,0 \mid \underline{H}_{int} \mid 1,0\right) = -\tfrac{1}{2}\left(g_J \mu_0 - g_F \mu_N\right) B \cos \omega_0 \left(t - \tfrac{x}{c}\right) \quad (6)$$

The Schrödinger equation then yields the equations for the coefficients of states (2,0) and (1,0)

$$\begin{aligned} i\hbar\, \dot{a}_0^2 &= -E\, a_0^1 + b \cos(\omega_0 t + \delta)\, a_0^2 \\ i\hbar\, \dot{a}_0^1 &= E\, a_0^2 + b \cos(\omega_0 t + \delta)\, a_0^1 \end{aligned} \quad (7)$$

where a constant has been added to the total Hamiltonian to make the energy of state (2,0) equal to + E and the energy of (1,0) equal to - E. Also the abbreviations

$$\begin{aligned} b &= -\tfrac{1}{2}\left(g_J \mu_0 - g_F \mu_N\right) B \\ \delta &= -\omega_0 x/c \end{aligned} \quad (8)$$

have been introduced. (This phase angle δ does not appear in the diagonal elements of the ground state density matrix describing the absorption).

In spite of their seeming simplicity equations (7) cannot be solved without resorting to expansion in series or to other approximation procedures. They are of the same form as the equations describing a spin $\frac{1}{2}$ system subjected to an oscillating magnetic field at right angles to a static magnetic field. For such a system one may neglect the component of the oscillating field rotating oppositely to the Larmor precession. A similar approximation can be used here, expanding the cosine into a sum

of exponentials and neglecting the "oppositely rotating" one. With this approximation the resonant solution for $\omega_0 = 2E/\hbar$ is conveniently written as

$$\begin{bmatrix} a_0'(t) \\ a_0^2(t) \end{bmatrix} = \underline{\underline{U}}_{HF}(t - t_0) \begin{bmatrix} a_0'(t_0) \\ a_0^2(t_0) \end{bmatrix} \tag{9}$$

where the unitary matrix $\underline{\underline{U}}_{HF}(t-t_0)$ is given by

$$\begin{pmatrix} \cos\eta\, e^{\frac{i}{\hbar}E(t-t_0)} & \sin\eta\, e^{i(\delta-\frac{\pi}{2})} e^{\frac{i}{\hbar}2Et_0} e^{\frac{i}{\hbar}E(t-t_0)} \\ \sin\eta\, e^{-i(\delta+\frac{\pi}{2})} e^{-\frac{i}{\hbar}2Et_0} e^{-\frac{i}{\hbar}E(t-t_0)} & \cos\eta\, e^{-\frac{i}{\hbar}E(t-t_0)} \end{pmatrix} \tag{10}$$

$$(\eta = b(t-t_0)/2\hbar)$$

A better approximation to the solution of equations (7) has been obtained by A.F. Stevenson[59] by expanding in powers of $b/2E$. To first order in $b/2E$ the amplitudes receive corrections of order $1/4$ ($b/2E$), while the calculated angular frequency that gives the maximum transition probability from one state to the other is corrected according to

$$\omega_r = \omega_0 \left(1 + \frac{1}{4}(b/2E)^2\right) \tag{11}$$

This result was first obtained by Bloch and Siegert.[60]

3. Perturbations of the Resonance

Several sources of line breadth and the method of reducing the Doppler breadth have been discussed elsewhere[61] and will not be elaborated here. During the course of the present work several groups have obtained information on the shifts caused by collisions with various buffer gases, including both positive and negative variations with pressure increases.[62]

The presence of optical radiation for the purposes of pumping and detection can be a source of both line broadening and of a shift in the hyperfine resonance. If the average rates of interactions with photons for the (2,0) and (1,0) states are $\Gamma_{2,0}$ and $\Gamma_{1,0}$ then by the Weisskopf-Wigner relations[63] the breadth will be

$$\Delta\nu = \Gamma_{2,0} + \Gamma_{1,0} \tag{12}$$

(Such average interaction rates can be obtained from the optical pumping theory given in Section II A)

A careful treatment of the interaction of the optical radiation reveals the possibility of a shift ΔE in an energy level due to this interaction[64]:

$$\Delta E = (\ ) \mathcal{P} \int \frac{|(i|\vec{P}\cdot\vec{A}|f)|^2}{k_0 - k} \rho_k \, d\Omega \, dk \tag{13}$$

Here ρ_k is the density of optical radiation oscillators having wave number k and k_0 is the value of k at the central optical frequency. $\mathcal{P}$ denotes principal value integral.

A similar expression will hold for each of the hyperfine levels. If there is a lack of symmetry in the distribution ρ_k about k_0 this term can be non-zero. The possible existence of such shifts was recognized when this work was begun and was estimated to be very small. Recent work by Barrat and Cohen-Tannoudji[65] predicted that under some experimental conditions they could be observed and succeeded in doing so. This effect serves to explain frequency shifts as a function of light intensity observed by Arditi[66] and also by Bender.[67]

The desirability of eliminating the optical transitions as a source of disturbance for the hyperfine resonance is apparent from this discussion. The phase destructive method makes it possible to interrupt the light beam and to detect the microwave resonance only when the optical radiation is not present. This is discussed further in Section II E and in Section III. Other methods of detection can also be devised which involve the pulsing on and off of the light source to eliminate these undesirable effects, as will be discussed in Section V.

E. Phase Destruction Method

1. Description

A non-mathematical discussion was given in Section I. In this section calculations will be carried out using the theory developed for this purpose.

An experimental program of allowing the several oscillatory electromagnetic fields, at optical, microwave, and radio frequencies, to act separately is convenient, as illustrated in Figure 4. It is fortunate that such a program enables calculations to be performed much more readily than if the several different frequency fields acted simultaneously.

The particular property of the density matrix to be exploited is that one may regard a given density matrix which contains all of the information on the system as capable of decomposition into a sum of density matrices in arbitrary ways.[68] Some one of these ways may be especially useful in some computations. Here the useful decomposition is into the density matrices corresponding to pure

(F, m_F) states with statistical weights given by the diagonal elements of the original density matrix, obtained by the optical pumping process described in Section II A. One is clearly not allowed to think of atoms being definitely in single pure (F,m_F) states for they could be in pure superposition states formed from the (F,m_F) states, but if the density matrix is diagonal, such an interpretation is allowable. It is in accord with the usual naive way of considering the populations of atomic states and constitutes a justification of that procedure.

The unitary matrices given in the preceding sections for the action of the coherent microwave and rf fields can be used to describe the time development of the pure (F,m_F) states of the atom. The wave functions resulting from such successive unitary transformations can be used to form density matrices which can be combined with the statistical weights from the original diagonal density matrix to yield the final density matrix.

2. Change in Density Matrices Produced by Pulse Sequence

The calculation as described above is straight forward but tedious and will not be given in detail. The wave function for the result of operating successively with the unitary operators is

$$\underset{\sim}{\psi}_{Final} = \underset{\sim}{U}(-90^\circ)\ \underset{\sim}{U}_{HF}(\gamma)\ \underset{\sim}{U}(+90^\circ)\ \underset{\sim}{\psi}_{Initial} \qquad (1)$$

It is convenient to use a column vector notation in terms of the

coefficients of the wave functions. For the initial state $(F, m_F) = (2, +2)$ one obtains

$$\underline{\underline{U}}(90^\circ)\,\underline{\psi}_{initial} = \begin{bmatrix} 0 \\ 0 \\ 0 \\ \frac{1}{4}\, e^{i2\omega t} \\ -\frac{1}{2}\, e^{i\omega t} \\ \frac{\sqrt{3}}{2\sqrt{2}} \\ -\frac{1}{2}\, e^{-i\omega t} \\ \frac{1}{4}\, e^{-i2\omega t} \end{bmatrix} \tag{2}$$

$$\underline{\underline{U}}_{HF}\,\underline{\underline{U}}(180^\circ)\,\underline{\psi}_{initial} = \begin{bmatrix} 0 \\ \frac{\sqrt{3}}{2\sqrt{2}}\, \sin\eta\, e^{-i(\delta+\frac{\pi}{2})}\, e^{-\frac{i}{\hbar}Et} \\ 0 \\ \frac{1}{4}\, e^{i2\omega t} \\ -\frac{1}{2}\, e^{i\omega t} \\ \frac{\sqrt{3}}{2\sqrt{2}}\, \cos\eta\, e^{\frac{i}{\hbar}Et} \\ -\frac{1}{2}\, e^{-i\omega t} \\ \frac{1}{4}\, e^{-i2\omega t} \end{bmatrix} \tag{3}$$

$$\underline{\underline{U}}(-90^\circ)\,\underline{\underline{U}}_{HF}(\eta)\,\underline{\underline{U}}(+90^\circ)\,\Psi_{initial} =$$

$$\begin{bmatrix}
\frac{\sqrt{3}}{4}\sin\eta\, e^{i(\delta-\frac{\pi}{2})}\, e^{-\frac{i}{\hbar}Et}\, e^{-\frac{i}{\hbar}(E+\hbar\omega)t} \\
0 \\
-\frac{\sqrt{3}}{4}\sin\eta\, e^{i(\delta-\frac{\pi}{2})}\, e^{-\frac{i}{\hbar}Et}\, e^{-\frac{i}{\hbar}(E-\hbar\omega)t} \\
\frac{3}{8}(1-\cos\eta)\, e^{-\frac{i}{\hbar}(E-2\hbar\omega)t} \\
0 \\
\frac{\sqrt{3}}{4\sqrt{2}}(1-\cos\eta)\, e^{-\frac{i}{\hbar}Et} \\
0 \\
\frac{5}{8}\left(1+\frac{3}{5}\cos\eta\right) e^{-\frac{i}{\hbar}(E+2\hbar\omega)t}
\end{bmatrix} \qquad (4)$$

The diagonal elements of the final density matrix are

$$\begin{pmatrix}
\frac{3}{16}\sin^2\eta & & & & & & \\
& 0 & & & & & \\
& & \frac{3}{16}\sin^2\eta & & & & \\
& & & \frac{9}{64}(1-\cos\eta)^2 & & & \\
& & & & 0 & & \\
& & & & & \frac{3}{32}(1-\cos\eta)^2 & \\
& & & & & & 0 \\
& & & & & & \frac{25}{64}\left(1+\frac{3}{5}\cos\eta\right)^2
\end{pmatrix} \qquad (5)$$

One can perform similar calculations for each state (F, m_F) as the initial state. The final density matrix is the same as the initial one for the initial states (1,0), (2,-1) and (2,1) since the action of $\underline{\underline{U}}$ (90°) lends to a coefficient of zero for the (1,0) and (2,0) states so that $\underline{\underline{U}}_{HF}(\eta)$ has no effect and $\underline{\underline{U}}(-90^\circ)\,\underline{\underline{U}}_{HF}(\eta)\,\underline{\underline{U}}(90^\circ) = \underline{\underline{II}}$

3. Change in Effective Oscillator Strengths

Using the equation

$$f_{eff} = f_0 \, Tr \, \underline{\rho} \, \underline{A}$$

one can calculate this as a function of η. For the operator $\underline{A}$ corresponding to σ^+ radiation directed along the axis of quantization the result is

$$\begin{aligned} D_1: \quad & f_{eff}^{(\sigma^+)} = \tfrac{3}{4} f_0 [1 - \cos\eta] \\ D_2: \quad & f_{eff}^{(\sigma^+)} = 3 \cdot \tfrac{3}{4} f_0 \left[1 + \tfrac{1}{3}\cos\eta\right] \end{aligned} \tag{6}$$

for the density matrix corresponding to the initial state (2,+2). Similar calculations for final density matrices for other states can be made. When these are combined using as statistical weights the diagonal elements of the initial density matrix, the result for the change $\Delta f = f_{final} - f_{initial}$ in the effective oscillator strength is

$$\Delta f_{D_1}^{(\sigma^+)} = f_0 \left[\tfrac{1}{2}(\rho_{33} - \rho_{11}) + \tfrac{3}{4}(\rho_{44} - \rho_{88})\right](\cos\eta - 1)$$

$$\Delta f_{D_2}^{(\sigma^+)} = - \Delta f_{D_1}^{(\sigma^+)} \tag{7}$$

The ρ_{ii} are the initial populations of the states.

The effect of the resonance for σ^- radiation can be obtained by an exchange in the coefficients

$$\begin{aligned} \rho_{11} &\rightleftarrows \rho_{33} \\ \rho_{44} &\rightleftarrows \rho_{88} \end{aligned} \tag{8}$$

and is seen to give just the negative of the above values. It seems remarkable that only the differences in initial populations between the states (1,-1) and (1,1) and between the states (2,-2) and (2,2) contribute to the final result.

Such equal and opposite intensity changes could enable the use of a bridge type of detection to balance out fluctuations in the light source.

The maximum change is found for $\eta = \pi$, corresponding to a change in sign of the (2,0) state with respect to its partner states of total angular momentum F = 2 in the superposition state wave function following the 90° pulse. The magnitude of the change in absorption resulting from this change in the effective oscillator strength is clearly of the same magnitude as that obtained by inverting the oriented populations by means of a 180° pulse which is (See Section II B 4)

$$\Delta f_{D_1}^{(\sigma+)} = f_0 \left[(\rho_{11} - \rho_{33}) + 2(\rho_{88} - \rho_{44}) + (\rho_{77} - \rho_{55}) \right]$$
$$\Delta f_{D_2}^{(\sigma+)} = -\Delta f_{D_1}^{(\sigma+)} \qquad (9)$$

It should be noted that there need be no energy absorbed from the microwave radiation serving to mix the (2,0) and (1,0) states since only a phase change and not a change in the amplitude of these states need be established.

Other modes of operation than the pulsed microwave one are possible in which the microwaves are present continuously. They are only effective between the 90° pulses however, and a similar theoretical description applies.

The effect of relaxation, which has been neglected in the foregoing analysis, will be to degrade the signal from that

calculated. As one increases the interval τ between the two 90° pulses the signal will then become weaker, but since it is so strong one can proceed quite far in increasing this time interval τ . The line width for the hyperfine resonance is then expected to be $\Delta\nu \sim (2\pi\tau)^{-1}$ If the hyperfine excitation is applied in two coherently phased pulses one can narrow the resonance by a factor of 2 as is accomplished in the Ramsey method of separated oscillatory fields in atomic beam work.(69) In addition, this two coherent pulse method should allow one to narrow artificially the resonance beyond that determined by the T_2 relaxation time, by selecting just those atoms which live a time τ , which can be made greater than T_2 by this sensitive means of detection, as discussed in Appendix C.

There is also the possibility of applying quite complicated pulse sequences to study their effects on atoms in a way which would be quite involved for atomic beams.

III. EXPERIMENTAL METHODS AND INSTRUMENTATION

In this section the details of the apparatus used are given, along with some design considerations. The difficulties encountered with some approaches that were not successful are discussed. Separate parts are devoted to a description of the source of rubidium resonance radiation; to the making of gas cells, with considerable attention to the technique of preparing walls by treatment with alkylchlorosilanes; to the rf pulse circuitry for the Zeeman resonances; to the hyperfine microwave frequency stabilization system; and to the electro-optical pumping and detection system.

Figure 5 shows an early view of the optical system and magnetic field and gas cell arrangement, while Figure 6 shows the changes made when using the shielded solenoid. Figure 7 shows the microwave frequency stabilization system. The electronic apparatus used for the pulsed resonances is shown in Figure 8.

Diagram 1 presents a schematic block diagram of the major parts of the experiment and their relations to each other.

A. Light Source

1. Spectroscopic Line Structure and Line Breadth

The structure of the two D lines resulting from the fine structure splitting in the 5 p state of rubidium are shown in Figures 9 (a) and 9 (b) which display the hyperfine splitting caused by the nuclear spin I for the ground state and for the excited states.($I = 3/2$ for rubidium 87; $I = 5/2$ for rubidium 85) The figures also show the ten hyperfine components of the optical transitions

FIG. 5 VIEW OF EARLY OPTICAL AND MAGNETIC FIELD ARRANGEMENT

FIG. 6 VIEW OF OPTICAL SYSTEM AND SHIELDED SOLENOID.

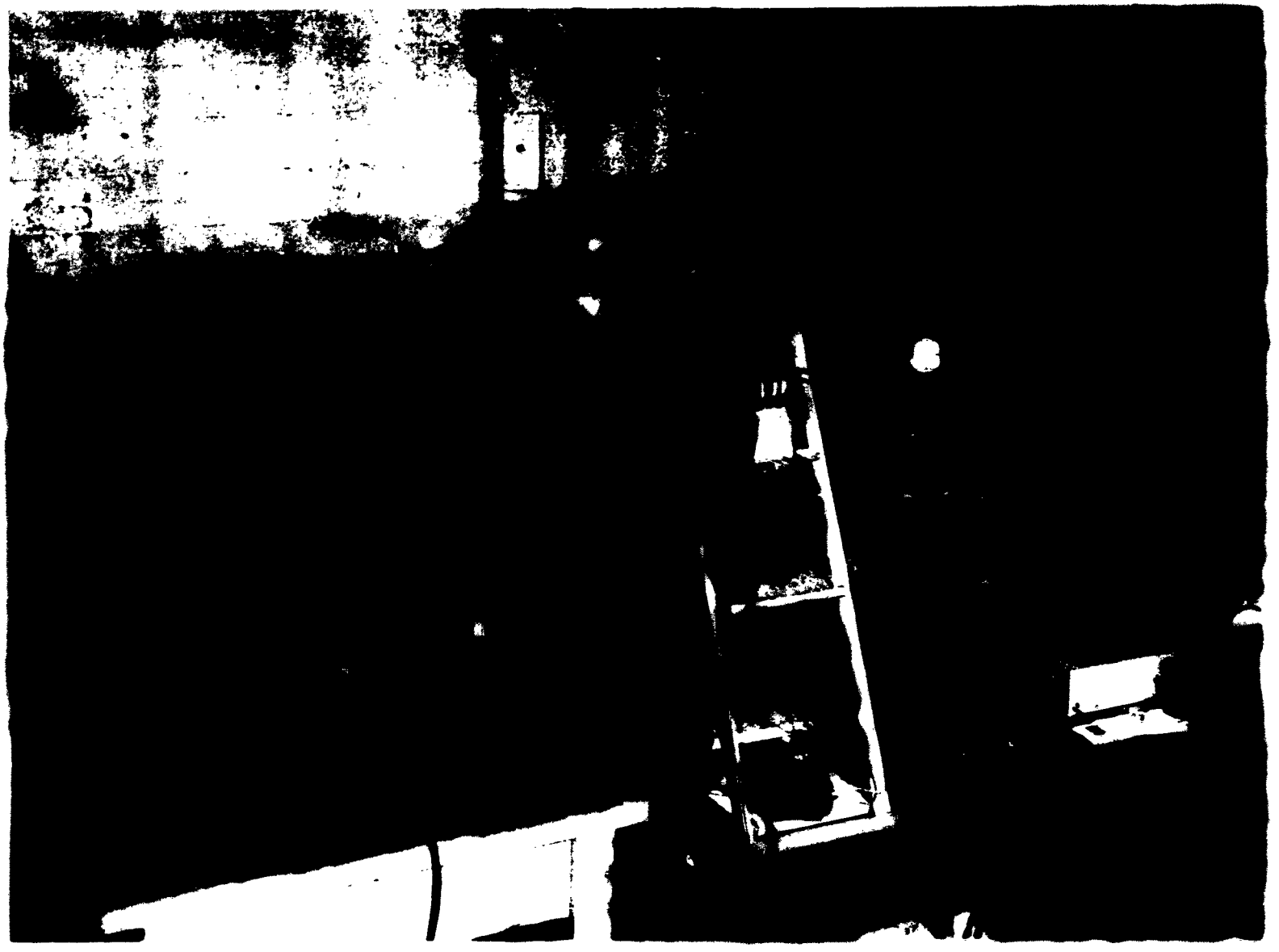

FIG. 7 VIEW OF MICROWAVE FREQUENCY STABILIZATION SYSTEM.

FIG. 8 VIEW OF ELECTRONIC APPARATUS

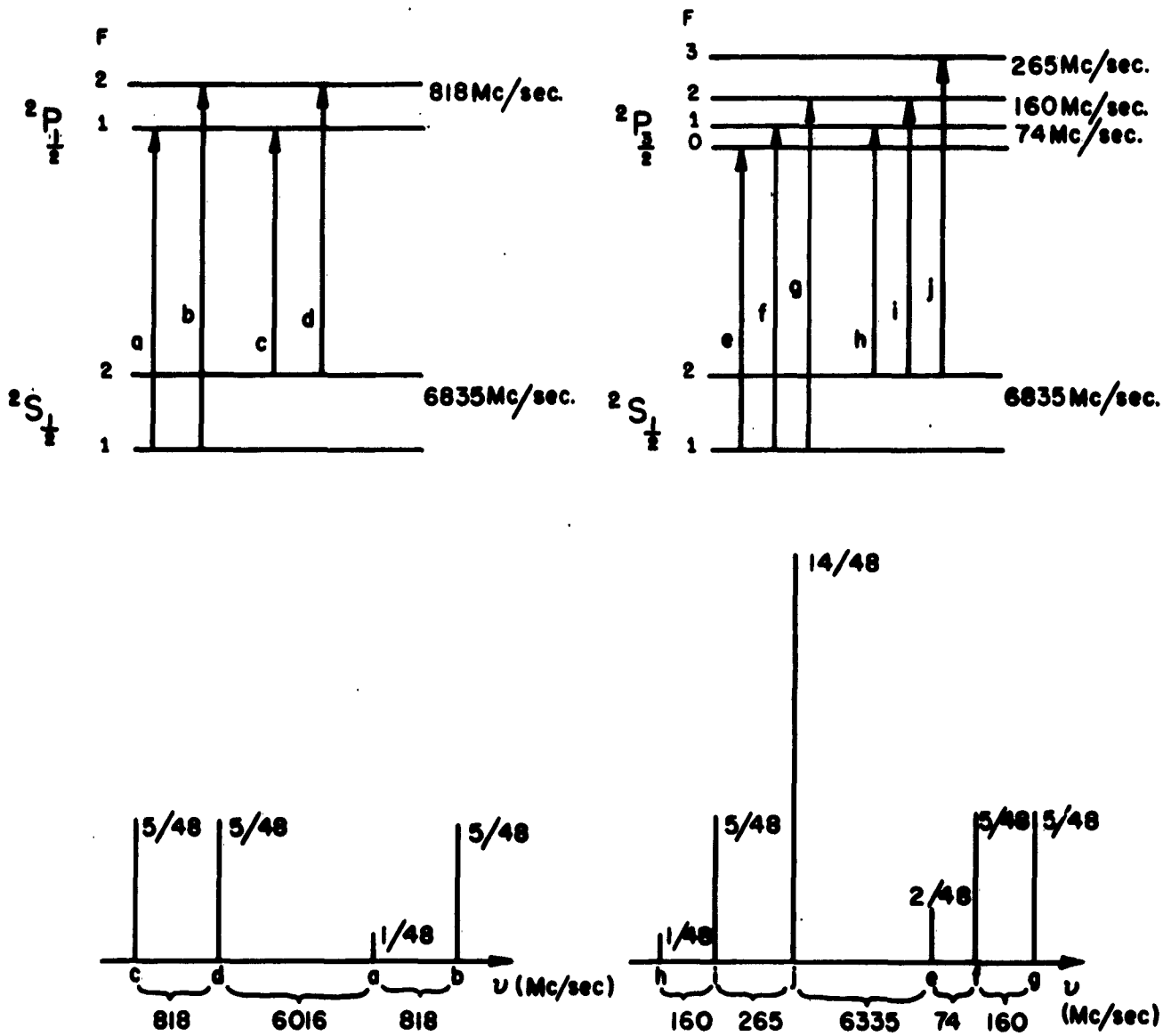

HYPERFINE STRUCTURE AND OSCILLATOR STRENGTHS FOR Rb^{87}

FIG. 9a

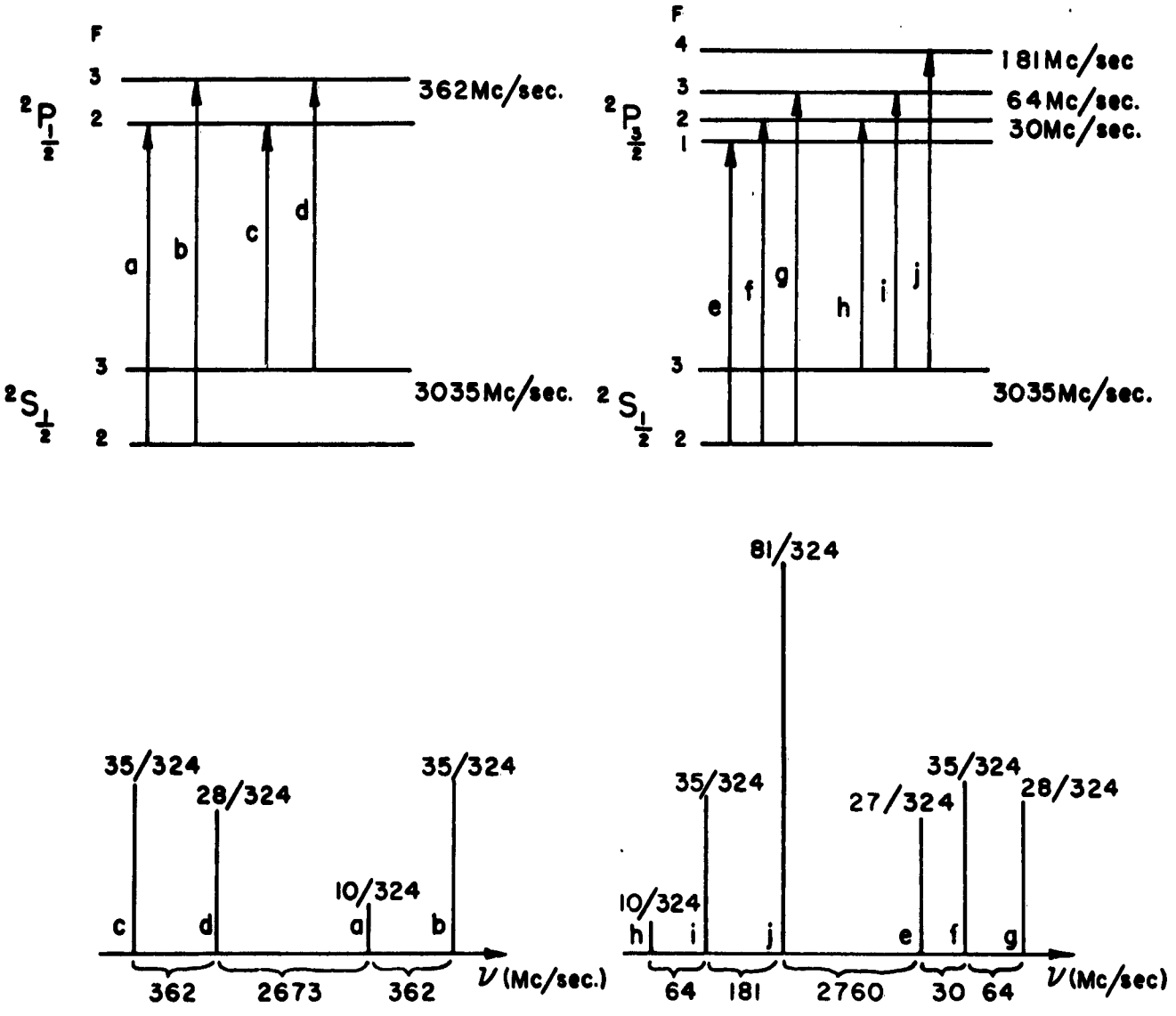

HYPERFINE STRUCTURE AND OSCILLATOR STRENGTHS FOR Rb^{85}

FIG. 9b

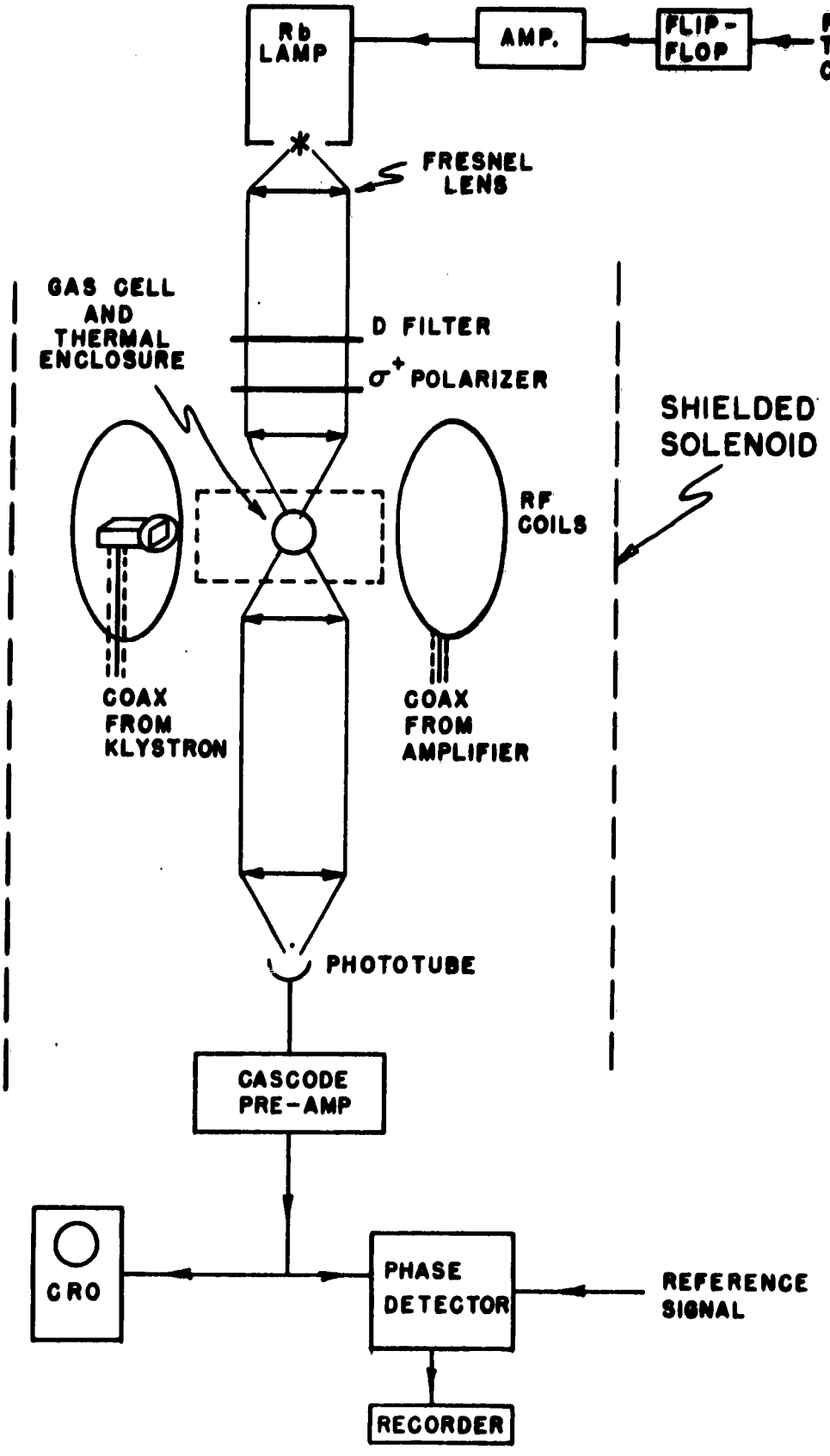

SCHEMATIC DIAGRAM OF EXPERIMENT

DIAGRAM 1 (continued overleaf)

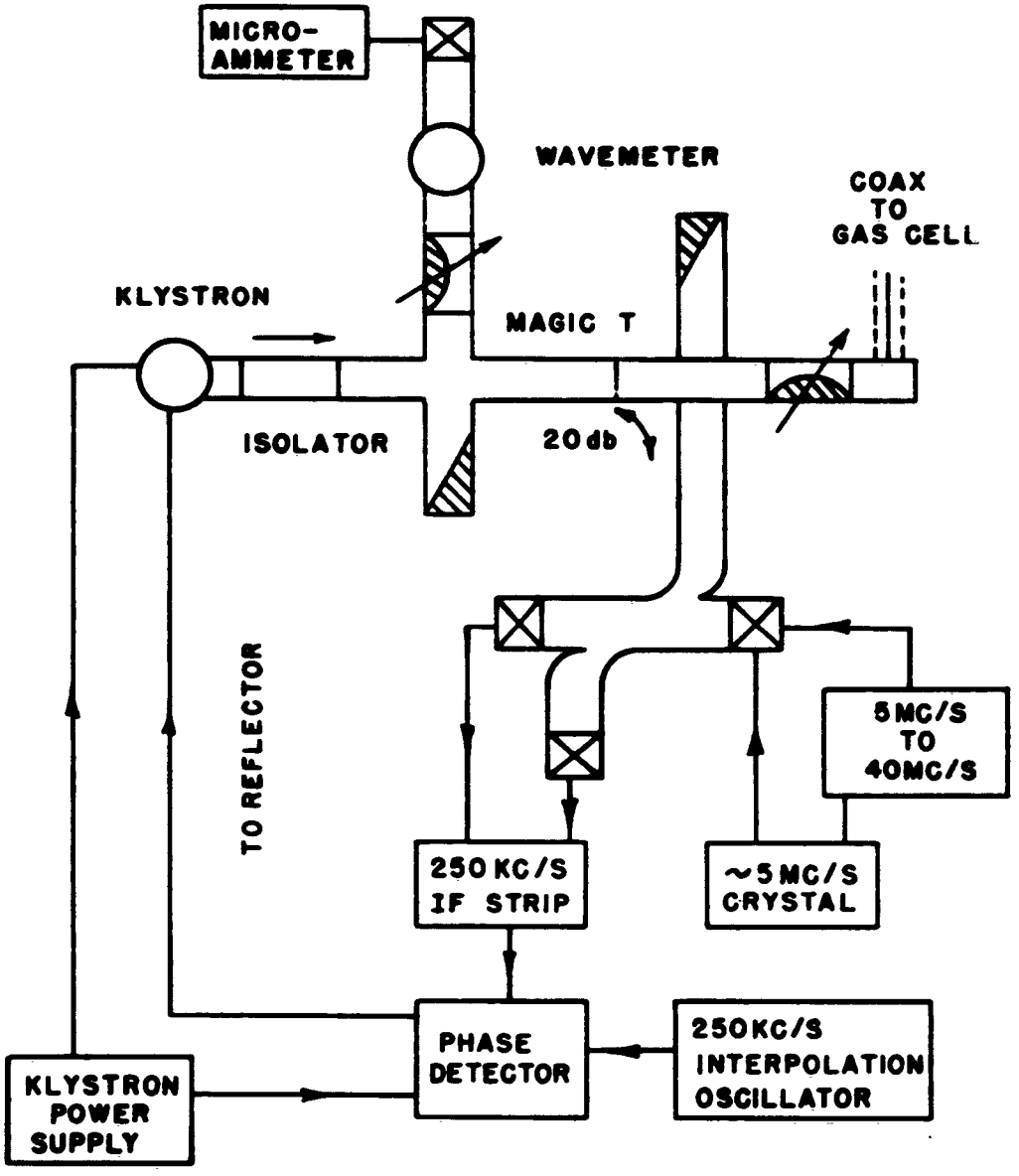

FREQUENCY STABILIZATION SYSTEM

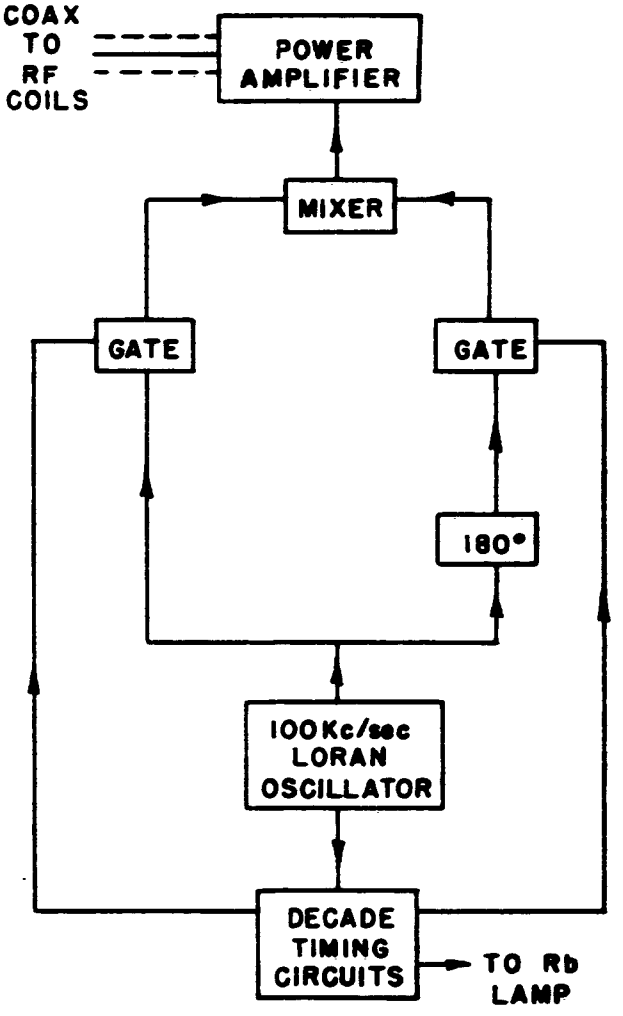

RF PULSE SYSTEM

DIAGRAM 1 (continued)

along with their oscillator strengths. The excited state hyperfine splittings are those determined by Rabi and Senitzky[70] using optical excitation in atomic beams.

The amount of overlap among the hyperfine components can be determined from the Doppler width. This is 520 Mc/sec for rubidium at temperature of 300° C. The optical radiation from an electrically excited discharge in rubidium vapor has a spectral breadth at least 3-4 times the room temperature Doppler breadth,[71] and under most conditions perhaps ten times larger, due to collision broadening and self-absorption in the discharge tube. Under these conditions the overlap is considerable and results in each of the hyperfine components in D_1 or D_2 having the same peak intensities.

Naturally occuring rubidium is composed of 72 % Rb^{85} and 28% Rb^{87}, so the Rb^{85} structure will dominate. However, by exciting a discharge in pure Rb^{87} the hyperfine structure could be resolved using a large concave grating spectrograph.

Reduction of the peak intensity at the center of the broadened line by self-absorption can be a serious problem, for this is the spectral region in which the cooler alkali vapor in the optical pumping cell absorbs and reradiates the radiation. Methods of avoiding this are discussed below.

2. Types of Lamps and Electrical Excitations of the Discharge

In the initial work commercial rubidium vapor lamps made by Phillips and by Osram were used. These consist of a discharge tube using argon as a carrier gas containing similar electrodes at each end which is enclosed in a non-evacuated glass

envelope for purposes of thermal stabilization. They are intended to be excited by several hundred volts at 60 cycles, in series with a ballast resistor. Such excitation gives 120 cycle pulsations in the light output which would be undesirable for the type of pulse work used in the present research. Accordingly other excitation methods were tried on these lamps: rf, microwave, and dc.

Some difficulty was encountered in coupling rf energy at 14 Mc into the electrode structure of the Osram lamp, although if the lamp was started independently and warmed up, for example by microwave excitation, the rf energy served to maintain the discharge steadily but not as brightly as one might desire.

Microwave excitation using a Raytheon Microtherm unit consisting of a magnetron oscillator at 2450 Mc/sec coupled to a dipole antenna and reflector could give quite an intense discharge. However, the power supply in the unit had a large 60 cycle modulation which affected the power output. Although this could have been removed by suitable filters in the power supply, this was not done.

Excitation using direct current was found to be quite satisfactory. An inductance of $\sim$ 10 henries having a resistance of about 1 ohm was placed in series with an Osram discharge tube and fed from a rotating d-c generator with low commutator noise. The voltage was remotely controllable by means of a field rheostat for starting the lamp. Without the inductance, instabilities leading to relaxation oscillations would develop in the discharge. The large inductance was considerably more effective in suppressing such oscillations than a transistor regulated constant current source

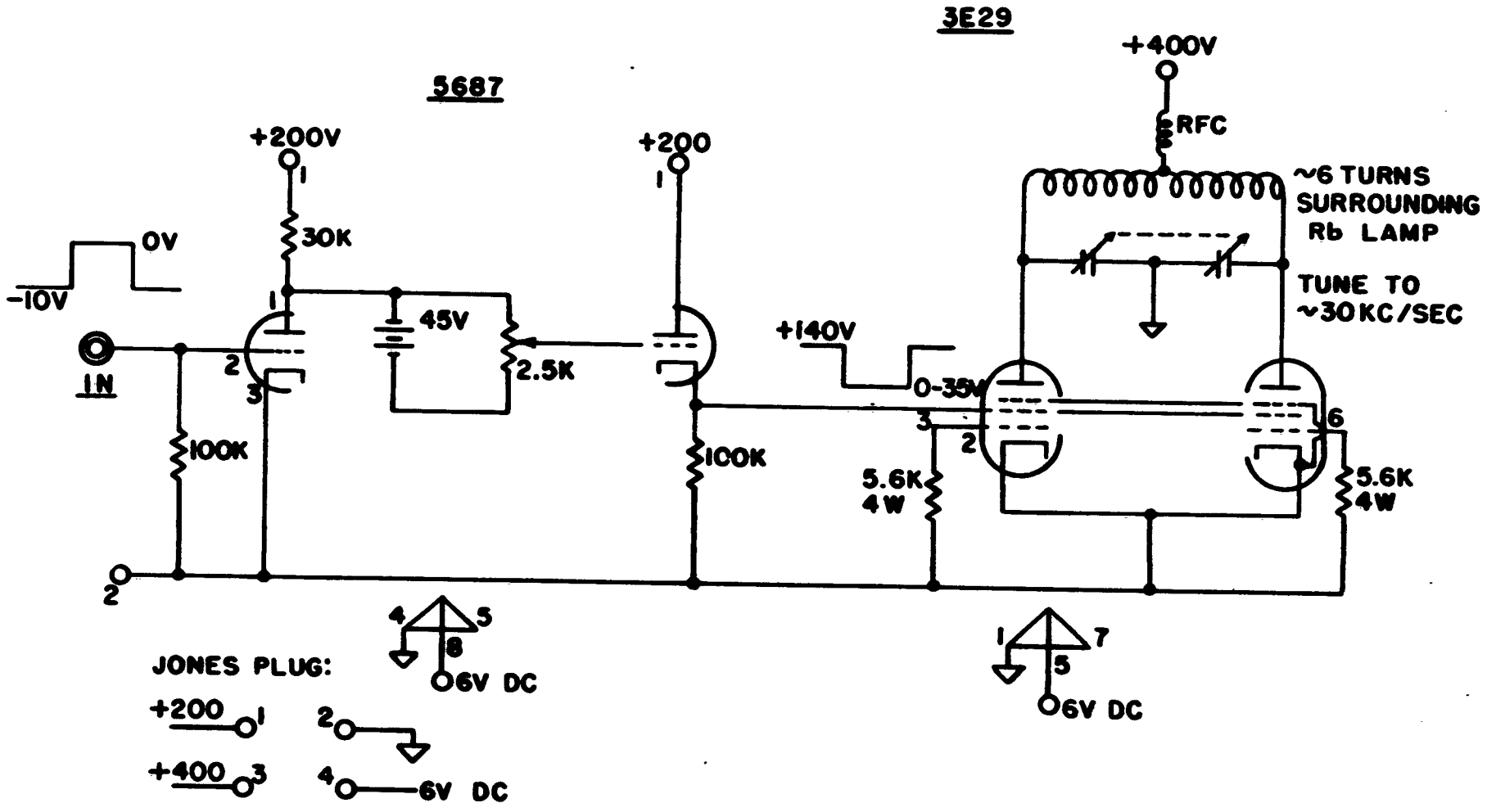

PULSED RF OSCILLATOR FOR RUBIDIUM LAMP EXCITATION

DIAGRAM 2

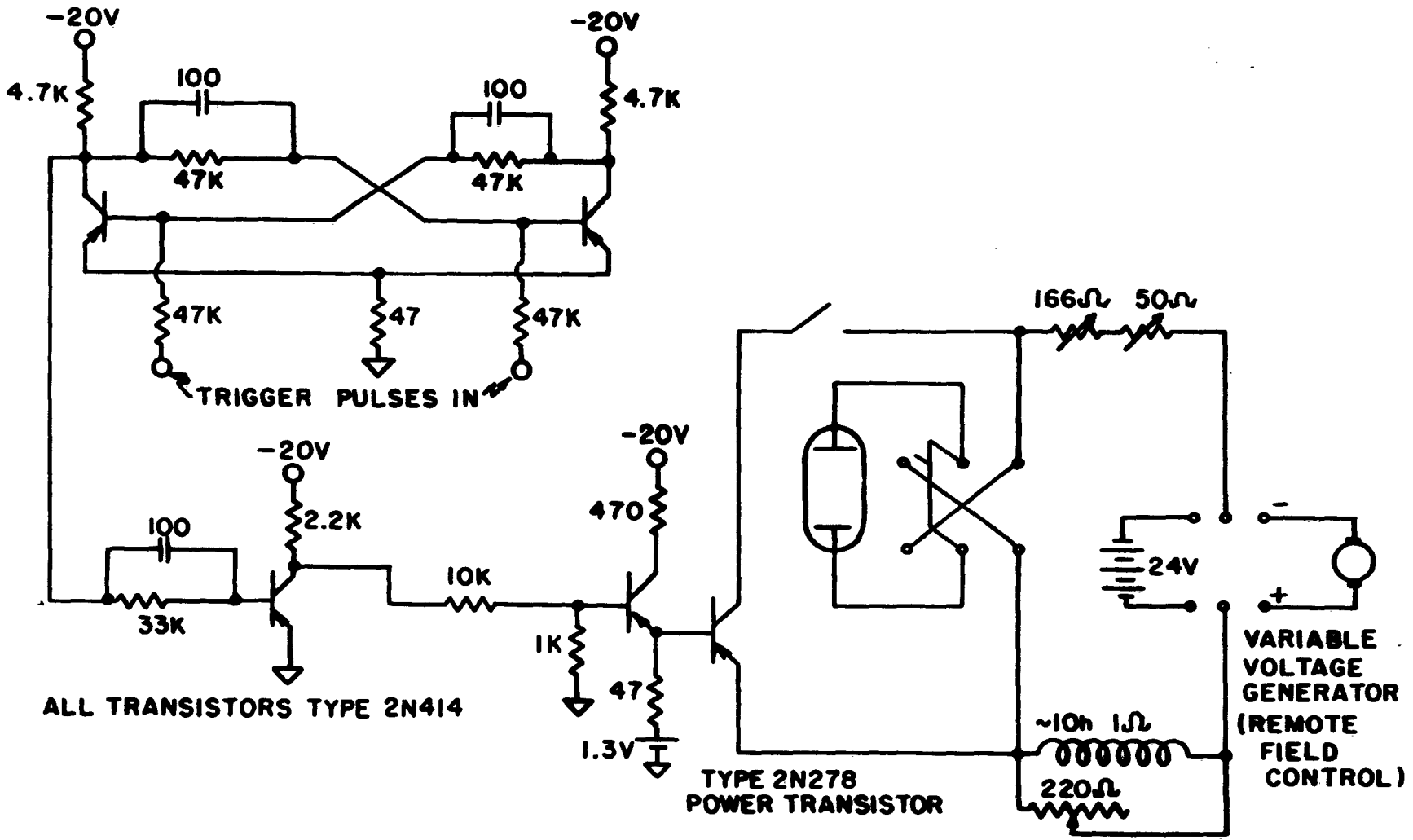

DC RUBIDIUM LAMP EXCITATION AND TRANSISTOR SHORTING SWITCH

DIAGRAM 3

especially constructed for the purpose. The probable reason for this is that the voltage swings available from the stored energy in the inductance were not limited by the voltage source as in the case of the transistor circuit. With time the generator became more noisy and it was convenient to transfer operation after starting to five 6 volt storage cells in series, by rapid manual switching. A reversing switch was incorporated to change the polarity of the lamp when being excited by dc to allow both electrodes to age equally. The circuit is given in Diagram 3.

Some laboratory made electrodeless lamps were also tried. One geometry utilized a flat strip envelope about one inch by 1/8" internal dimensions terminated in circular cylindrical chambers about which cylindrical electrodes were placed to enable excitation by capacitive coupling. This geometry was chosen to minimize self absorption by letting the depth of the discharge source be on the order of the "mean free path" for the emitted photons. The carrier gas was neon at a few mm Hg pressure, and the excitation source was an amateur radio transmitter at 25 Mc/sec kindly lent by R.A. Naumann. Instabilities developed in the discharge, however, the most serious being changes in the mode of the discharge every several seconds.

The most successful lamp was one constructed by C. Varnum at the suggestion of T.R. Carver and kindly lent by them. It consisted of a circular flat button enclosure having a slightly concave front surface, about 1 ½" in diameter and ¼" deep and used a few mm of argon on the carrier gas. It was placed in the tank coil of an rf oscillator having a frequency

of about 30 Mc/sec and excited by a magnetic type of coupling, the electric field being produced by the oscillating rf magnetic field. About 30 watts could be coupled into the discharge. The diagram for this circuit is given as Diagram 2. When run with dc on the filaments it was exceptionally stable and bright. The large area enabled it to be imaged on the central part of the gas cell with a one to one magnification. It may be seen on top of the Dexion structure in Figure 6.

During the later stages of the investigation a rubidium lamp made by the Varian Associates for use with their magnetometers and atomic clocks was acquired. This lamp was the result of much experimentation on temperature balance and excitation rates and has been described in the literature.(72) The power consumed by the lamp is only a few watts. It worked adequately well but was about ten times less effective in producing orientation as measured by 180° pulses (See Section III C below) than the large area high power lamp described immediately above.

3. Questions of Self Reversal and Intensity

Examination of the spectral output of lamps under several types of excitation during the early stages of the investigation by means of a large 3" concave grating spectrograph emphasized the ease with which the D lines could be self reversed. This happened whenever too much power was fed into the discharge to be removed by the cooling, resulting in the lamp running at too high a temperature. The practical remedy was simply to increase the efficiency of the cooling.

Two methods of cooling were utilized: blowing air by the discharge tube from the building pressure line; and immersing the tube in a bath of silicone oil which was itself cooled by cold water flowing through copper tubes immersed in the oil. When cooling the Osram lamps it was found expedient to remove the outer jacket. Care must be taken not to cool too much for the vapor pressure of the rubidium depends on the temperature and one can lose intensity in the rubidium radiation.

When using the silicone oil bath surrounding the discharge tube (silicone oil is quite transparent in the near infra-red[73]) a good temperature was found to be about 140° C. Figure 17 shows a picture of such a lamp. An increase in emitted radiation by approximately a factor of 2 was obtained by surrounding the envelope containing the silicone oil with a reflecting aluminium foil layer opposite the aperture for the emmission of the light. The entire envelope was wrapped with two alternate layers of asbestos tape and aluminum foil. This was necessary in order that the energy put into the discharge raise the temperature sufficiently to yield the optimum rubidium vapor pressure.

Some years ago D.A. Jackson[74] demonstrated that it was possible to increase the intensity of radiation from discharges in alkali vapors without self-reversal if one cooled adequately while increasing the excitation current density. This was one of the motivations for the cooling employed and it was observed that the intensity increased more or less linearly up to the maximum current tried, about 2-amps (the rated current is about 0.7 amps). This represented a power input of about 30 watts.

No careful measurement was made of actual intensities, but from observations on photo currents, assuming a photon efficiency of 1/250 for an S-1 cathode at $\sim$ 8000Å, an overall photon emission rate in the D lines of about 10^{16} photon/sec-steradian was achieved from the dc excitation. The larger area of the rf excited button source described above resulted in its being more effective for orientation (measured by 180° pulses) than the dc source by about a factor of 3.

4. Methods of Pulsing the Light Source

Although mechanical interruption of a beam of light by means of a rotating wheel containing suitable apertures, or perhaps a combination of wheels rotating at different speeds to achieve a vernier effect for rapid rise and fall times, affords a means of pulsing with large solid angles of acceptance, difficulty in making rapid changes in the duty cycle and repitition rate would be experienced. An electrical method was therefore sought which would respond to the action of triggering pulses from some master timing arrangement possessing easy flexibility for adjustment during experimentation.

Mechanical shutters activated by solenoids or compressed air were soon found by calculation to require too much power for operation in times of the order of a millisecond, as was desired, given the necessary mass of such devices. Very lightweight shutters for cameras have been made by the Graflex Corp. to operate in this time range, but upon examination they proved to be ill-adapted for continuous cyclic operation as was desired.

Electro-optical shutters utilizing the bi-refringence in a solid such as potassium dehydrogen phosphate (KDP) induced by an electric field suffer from the need to use highly collimated light and thus the available photon flux for orientation and detection purposes is reduced. Also, the commercially available aperture sizes are small.

The method finally adopted was to turn the discharge in the lamp on and off. Although this produced time constants on the order of several milliseconds due to recombination effects, the speed was adequate and such operation did not promote instability in the discharge as had been initially feared.

For the dc discharge excited lamp a Delco 2N278 power transistor capable of carrying 2 amperes was placed in parallel with the lamp and used as a switch. Since the combination was fed from a very effective constant current source (the large inductance previously mentioned) the current could be transferred very cleanly back and forth between the discharge and the transistor. Some of the switching transients are shown in Figure 10. The circuits for the transistor binary and power amplifier used to drive the power transistor are shown in Diagram 3. In order that the magnetic field at the position of the gas cell resulting from the dc excitation be changed a little as possible during the switching, the power transistor, mounted on a large aluminum plate for power dissipation, was placed near the light source, as can be seen in Figure 5.

For the rf discharge excited light source using the button shaped tube and magnetic excitation described above, the pulsing was accomplished by swinging the screen grid on the 3E29

oscillator tube. The electron tube amplifier circuit enabling this to be driven from the same binary which drove the power transistor is given in Diagram 2.

This light source can be seen atop the Dexion scaffolding in Figure 6. An oscillogram of a transient is shown in Figure 10 (c).

B. Rubidium Vapor Cell Preparation and Wall Coatings

1. Glass Bulbs

These were blown from Pyrex glass by the Palmer Laboratory glassblower, Leigh Harris. The size was not critical but most were spherical with a diameter of 2 inches. For buffer gas bulbs this gives an adequately long time for diffusion to the walls for the pressures of buffer gases used (see discussion in Appendix to Reference (1)). The size of the orifice for such buffer gas cells is not critical.

For bulbs having coated walls, the size of the orifice is important since nearly complete relaxation occurs when an atom strikes the reservoir of rubidium in the tube adjoining the orifice. The following approximate calculations are relevent. The probability of an atom leaving the cell is the ratio of the orifice area to the area of the wall

$$\text{Prob. of leaving} = \frac{A_1(\text{orifice})}{A_2(\text{wall})} = \frac{1}{4}\,\frac{d_1^2}{d_2^2} \qquad (1)$$

d_1 = diameter of orifice (assumed circular)

d_2 = diameter of spherical bulb

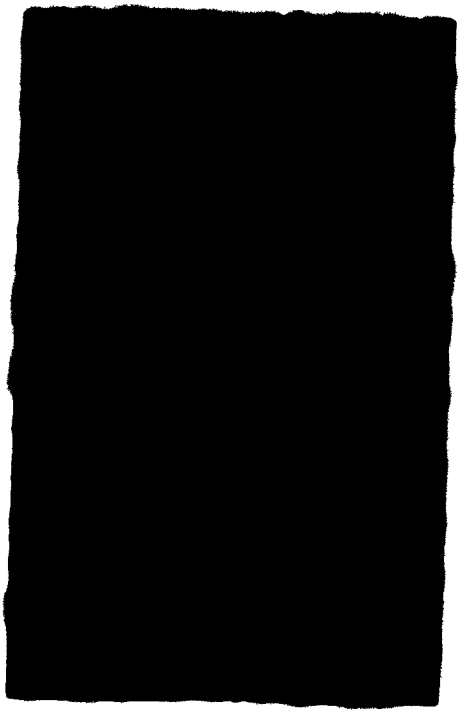

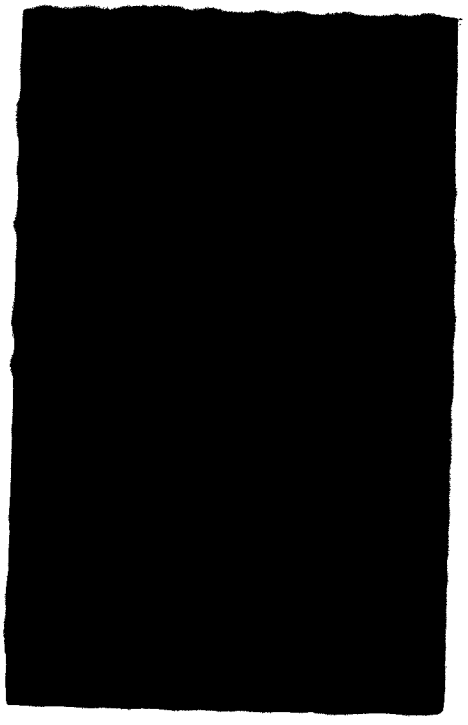

(a) 2ms INTERVAL

(b) 10ms INTERVAL

D.C. TRANSISTOR SWITCHING

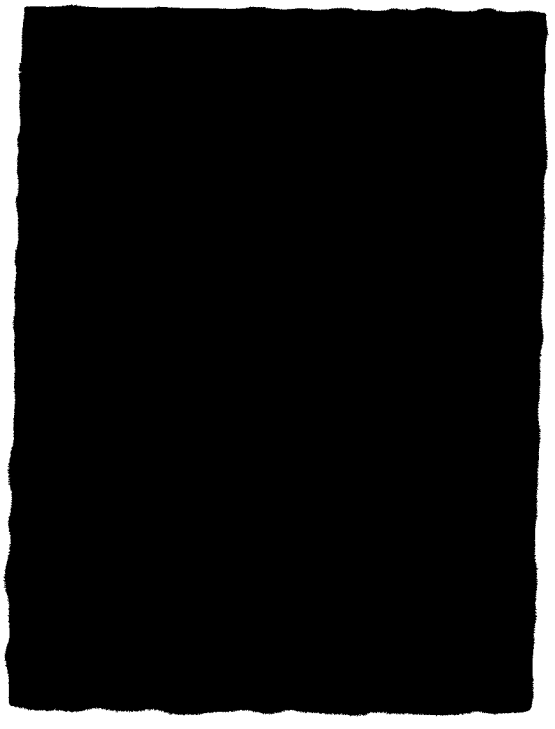

(c) RF SWITCHING (2ms INTERVAL)

FIG. 10 LIGHT PULSING TRANSIENTS.

The probability per unit time is obtained by multiplying by the number of collisions per second, τ_o^{-1}, where τ_o is the average transit time across the cell, $\tau_o^{-1} = \frac{\bar{v}}{d_2}$, $\bar{v}$ being the average velocity. The probability of an atom having left the cell after a time τ is

$$\rho(\tau) = e^{-\frac{A_1}{A_1}\frac{\tau}{\tau_o}} \tag{2}$$

and a convenient criterion is set by placing

$$\frac{A_1}{A_2}\frac{\tau}{\tau_o} = 1 \tag{3}$$

For a 2 inch diameter bulb of Rb atoms at room temperature $\tau_o = 3 \times 10^{-4}$ sec and the following relation between τ and d_1 is obtained:

$$\tau = \frac{4 d_2^3}{\bar{v} d_1^2} = \frac{2.1 \times 10^{-3}}{d_1^2} \text{ sec} \tag{4}$$

This yields $\tau = 0.2$ sec for $d_1 = 10^{-1}$ cm. It is to be noted that τ goes as the cube of the cell diameter.

"Lobsterpot" types of cells having very small orifices were made (as shown in Figure 12) to give calculated relaxation times of several seconds in order that this be a negligible source of relaxation when examining the performance of wall coatings. Some 1 inch diameter cells were made in order to improve the Dicke Doppler reduction in such wall coated cells and this necessitated orifice openings of only several tenths of a millimeter which were prepared by Mr. Harris by grinding the end of a tapered tube.

2. Rubidium Distillation and Buffer Gas Handling

The only change from the methods described in reference (1) was concerned with the manner of obtaining the rubidium from the rubidium chloride form in which it is readily available. Instead of replacing the Rb by Na as described there, a technique of using calcium for this purpose as described by Strong[75] was employed. Calcium chips were filed to yield a fine powder which was mixed with RbCl in roughly stoichiometric proportions. The mixture was placed at the bottom of a 1/2" pyrex tube joined from its side to the bulb to be filled by constricted tubing to be sealed off at successive constrictions in the distillation process. The top of the tube was sealed off near the connection to the bulb. After a good fore vacuum was achieved the powder mixture was torched to release water and adsorbed gases. The volume of gas evolved was considerable and sometimes came off explosively, blowing the powder throughout the system. This effect was eliminated by placing some glass wool above the powder in the tube and tamping it gently into place. This trapped the powder particles but was sufficiently porous to allow rubidium vapor to pass through. It was necessary to heat the mixture until the pyrex was glowing red in order to effect the replacement, but the use of an iron boat as described by Strong[75] was not required. After a sufficient amount of rubidium was produced and moved beyond the first constriction, the pyrex tube was removed from the system. It was often found possible to use the mixture again for the production of more rubidium, in which case the problems associated with the evolution of gas were eliminated.

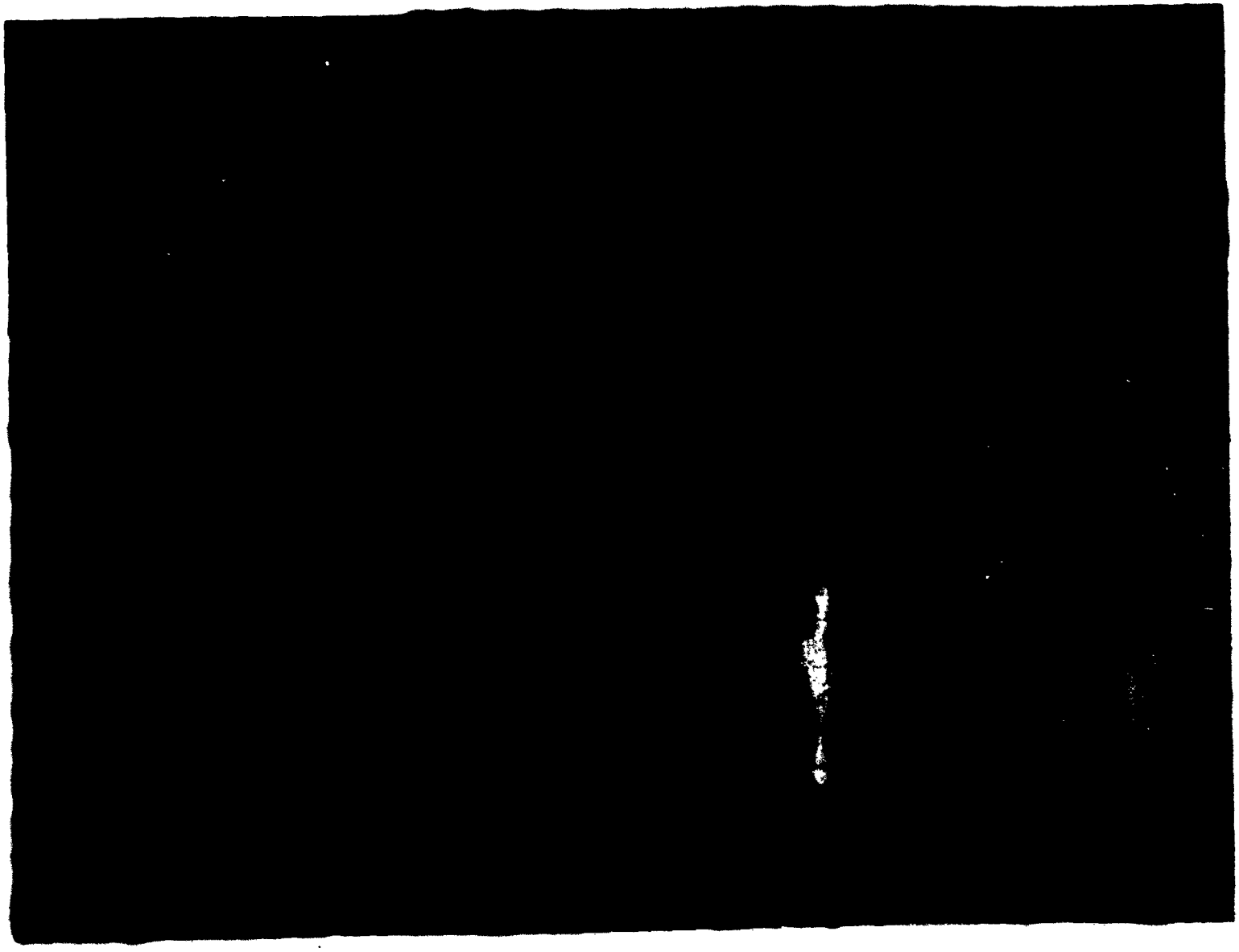

FIG. 11 VIEW OF VACUUM SYSTEM

During the early stages of the work rubidium was distilled into bulbs singly. However, during the investigations of the alkylchlorosilane wall coatings, several bulbs were filled simultaneously, as shown in the photograph of the vacuum system in Figure 11. Distillation of the natural rubidium has been completed in the photograph. The oven shown lowered was used to bake the bulbs at 300-400° C under mercury diffusion pump vacuum before final distillation of rubidium into the bulbs, the deposits of metallic rubidium being prevented from evaporation by cool moistened cloths wrapped around the tube. Pressures between 5×10^{-7} and 10^{-6} mm Hg could be achieved with this vacuum system.

3. Wall Coatings

a. Introduction

The desirability of finding wall coatings which will only slightly perturb the internal states of atoms during collisions has been recognized since the proposal of Prof. R.H. Dicke[3] for the reduction of the Doppler width by confining the atoms to a region smaller than or comparable with the wavelength of the transition between the states. Another motivation has been the success of optical pumping experiments in buffer gases.[6,10]

Some evidence that spin orientation is preserved after bounces from hot metal surfaces was obtained by W.B. Hawkins.[76] A suggestion that saturated straight chain hydrocarbon waxes might provide such a surface was made by T.R. Carver in a talk at the 1957 Frequency Control Symposium[77] Independent optical pumping experiments by H.G. Robinson, E.S. Ensberg, and H.G. Dehmelt[78] first demonstrated that eicosane, a $C_{20}H_{46}$ straight chain hydrocarbon

formed a very successful wall coating. Careful experiments by W. Franzen[79] using an optical monitoring technique indicated that the longer the chain of the hydrocarbon wax, the longer the relaxation time.

The possibility of using a "storage box" with suitable walls to interrupt the passages of atoms between the two oscillating fields in an atomic beam resonance apparatus was proposed by Prof. N.F. Ramsey[80] and subsequent experiments by him and his colleagues have yielded much information on the relaxing and absorbing properties of various kinds of surfaces.[81]

b. Alkylchlorosilanes

The merits of methylchlorosilane treatments of glass surfaces for the production of spin-relaxation inhibiting coatings were first confirmed during the course of this work by optical orientation experiments in rubidium vapor. This knowledge was communicated privately to workers in several laboratories where subsequent experience has produced additional evidence for the usefulness of the technique.[82]

The treatment of walls with such materials for the purpose of atomic physics experiments was first suggested by Prof. R.A. Naumann of Princeton University. He proposed it to inhibit the recombination of atomic hydrogen on the walls of glass tubing leading from Wood's discharge regions in connection with resonance experiments being done on the properties of atomic hydrogen by J.P. Wittke and E.B.D. Lambe in Prof. Dicke's laboratory,[2,83] for which purpose it was very successful.

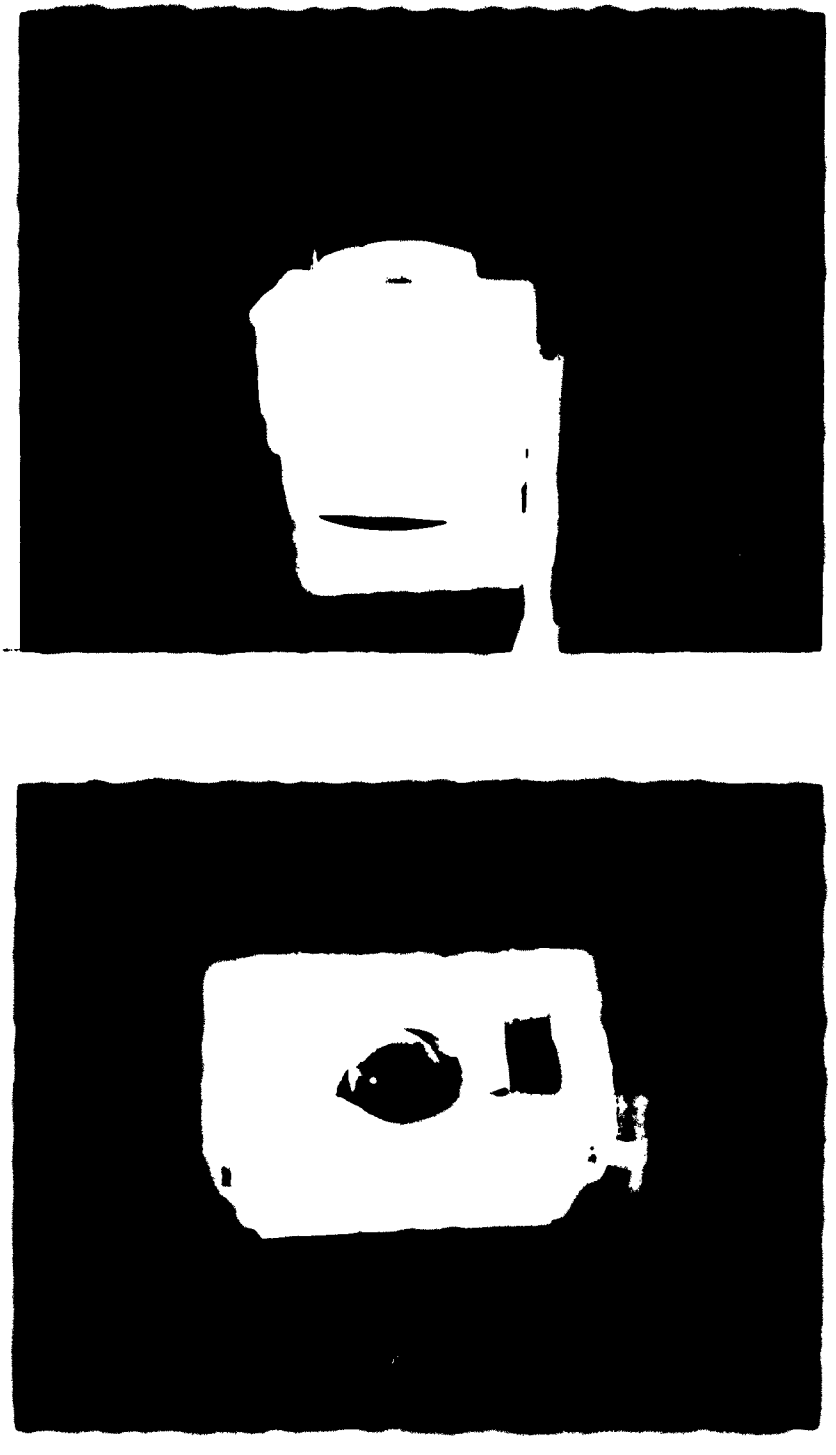

FIG. 12 THERMAL ENCLOSURE AND TYPICAL GAS CELLS.

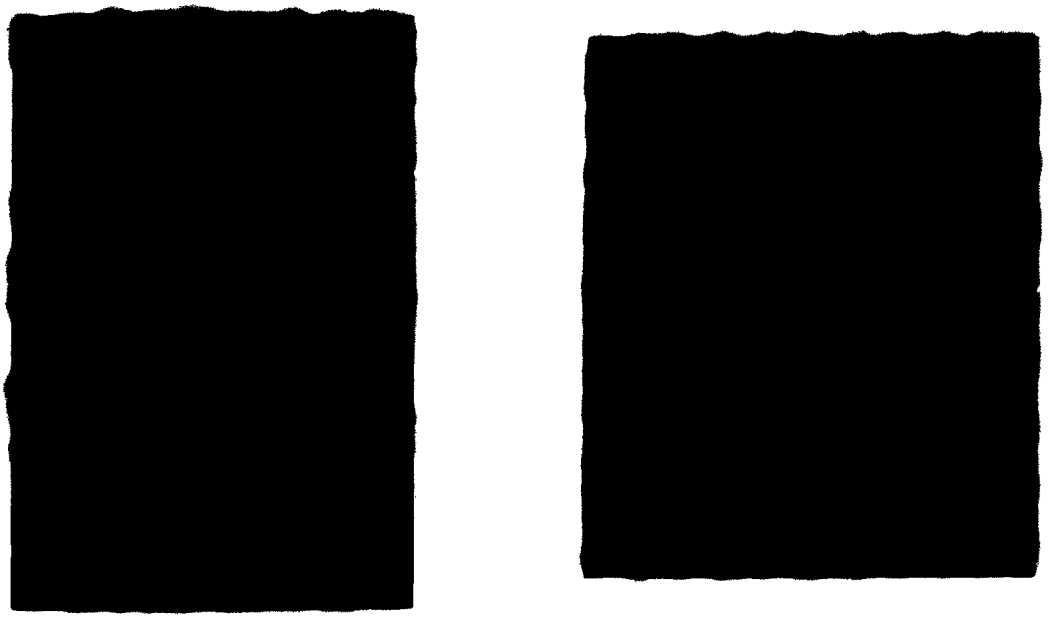

+90° PULSE
−90° PULSE

OUTPUT OF
POWER AMPLIFIER

FIG. 13 90° PULSE WAVEFORMS

The actual material used was a mixture of methyltrichlorosilane and dimethyldichlorosilane manufactured and sold by the General Electric Co., Silicone Products Division, Waterford, N.Y. under the name "Dri-Film" SC-77. It was originally developed as a coating for insulators to prevent the formation of continuous moisture films.(84) A variety of other Dri-Film products to be applied to various substrates, including metals, from either the vapor or liquid phase, are available from GE along with information on uses and techniques of applying.

Dri-Films SC-77 and SC-02 (pure dimethyldichlorosilane) were first used in the optical pumping experiments. They are liquids with very high vapor pressure, so that one can easily use the vapor to form the wall coating. An idealized description of the chemical process is indicated in the following schematic formula:

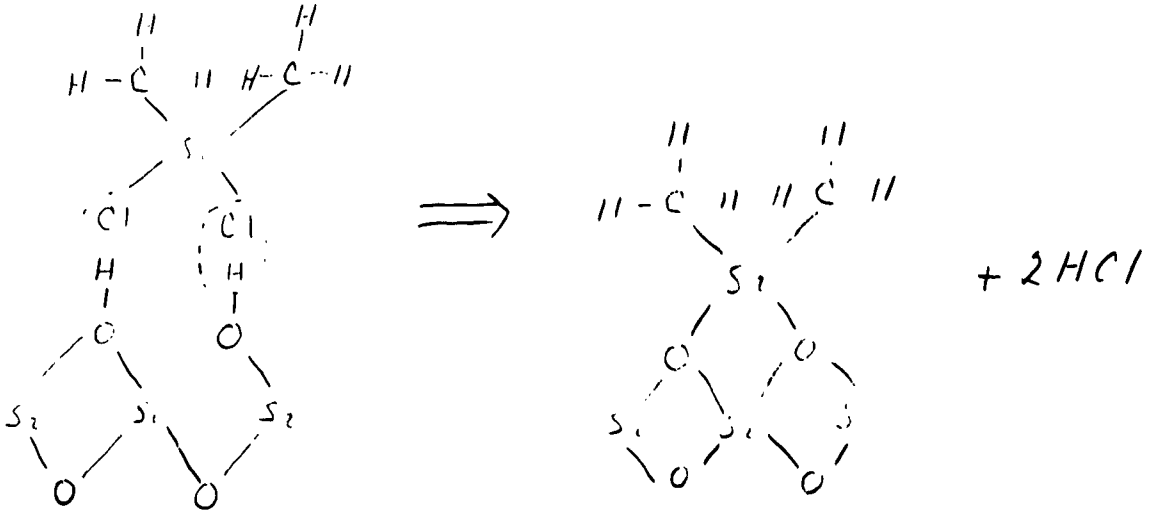

The H atoms are normally present on the oxygen atoms on the glass surface. However, after baking the glass bulb under vacuum, it is desirable to admit some distilled water vapor to insure their presence. The presence of a thin film of water on the surface will

promote linking of the silanes along the surface and the formation of a layer many molecules thick. The presence of too much water results in a visible cloudy coating. The final coating should be invisible. Excess water vapor in the volume of the cell should be avoided and the unreacted Dri-Film vapor should be flushed out. The reaction with the surface water seems to be completed in less than a second. Care should be taken not to inhale the Dri-Film vapor because of the formation of HCl.

The vapors may be introduced into the bulb by means of thin glass tubes attached to a rubber syringe bulb or by means of a system of stopcocks allowing for evacuation of the bulb and subsequent opening to the reservoirs of the appropriate vapors. Unfortunately Dri-Film reacts with most stopcock greases, so frequent regreasing is necessary.

A test for a successful coating before distilling rubidium into the cell and looking for optical pumping signals is to admit a drop of distilled water. It should not wet the surface, but exhibit a large angle of contact and run freely about. The coated bulbs may be baked under vacuum at 350°C -400°C for several hours without deterioration of the surface.

After baking, rubidium is distilled into the neck of the bulb in the usual way. Frequently there is a time lag before optical pumping signals can be seen. It is not completely clear what causes this behaviour. It may be connected with the gettering by the rubidium of gases evolved during the sealing off process and with the trapping of rubidium atoms in interstices and imperfections of the surface. Reactions with unhydrolyzed chlorine atoms in

the surface may also be taking place. The time lag can sometimes be reduced by heating the bulb or even by driving rubidium into the chamber and moving it around with a torch.

The pyrex glass which has been used has a surface different from that indicated in the diagram due to the presence of impurities such as boron and this doubtless affects the coating.

The increased effectiveness of the longer chain paraffins for the inhibition of spin relaxation[79,81] suggested the investigation of higher alkylchlorosilanes.[85] These were obtained up to octadecylchlorosilane ($C_{18}H_{37}$) and applied to glass surfaces. The vapor pressure of the higher alkyls decreases rapidly, making vapor treatments more difficult. However, by waiting sufficiently long (2 hours for octadecylohlorosilane) the vapor will react completely with the water film. Alternatively, a solvent such as toluene can be used, but this is more difficult to get into and out of bulbs with small orifices (which are desirable in practice to minimize the relaxation of atoms on the free rubidium surfaces in the neck of the bulb as compared with wall relaxation) and in addition tends to leave a waxy deposit which must be cleaned off.

Sets of coated bulbs for comparison purposes were made by opening the tubes leading into them in a constant humidity environment (a dry box converted into a "wet box") after they were baked under vacuum and sealed off, allowing the humidity to determine the thickness of the surface film so that it would be the same for each bulb. Excellent coatings were achieved, as judged by the water droplet test, with the higher alkyl coatings exhibiting the larger

contact angles. However, the optical pumping signals from all but the ethyl coatings were very poor, some worse than for uncoated glass surfaces. The reasons for this are not clear. It may be that the coatings decomposed during the baking before distilling in the rubidium, although for the higher alkyls the temperature was kept $\sim$100°C. The surfaces formed may be capable of absorbing rubidium atoms for a very long time. Further studies of these coatings should be conducted.

Although consistent results can be obtained with care on applying the alkylchlorosilane wall treatments, there are many ill-understood effects which make the techniques still something of a "black art". Some of these effects are doubtless associated with the complicated nature of glass surfaces.[86,87]

Better understood results can probably be achieved by using very clean surfaces made possible by ultra-high vacuum systems and by careful attention to the purity of the silane and water vapors and the alkali metal.

c. Paraflint Wax

A search for long straight-chain saturated hydrocarbon waxes led to a discussion with Professor J.A. Dixon of the Pennsylvania State University, the director of an American Petroleum Institute research project on the chemical synthesis of pure heavy paraffin hydrocarbons, who suggested the commercial material Paraflint.[88] It is a mixture of normal paraffins having an average molecular weight corresponding to $C_{50}H_{102}$ and has a melting point of $\sim$ 100° C.

Successful cells were prepared by distilling in the Paraflint and then achieving a thin layer by putting the cell in an oven, melting the wax and allowing it to drain off the walls and out of the orifice. It was not studied extensively, but has been used subsequently by several research groups.(81,82)

d. Vydax Fluorocarbon

An experimental fluorocarbon dispersion having the trade name Vydax , Code DV9233 was furnished by the research division of the DuPont Company.(89) It is a low polymer of tetrafluoroethylene dispersed in Freon-113 and was made for the purpose of forming a thin coating of flurocarbon on various substrates.

It could be applied to the inside of a glass bulb by filling with the dispersion and then allowing it to drain and dry. According to the manufacturer's information, such coatings could withstand temperatures of 265°C before melting.

When rubidium was distilled into a bulb that had been baked under vacuum at 150° C for a few hours, there was a tendency for the surfaces to become blackened in places. No orientation signal could be detected when optical pumping was tried.

This negative result is in accord with the experience of the Harvard group with cesium on Teflon surfaces.(81)

Since the material was acquired only during the last weeks of experimentation, it was not possible to study it further.

e. Relaxation Effects

These are discussed in Section IV C. Some direct measurements of T_2 relaxation times were carried out in collaboration

with P.L. Bender of the National Bureau of Standards. Most measurements were of relative T_1 relaxation times as indicated indirectly by the degree of optical orientation.

4. Thermal Enclosure

Although the vapor pressure of rubidium at room temperature is about 10^{-7} mm Hg, giving sufficient density of atoms for optical pumping effects, larger effects for some purposes can be obtained by operating at higher temperatures. An enclosure of 1" thick polystyrene foam slabs, held together with 1/8" lucite rod skewers made an effective thermal enclosure. It was fitted with optical windows made of glass that transmits readily in the near infra red. Hot air was blown into the enclosure through a rubber hose covered with an asbestos sheath. This air was supplied from a commercial hair dryer operated from a variac to enable the temperature of the gas cell to be varied. It was easily possible to reach temperatures of 50-60° C, these being measured with an alcohol thermometer inserted into the enclosure near the gas cell.

It was necessary to use no metal in the construction so as not to interfere with the rf or microwave radiation. The enclosure is shown in Figure 12 and can be seen in place in Figure 5.

C. Zeeman Resonance

1. Radio Frequency Coils

These were made fairly large and of approximate Helmholtz spacing in order that the rf field might be fairly uniform over the volume of the gas cell. (See Section II C) The first

rf coils used were wound over the Helmholtz coils serving to cancel the laboratory horizontal magnetic field. However, induced currents in these coils severely reduced the amplitude of the rf field which could be achieved at the resonance cell and the resonance could not be saturated. These were replaced with circular coils consisting of 10 turns of #14 cotton covered copper wire with a radius of 10.5 cm. For reasons of convenience they were placed 14 cm apart, rather than the conventional Helmholtz spacing. The field at the center was given by

$$B_1 = 0.46\, i \quad \text{milligauss} \qquad [i \text{ in ma}]$$

and could be expected to differ from this by no more than 10 percent over the volume of a 2" gas cell. The coils were connected in series by RG58U 50 ohm coax cable to minimize the distortion of the field from this connection and were fed by the same type cable through a shielded series resistor from the 8 ohm output of a Heathkit audio power amplifier Model W-5M which posessed an adequate frequency response. The rf coil circuit was predominately resistive.

A frequency of 100 kc/s was chosen since a very stable Loran crystal controlled oscillator at this frequency was readily available. The power amplifier responded well to the gated pulses with which it was supplied, as shown in Figure 13 illustrating the form of the pulse supplied to the coils, indicated by the voltage wave form across the series resistor.

The magnetic field B_1 in milligauss needed for a 90° pulse was given by $nB_1 = 35.7$ where n is the number of cycles of the 100 kc/s field applied. For n = 10, the number generally used, one needs for the oscillating field, which is twice B_1, approximately

7 milligauss. For a 180° pulse one could use twice this value for the same number of cycles or one could double the number of cycles. This latter procedure was followed.

2. D.C. Magnetic Field Configurations

a. Helmholtz Coils

The initial work and first demonstration of the phase destructive method of optical detection were carried out using two sets of Helmholtz pair coils. These were used first by J.P. Wittke [2] and later by T.R. Carver[1] in the same location. Each was about 14 inches in radius and was fed from storage batteries through a series parallel combination of rheostats to enable precise control of the fields. One set of coils was oriented and the current adjusted to cancel the horizontal component of the local laboratory field, while the other set was used to reduce the value of the vertical component of the local field to $\sim$ 140 milligauss, the value of B_o required for resonance at 100 kc/s. For Helmholtz pairs the inhomogeneity along the axis is

$$\frac{\Delta B_o}{B_c} = -4\left(\frac{\Delta z}{r}\right)^4$$

where r is the radius, and Δz is measured from the center, a similar expression holding off-axis. This would predict an inhomogeneity of about 10^{-4} for a 2 inch diameter gas cell if only the coils themselves contributed. Unfortunately local ferromagnetic materials around the laboratory contribute to a much larger inhomogeneity: $\sim 10^{-2}$ as determined from the width of the 100 kc/s resonance, which was about 1000 cps. Another indication of the large inhomogeneity was the impossibility of preserving phase memory between 90° pulses

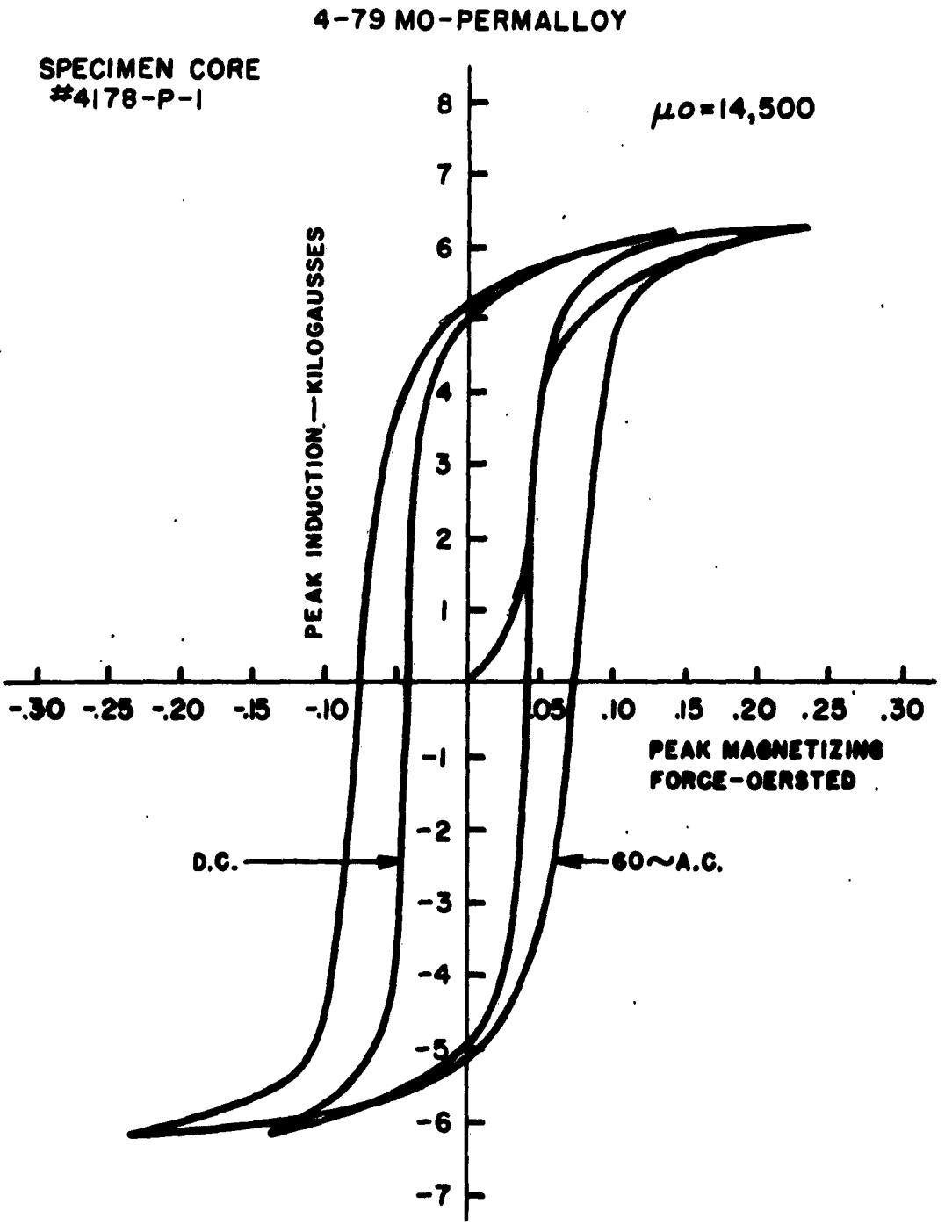

D.C. AND A.C. MAGNETIZATION CURVES
AND HYSTERESIS LOOPS
OF 4-79 MO-PERMALLOY

FIG. 14

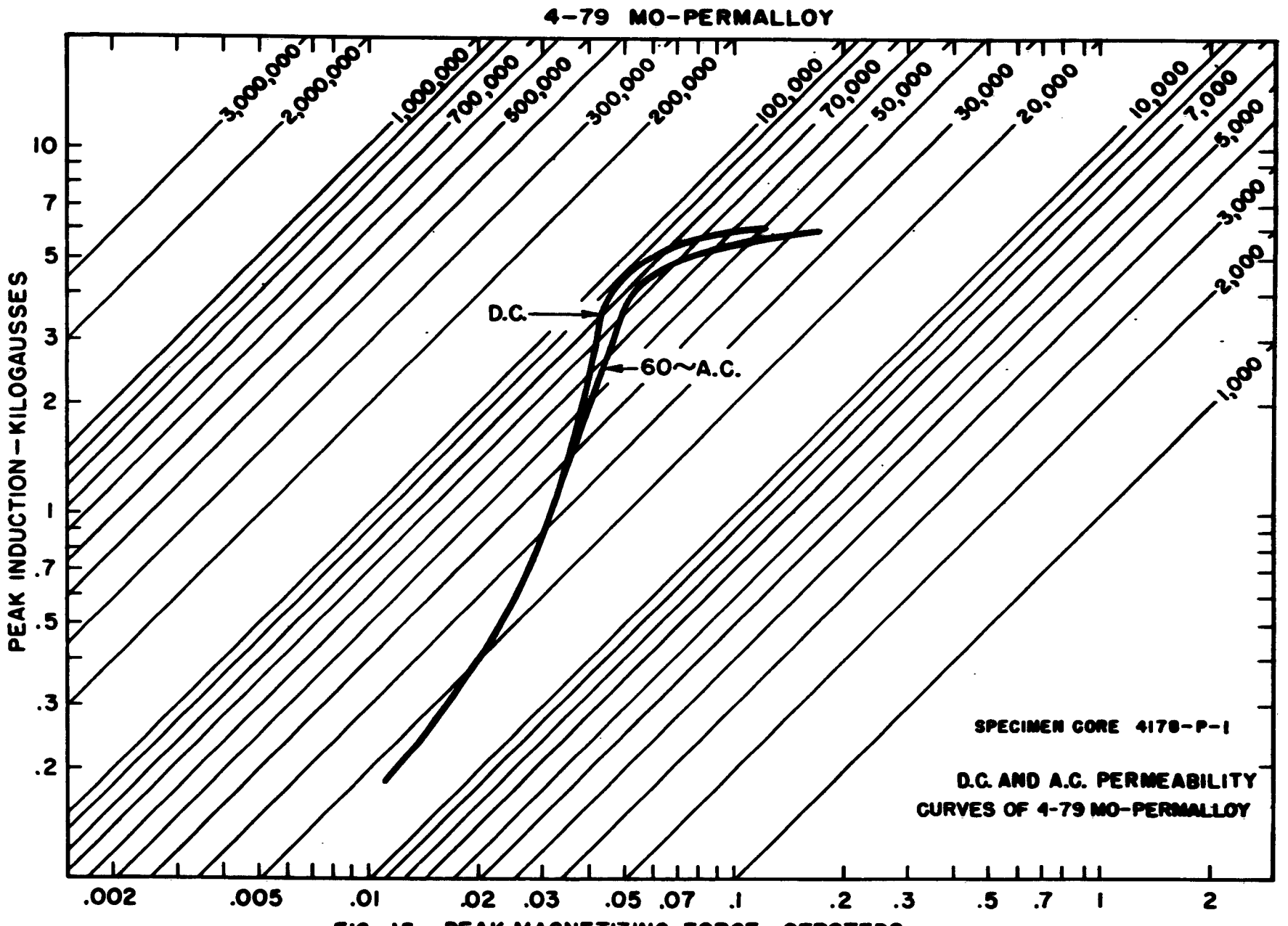
4-79 MO-PERMALLOY
PEAK INDUCTION-KILOGAUSSES
10
7
5
3
2
1
.7
.5
.3
.2
3,000,000
2,000,000
1,000,000
700,000
500,000
300,000
200,000
100,000
70,000
50,000
30,000
20,000
10,000
7,000
5,000
3,000
2,000
1,000
D.C.
60~A.C.
SPECIMEN CORE 4178-P-1
D.C. AND A.C. PERMEABILITY
CURVES OF 4-79 MO-PERMALLOY
.002
.005
.01
.02
.03
.05
.07
.1
.2
.3
.5
.7
1
2
FIG. 15 PEAK MAGNETIZING FORCE-OERSTEDS

beyond a time interval of 2 milliseconds, even with one 180° pulse interposed.

Another configuration was adopted in an attempt to remove this difficulty and is described below.

b. Shielded Solenoid

Laboratory sources of magnetic fields produced the large inhomogeneities, so it was decided to shield the region of the gas cell from their influence and to produce the desired field by controlled currents in an appropriate coil configuration designed to give the required homogeneity as computed in Section II C 6.

Several shielding geometries were seriously considered including the use of large Armco iron slabs around the outside of the Dexion framework keeping the same Helmholtz coils or several concentric mu-metal cylinders surrounding a solenoid.

A large amount of 4 inch by 4 mil moly-permalloy strip was available in the laboratory which had been acquired earlier for the purpose of magnetically shielding a gravitational experiment but never used, so it was decided to build a large solenoid and wrap it with this material. The magnetic characteristics of the 4-79 Mo-Permalloy are shown in Figures 14 and 15.

The soleonoid was wound under tension on a form of thick cardboard 1 meter long, 10 inches inside diameter with $\frac{1}{4}$" thick walls. The winding consisted of a single closely spaced layer of 1200 turns of #20 wire insulated with heavy formvar having a total resistance of 30 ohms. The winding was greatly facilitated by the use of a large lathe. Figure 16 shows the completed winding before

the magnetic shielding was applied, and a section of the permalloy strip. A layer of ¼" wide thin yellow mylar pressure sensitive tape was applied to hold the winding in place before proceeding with the shielding.

The first three layers of magnetic shielding were each formed of 11 pieces of the 4" by 4 mil strip slightly shorter than the solenoid form. They were arranged in venetian blind fashion with 1" overlap and wound with a layer of yellow mylar tape, followed by a layer of black electrical tape to increase the separation between successive shielding layers. Such separation is desirable for better shielding.

The four outer layers of shielding were wound in spiral fashion, the second layer being centered over the butt joints made by successive turns of the first layer, and the whole wound with black tape. The third and fourth layers were wound in the same way but with the opposite helicity and were secured with a final layer of yellow mylar tape.

The completed shielded solenoid can be seen in place in Figure 6. The application of so many layers under tension on the lathe caused the cross-section to be very accurately circular, although uniformity of cross-section along the length is all that is required for field homogeneity.

The effectiveness of the shielding was measured with an electronic fluxmeter[90], and found to be not as good as had been hoped. The reduction of a field at right angles to the axis of the solenoid was by a factor $\sim 3 \times 10^{-3}$. The reduction factor for fields along the axis was $\sim 3 \times 10^{-2}$.

FIG. 16 CONSTRUCTION OF SHIELDED SOLENOID.

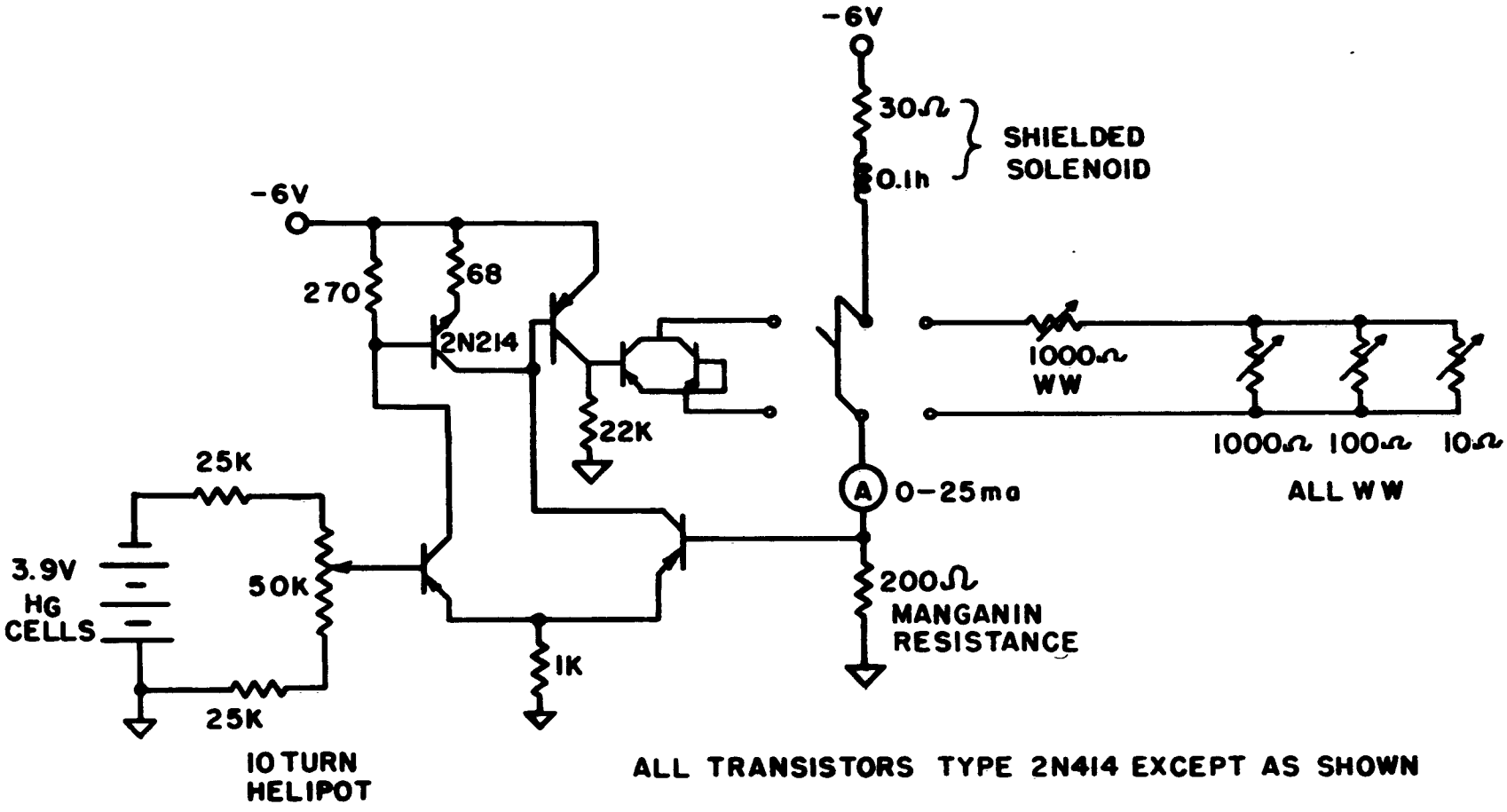

SHIELDED SOLENOID SUPPLY CIRCUITS

DIAGRAM 4

The internal field at the center produced by such a shielded solenoid is expected to be just that of an unshielded solenoid, the shielding simply providing a path for the external flux. This was found to be indeed the case with the field given by

$$B_o = 15.1\, i \quad \text{milligauss} \qquad [i \text{ in ma}]$$

as given by the geometry and confirmed by measurement of the 100 kc/s resonance is Rb^{87} at 143 milligauss for i = 9.5 ma. There was some residual field produced by the shield, for reversal of the field direction required a current differing from this by about 5%. Demagnetization was attempted by energizing the coil with 60 cps current and reducing the current to zero, but it was unsuccessful.

The current was provided by a transistorized constant current source designed for the purpose. Very fine control was provided by a ten turn helipot. It was also possible to supply the current directly from a storage battery through a series-parallel connection of variable resistors for fine control. The circuits are shown in Diagram 4.

c. Time Varying Fields

The presence of magnetic fields changing at 60 cps and higher harmonics of this frequency was a continuous source of annoyance, although it was used as a modulation source in some of the experiments (See Sections II C 8 and IV A) when it proved difficult to compensate it. Another magnetic field at $\sim$20 cps was frequently present from a model magnet being studied by the physicists and engineers associated with the Princeton-Pennsylvania Accelerator in a laboratory about fifty feet away. This field was about six to ten

times the 60 cycle field, depending on the amount of use of various pieces of equipment in the laboratory.

It had been hoped that the shielded solenoid described above would shield these time varying fields effectively. However, they were reduced by only a factor of 3-4 in the longitudinal direction for which they were most serious under Zeeman resonance conditions. Accordingly some attempts were made to compensate them at the position of the resonance cell.

Using a pickup coil at the position of the gas cell, one could acquire a signal depending on the time varying magnetic field and use it to vary the current in the main solenoid so as to just cancel this time varying field by the use of appropriate feedback circuits.

A coil was made consisting of 2650 turns of #36 wire wound on a form having an average diameter of 9" and a resistance of 2600 ohms. The coil was wrapped with thin copper tape for electrostatic shielding purposes. The coil constant NA was such as to give an rms voltage of 1 millivolt for an rms 60 cycle field of $\frac{1}{4}$ milligauss, which was a typical value for this type of field at the center of the solenoid.

The voltage output of the coil was amplified by about 1000 by a chopper stablilized d-c amplifier made by Electro-instruments, Inc., having an equivalent input noise of $\sim 10\,\mu v$ between 0 and 50,000 cps and posessing a very low drift rate. Because of a quirk in the design which used the internal resistance of the source, this could not exceed 3000 ohms. The output of the d-c amplifier was fed into an integrator made from a Philbrick

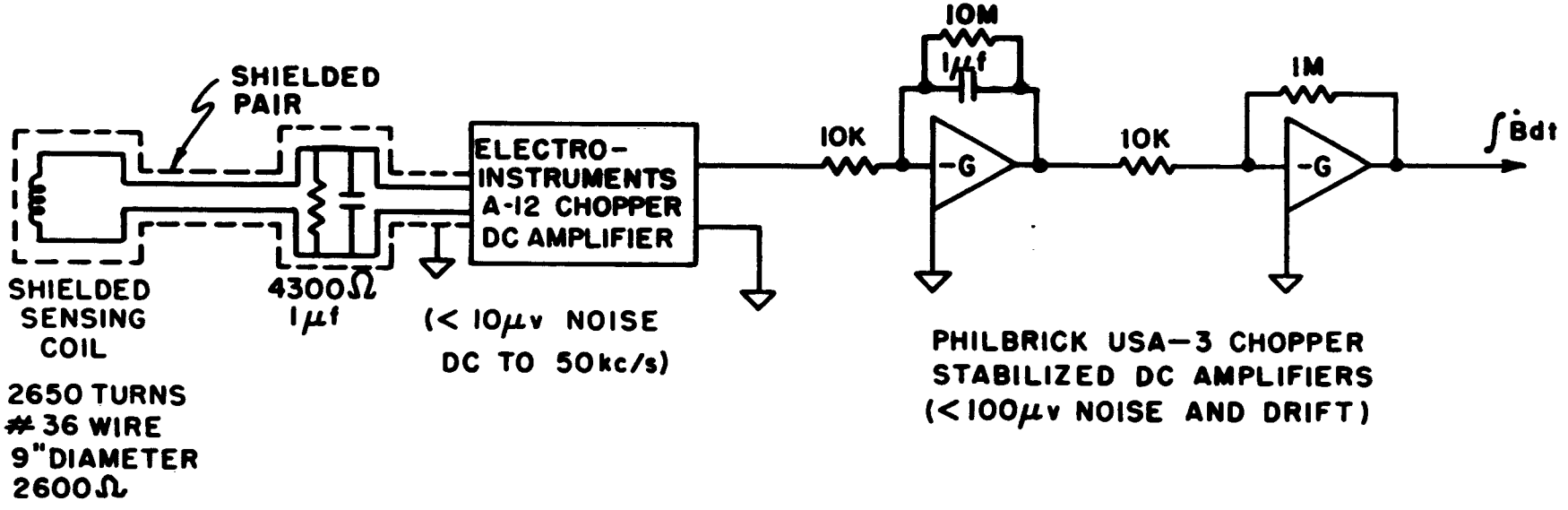

SENSING AND INTEGRATING CIRCUITS FOR TIME-VARYING MAGNETIC FIELD.

DIAGRAM 5

chopper stabilized operational amplifier having a time constant sufficient for good integration down to 1 cps. The integrated output was amplified by another Philbrick operational amplifier using resistive feedback. The circuits are given in Diagram 5.

Difficulty was experienced in producing a time varying current in the solenoid coil proportional to the time varying component of magnetic field as obtained from the integrator by incorporating a fast feedback loop into the constant current source already constructed. Although such a combination of a varying current for cancellation of the time varying external magnetic field superposed on an average current is certainly possible, practical difficulties associated with the earlier design which had not anticipated this feature prevented the time varying fields from being reduced beyond a factor 2 or 3 before oscillations in the feedback circuit built up. Because of the press of time and the desire to perform experiments which were not prevented from accomplishment by the time-varying field, the appropriate new circuitry incorporating the frequency dependence to avoid the Nyquist oscillations was not built.

A much simpler way to suppress the externally produced time varying field would be to have several independent solenoid windings. One could be used to produce the desired d-c field. Another could produce the time varying field designed to cancel the externally produced field, deriving its current from an amplifier driven by the induced voltage in a third coil. It is not necessary to integrate this voltage to get a signal proportional to the time varying field, for one can simply require in the feedback

circuit that the induced voltage be reduced to zero (i.e. to the input noise level of the amplifier). Such a flux stabilization worked well on a Varian magnet in this laboratory.(91)

3. Radio Frequency Pulses

a. Early Circuits

The first system used to give two 90° pulses separated by a time interval will be described but only given in block diagram form since it lacked flexibility for experimentation and was replaced by the circuits to be described below. For some of the circuits such as flip-flops and one-shot multivibrators, commercial units made by Eeco were acquired and adapted.

The block diagram of the arrangement of the various circuits is shown in Diagram 6. The first pulse should produce a 90° rotation of the spin system and the second pulse should produce the inverse 90° rotation. This can be accomplished by tuning the frequency and magnetic field for exact resonance and having the second pulse identical to the first except that it is 180° out of phase, or by having the pulses identical and detuning slightly from exact resonance. This latter method was chosen for the first attempt, whereas later circuits used the former method.

In order to achieve exactly similar pulses the starting time of the pulses is determined by a pre-set electronic counter which counts a given number of cycles of the Zeeman frequency and then triggers the appropriate circuits.

The sequence of operations is as follows. A low frequency function generator operating at~30 cps (this frequency to

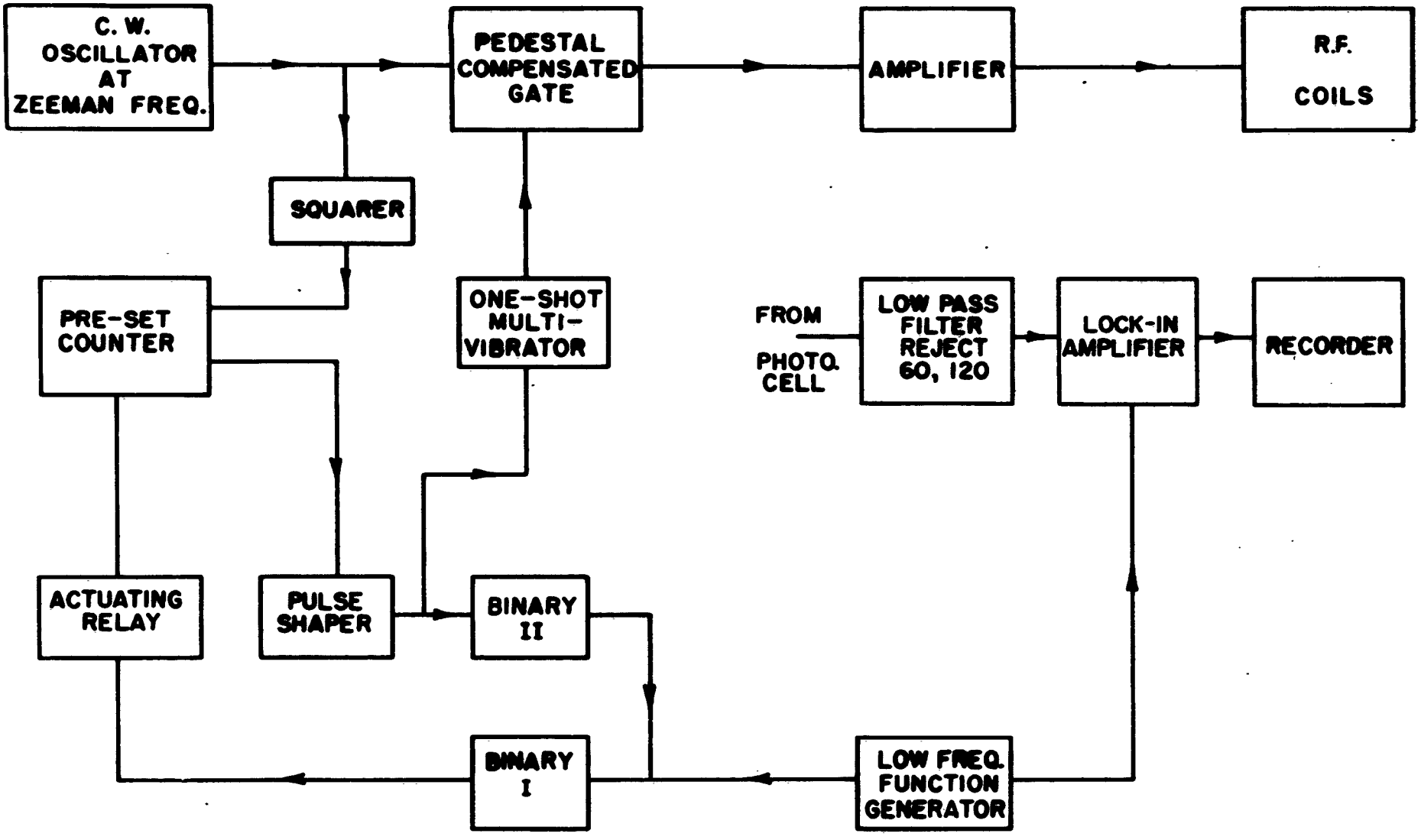

BLOCK DIAGRAM OF FIRST DOUBLE PULSE RESONANCE SYSTEM

DIAGRAM 6

be reduced as the experiment proceeds) provides an initiating pulse and also a square wave reference signal for a lock-in amplifier. The initiating pulse triggers a binary which actuates a relay which turns on the pre-set counter. After 1000 cycles of the Zeeman frequency from a continuously running oscillator ($\sim$ 200 kc/s, this frequency being reduced to 100 kc/s later) a pulse is obtained which is shaped and applied to a one-shot multivibrator and also to a second binary. The pulse from the one-shot multivibrator opens a pedestal compensated gate which lets pass a pulse of the Zeeman frequency from the oscillator. This pulse is sent to a power amplifier and produces the desired pulse of current in the rf coils.

After another 1000 cycles an identical pulse is formed in the same way. However, the process stops here for the output pulse from the second binary actuates the first binary and opens the actuating relay for the pre-set counter, turning it off.

The system worked very reliably, after remedying electronic difficulties in the lock-in amplifier and in the pre-set counter. The time interval between the pulses could be changed by changing the number set on the counter, which could be 10^3 or 10^4 or 10^5, and also by changing the frequency of the oscillator. The variable frequency oscillator used was not very stable, so the Loran crystal controlled oscillator at 100 kc/s was incorporated into the system. The lock-in amplifier was sensitive to 60 and 120 cps signals and since these were large in the optical detection signal for the Zeeman resonance because of the presence of time-varying magnetic fields at these frequencies, it was necessary to construct a low pass filter containing also twin T rejection networks at 60 cps and 120 cps.

A desire to interpose 180° pulses to combat the field inhomogeneity as described in Section II C 7 and the need for more flexible pulse programming to be used with the light source and with the microwave resonance led to the design of a new digital timing system described below.

b. Digital Timing Circuits

Considerable thought was given to a type of flexible timing system that might be assembled at moderate expense. The most promising system seemed to consist of a sequence of decade scalars (without feedback) and many multilegged coincidence circuits so that a pulse could be obtained at any desired time in the cycle of the cascaded decade counters, one leg of each coincidence circuit going to a position in each of the decades. The minimum time interval between pulses with such a system would be determined by the rate of driving the fastest decade. One needs decades which will allow a number of legs from different coincidence circuits to be placed in the same digital position. This last requirement rules out the easy use of commercial decade single tube counters, for a vacuum tube amplifier or cathode follower would have to be added for each digital position on each decade.

A satisfactory solution was found in some of the flexible pulse programming equipment offered commercially by the Navigation Computor Company (Navcor) all of which utilizes transistor circuits. The basic unit was a shift register, consisting of ten binaries so connected that upon receipt of an advance pulse the state of each binary, "0" or "1" is transferred to the next one. By inserting a "1" in one position and interconnecting the last and the

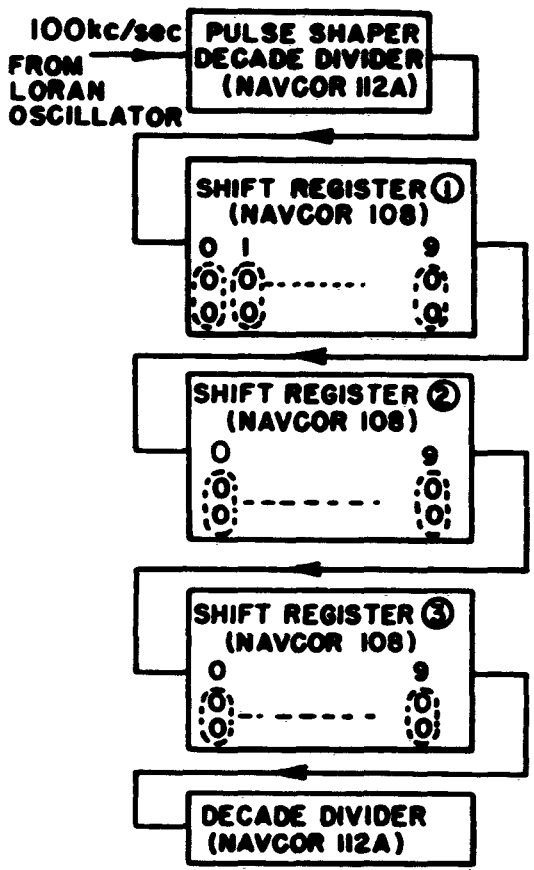

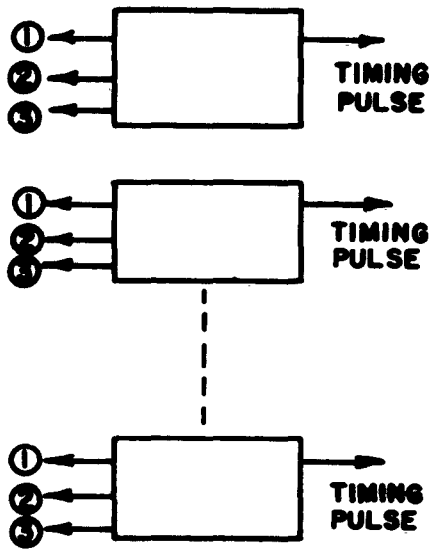

DIODE COINCIDENCE GATES

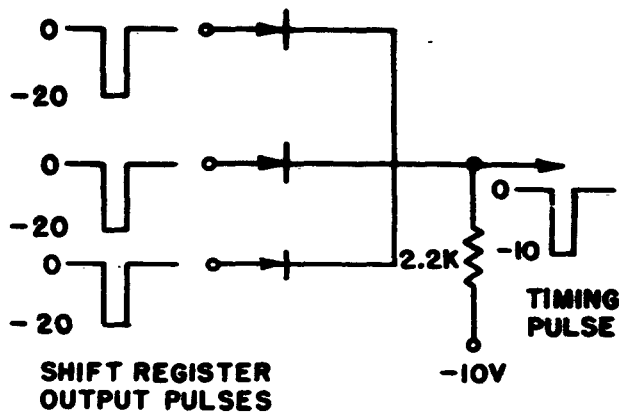

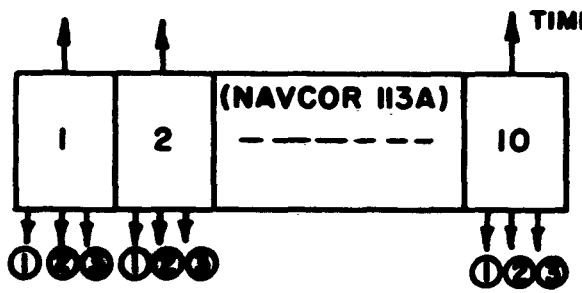

TRANSISTOR COINCIDENCE GATES

DIGITAL TIMING CIRCUITS

DIAGRAM 7

first, one has a decade scaler. Each of the binaries was fitted with a transistor current amplifier leading to an output Johnson pin jack, either "0" or "1" ("1" =-10 volts) being available. Diode coincidence circuits of the Rossi type as shown in Diagram 7 were made for use with these shift registers. Navcor also supplied three legged transistor coincidence circuits, a set of ten of these on one chassis being acquired. Two decade scalars were obtained for the high speed and low speed scaling without provision for coincidence circuits, along with a transistorized power supply to energize the entire unit. A view of the unit can be seen in Figure 8. The maze of wires is needed for the pulse sequence described below, but it was quite easy to program, a number of multiple connections having been made with Johnson pin-Jacks after the manner of power distribution panels. New arrangements could be made by simply replugging leads. The low impedance of the circuits presented interference from pick-up and cross-talk. Some of the relevent circuits are given in Diagram 7.

The first decade scaler contained a pulse shaping circuit so that it could be driven by a sinusoidal wave form obtained from the Loran crystal controlled oscillator at 100 kc/sec. Pulses were obtained to open and close transmission gates to allow this same 100 kc/sec signal to be applied to the power amplifier and thence to the rf coils. The use of the same signal for both purposes means that the pulse sequence will be identical from one repetition to the next as to phase.

c. Transmission Gates

The requirements of rapid operation, no pedestal, and low leakage in the non-transmitting position were achieved by using a combination of 6-diode gates.(92) Solid state diodes were used and at 100 kc/s, feedthrough was sufficiently serious for a long interval between 90° pulses that a second 6-diode gate was used to shunt the output of the first gate. The circuits are given in Diagram 8. The voltage change for the 6-diode gates was supplied from a vacuum tube binary, as shown in Diagram 8 a. After being opened by a pulse on one grid, another pulse was required on the other grid to close the gate. The actuating pulses came from the coincidence circuits described above and were fed onto the grids of the binary through a diode mixer to avoid interactions among the many coincidence circuits, as shown in Diagram 8 a. Input to the gate was by means of a vacuum tube cathode follower as was the output from the gate, as shown in Diagram 8 b. The individual gates were incorporated into 3 tube vector boxes.

Two identical transmissions gates were constructed, the 100 kc/sec signals with which they were fed differing in phase by 180°, thus enabling the second 90° pulse to be exactly 180° out of phase with the first. The 180° phase splitting was obtained from a difference amplifier, the large cathode resistance for this "long-tail pair" being obtained from an n-p-n transistor acting as a current cource. Provision was made for shifting the phase of the 100 kc/sec signal fed to the digital timing circuits with respect to that fed to the transmission gates in order that the initial phase of the pulses could be controlled. Provision was also made for attenuating

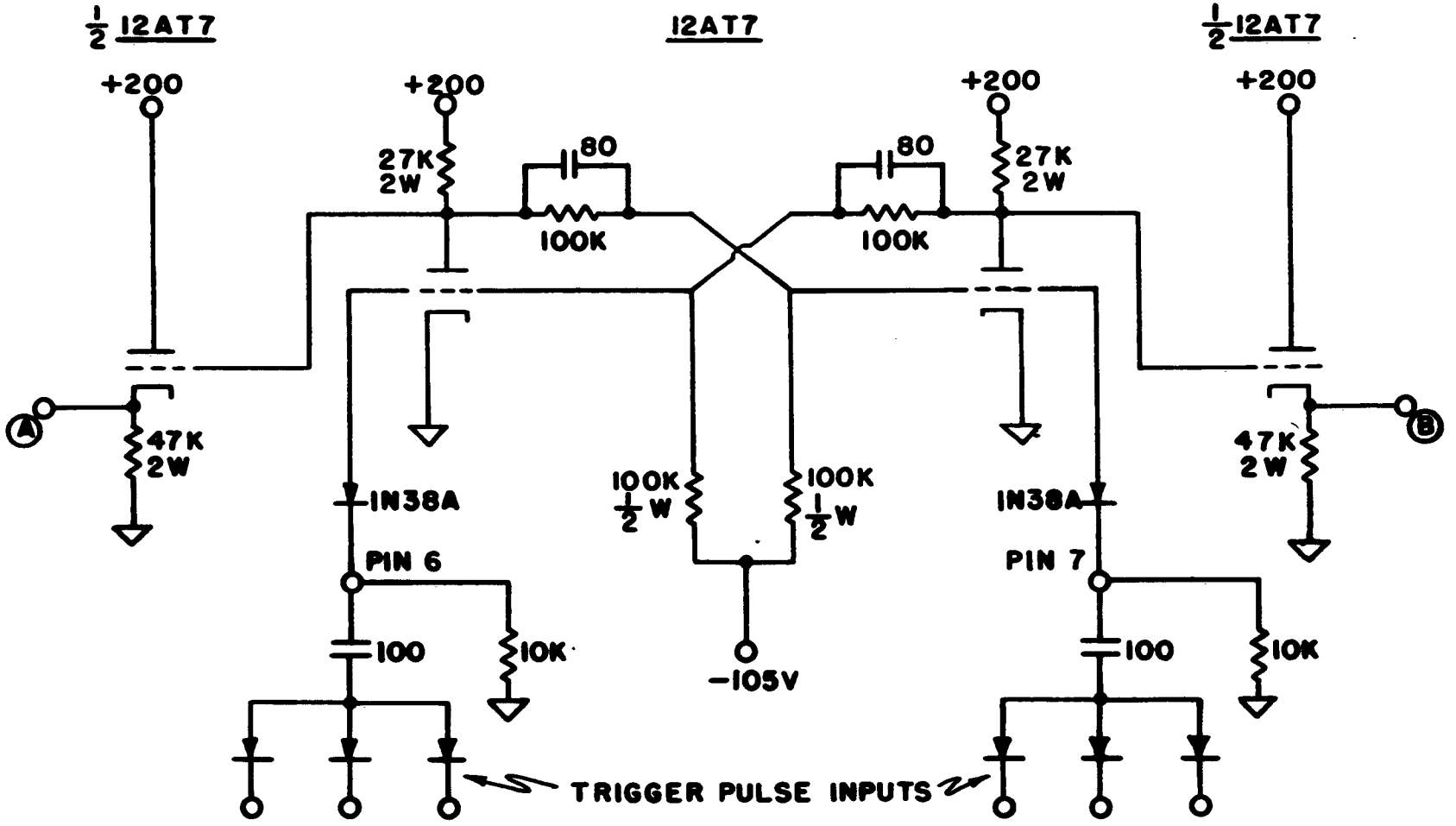

DRIVER BINARY FOR 6 DIODE TRANSMISSION GATE

DIAGRAM 8a

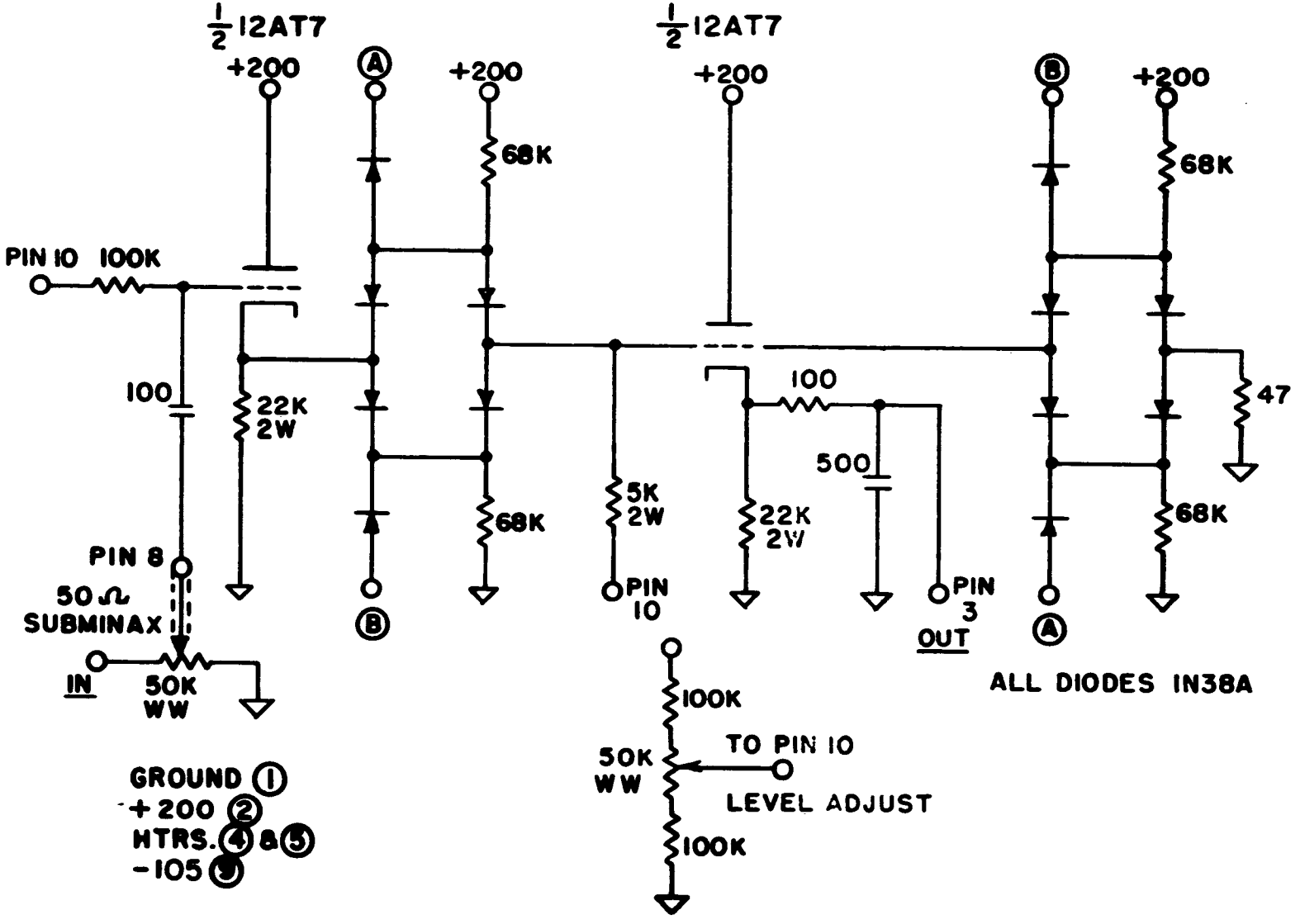

6 DIODE TRANSMISSION GATE

DIAGRAM 8b

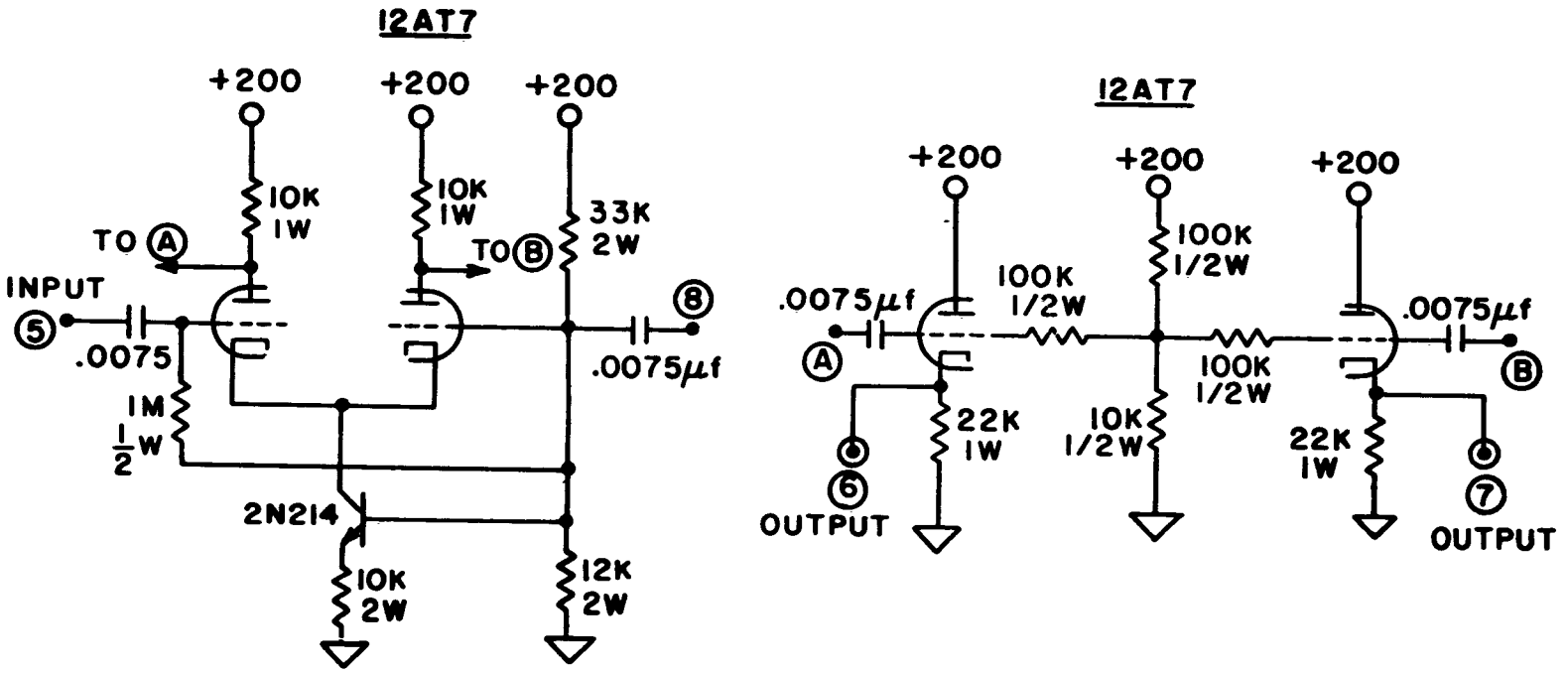

VECTOR BOX PINS

1. GROUND
2. B+
3.+4. HEATERS

DIFFERENCE AMPLIFIER PHASE INVERTER

DIAGRAM 9-a

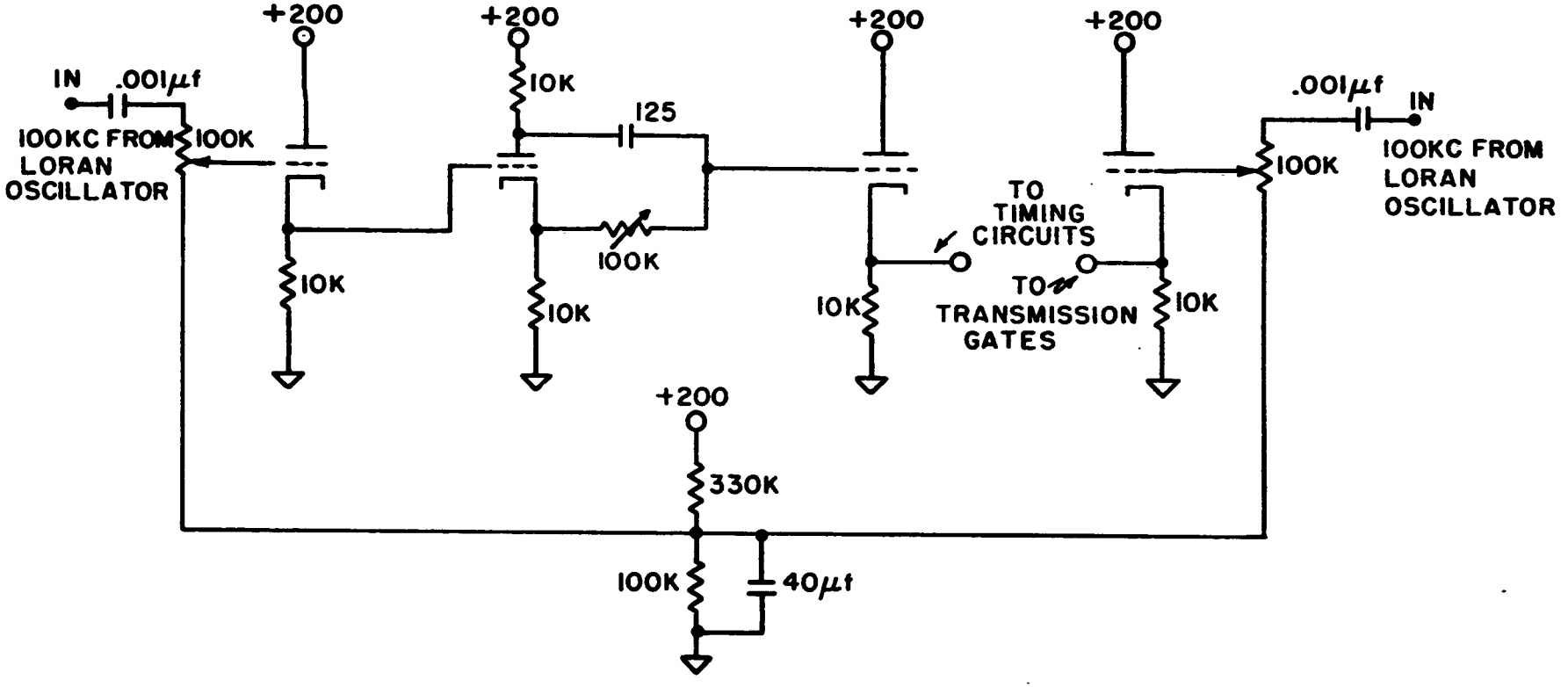

VARIABLE PHASE SHIFTER
FOR
100kc/sec TIMING SIGNAL

DIAGRAM 9b

these two signals independently, for the pulse shaping circuit of the digital timing array worked satisfactorily only for a narrow range of amplitudes. These circuits are shown in Diagrams 9 a and 9 b.

4. Response of Oriented Atoms to Pulses

a. Adjustment for Desired Rotation

The analysis given in Sections II B and II C shows that the change in the optical absorption of a beam of σ^+ radiation in the z-direction when an oriented assemblage produced by this beam is rotated by an angle β about an axis in the x-y plane is precisely the same as that resulting from free precession modulation of a beam in the x-y plane, provided one takes proper account of the opposite g-factors for the F = 1 and F = 2 states. When the rotation is caused by an oscillatory rf field B_1, the effective oscillator strength as a function of β is

$$D_1: \quad f_{eff}^{(\sigma+)} = f_0 \left\{ 1 - \left[(N_8 - N_4) + \tfrac{1}{2}(N_7 - N_5) - \tfrac{1}{2}(N_3 - N_1) \right] \cos\beta \right.$$

$$D_2: \quad f_{eff}^{(\sigma+)} = f_0 \left\{ 2 + \left[(N_8 - N_4) + \tfrac{1}{2}(N_7 - N_5) - \tfrac{1}{2}(N_3 - N_1) \right] \cos\beta \right. \qquad (1)$$

where the N_i refers to the populations before the pulse ($N_i = f_{ii}$). The maximum change is obtained for $\beta = \pi, 3\pi, 5\pi, \ldots (2n+1)\pi, \ldots$.

The timing pulse program was arranged to obtain a 90° pulse by opening the gate for 10 periods of the 100 kc/sec rf signal. By starting from zero amplitude one can increase β by increasing the rf amplitude while observing the rise and fall of the optical transmission signal in response to the pulse. The first maximum corresponds to $\beta = \pi$ and the amplitude for $\beta = \pi/2$ is easily obtained by reducing the amplitude until the change in the optical transmission

signal is $\frac{1}{2}$ that for $\beta = \pi$. Pulses for 180° rotations to be interposed between the +90° and -90° pulses were obtained by opening one of the gates for 20 cycles at the appropriate time, and using the same amplitude of rf field for all pulses.

b. Measurement of "Longitudinal" Relaxation Time T_1

The change in optical transmission following a 180° pulse is a measure of the degree of orientation achieved, as shown by equation (1) in the preceding paragraph. For the same light intensity such changes for different bulbs give a measure of the relative orientations. The orientation achieved will depend on the ratio ρ of optical pumping time Γ^{-1} to relaxation time T as given in Section II A 8 and in Appendix E. T is here a "longitudinal" relaxation time, affecting populations. Although the relationship between T and the orientation achieved in this way is not linear, a crude relative measurement of such times is readily achieved. Better values could be found using the computer solutions of the optical pumping equations as discussed in Section II A 8 and Appendix E.

This method was used to obtain a measure of relative relaxation times for various wall coatings and the results are given in Section IV C.

c. Measurement of "Transverse" Relaxation Times T_2

A value of the relaxation time T_2, which is a characteristic time for atoms to lose their relative phase relations, can be obtained by monitoring the decay of the envelope of the Larmor frequency using the transmission modulation of a beam of σ^+ light.

This detection light beam should be so weak that the optical pumping time associated with it is much longer than the e -folding decay time of the envelope.

It is essential in such an experiment that the magnetic field be sufficiently homogeneous that no spurious decay time results from the inhomogeneities, as described in Section II C 6.

Some experiments of this sort were carried out in collaboration with P.L. Bender of the National Bureau of Standards using the facilities of the U.S. Coast and Geodetic Survey Magnetic Observatory at Fredericksburg, Virginia. A single beam of σ^+ D_1 radiation was oriented at 45° with respect to a weak homogeneous field of a few milligauss, corresponding to a precession frequency of a few kilocycles per second, and at 45° to an rf field used to apply a pulse to tip the oriented atoms, initiating the free precession. It is clearly not necessary to rotate through 90° in order to observe modulation at the Larmor precession frequency.

The results of some measurements of this type on bulbs having alkylchlorosilane wall coatings are given in Section IV C.

D. Hyperfine Resonance Between States (2,0) and (1,0)

1. Klystron Stabilization

a. Earlier System and Modifications

The system for stabilizing the Varian X-26D klystron by phase locking it to the 1367th harmonic of a 5 Mc/sec crystal controlled oscillator differed only in minor ways from the system described in reference (1) which was an adaptation to higher frequencies of a circuit described by C. L. Searle (93). A block diagram is shown in Diagram 1 and several critical circuits are reproduced here in Diagrams 10 a through 10 e.

Since there was no need for a 30 Mc/sec offset , a new crystal cut to 4.99996 Mc/sec was acquired to replace the 4.999250 Mc/sec crystal, using the same circuits however. Slight retuning of the resonant circuits in the IF strip and phase lock system was necessary to use an intermediate frequency of 250 kc/sec rather than 200 kc/sec. In the later stages of the work an ultra-stable 5 Mc oscillator (to be described below) was kindly made available by Dr. E. Hafner of the Signal Corps Research and Development Laboratory whose use required slight additional retunin s.

Since 1367 is a prime harmonic of 5 Mc/sec, it was found that an improvement in the strength of the phase lock system could be achieved by mixing on the multiplier crystal some 5 Mc/sec signal directly from the oscillator along with the 40 Mc/sec from the electronic multiplier. This signal was fed through a series tuned circuit so as to present a high impedance for other frequencies. Before doing this it was necessary to rely on some fundamental frequency being present in the output of the 5 to 40 Mc/sec multiplier.

b. Locking Procedure

Care had to be exercised in locking to the correct harmonic. This could generally be measured by means of a microwave wavemeter in combination with a crystal and microammeter loosely coupled to the klystron. The wavemeter could easily be read to 5 Mc/sec. However, much time was lost in searching for the $0 \leftrightarrow 0$ resonance using the phase destruction scheme because the wavemeter was reading in error by 10 Mc/sec. The appropriate correction was found by measuring the frequency directly using a Hewlett-Packard transfer

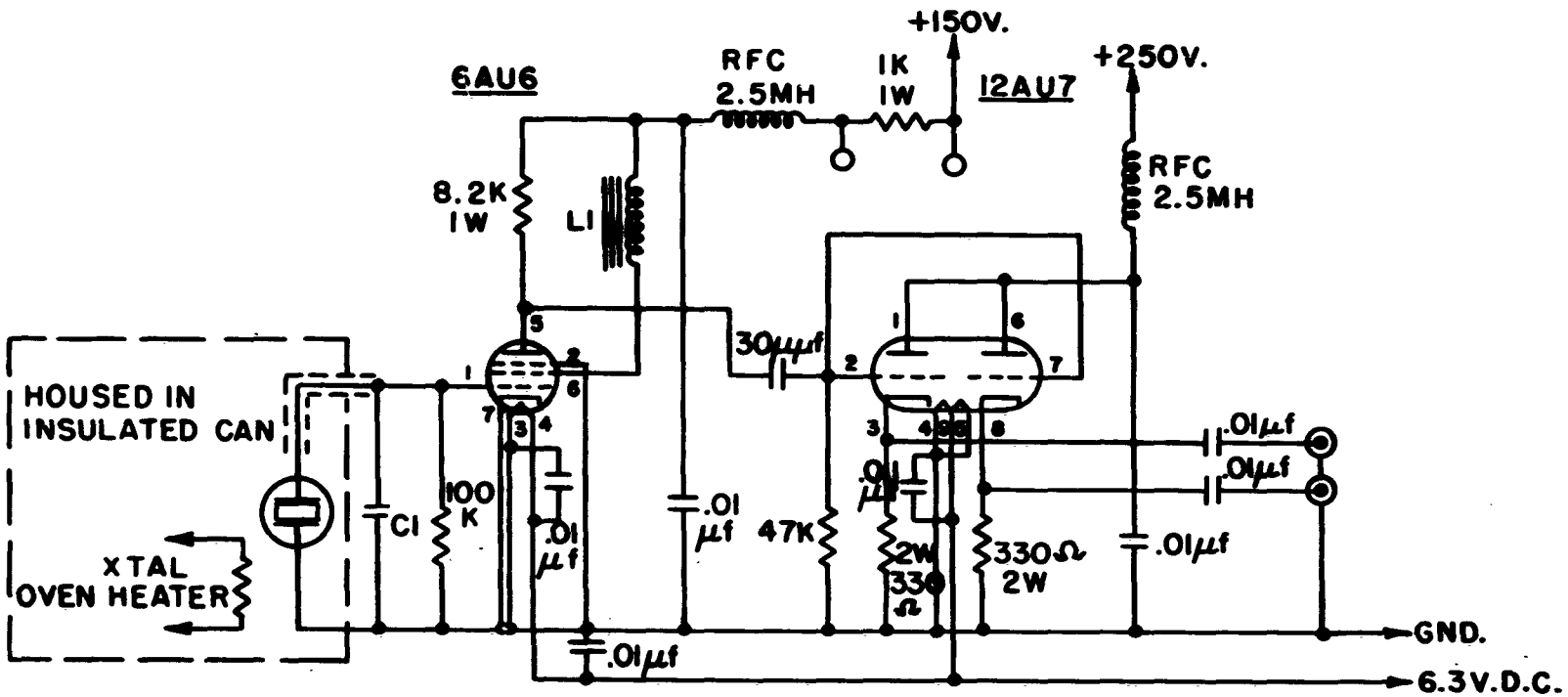

C1= 35μμf
L1= 150-250μf SLUG TUNED UNIT SCREWDRIVER ADJUST.
RFC = 2.5 MH CHOKE.

XTAL CONTROLLED 5MC OSCILLATOR

DIAGRAM 10-A

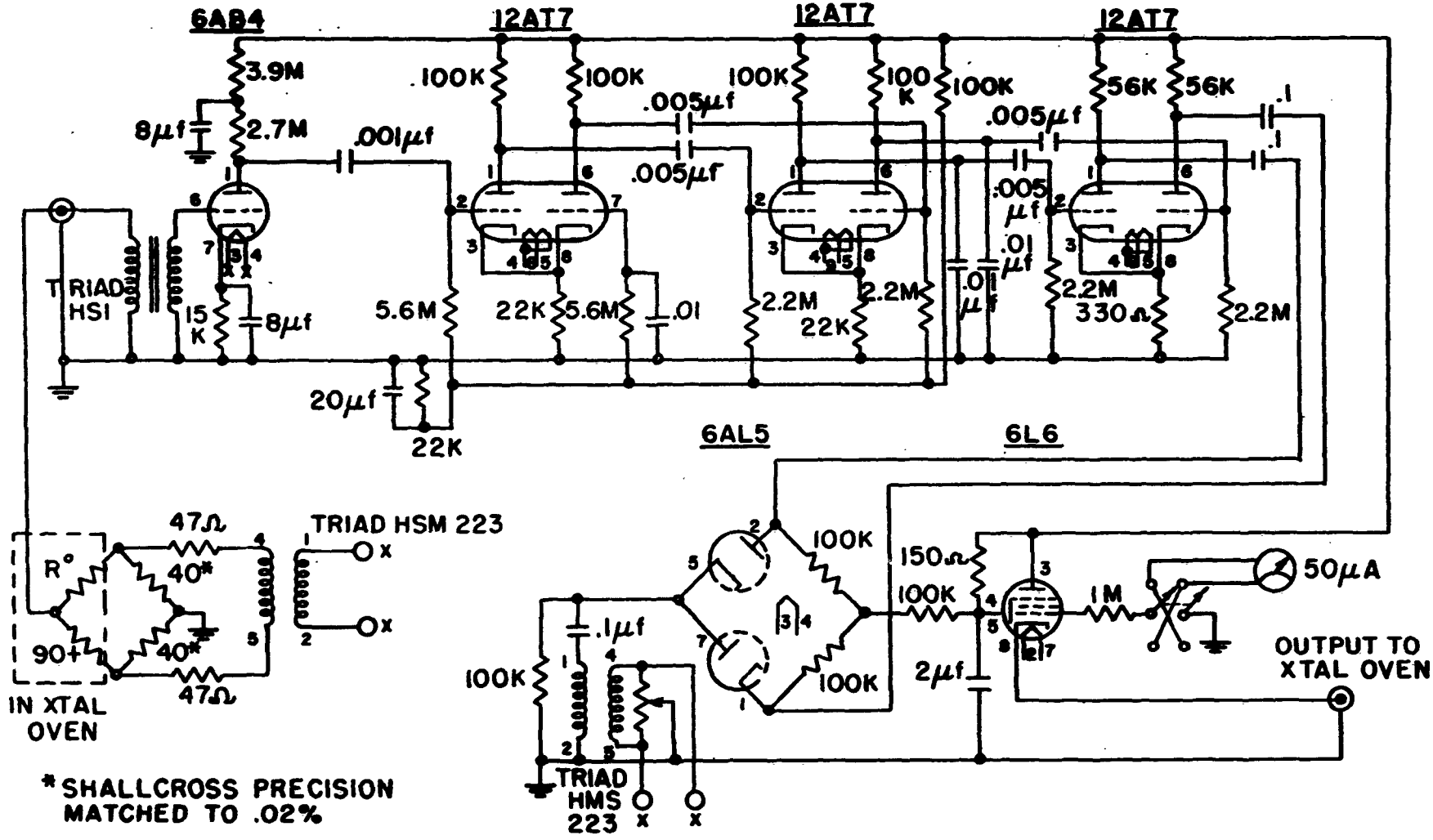

*SHALLCROSS PRECISION MATCHED TO .02%

R° RDF STIKON, TEMPERATURE SENSITIVE

xx 6.3 FILAMENTS

XTAL OVEN CONTROL AMPLIFIER

DIAGRAM 10-B

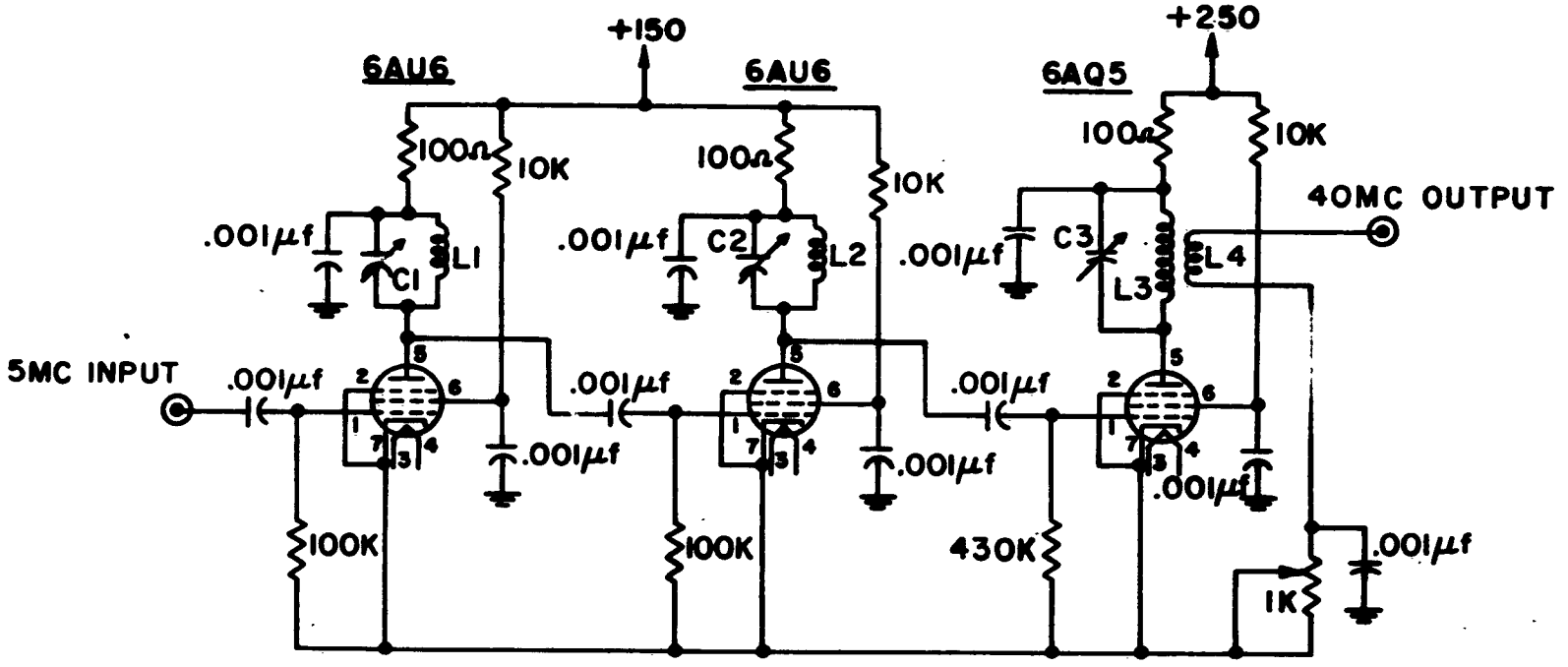

C1-L1 TUNED TO 5MC
L2 TUNED TO 20MC
L3 PRIMARY TUNED TO 40MC
L4 SECONDARY APPROX. 2 TURNS #25 WIRE

5-40MC/SEC. MULTIPLIER

DIAGRAM 10-C

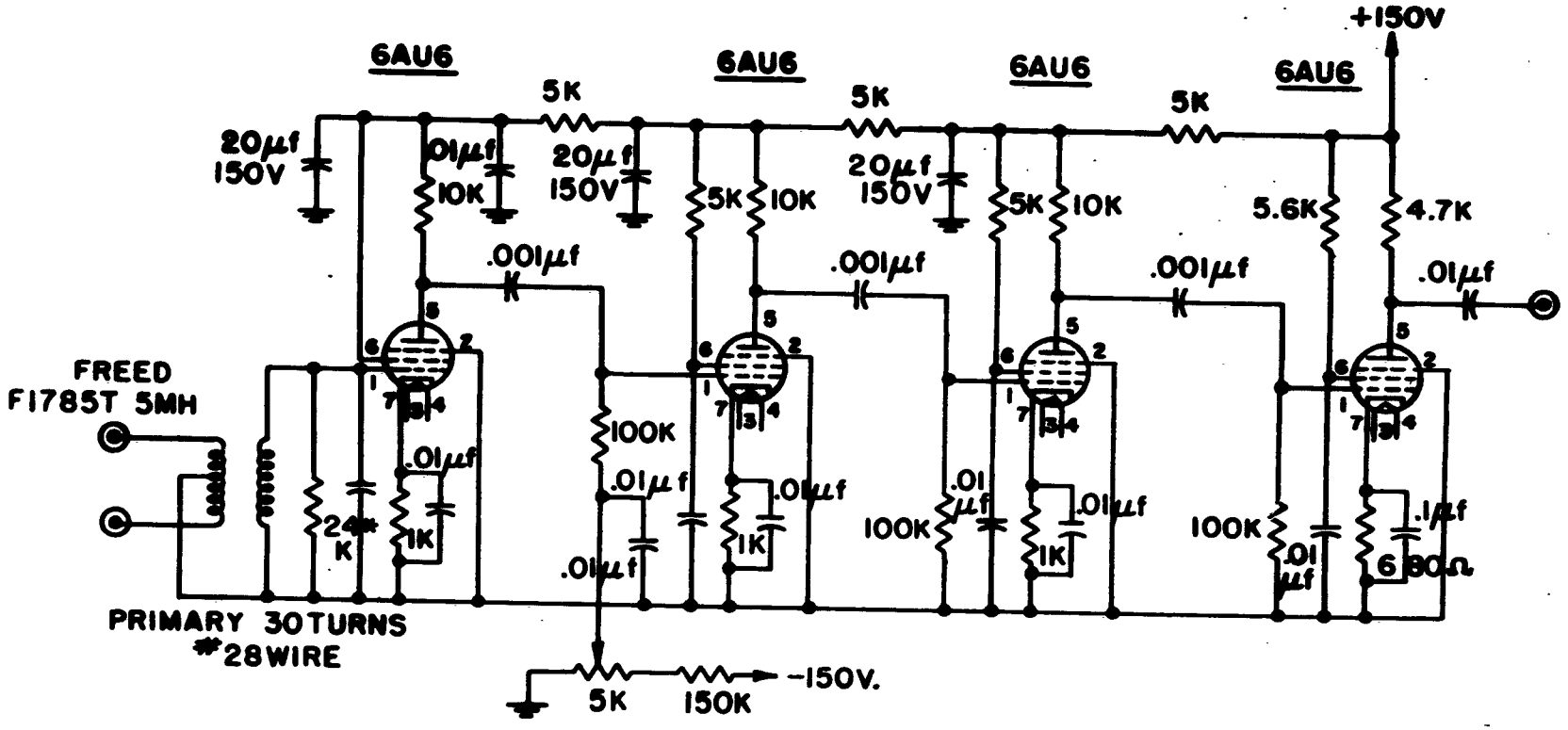

* TUNE TO 200KC APP. 40μμf

B.W.–90KC

GAIN–120DB

200KC IF AMPLIFIER

DIAGRAM 10-D

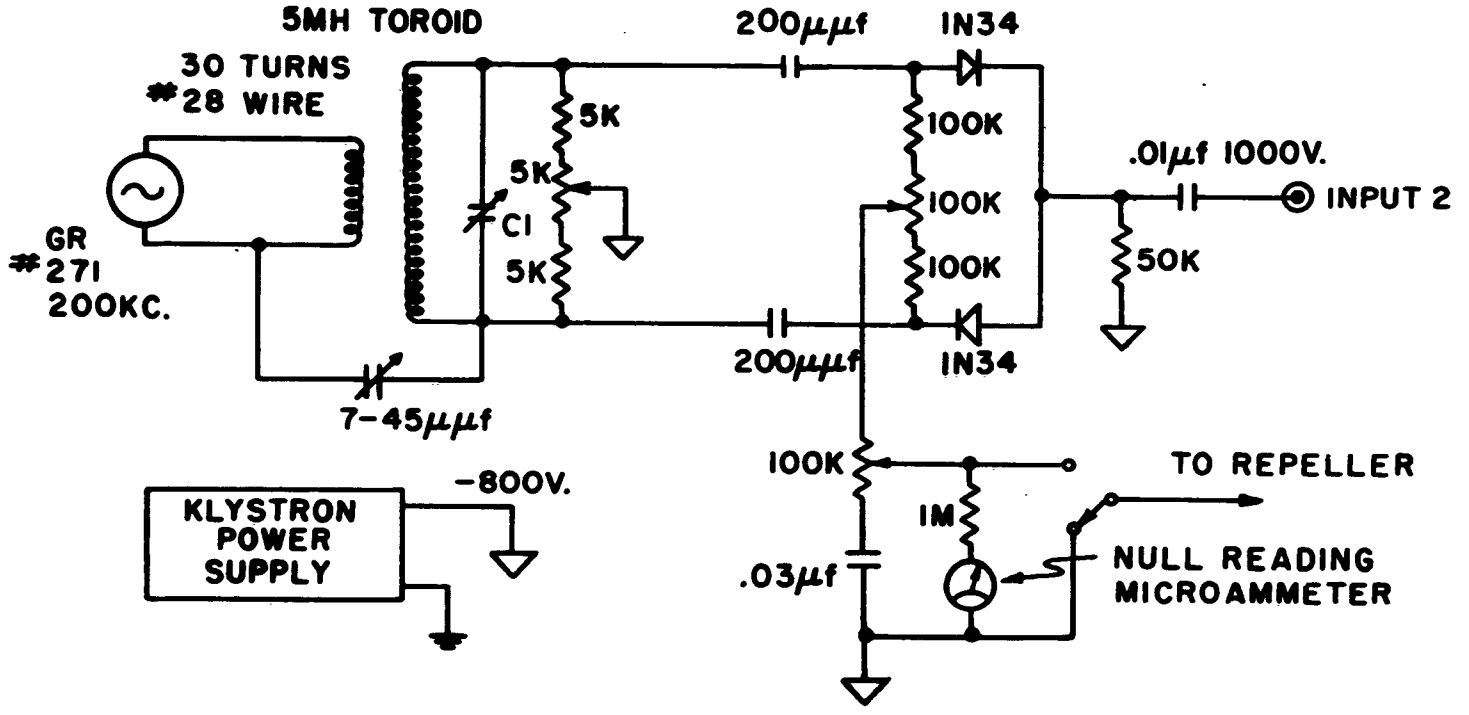

C1-TUNED TO BALANCE.

▽-COMMON INTERNAL CONNECTION AT -800VOLTS.

BALANCED PHASE SENSITIVE DETECTOR

DIAGRAM 10-E

oscillator which responded to 6835 Mc/sec although this was above its nominal range.

Caution also had to be taken in locking on the right side of the 1367th harmonic with the interpolation oscillator, its frequency needing to be subtracted from the harmonic frequency to give the klystron frequency. The condition of phase lock was maintained by using a Lissajous pattern between the IF difference frequency and the frequency of the interpolation oscillator as displayed on a 3 inch oscilloscope. At times the lock was very precarious and constant adjustment of the reflector voltage was necessary to keep the klystron locked. Frequent adjustment of multiplier crystal bias and 5 Mc/sec signal amplitude was also needed.

c. Ultra Stable Oscillator

Observation of narrow resonance lines requires high stability in the frequency being used to scan the line during the time of scanning. Since it was hoped that widths of less than 10 cps might be observed, a 5 Mc/sec crystal oscillator having a stability of at least 10^{-10} over seconds was required. An oscillator that had given evidence of stabilities of 10^{-11} over a few seconds was kindly lent by Dr. E. Hafner of the Signal Corps Laboratories. It had been constructed by him in connection with experiments on stabilizing crystal oscillators using feedback circuits of the type employed in passive atomic frequency standards, crystals of very good short term stability being combined with crystals of very low drift rate. The circuits are similar to those developed by Warner and Smith at the Bell Telephone Laboratories[37] under contract

with Dr. Hafner's group at the Signal Corps.

Physically the crystal is located in a brass cylindrical can designed to be immersed in a commercial thermally stabilized oil bath and joined to the chassis containing the circuits by three 1/8" diameter stainless steel tubes containing the leads. It required input voltages of 150 V dc, highly stabilized, and a stabilized filament voltage of 6.8 v, producing a 5 Mc/sec signal at 0.3 volts. This was not sufficient to drive the klystron phase lock system so it was amplified by a Tektronix 121 amplifier to 2 volts before being introduced.

A commercial thermally stabilized bath of the type for which the oscillator was designed was not available, so one was made using a large Dewar flask containing Prestone anti-freeze, which has a high boiling point and a large specific heat. Heat was supplied from a blade heater actuated by a mercury thermometer contact and external transistorized relay. A motor driven stirrer was used to mix the bath. This thermal control apparatus was borrowed from the Princeton Chemistry Department, and served to keep the temperature constant to within 0.01° C over minutes. During actual measurements the stirrer was disconnected for fear of vibrations causing frequency shifts although these were not severe and there was no actual evidence for such an effect.

The crystal frequency was monitored as a function of temperature using a Berkeley frequency counter and found to have its minimum around 77° C at 4.9999910 Mc/sec. The frequency as monitored on the counter would stay within 2×10^{-8}, the limit of measuring precision, over minutes but there was sometimes a drift of

5×10^{-8} over an hour. It was known before obtaining it that the crystal oscillator suffered from a large drift rate, this being the price paid for good short term stability.

The oscillator in its thermal bath can be seen in Figure 7.

2. Frequency Measurement

In the early stages of the work a system of monitoring the Loran 100 kc/sec crystal oscillator with respect to transmissions of WWV was used, as described in reference (1). However the loan by the Signal Corps of a National Company Atomichron, NAFS-1, No. 9, cesium beam atomic frequency standard, and the acquisition by the laboratory of a Hycon-Eastern 1 Mc/sec crystal controlled oscillator simplified the frequency measurements considerably. Several techniques were possible. One could use the 1 Mc/sec output of the Atomichron, certainly accurate to better than 10^{-9}, as an external timing source for a Berkeley crystal controlled counter, a precision in measuring the 5 Mc/sec crystal of 2×10^{-8} being possible in a 10 second count. Frequently the Atomichron was used to monitor the drift rate of the Hycon 1 Mc/sec oscillator, this being offset slightly, and the two signals compared in a transistorized phase detector shown in Diagram 11. The Hycon oscillator displayed drift rates of less than 10^{-10} per day. It could then be used as the timing base for the Berkely counter rather than the Atomichron itself, the Atomichron being used only occasionally to check the crystal frequency.

The presence of the Atomichron was indispensable to an experiment on gravitation carried out by W.F. Hoffmann which required monitoring the period of a high frequency ($\sim$ 22 cps) gravitational pendulum during the course of a year.

During the last several months of the investigation, the Atomichron was required by the Signal Corps for use in experiments on the world wide synchronization of atomic clocks (WOSAC)[95] and was subsequently lent to Harvard for use in the hydrogen maser investigations..[96] Reliance on the measurements of hyperfine line shifts due to wall coatings was then placed on the continued stability of the Hycon oscillator.

During the WOSAC experiments a 133 1/3 kc/sec atomichron stabilized signal was radiated from the Signal Corps Laboratories at Fort Monmouth, about 50 miles from Princeton. Using simple receiving circuits consisting of an antenna, tuned circuits and an amplifier, the signal was recognized by comparing it with the 100 kc/sec signal from the Atomichron before it was removed, a stationary lissajous pattern resulting. However, the reception was not always good, the signal was propagated only at certain times, and during the last months of investigation was not available, so that the method was not effective as a replacement for the Atomichron, although in principle it could have been.

The internal crystal of the Berkeley counter was adjusted frequently to agree with the Atomichron or the Hycon oscillator, and provided sufficient stability for measurements of the interpolation oscillator frequency to 10^{-6}.

The interpolation oscillator used to sweep through the hyperfine resonance was a General Radio Model 271, designed primarily for measuring frequencies, which was stable to a cycle at 250 kc/sec and posessed an internal circuit enabling frequency changes to be monitored to a few cycles by a moving pointer and dial. This feature was used in estimating the line width of the $0 \leftrightarrow 0$ hyperfine resonance when it proved difficult to display it on a chart recorder (See Section IV B 2 below).

3. Coupling of Microwave Field to Gas Cell

Before the shielded solenoid was introduced, a section of wave guide was extended using a half twisted section to allow energy to be radiated onto the gas cell from the open end of the wave guide with the B field parallel to the vertical field B_o. Very little field strength was needed to connect the (2,0) and (1,0) states so there was no need of a cavity to enhance the field strength.

There was not sufficient space in the shielded solenoid to bring in wave guide sections so a UHF to waveguide adapter was used as the radiating element inside the solenoid. It was joined to a similar adapter by a 6 foot length of low loss coaxial cable, contributing only a few db loss. There was sufficient power available from the klystron ($\sim$50 mw) that this price could easily be paid, and indeed an attenuator before the coaxial connection was used to avoid saturating the resonance.

The possible desirability of placing absorbing material for the microwave energy to avoid reflections and standing waves was recognized but this was not tried.

4. Detection of the Resonance by the Phase Destruction Method

Most observations were made visually on an oscilloscope screen on the manner in which the second 90° pulse affected the light intensity, as described in detail in Section IV A. The observable effect was the vanishing of the 60 cps modulation of this transmitted light intensity when the phase relations were altered by the microwave field.

Since it proved difficult to eliminate this 60 cps modulation, it was decided to exploit it in a phase detection system to display the resonance as a dc signal on a chart recorder as one swept through the resonance using the interpolation oscillator.

A variable phase 60 cps signal was obtained by rotating the rotor of a synchro generator which was provided with a rotating field from a 60 cps three-phase source. This was used as the reference signal for the type of transistorized phase detector shown in Diagram 11. Since the rubidium $\sigma^{+}D_1$ detection and pumping light beam was cut off during the interval between the two 90° pulses, this constituted a very large signal in contrast to the variation caused by the 60 cps modulation after the pulse sequence ($\sim$100 volts compared with $\sim$1 volt). Accordingly a gating circuit was made to interrupt the signal from the phototube pre-amplifier combination and allow it to pass only after the occurrence of this unwanted signal. The signal, consisting of a decaying exponential caused by the recovery of the spin orientation under optical pumping and the consequent change in light transmission, recurring say 22 times per sec (one repetition frequency used), and having its amplitude modulated at 60 cps was the

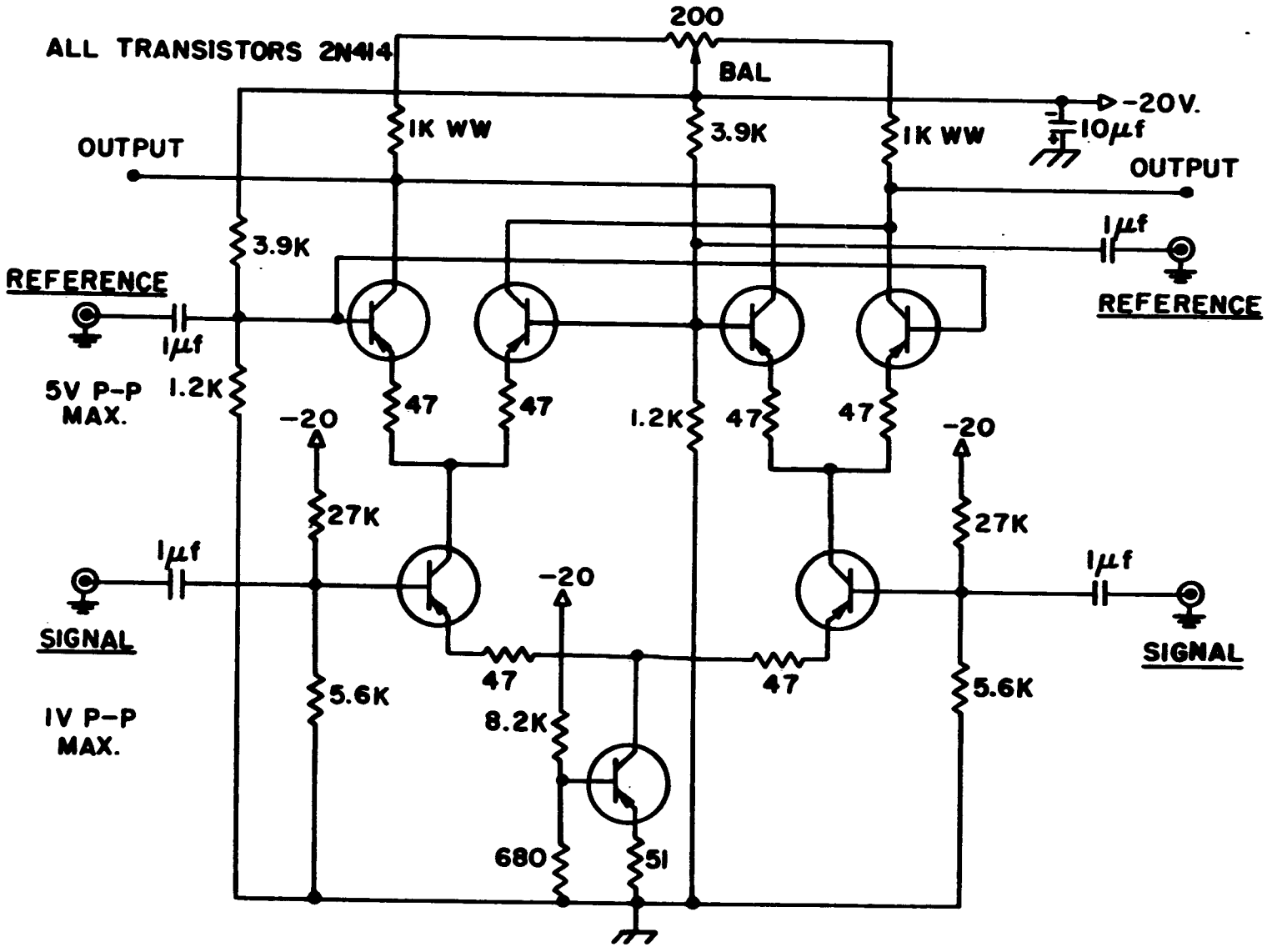

BALANCED TRANSISTOR PHASE DETECTOR

DIAGRAM II

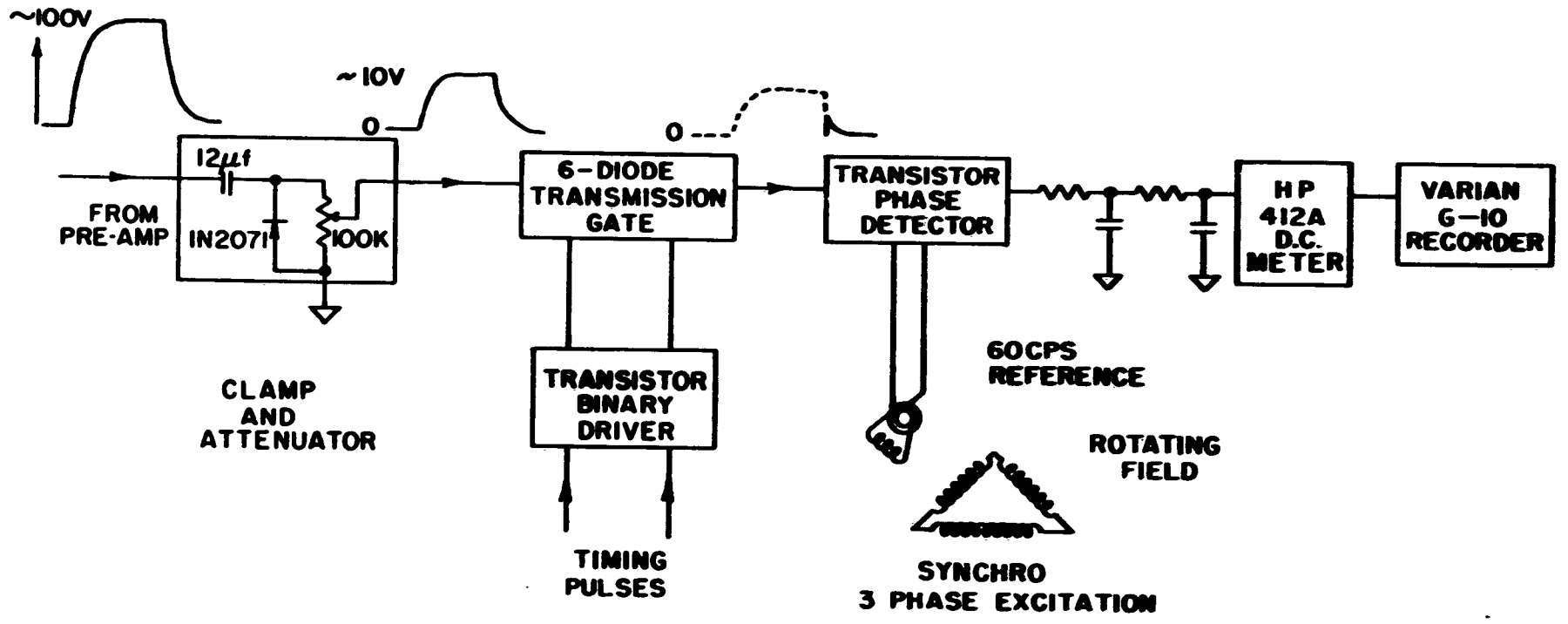

PHASE DETECTION WITH 60cps REFERENCE

DIAGRAM 12

input to the phase detector. The phase detector served the purpose of creating a dc signal by synchronous rectification of the 60 cycle component of the signal. The output of the phase detector was amplified by a HP 412 A chopper stabilized dc meter and applied to a Varian G-10 recording potentiometer. Some of the circuits are shown in Diagram 12.

5. Possible Methods of Pulsing the Microwave Resonance

Narrowing of the resonance beyond the width predicted from the T_2 relaxation time could be expected to result from applying the microwave radiation in two coherently phased pulses at the beginning and at the end of the interval between the 90° pulses, as discussed in Section I D and in Appendix C.

Since the resonance is so narrow a shift of frequency by a few kilocycles is equivalent to having the radiation completely absent. One scheme which was briefly explored experimentally was to shift the klystron in and out of phase lock by changing the reflector voltage by means of a transistor flip-flop circuit in series, having its own floating battery supply. Difficulty was experienced in triggering the floating flip-flop circuit and the matter was not pressed further although such a scheme would probably work. The question of the speed of response of the phase lock in recovering the locked state would be the most critical one.

The use of a ferrite microwave switch employing the Faraday effect was studied but it was concluded that too much power would be necessary to switch the condition in a millisecond or less, since the magnetic fields needed are not small.

A crystal diode microwave switch relying on the change in reflection as the crystal bias is changed was actually acquired but the change in transmission that was possible was not great enough. Several such switches in cascade would have been required.

The most promising scheme would be to use a type of balanced modulator and mix in a frequency of, say, 10 kc/sec to shift the resonance, leaving the amplitude and phase lock system unchanged. It is quite easy to pulse such a low frequency signal, which could be derived from the 5 Mc/sec frequency in the phase lock system.

E. Optical and Photo-Detection System

1. General Considerations

The optical requirements for optical pumping purposes are not all severe, it being necessary merely to illuminate the resonance cell with a large photon flux, having the directions of propagation more or less along an axis, but angles of deviation of 20° to 30° can be tolerated. For a given source of optical resonance radiation, (See Section III A), the problem is then one of collecting the radiation over as large a solid angle as possible. After the light has passed through the cell the problem is again simply one of collecting it and conveying it to a suitable photodetector for conversion to a current. One needs to worry about collimation only if spectral filters are used at some point in the system.

The use of a vertical system enabled gravity to be employed in positioning components of the system, as can be seen in Figures 5 and 6.

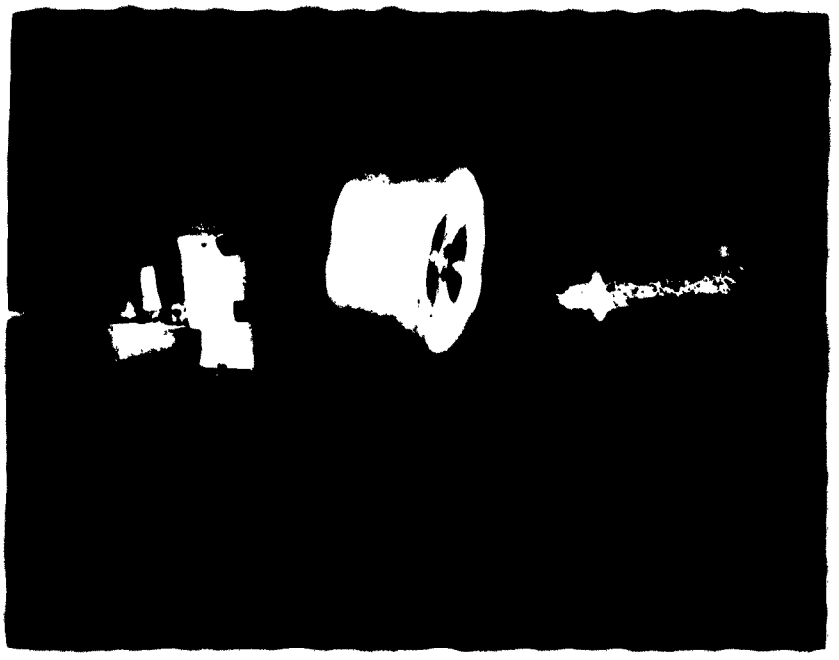

FIG. 17 SOME ELEMENTS OF THE OPTICAL SYSTEM

2. Collection of Light

If lenses are used they need to be of low f number but can be of poor optical quality. The use of plastic Fresnel lenses was found to be quite satisfactory. The first kind used were 15" in diameter having an f value of 1, commercially offered to serve as "solar furnaces." The use of two of these adjacent to one another improved the f number. Later, better quality plastic Fresnel lenses[97] were obtained having an f value of 0.6 and a four inch diameter. One of these lenses can be seen in Figure 17. It was fitted into a polystyrene foam disk which made a snug fit into the cardboard tube shown in the figure, adjustments in its vertical position being easily made for the purpose of focusing.

The most effective system used the large area source described in Section III A, with one of these lenses placed to roughly form the light into a parallel beam. A second identical lens about 3 feet away was incorporated into the thermal enclosure of the bulb described in Section III B 4, and formed an image of the source at the center of the bulb. A third similar lens was incorporated into the bottom structure of the thermal enclosure to collect the light from the cell and a fourth similar lens about 2 feet further on focused the light onto the cathode surface of the phototube. Optical pumping time constants $1/\gamma'$ on the order of 1 millisecond could be achieved under the most favorable conditions in the source.

3. Polarizing Filters

Land Polaroid HN-22 polarizers were found to be effective near 8000 A where the D lines of rubidium lie. They were combined

with plastic quarter-wave retardation plates made especially by Polaroid for this near infra-red region to give circularly polarized radiation.

The plastic Fresnel lenses described in the preceding section were found by experiment not to disturb the polarization appreciably, which seems remarkable. Therefore the σ^+ polarizer could be placed before the lens which forused the radiation onto the resonance cell, which was a convenience.

In experiments with polarizers suitable for use in the polarization bridge discussed in Appendix B, Polaroid types HN-7 and HR were found to be more effective for extinction when crossed than the type HN-22. However, this has a greater transmission and was thus more useful for polarization purposes.

4. Spectral Filters for the D Lines

Suppression of one of the D lines is very desirable for optical orientation and optical detection of resonances as is explained in detail in Section II A. Very effective dielectric multilayer filters for the purpose were obtained from Spectrolab, Inc.[98] They possessed an acceptance angle of $\pm$ 12° and had a transmission of 80-90%. Both 3 inch diameter round and 2 inch square filters were obtained to pass either the D_1 or the D_2 line.

This type of filter was mounted in a lucite frame and placed adjacent to and above the polarizing filter, where the light was fairly well collimated.

For some experiments on wall coated cells, for which both D_1 and D_2 σ^+ pumping orient in the same sense, as explained in

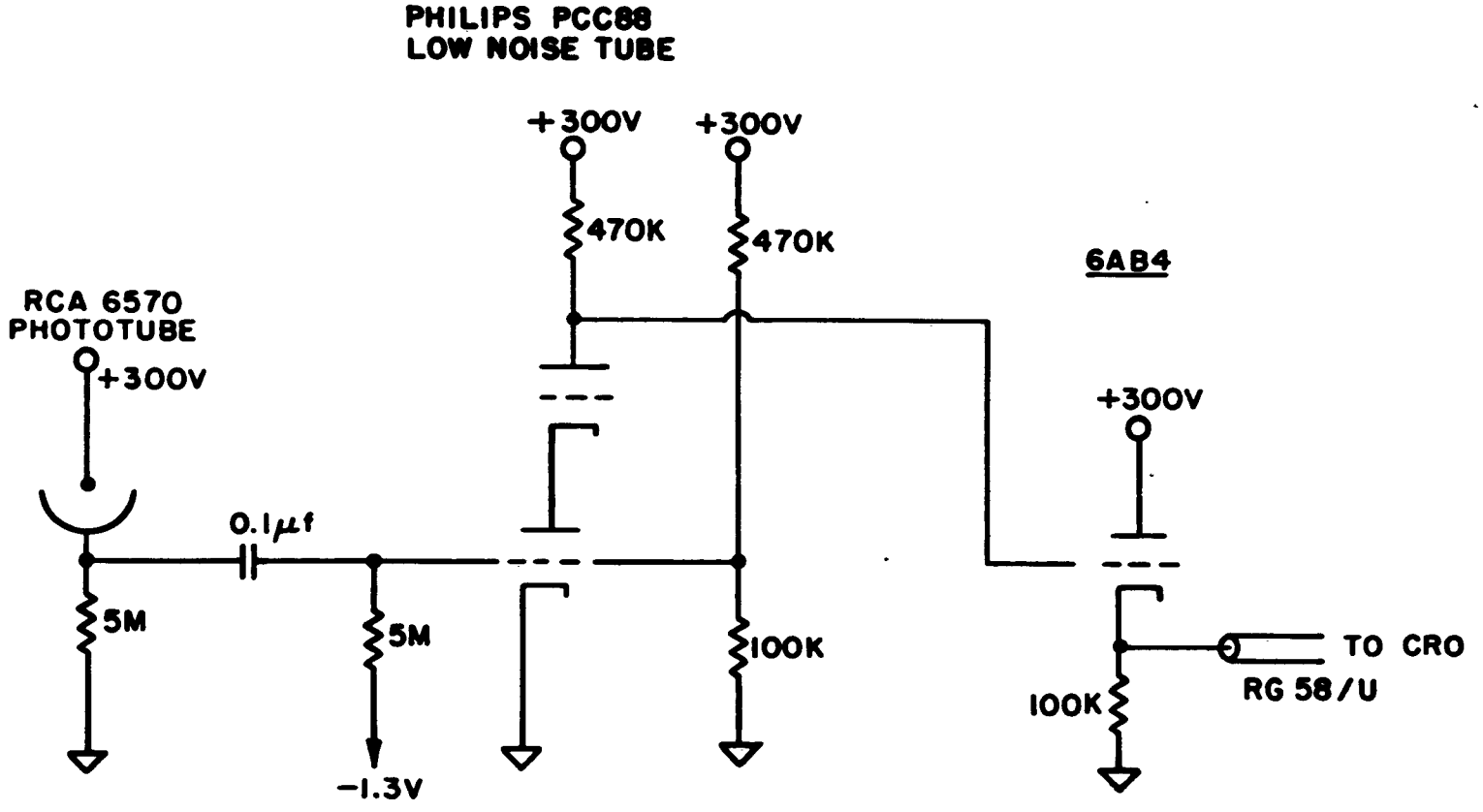

ALL FILAMENTS FROM 6V STORAGE BATTERY

PHOTOTUBE CASCODE PRE-AMPLIFIER

DIAGRAM 13

Section II A, no filtering of the incident radiation is necessary. However, it is sometimes desirable to filter the radiation before it is incident on the photo detector since the detection signals are of the opposite sign for D_1 and D_2.

5. Photo-Detection

Vacuum photo tubes were used throughout the investigation, the type RCA 6570 being used almost exclusively. It has an S-1 surface which is suitable for the near infra-red region, and has the electrodes ruggedly supported at both ends of the structure. The efficiency of photons for the production of electrons at an S-1 surface is not very high: only 1 electron for every 250 photons around 8000 Å using information from the tube data sheet.

The phototube was used with several different pre-amplifiers during the development of the research, the most successful of which was a cascode type having a gain of several hundred using a double diode. The Philips type PCC88 double triode gave the best noise figure. The circuit is shown in Diagram 13. It was necessary to energize the filaments with dc from a storage cell to reduce 60 cycle pick up.

Signals for a 180° rotation of oriented spins by pulsed Zeeman resonance could be achieved of nearly 10 volts amplitude under favorable circumstances for the light source, with a noise of less than one millivolt, this coming chiefly from the photon shot noise associated with the beam of detection light, with no bandwidth limitation other than the cathode ray oscilloscope response of 5 Mc/sec. Signals of a few volts were more usual. The phototube housing and pre-amplifier combination can be seen in Figure 17.

IV. EXPERIMENTAL RESULTS

A. Demonstration of the Phase Destruction Method of Detecting the (2,0)←→(1,0) Resonance

1. Initial Results

a. Single 180° Pulse; 60 cycle Modulation

With the very inhomogeneous magnetic field described in Section III C, no effects of the microwave field on the intensity after the second 90° pulse were observed until the time interval between the 90° pulses was reduced to 2 milliseconds and a 180° pulse interposed to utilize the spin echo effect as described in Section II C 7. The observations are best described by referring to Figure 18 showing oscillograph traces of the output of the photocell preamplifier combination during the rf pulse sequence-- + 90°, 180°, - 90°--described in Section II E, which is shown at the top of the figure. The gas cell contained Rb^{87} with 5 cm Hg of Neon as a buffer gas and was held at a temperature of 45° C.

The transmitted intensity of the $\sigma^+ D_1$ light sometimes increased and sometimes decreased after the second 90° pulse with a beat frequency between the pulse sequence repetition rate (about 25 cps) and the 60 cps external time varying field, as shown in the middle picture of Figure 18 (a). The interpretation of this is that the 60 cycle field is detuning the resonance so that sometimes the second "90" pulse is + 90°, sometimes - 90° and sometimes an intermediate rotation, depending on the strength of B_o as modified by the 60 cycle magnetic field, as described in Section II C 8.

The effect of the continuously applied 6835 Mc/sec microwave field coupling the (2,0) and (1,0) states on resonance is shown in the bottom picture of Figure 18 (a). It seems to destroy the phase relations in such a way that the average effect on the bulb is to completely remove the beating in the response to the -90°pulse.

The size of the obtainable signal is clearly comparable with that resulting from a 90° rotation of the oriented atoms, this being given by the change in light intensity following the first 90° pulse. The noise is not nearly so large as would appear from the pictures. There was a slight oscillation in the light source which appears as noise in the photographs, but this was subsequently eliminated.

b. Pulsing of Lights

The relaxing effects of the incident light during the interval between the 90° pulses is evident in Figure 18 (a). The sudden change produced by the 180° pulse is a measure of the degree of orientation produced by the j^{+} pumping light. Absorption of a photon by a freely precessing atom results in practically complete destruction of the phase relations. There is probably some small preservation of coherence in the ground state in the resonance radiation process, but this question needs further study.

The advantage of removing this optical relaxation during the free precession interval is clear from Figure 18 (b). The other experimental conditions were the same as for Figure 18(a), the center trace showing the removal of the 60 cycle induced variation of the light intensity by the microwave resonance. The lights were pulsed off using the transistor switch described in Section II A 4. The gain

differs from the conditions in Figure 18 (b) by a factor 10, so an increase in the signal by a factor of 3 or 4 has been achieved.

It was not possible to lengthen the interval between 90° pulses beyond 2 milliseconds even with the elimination of optical pumping relaxation because of the large inhomogeneities.

c. Multiple 180° Pulses

A demonstration of the effectiveness of the Carr-Purcell technique[24] of preserving the phase memory of freely precessing atoms as they diffuse in a region of inhomogeneous magnetic field as described in Section II C 7 was made by inserting 5 180° pulses between two 90° pulses separated by an interval of 10 milliseconds, the other conditions remaining as before. The top trace in Figure 18 (c) shows the spacing of the pulses, while the lower two traces show the effect on the transmitted light, the bottom one being taken with the microwave radiation continuously on resonance. The 60 cycle induced variation after the second 90° pulse and its removal by the microwaves were clearly visible in the original oscilloscope traces, but do not show up well in the reproduction.

Blanking of the incident light gave an increase in the signal, although not as much as for the 2 millisecond interval, due to the action of other dephasing relaxation processes during the 10 millisecond interval. This is shown in Figure 10 (b).

d. Lock-in Amplifier Recorder Trace

The signal described in Section IV A 1 a above was fed into a phase detector whose reference was a square wave at

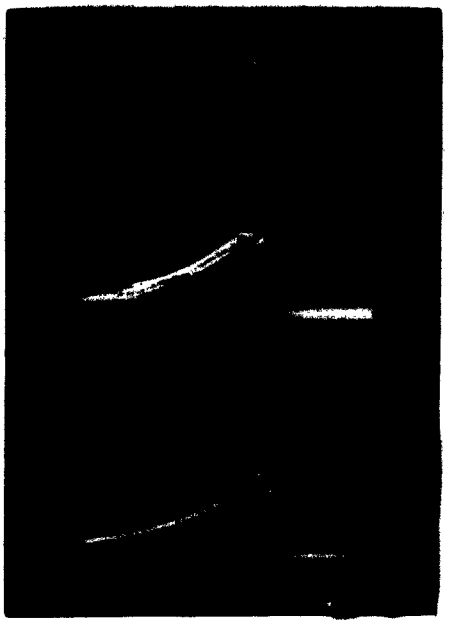

(a) 2 MILLISECONDS BETWEEN 90° PULSES.

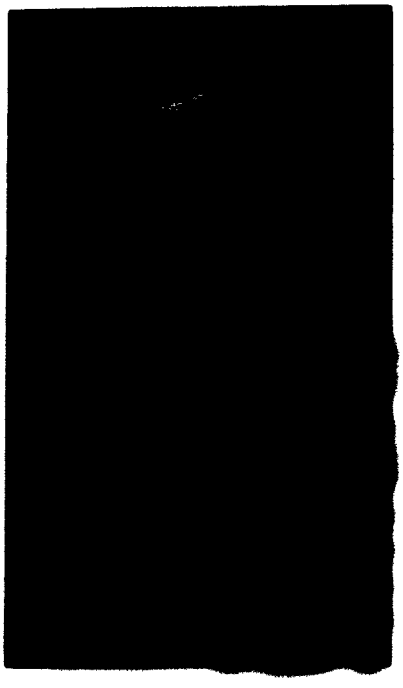

(b) LIGHTS OFF DURING INTERVAL OF (a)

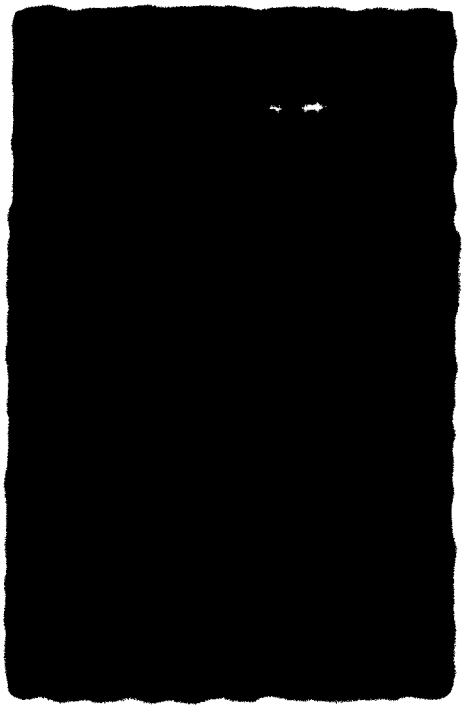

(c) MULTIPLE 180° PULSES 10MS TOTAL INTERVAL

TIME INCREASES FROM RIGHT TO LEFT

FIG. 18 PHASE DESTRUCTIVE DETECTION

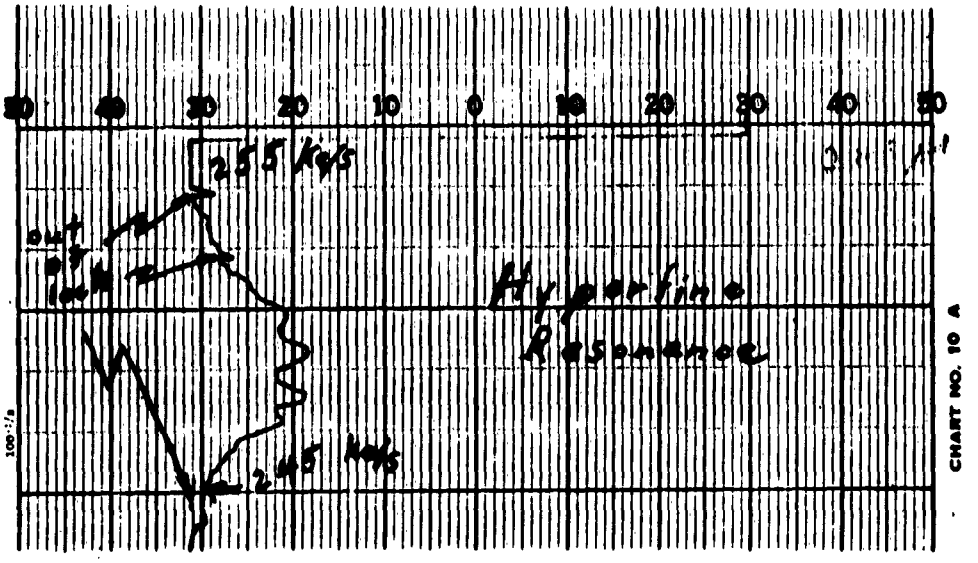

FIG. 19 RAMSEY PATTERN FOR PHASE DESTRUCTIVE DETECTION.

the pulse sequence repitition frequency of about 22 cps. The 60 and 120 cps suppression filter described in Section II C 3 was used. As the microwave frequency was manually swept through resonance the dc output as displayed on a Varian G-10 chart recorder showed a plateau about 10 kc/sec wide on which was superposed an inverted Ramsey pattern,[99] the central peak being about 500 cps wide. The recorder trace is shown in Figure 19.

This was the type of resonance expected, the 10 kc/sec plateau width being attributed to the 10^{-4} second 90° pulses and the 500 cycle width being that expected from the 2×10^{-3} second effective measurement time between the 90° pulses.

Most subsequent work involved visual observation of the resonance in which line widths could be estimated by the method described in Section III D 4.

Since the observation of the $(2,0) \leftrightarrow (1,0)$ resonance was so readily made visually using the oscilloscope presentation of the response to the second 90° pulse, the further development of a phase detection system to record the resonance was not pressed. The system mentioned above used a lock-in amplifier of relatively ancient vintage which gave considerable trouble in this particular application, particularly because of the difficulty in removing its tendency to respond to very weak 60 cps signals.

In the last stage of the investigation when the ultra-stable oscillator crystal oscillator described in Section III D 1 c was available, an effort was made to obtain a dc signal from the (2,0) ··(1,0) resonance for use with a chart recorder. This is described below in Section IV A 2b.

2. Later Results

a. Visual Detection for Longer Intervals

With the increased homogeneity brought about by the shielded soleonoid described in Section III C 2 b, it was possible to preserve phase relations in the freely precessing atoms for much longer intervals. Using a single 180° pulse between the two 90° pulses, an interval of 22 milliseconds for a 5 cm Ne Rb^{87} bulb was readily demonstrated by the 60 cycle modulation described above. The time interval could probably have been lengthened further since the signal was quite strong, although because of certain experimental inconveniences this was not done. The improvement in the homogeneity was thus in excess of a factor 10. The switching off of the lights during this interval was, of course, essential.

Observation of the $(2,0)\leftrightarrow(1,0)$ resonance by means of variation of the oscilloscope trace, as described before, was equally easy, although the variation caused by the 60 cycle magnetic field was different because of the shielding (See Section II C 8).

Figure 20 shows the effect of the microwave radiation at the $(2,0)\leftrightarrow(1,0)$ hyperfine frequency on a different time scale from that previously presented in Figure 18 so that the reduced beat frequency between the pulse repetition frequency and the 60 cycle magnetic field variation is apparent, as discussed in Section II C 8. The time interval τ between 90° pulses (no 180° pulse is interposed) are 2, 3, 4, and 6 milliseconds, respectively for Figures 20a,b,c and d. The upper trace in each of the dual trace pictures is the magnetic field at the position of the gas

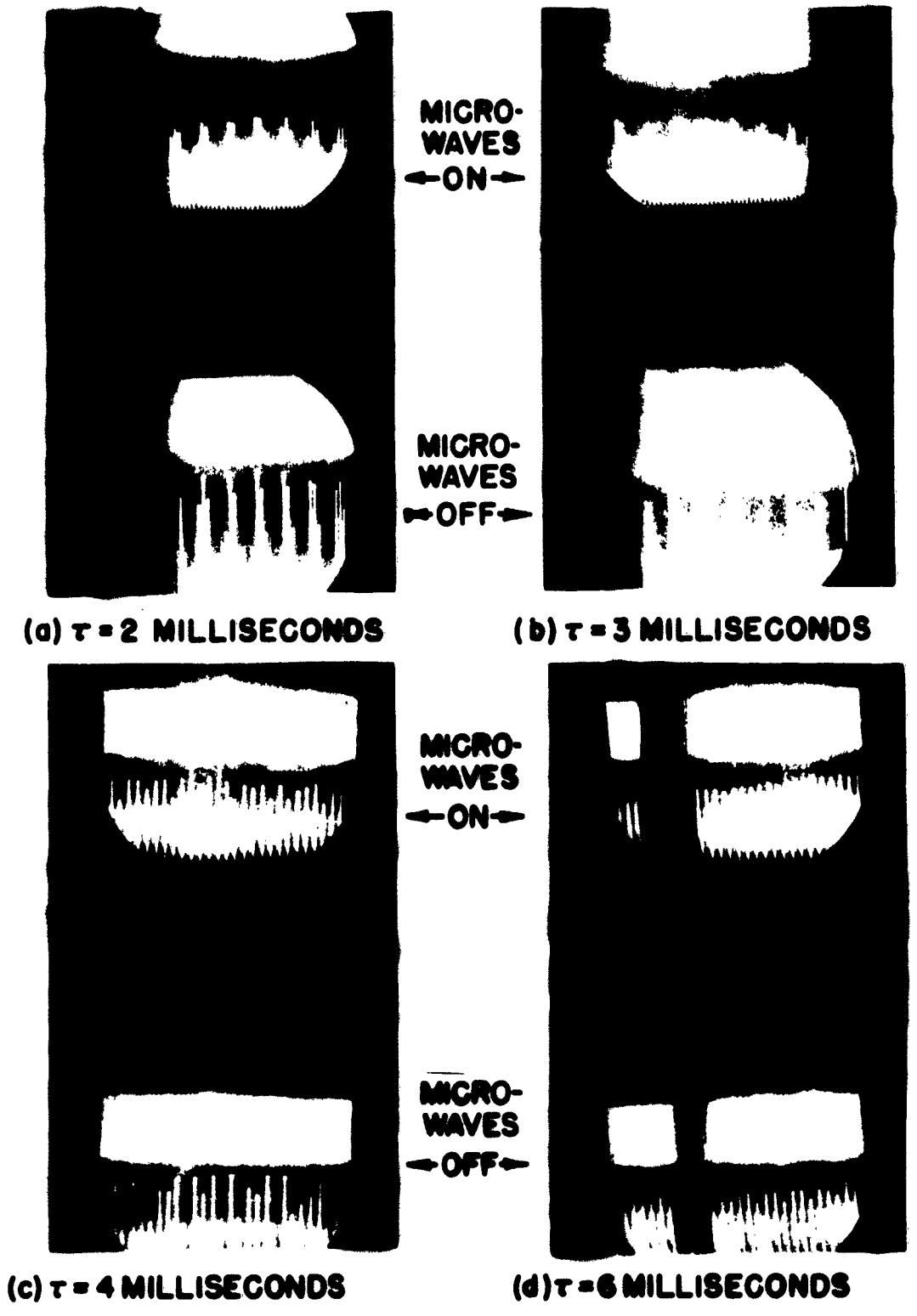

FIG. 20 PHASE DESTRUCTIVE DETECTION FOR SEVERAL INTERVALS BETWEEN 90° PULSES, τ

cell which had a peak to peak amplitude of about 1/2 milligauss. This cell was coated with SC-02 Dri-Film and was of the "Lobster Pot" type. Similar traces were obtained for other cells.

As the interval t is lengthened, the magnitude of the variation after the second 90° pulse is reduced because of the greater relaxing effect of the light. Also the strong periodicity at the reduced beat frequency is diminished at longer intervals, being replaced by a more nearly random variation, which is still strongly affected by the microwave resonances, however. The randomness is only apparent and results from the appearance of higher harmonics as the interval t is increased, since this affects the arguments of the Bessel functions which are the amplitudes of these harmonics, as explained in the analysis in Section II C 8. From this analysis, since the argument of the Bessel functions is proportional to $\sin \frac{\pi}{T_c} \tau$, one would expect the single periodicity to be recovered as one continues to increase τ . There was not a sufficient increase made of τ to show this experimentally, however.

b. Phase Detection

Although it was not necessary to use phase detection to observe the $(2,0) \leftrightarrow (1,0)$ resonance using the phase destruction method since the visual oscilloscope signal was so strong, a method of deriving a dc signal from the variations in light intensity following the second 90° pulse is desirable for recording the resonance. The situation is complicated considerably by the presence of the 60 cycle magnetic field which, because of practical difficulties in the existing apparatus, it was not possible to reduce to a sufficiently low

level, as discussed in Section II C 2 c., and by the need to cut off the lights during long intervals τ, creating a large signal at the pulse repetition frequency. Although the use of this frequency as a reference in the phase detection system described above in Section IV A 1 d seemed to be satisfactory in principle, it would not be satisfactory when the lights were being pulsed without modification.

The light pulsing signal was strongly reduced by making an electronic transmission gate to pass the output of the phototube preamplifier only during an interval following the second 90° pulse, when the transmitted light had very nearly recovered its former value, variations in this value constituting the signal, as described in Section III D 3.

The use of the other reference frequencies was explored experimentally. The reduced beat frequency was produced by using a transistor phase detector of the type shown in Diagram 11 to mix a square wave at the repetition frequency with the variable phase 60 cycle signal derived from the synchro as described in Section III D 3. A second phase detector of the same type was then used with the reduced beat frequency serving as reference and the signal from the phototube described above serving as the input. The output of the second phase detector was amplified by a HP412A chopper stabilized dc meter-amplifier and applied to a recorder, as described in Section III D 3.

The system worked well at times, but since there was no fixed phase relation between the repetition frequency and the 60 cycle field, it required frequent adjustment of the phase of the

60 cycle reference. Thus it was not suitable for continued experimentation on different gas cells under a variety of conditions.

The use of the 60 cycle field as reference in single phase detection was tried as discussed in Section III D 3. This was more stable than the double phase detection described immediately above and gave very strong signals but still suffered from defects. It was not sufficiently sensitive to the signal produced by the microwaves during the active interval τ so that the characteristic Ramsey pattern did not appear. The time constant of the dc amplifier recorder combination was too slow (several seconds) to sweep through the lines rapidly, thus preventing the recording of very narrow lines, for the ultra-stable (short term) crystal oscillator controlling the klystron frequency drifted badly.

Even with these defects it was possible to demonstrate the broadening of the lines by increased microwave power and the increase in the signal strength by cutting off the lights during the active interval.

B. $(2,0) \leftrightarrows (1,0)$ Hyperfine Resonance

1. Line Shifts

a. Buffer Gases

The only buffer gases used were neon and argon. No special effort was made to measure the pressure shifts but the results were in agreement with the data published by P.L. Bender[100] and M. Arditi[101] for those few pressures used in the experiments:

$$\text{e.g.,}\quad 5 \text{ cm Hg Ne},\ R_b^{87} \Longrightarrow +17{,}400 \text{ cps}$$

The frequency 6834.6826 Mc/sec is taken as the unperturbed value. (102)

b. Wall Coated Cells

The measurements were made during the last months of the research when the Atomichron was no longer available so reliance was placed on the continued stability of a Hycon Eastern 1 Mc/sec oscillator, as discussed in Section III D 2. They were complicated by the rapid drift rate of the ultra-stable (short term) oscillator used to stabilize the klystron in the hope of obtaining narrow lines, as discussed in Section III D 1 c. Furthermore, the center of the resonance was determined visually because of the rather unsatisfactory performance of the recording system used. These factors made it difficult to determine the center of the resonance to better than 100 cycles.

Some measured shifts at a temperature of 40° C were:

Paraflint	- 6900 cps
Sc-02 Dri-Film	- 4200 cps
Sc-77 Dri-Film	- 4600 cps
Diethyldichlorosilane	- 6000 cps
Sc-77 Dri-Film (1" cell)	- 7800 cps
Diethyldichlorosilane (1" cell)	- 5400 cps

All bulbs were 2" in diameter except where noted and contained natural rubidium. The data were taken with a 4 millisecond interval between the 90° pulses.

Except for the general large negative shift, one should not attach too much significance to the relative values of these numbers, since the technique of applying the coatings is still something of a "black art."

The shift is much larger than was expected and represents a phase shift per wall collision much larger than for buffer gas collisions, since there are about 10^{-4} fewer wall collisions per second than buffer gas collisions at a few cm Hg buffer pressure. It is much larger (by $\sim$ 10) than similar results reported for cesium in the storage box atomic beam experiments at Harvard.(81)

c. Light Intensity Shifts

The evidence for the effectiveness of removing the light during the active resonance interval between the 90° pulses for removing this type of shift is rather inconclusive because of the experimental difficulties mentioned above in measuring the shifts. However, measurements were made both with lights on and with lights off and there was some slight evidence for a shift in the resonance frequency between the two conditions.

If the spectral distribution in the light source is sufficiently asymmetric to produce a light shift as discussed in Section II D 3, the method of pulsing the lights should be an excellent one for avoiding the effect and still retaining the advantages of optical detection.

2. Line Widths

a. Visual Observation

Using the Bliley 5 Mc/sec crystal in the klystron stabilization system the line widths seen were about 200 cps even with very long separations T_1 between 90° pulses which should give widths

$$\Delta \nu = \frac{1}{2\pi t}$$

of a few cycles. This was attributed to the poor short term stability of this crystal. It was not the same crystal (although of the same type) as the one used in the microwave detection experiments which yielded a line width of $\sim$80 cps in reference (1).

With the ultra-stable (short term) oscillator it was hoped that such very narrow lines might be seen. However, the narrowest lines observed were about 60-80 cps with both buffer gas and wall coated cells, a visual estimate being made as described in Section IV A 2, independent verification being made by several colleagues. The time intervals were such as to predict widths of about 10 cycles. The reason for this discreppancy is not clear. It may be that the oscillator was not being operated under the conditions to elicit its maximum short term spectral purity.

No great effort was made to obtain these narrow lines with the existing equipment since it is clear that the method will yield such narrow resonances with improved electronic instrumentation.

b. Recorder Observation

The narrowest lines recorded were several hundred cycles in width the under conditions which yielded lines less than

100 cycles in width for visual observation. This was attributed to the several second time constant of the amplifier recorder combination necessitating slow traversals of the resonance, allowing the crystal to drift, and to the "random" element entering the signal input to the phase detector, as discussed in Section IV B 2 a.

It is clear that changes in the electronic instrumentation will enable the recording of the same width lines as are observed visually.

4. Reduction of Doppler Width by Wall Coated Cells

Since the line widths for the hyperfine resonance obtained above for wall coated cells are much less than the Doppler width of 10 kc/sec, it is clear that the Doppler reduction method proposed by Professor R.H. Dicke[3] works as predicted for confinement of atoms to dimensions on the order of a wavelength. Most previous use of this technique had confined the atoms to regions very much smaller than a wavelength, an exception being the work of Ramsey and his associates using coated wall storage cells in the hydrogen maser.[96]

C. Wall Coated Cells

1. Longitudal Relaxation Times T_1 for Zeeman Transitions

a. Alkylchlorosilanes and Waxes

A relative measure of these times was obtained by a change in absorbtion of $\sigma^+ D_1$ light of an oriented vapor subjected to a 180° pulse, as described in Section III C 4 b. Some typical photographs of oscilloscope traces under such conditions are shown in Figure 21.

All the cells contained natural rubidium except for the 5 cm neon one which contained Rb^{87}. This accounts for the larger changes in optical signal with this cell.

All good wall coated cells give orientations within 30% of each other. The Dri-Film methylocholorsilane coatings were fully as effective as the Paraflint wax and one can infer T_1 times of around 100 milliseconds.

The experiments with higher alkylcholorsilanes as described in III B 3 were somewhat disappointing in that useful coatings were only obtained with ethyl groups. However, the orientations achieved with such coatings were somewhat better than for any other material tried.

It is worth noting that in an effort to determine whether any gas had gotten into an ethyl cell that could be acting as a buffer gas, a leak tester discharge was applied to the cell. There was no evidence for gas, but the signal was completely destroyed. It was recovered slowly, but after hours was only 1/3 its former value and never fully reached this value.

b. Uncoated Glass Walls

In order to have some reference for the T_1 relaxation experiments, the relaxing effects of glass were investigated, the expectation being that no orientation would be observed. It was thus surprising to find an orientation as measured by the response to 180° pulses about 1/30 that for the best wall coatings. A trace of such a response is shown in Figure 22 (a). The decay time after the pulse is much shorter than the usual optical pumping time, enabling one to attribute the relaxation to wall collisions and thus to

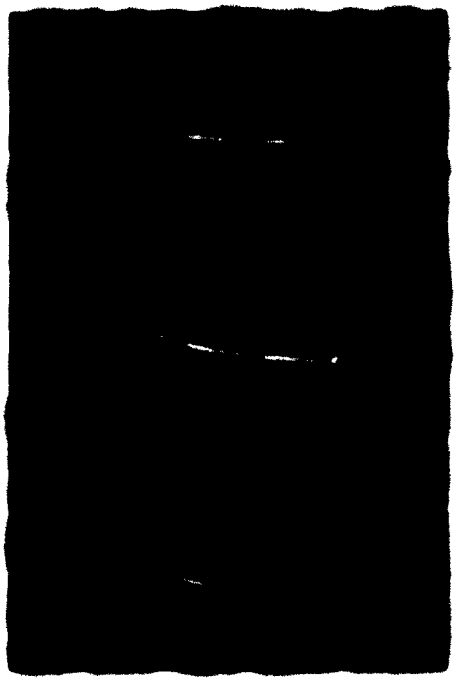

SC-02 LOBSTER POT CELL

SC-02 NORMAL ORIFICE

SC-77 LARGE ORIFICE

(a) DRI-FILM WALL COATED CELLS
(STUDIED ALSO BY FREE PRECESSION)
NATURAL Rb, 40°C
2 ms./cm. 1 v/cm.

(b) Rb^{87}, 5cm. Ne BUFFER GAS
40°C, 2 ms./cm. 1 v/cm.

FIG. 21 RESPONSE TO 180° PULSE (D_1 σ^+ PUMPING AND DETECTION)

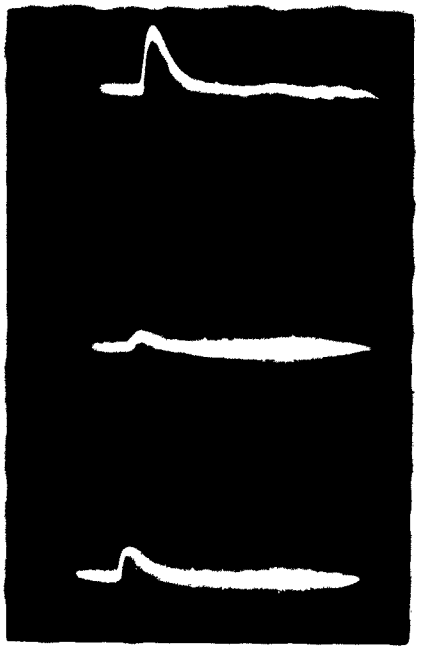

D_1 , Rb^{85} REVERSAL

D_1 , Rb^{87} REVERSAL

D_1 & D_2 Rb^{87} REVERSAL
(NO FILTERING)

(a) UNCOATED GLASS WALL
NATURAL Rb 1ms./cm., 0.1V/cm.

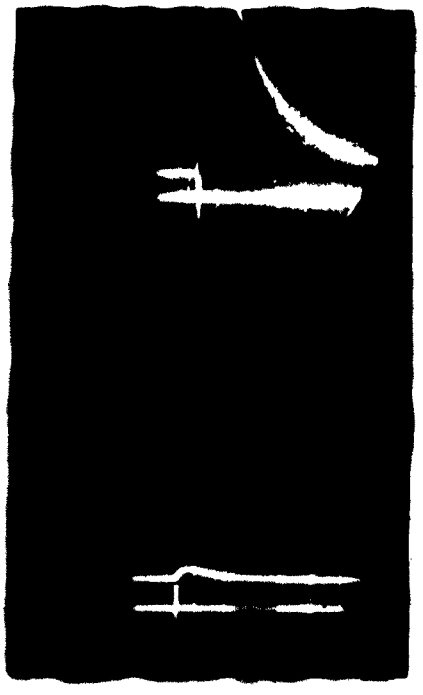

D_1 PUMPING AND DETECTION

D_2 PUMPING AND DETECTION

(b) Rb^{87} 5cm. Ne BUFFER GAS
1ms./cm. 1V/cm.

FIG. 22 RESPONSE TO 180° PULSE

estimate the average number of such collisions to relax 1/e of the oriented atoms. In this way one estimates 5 to 10 collisions being required for disorientation by a pyrex walled cell containing natural rubidium.

The most effective combination of light source and optical and detection configurations as discussed in Section III was required for the measurement of orientation in such clean, baked glass cells.

It was learned shortly after these observations that similar effects had been seen by Professor H.G. Dehmelt.[103]

2. Transverse Relaxation Times T_2 for Zeeman Resonances

A few measurements were carried out in the homogeneous magnetic field available at the Magnetic Observatory maintained by the U.S. Coast and Geodetic Survey at Fredericksburg, Va. in collaboration with P.L. Bender of the National Bureau of Standards. The technique is described in Section III C 4 c. The higher alkylchlorosilane cells had not been prepared at the time of the measurements. The only cells measured were coated with Dri-Film and were 2 inches in diameter, two having fairly large orifices, giving relaxation times by migration into the neck, according to the simple theory of Section III B 1, of about 50 milliseconds.

The cells contained natural rubidium at room temperature and it was necessary to monitor the Rb^{85} resonance in order to obtain a usable signal with the weak light used. The g-factors for this spin 5/2 nucleus ground atomic state were

$$g_{F=3} = 1/3$$

$$g_{F=2} = -1/3$$

An SC-02 Dri-Film coated bulb gave T_2= 40 milliseconds while an SC-77 Dri-Film bulb gave T_2 = 60 milliseconds. An SC-02 coated lobster pot type cell gave a T_2 of only 8 milliseconds.

These results were somewhat surprising. First of all the method of measuring relative T_1 values had indicated that the SC-02 coating was slightly better than the SC-77 coating, and that the lobster pot SC-02 cell was almost as good as the others, as shown in Figure 21. This emphasizes the caution with which the non-linear dependence upon T_1 of the 180° response must be interpreted, for one probably does not expect a large difference between T_1 and T_2.

The poor performance of the lobster pot cell in comparison with the performance of the same coating in the large orifice bulb is doubtless due to the poor quality of the coating achieved through the small hole, since it was one of the first such coatings attempted on a lobster pot cell. Coated lobster pot cells made subsequently performed well.

3. Averaging of Magnetic Field Inhomogeneties

Although the use of a wall-coated cell to average out magnetic field inhomogeneities by the motion of the atoms was one of the motivations for investigating wall coatings, very little systematic attention was given to this aspect of the problem using the coatings that were developed.

If one accepts a value of 10 milliseconds as the dephasing time due to inhomogeneities as determined from the measurement of 22 milliseconds preservation of coherence using a single 180° pulse in a buffer gas cell described in Section IV A 2 a, a frequency spread

of $\Delta\omega' = 100$ should be expected in the Zeeman resonance. Using the expression developed in Section II C 7, one would expect a factor of improvement in a wall coated cell of

$$\frac{1}{\Delta\omega\,\tau_0} = 10^{-2} \times \frac{10^4}{3} \approx 30$$

Although the preservation of coherence among the freely precessing atoms was somewhat easier in a wall coated cell, there being no need of 180° pulses, for example, the factor was by no means this large. No attempt was made to determine the actual factor. Probably the value of 10 milliseconds assumed above represents a time for which the phase spread is considerably in excess of one radian, which would bring the observations more in line. However, there was direct evidence that in a weak magnetic field corresponding to a precession frequency of abous 3 kc/sec for Rb^{87}, the phase was preserved in a buffer gas cell for an e-folding time of about 6 milliseconds. This is discussed in Section IV D 1 below.

A very cursory comparison was made of the line widths in a buffer gas cell (5 cm Ne and Rb^{87}) and in a wall coated cell (SC-02 Dri-Film, natural rubidium) using continuous rf and 60 cycle modulation--an adaption of the recording system for the hyperfine resonance described in Section III D 4. The result was a narrowing of the resonance by the wall coated cell by only a factor 2. It is possible that the difference between Rb^{87} and natural Rb contributed to lessening the effect.

D. Other Results

1. Effect of (2,0)$\longleftrightarrow$(1,0) Resonance on The Larmor Frequency Modulation of Light

It was found that a weak magnetic field could be established in the shielded solenoid at an angle to the axis by reducing the axial component to a very small value. This was done by establishing a small field to oppose the residual field. Any kind of a sharp pulse (rf or dc) applied to the rf coils would set the oriented atoms into coherent free precession about the field direction, thus providing modulation of the σ^+ D_1 light at the Larmor frequency as discussed in Section II B 4.

The small magnitude of the field resulted in a Larmor precession frequency of about 3 kc/sec for Rb^{87}. The e-folding time for the decay of the oscillations was about 6 milliseconds.

Application of the microwave field to couple the (2,0) and (1,0) states during the free precession reduced the persistance of the free precession sharply, as was to be expected, since the effect is clearly very closely related to the phase destruction method using the 90° pulses.

Figure 23(a) shows the effect. The possibility of simultaneously monitoring the magnetic field and the hyperfine resonance by means of modulation of σ^+ light at the Larmor frequency is clear.

2. Optical Pumping with D_2 Radiation

As discussed in Section II, alkali atoms in wall coated cells may be oriented in the same direction by both D_1 and D_2 radiation, since there is no mixing in the excited state, and one can hope to gain

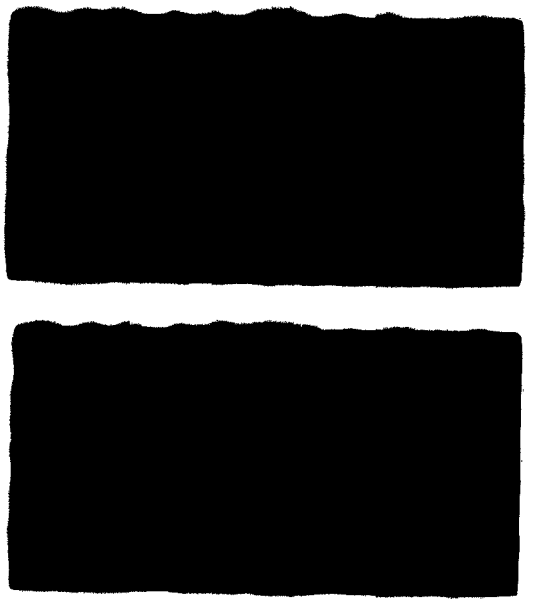

(a) EFFECT OF O⟷O RESONANCE
ON FREE PRECESSION
Rb^{87} 5cm. Ne Buffer Gas
1ms./cm., 0.5volts/cm.

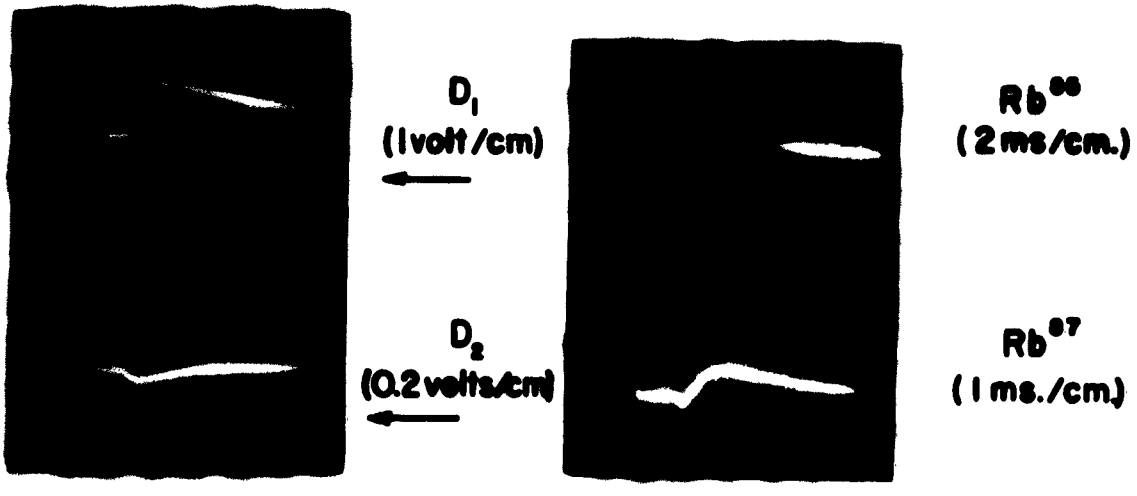

(b) SC-02 COATED LOBSTER
POT CELL
NATURAL Rb, Rb^{85} REVERSAL
1ms./cm.

(c) SAME CELL AS (b)
$D_1 + D_2$ PUMPING,
D_2 DETECTION
0.5volts/cm.

FIG. 23 INTERESTING RESPONSES TO PULSES

in orientation efficiency by using both fine structure components.

Since no data existed on the dynamics of optical pumping with D_2 radiation alone, solutions by 650 digital computer were obtained for this case as discussed in Section II A 8. Some integral curves for the change of ground state populations with time are given in Appendix E.

Some pictures of the change in light intensity for D_2 σ^+ light following a 180° pulse are given in Figures 22 (b) and 23 (b) and (c) under several conditions. Figure 22 (b) shows the response when D_2 σ^+ pumping and detection is used in a 5 cm Ne Rb^{87} bulb as compared with that for D_1 under the same conditions. The orientation produced by D_2 is much smaller, as expected, since there is excited state mixing.

Figure 23 (b) shows the response for an SC-02 coated lobster pot cell containing natural Rb (Rb^{85} resonance) to D_1 and to D_2 separately. The trace for D_2 is much smaller than that for D_1. The reasons for this large discrepancy are probably associated with a large amount of self reversal in the source for D_2.

Figure 23 (c) shows the same cell being pumped with both D_1 and D_2 σ^+ light simultaneously. The detection is with D_2 light. The upper trace is for Rb^{85} with a time scale of 2 ms/cm and the lower trace for Rb^{87} with a time scale of 1 ms/cm. The change in sign of the response transient and the long recovery time for the Rb^{85} represent interesting relaxation effects that should be studied further.

V SUMMARY AND CONCLUSIONS

A. Optical Detection of the $0 \leftrightarrow 0$ Hyperfine Resonance

A new method of optically detecting the field independent magnetic hyperfine resonance between the magnetic substates in the ground state of an alkali atom has been devised, analyzed, and experimentally demonstrated for the case of rubidium 87. It relies on producing a change of phase between an $m_F = 0$ state and its partner states of the same F value during the coherent superposition state describing free precession.

A major advantage of the new method is that it yields very strong signals, easily observable on an oscilloscope without bandwidth limitation with a signal to noise amplitude ratio greater than 10^3. This strong signal can be sacrificed in favor of narrowing the line width to the limit set by the T_2 relaxation time in the gas cell, and even beyond, using a method for artificially narrowing the resonance by observing only those atoms which are not relaxed during a time interval greater than T_2. Because of practical experimental difficulties described in Section IV, the line widths of a few cycles per second that seem certainly possible were not realized. Also, because of the interest in investigating other matters, described below, the microwave resonance was not actually applied in two coherently phased pulses to select the longer lived atoms and thus to narrow the line artificially. The method of detection is well adapted to accomplishing this however.

Other methods of optical detection were devised also, as described in Section I, but not investigated experimentally.

One of these, the selective hyperfine absorption method, improved for rubidium 87 by the use of a rubidium 85 filter cell, (independently conceived by several investigators, see Introduction, p. I-7). is the method of optical detection used in all the optically pumped rubidium vapor cell frequency standards developed so far. More information on this is given in Appendix A. The use of a polarization bridge to permit the signal to appear on a null background, as mentioned in Section I and described in Appendix B, was not tried experimentally.

B. Wall Coatings

The effectiveness of coatings formed by treatment of glass with alkylchlorosilanes for the inhibition of relaxation in oriented atoms colliding with the walls was demonstrated. These coatings are quite easy to apply and form a chemical bond with the glass permitting the cell to be baked at 350° - 400° C after the coating is formed without deterioration of the surface.

The relaxing properties of these coatings were found by experiments to be about the same as those of the long chain saturated by hydrocarbon waxes, in particular, Paraflint, a commercial mixture averaging $C_{50}H_{102}$, a material first uncovered in this work and found useful by several other groups.

Orientation in a coated wall cell can be produced by both D_1 and D_2 σ^+ radiation simultaneously in contrast with the use of a buffer gas, for which, at a few cm pressure, the excited state mixing requires the production of an intensity difference between D_1 and D_2 since they tend to orient in opposite directions in this case.

Under some conditions, the rapid motion across the cell of precessing atoms in wall coated cells results in averaging out magnetic field inhomogeneities which would otherwise constitute a serious limitation to the duration of a free precession state before dephasing in a buffer gas cell.

The visual observation of the 6835 Mc/sec $0 \longleftrightarrow 0$ hyperfine resonance in 2" diameter wall coated cells with widths of 60-80 cps certainly shows the effectiveness of the Dicke method of Doppler reduction when the atoms are confined to a region whose extent is on the order of a wavelength. Instrumentation difficulties described in Section IV make it difficult to say what is the contribution to the width from wall collisions.

There was found to be a negative pressure shift for the $0 \longleftrightarrow 0$ resonance of several kc/sec for the wall coatings, it being difficult to attribute specific values to the several materials because of a lack of knowledge of the quality of the coatings, Ethylchlorosilane seemed to give the least shift, however. Because of the many fewer collisions per second with the walls than with buffer gas atoms in a buffer cell, one would expect the resonance frequencies to be much less sensitive to environmental changes such as temperature, although because of experimental difficulties discussed in Section IV no real evidence was obtained to support this.

C. Coherently Pulsed Zeeman Resonance

The theoretical and experimental study of the response of optically oriented atoms to coherent pulses at the Larmor precession frequency formed a large part of this investigation. The + 90°,

- 90° sequence separated by a time interval τ is essential in the phase destruction method of detecting the $0 \longleftrightarrow 0$ resonance.

The spin echo techniques of Hahn, using a 180° pulse to alleviate the dephasing action of an inhomogeneous magnetic field on an assemblage of freely precessing atoms have been successively employed on optically oriented vapors for the first time in this investigation. The extension of spin echo methods by a series of 180° pulses as developed by Carr and Purcell to maintain free precession phase relations in an inhomogeneous magnetic field when the atoms are diffusing in a medium has also been used with success in the case of a buffer gas.

The change in the transmitted intensity of σ^+ light following a 180° pulse is a measure of the orientation of the assemblage. This technique has been used to obtain relative values of orientation for vapors in cells coated with different materials, and hence some measure of the T_1 relaxation time, although the relationship is non-linear.

Using a weak beam of σ^+ light in the plane of free precession induced by a pulse of rf, the T_2 relaxation time can be measured by observing the decay of the modulation envelope. A few experiments of this nature on wall coated bulbs were made in collaboration with P.L. Bender of the National Bureau of Standards.

D. Pulsed Optical Radiation

This was accomplished satisfactorily by turning on and off the discharge tube excitation as described in Section III A. It is desirable to do this since the absorption of optical resonance radiation is a potent relaxing agent and can contribute to the line

breadth of the hyperfine resonance and to the destruction of the phase relations in a coherent superposition state produced by an rf pulse. It is thus necessary to interrupt the light absorption during an interval of free precession τ greater than several times the optical pumping time constant Γ^{-1} (See Section III).

Another advantage of cutting off the light during the sensitive time for the action of the microwave hyperfine resonance is the avoidance of possible shifts in the hyperfine resonance frequency induced by an asymmetry in the spectral distribution of the light, as discussed in Section II D.

E. Theoretical Formulation

The manner of describing optical pumping presented in Section II A provides a convenient formalism in which the effects of several kinds of optical pumping acting simultaneously is readily assessed.

The derivation of the stochastic equations from the differential equations under certain conditions should be emphasized, since the use of stochastic equations has sometimes been criticized.[15]

Explicit incorporation into the optical pumping formalism of relaxation based on decoupling of the electron and nuclear and randomization of the electron spin is new, as are the computer solutions for some cases given in Appendix E. One consequence of the above relaxation assumption for ground state relaxation is a crossing of some of integral curves giving the populations as a function of time. The existence of such effects could be looked for experimentally by pulsed resonances between states in a strong magnetic field

to investigate the reality of the assumption.

The use of the density matrix formulation, along with absorption operators and effective oscillator strengths, has proved to be a technique lending clarity to complex situations. Another powerful technique is the application of rotation operators to describe the effect of pulsed rf fields.

F. Recommendations for Further Research

A number of directions for further study are mentioned at various points in the preceding exposition, particularly in Sections III, IV, and V. Some of them are emphasized here.

1. Using improved instrumentation, as discussed in Sections III D and IV A and IV B, more information should be obtained on hyperfine line widths achievable with time intervals of $\sim$100 milliseconds between 90° pulses, which one knows are possible from T_2 measurements. It seems that approximately 1 cps line widths should be possible.

2. The method of coherently pulsing the microwave radiation at the beginning and end of the active interval between pulses should be investigated as a means of artificially narrowing the line through sacrifice of the large signal in favor of selecting the longer lived atoms. Such a technique could be used with the selective hyperfine absorption method of detection also, cutting the lights off to establish an active time interval. The signals would not be as strong

but they may be usable and the possibility should be experimentally studied since the difficulties with inhomogeneous magnetic fields and 60 cycle time varying magnetic fields would not exist. The polarization bridge discussed in Appendix B might also be used as a detection technique in connection with the coherently pulsed microwave resonance.

3. Further studies of alkylchlorosilane wall coatings should be made, including another attempt to make coatings from the higher alkyl groups, which may have been unsuccessful because of poor technique. Measurements of relaxation times should be made directly by observing the decay after a 180° pulse on an oriented system with a pulsed light source, after the method of Franzen, but using the electronic methods devised in this investigation. Circuits were built for just this purpose but there was not time to use them. More T_2 studies of the type described should be made on the same bulbs at some later time to determine the existance of long term deterioration of the coatings. This also should be done for the hyperfine resonance characteristics: line width and shift.

Information about the amount of absorption of alkali atoms by the wall coatings could be gained by a radioactive tracer experiment. Marked improvement in the surfaces should result from preparing them under ultra-high vacuum conditions ($\sim 10^{-9}$ mm Hg) and this should be explored.

4. More computer solutions of the equations of optical pumping dynamics should be obtained for various relaxation conditions. Some useful relations would be those between the orientation and relaxation time in the ground state, so as to make the method of 180° pulses for measuring relaxation times more meaningful. The detailed manner in which the populations change in recovering from a 180° pulse would also be interesting.

5. The method of populating the (2,0) state in excess of the (1,0) state by means of σ^+ optical pumping followed by an rf pulse at the Larmor frequency, or perhaps by a cw field, should be explored in relation to the problem of making an optically pumped alkali hyperfine maser, in particular for an atomic hydrogen 21 cm maser. Detailed calculations for optical pumping with Lyman α radiation in atomic hydrogen should be made. These are of particular interest because the interference terms [5] will dominate, as discussed in Section II A 1.

APPENDIX A SELECTIVE HYPERFINE ABSORPTION

In the introduction (Section I) and in Section II B 2, this method of optical detection is briefly described. Before the method was demonstrated experimentally, as discussed in the introduction, some detailed estimates of the magnitude of signals that could be expected were made using an approximate treatment. The estimates indicated that quite good signals could be achieved for transmission monitoring. The calculations were made in such a way that they could be applied to the polarization bridge described in Appendix B. The method used and some numerical results are presented here.

The complete problem of the dependence of the spectral composition of the light on the distance of penetration into the cell was not solved. A population distribution in the ground magnetic substates resulting from optical pumping with π polarization was assumed to exist uniformly throughout the cell (this assumption would be quite realistic for pumping in a wall coated cell, as described in Section II B 2, and is not too unrealistic if the change in intensity of the light as it passes through the cell is not large.) Twice as large an inverted population difference between the $m_F = 0$ states results from this type of optical pumping as compared with the use of σ polarized light.

The ten hyperfine components of the D lines are displayed in Figures 9(a) and 9(b) along with their oscillator strengths. The effective oscillator strengths introduced in Section II B to describe the absorption of light will differ from the intrinsic oscillator strengths in the aligned state produced by the π optical pumping.

The $m_F = 0$ states do not contribute equally for all the ten lines shown, and an equalization of their populations by a microwave field causes a selective hyperfine absorption which changes the overall transmission of the light. Furthermore the σ and π components are affected differently, this being of importance for the action of the polarization bridge described in Appendix B.

The effect of π pumping with both D lines in the presence of relaxation had not been calculated before, so an approximate solution of the optical pumping equations given in Section II A 6 was obtained for the case $\Gamma' T = 1$, with $\underline{R}$ the completely uniform relaxation matrix, by using the stochastic approach of Section II A 7.

If one takes $\Gamma T = 1$, the differential equation becomes

$$\dot{\underline{N}} = 2\Gamma\left[\frac{\underline{P}^T + \underline{R}^T}{2} - \underline{\underline{1}}\right]\underline{N} \tag{1}$$

Since the convergence of successive applications of the stochastic matrix is rapid, we have approximated $\underline{N}$ (∞) by

$$\underline{N}^{(3)} = \left[\frac{\underline{P}^T + \underline{R}^T}{2}\right]^3 \underline{N}(0)$$

$$= \begin{bmatrix} .115 \\ .141 - \delta \\ .115 \\ .102 \\ .132 \\ .141 + \delta \\ .132 \\ .102 \end{bmatrix} \tag{2}$$

δ = .01 before resonance

= 0 after resonance

The effective f-values before and after resonance may now be calculated.

For each frequency, the intensity per unit frequency obeys the equation

$$\frac{d}{dx} I_\nu = -n \sigma_\nu I_\nu \tag{3}$$

where n=number of Rb atoms per cm^3

x = distance of penetration into cell

The solution for a single frequency is

$$I_\nu(x) = I_\nu(0) \exp\left[-n \sigma_\nu x\right]$$

$$= I_\nu(0) \exp\left[-n \sigma_0 x e^{-\omega^2}\right] \tag{4}$$

where

$$\sigma_0 = \frac{2}{\Delta\nu_D}\sqrt{\frac{\ln 2}{\pi}}\,\pi c r_0 f_{eff}$$

$$\omega = \frac{2\sqrt{\ln 2}}{\Delta\nu_D}(\nu - \nu_0)^2$$

The other notation is given in Sections II A and II B.

The transmittance k is found by integrating over frequency

$$k = \frac{\int_0^\infty I_\nu \, d\nu}{\int_0^\infty I_\nu(0)\, d\nu} = \frac{\int_0^\infty I_\nu(0) \exp\left[-n\sigma_0 x e^{-\omega^2}\right] d\nu}{\int_0^\infty I_\nu(0)\, d\nu} \tag{5}$$

Such integrals can be evaluated by a series expansion. We will express k in such a way that tabulated values of an integral given by Ladenburg and Levy [104] can be used. We shall assume that the incident line is Gaussian in shape with a breadth $\propto \Delta\nu_D$ considerably greater than $\Delta\nu_D$. Then

$$k = \frac{\int_0^\infty I_\nu(0)\,d\nu - \int_0^\infty I_\nu(0)\left\{1 - \exp\left[-n\sigma_0 x\, e^{-\omega^2}\right]\right\} d\nu}{\int_0^\infty I_\nu(0)\,d\nu}$$

$$= 1 - \frac{\int_{-\infty}^{\infty} e^{-\frac{\omega^2}{\alpha^2}}\left\{1 - \exp\left[-n\sigma_0 x\, e^{-\omega^2}\right]\right\} d\omega}{\int_{-\infty}^{\infty} e^{-\frac{\omega^2}{\alpha^2}}\, d\omega} \qquad (6)$$

$$= 1 - \frac{1}{\alpha\sqrt{\pi}} \int_{-\infty}^{\infty} e^{-\frac{\omega^2}{\alpha^2}} \left\{1 - \exp\left[-n\sigma_0 x\, e^{-\omega^2}\right]\right\} d\omega$$

The function

$$n\sigma_0 x\, S(n\sigma_0 x) = \frac{1}{\sqrt{\pi}} \int_{-\infty}^{\infty} \left\{1 - \exp\left[-n\sigma_0 x\, e^{-\omega^2}\right]\right\} d\omega \qquad (7)$$

is the one tabulated. If α is large enough one may neglect the change in $e^{-\frac{\omega^2}{\alpha^2}}$ in the above integral to obtain

$$k = 1 - \frac{n\sigma_0 x\, S(n\sigma_0 x)}{\alpha} \qquad (8)$$

If more than one absorption line occurs within the breadth of the incident line, additional terms of the above form must be subtracted.

For the overlapping lines (e,f,g) and (h,i,j) one can find the total cross-section by a graphical addition of Gaussian shapes for each line. An exact graphical integration could then be performed.

Only the first graphic construction was done, approximating the result by a Gaussian line and using the above analytical method of calculation.

From a plot of the function $n\sigma_0 xS(n\sigma_0 x)$ one may readily obtain the transmittances and the changes in these on resonance for given values of n, x, σ_0 and α.

There is a maximum value for n determined by the hyperfine line width $\Delta\nu$ one wants and by the Rb-Rb exchange cross-section σ which determines the relaxation time T.

$$\Delta\nu \leq \frac{1}{\pi T} \tag{9}$$

Now

$$T = \frac{1}{n\bar{v}\sigma} \tag{10}$$

so that

$$n \leq \frac{\pi\Delta\nu}{\bar{v}\sigma} \tag{11}$$

For a velocity $\bar{v}$ corresponding to a temperature of 298° K and an exchange cross-section $\sigma = 10^{-13}$ cm^2, the maximum estimate of earlier work,[1]

$$n \leq 10^9 \Delta\nu \tag{12}$$

The following table gives values of transmittances before and after resonance for both σ and π polarizations for the values $n = 5 \times 10^{10}$, $x = 5$ cm, $\alpha = 4$.

The function $n\sigma_0 xS(n\sigma_0 x)$ exhibits saturation, that is, its derivative decreases monotonically to zero, so that there is a

Hyperfine Line		Transmittance k	
		Before Resonance	After Resonance
a	π	.948	.948
	σ	.944	.942
b	π	.794	.789
	σ	.791	.788
a+b	π	.742	.737
	σ	.735	.730
c	π	.775	.779
	σ	.800	.802
d	π	.818	.818
	σ	.782	.787
c+d	π	.593	.597
	σ	.582	.589
e,f,g	π	.632	.629
	σ	.634	.629
h,i,j	π	.522	.523
	σ	.522	.524

Change in Transmittances at Resonance for the Hyperfine Lines.

value of $n \sigma_0 x$ giving a maximum change in the transmittance k on resonance. Graphical analysis shows that the maximum is rather broad and occurs for $n \sigma_0 x \sim 2$.

Signal to Noise Considerations

Using the value of k and Δ k obtained above one can calculate the signal expected in either a transmission or a scattering detection arrangment. An unavoidable source of noise is associated with the random emission of photons from the lamp --the "photon shot noise".

If the number of photons per second passing through the gas cell and falling on a phtocathode is kI and the quantum efficiency of the photo-cathode is q, the signal in the electron stream coming off the photocathode is

$$\text{Signal} = q\, I\, \Delta\, k \text{ electrons per second}$$

Fluctuations in the electron stream due to the random arrival of photons will contribute noise for a band width of one cycle per second given by

$$\text{Noise} = \sqrt{q\, k\, I} \quad \text{electrons per second}$$

Thus we obtain

$$S/N = \sqrt{q}\ \sqrt{I}\ \frac{\Delta k}{\sqrt{k}} \tag{13}$$

It is assumed here that the noise in the dark current is less than the photon shot noise. For infra-red sensitive cathodes the dark current is high at room temperature because of the low work function. For S-1 (Cs -O-Ag) cathodes the dark current at room temperature is $\sim 10^{-9}$ amp/cm^2, which for q= 1/250, a value typical for these cathodes,[105] corresponds to a photon flux density of $\sim 10^{12}$ photons/sec-cm.^{2}

The absorption of an optical photon interrupts the hyperfine resonance so that if one wishes lines no wider than $\Delta\nu$ there is an upper limit to the intensity of the light source, given by

$$\Gamma = \int_0^\infty I_\nu \sigma_\nu \, d\nu \leq \pi \Delta\nu \qquad (14)$$

If the spectral width of the light source is $\Delta\nu_L$, the maximum intensity is approximately

$$I_o = \frac{\pi \Delta\nu}{f \pi c r_o} \Delta\nu_L \text{ photons/sec-cm}^2 \qquad (15)$$

For the values $\Delta\nu = 30$ cps, $\Delta\nu_L = 10^{10}$ cps, $f = 1$ (π-pumping, equal peak intensities of the D lines) one obtains the value

$$I_o \sim 10^{14} \text{ photons/sec-cm}^2$$

The preceding tabulation shows that for π radiation $k = 0.6$ and $\Delta k = 7 \times 10^{-4}$. If the effective area of the gas cell is $\sim 10^2$ cm^2 one finds for this maximum intensity

$$S/N \sim 5 \times 10^3$$

This figure could be improved still further by filtering of the hyperfine components before they are incident on the gas cell. An estimate can be obtained from the table but a more accurate calculation requires a knowledge of the equilibrium distribution $\underline{N}$ under the influence of hyperfine pumping which can be obtained as described in Section II.

Of course there will be sources of correlated noise depending on the method of exciting the light source, which are difficult to

520

DOPPLER WIDTH
AT 300°C

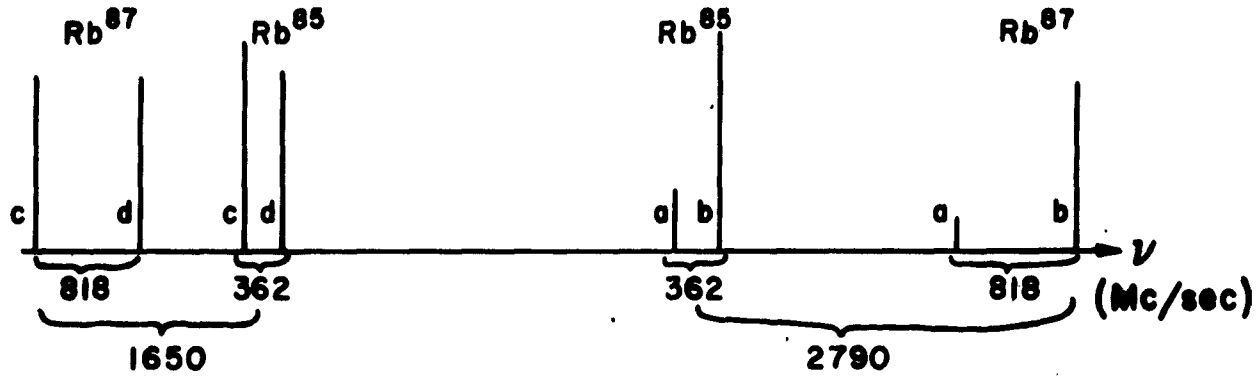

D_1 LINE

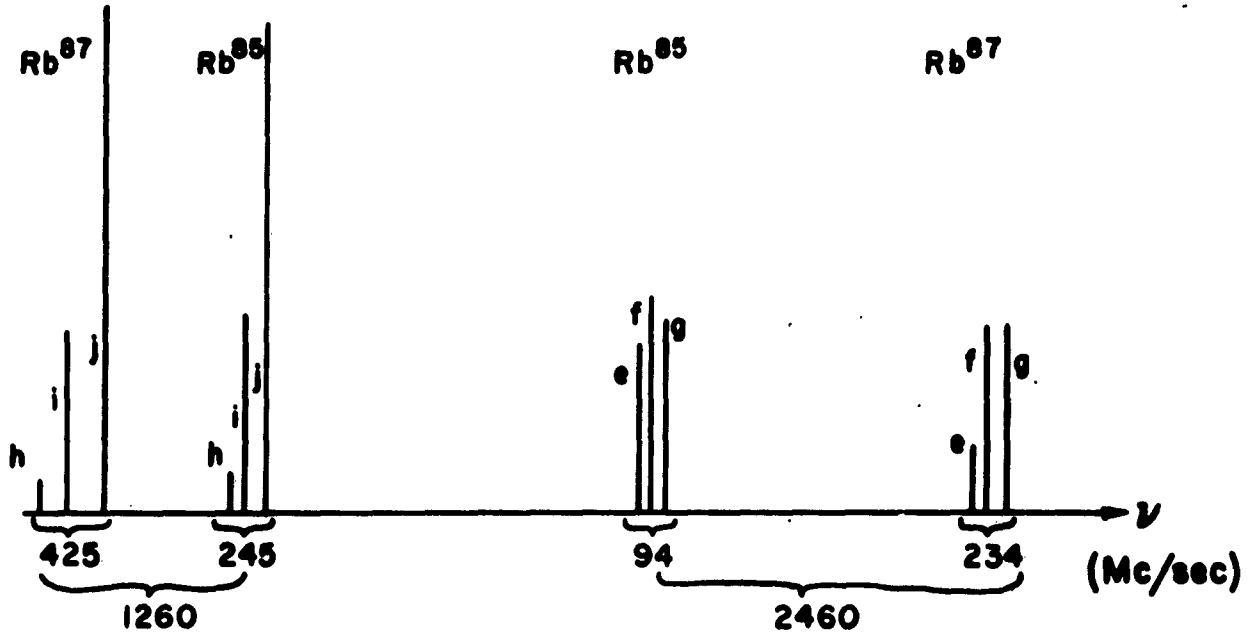

D_2 LINE

RELATIVE HYPERFINE STRUCTURE OF
RUBIDIUM ISOTOPES

FIG. 24

estimate, and the subsequent amplifiers will introduce some noise, but the above analysis yields a feeling for the ideal performance.

As mentioned in the introduction an excellent filter cell relies on a shift in the hyperfine components of Rb^{85} as compared with Rb^{87}. This is shown in Figure 24 which is adapted from work of Kopfermann and Krüger [106] on the optical hyperfine splittings and uses hyperfine splittings measured by Rabi and Senitzky[70] using atomic beam and resonance techniques. The figure is approximately to scale for both frequencies and oscillator strengths and displays the absorption Doppler width. Figures 9 (a) and 9 (b), should be consulted also for more details of the hyperfine components. The suppression to be expected, upon passage through a Rb^{85} cell, of the hyperfine components of Rb^{87} arising from the $F = 2$ level with respect to those arising from the $F = 1$ level is readily apparent.

Detailed numerical estimates of the signal to be expected using such a Rb^{85} filter cell were not made since the method was not explored experimentally at Princeton. Although other groups have used the technique, as discussed in the introduction, with considerable success,[19,20] some numerical calculations should be made in order to assess the experimental performance in relation to what might be ideally expected.

APPENDIX B POLARIZATION BRIDGE

A method of detecting optically the $0 \leftrightarrow 0$ hyperfine resonance as a signal imposed on a null background uses a small probing beam of light, linearly polarized at 45° to the axis of quantization of the system (taken here as the z-axis) which is passed

through a second polarizer oriented at 90° to the direction of polarization to block the light entering a photo detector. The action of a microwave field equalizing the population of the two $m_F = 0$ levels causes the π and σ components into which the 45° linearly polarized beam may be decomposed to be absorbed differently. The second polarizer no longer blocks the light and a signal appears.

An analysis using the calculus of Mueller[107] to describe the effect of imperfect polarizers and the gas cell on the transmission of light was carried out. It revealed the necessity of cooling to dry ice temperatures the S-1 photo cathode used for detecting the rubidium D lines in order that the dark current not mask the signal. Even by doing this, the analysis revealed that the method was inferior to the phase destruction technique which was therefore carried out in preference.

The manner of the analysis is useful in other situations involving imperfect polarizers and will therefore be summarized here.

A beam of light can be described by four parameters, as was first done by Stokes, which give full information on the intensity and state of polarization. In modern notation these are linear combinations of the elements of the density matrix, the basis vectors for which are two orthogonal states of polarization. It is usual to choose these basic vectors as π and σ polarizations, and this will be done here, but σ^+ and σ^- states are often used. These matters are discussed in many places in the literature.[108]

Stokes Parameters $\underline{S} = \begin{bmatrix} I \\ Q \\ U \\ V \end{bmatrix}$ (1); Density Matrix $\rho = \begin{pmatrix} \rho_{11} & \rho_{12} \\ \rho_{21} & \rho_{22} \end{pmatrix}$ (2)

$$\rho_{ij} = \langle c_i c_j^* \rangle_{\text{ensemble average}} \tag{3}$$

Electric Vector $\vec{E} = c_1 \vec{\epsilon}_1 + c_2 \vec{\epsilon}_2$

where
$$c_1 = A_1 e^{i\varphi_1}$$
$$c_2 = A_2 e^{i\varphi_2} \tag{4}$$

Relations between descriptions:

$$\begin{aligned} I &= \rho_{11} + \rho_{22} = A_1^2 + A_2^2 \\ Q &= \rho_{11} - \rho_{22} = A_1^2 - A_2^2 \\ U &= \rho_{12} + \rho_{21} = 2 A_1 A_2 \cos(\varphi_1 - \varphi_2) \\ V &= i(\rho_{21} - \rho_{12}) = 2 A_1 A_2 \sin(\varphi_1 - \varphi_2) \end{aligned} \tag{5}$$

Passage of the beam of light through many optical systems can be described as a transformation of one set of Stokes parameters into another set. The Mueller matrix of this transformation acts on the four Stokes paramaters regarded as a four component vector $\underline{S}$.

$$\underline{S}' = \underline{\underline{M}}\, \underline{S} \tag{6}$$

A polarizer is characterized by transmittances k_1 and k_2 in two perpendular principal directions which are defined exactly as

the transmittance in Appendix A. There may also be a relative phase retardation ξ between beams polarized in the principal directions. If the Stokes parameters are defined with respect to the y and z directions, x being the direction of propagation, the Mueller matrix $\underset{\sim}{M}(\theta)$ for a polarizer whose 2-axis has been rotated by an angle θ from the z-axis, in a positive direction about the x-axis, is

$$\begin{pmatrix} S & D\cos 2\theta & -D\sin 2\theta & 0 \\ D\cos 2\theta & S\cos^2 2\theta + P\cos\xi\sin^2 2\theta & (P\cos\xi - S)\sin 2\theta\cos 2\theta & -P\sin\xi\sin 2\theta \\ -D\sin 2\theta & (P\cos\xi - S)\sin 2\theta\cos 2\theta & S\sin^2 2\theta + P\cos\xi\cos^2 2\theta & -P\sin\xi\cos 2\theta \\ 0 & P\sin\xi\sin 2\theta & P\sin\xi\cos 2\theta & 0 \end{pmatrix}$$

where

$$S = \tfrac{1}{2}(k_1 + k_2)$$
$$D = \tfrac{1}{2}(k_1 - k_2)$$
$$P = \sqrt{k_1 k_2}$$
$$S^2 = P^2 + D^2$$

For two identical polarizers rotated by an angle θ with respect to each other the transmittance k_θ for unpolarized light, having Stokes vector

$$S = \begin{bmatrix} 1 \\ 0 \\ 0 \\ 0 \end{bmatrix}$$

is given by

$$k_\theta = \left[\underline{\underline{M}}(\theta)\, \underline{\underline{M}}(0) \right]_{11}$$

$$= S^2 + D^2 \cos 2\theta$$

$$= \frac{k_1^2 + k_2^2}{2} \cos^2\theta + k_1 k_2 \sin^2\theta \qquad (8)$$

The Land Polaroid Company defines

$$H_o = k_{0^\circ} = \frac{k_1^2 + k_2^2}{2}$$

$$H_{90^\circ} = k_{90^\circ} = k_1 k_2 \qquad (9)$$

and one has

$$k_\theta = H_o \cos^2\theta + H_{90^\circ} \sin^2\theta \qquad (10)$$

For good extinction it is clearly desirable to have a very small value of k_2.

The gas cell has principal transmittances k_π and k_σ, and one can probably neglect any relative phase retardation since the absorption lines are Doppler broadened, resulting in the absorption taking place effectively always at the center of the natural line where there is no phase shift. A more careful analysis may reveal some relative phase shift, but it will be taken to be zero for the present discussion. The transmittance of the system of gas cell between nearly crossed polarizers (departing from this condition by the angle φ) for initially unpolarized light is given by the 1,1 element of the product matrix

$$\underline{\underline{M}} = \underline{\underline{M}}\left(-\frac{\pi}{4}\right)\underline{\underline{M}}^{(cell)}(0)\,\underline{\underline{M}}\left(\frac{\pi}{4}+\varphi\right) \tag{11}$$

The result is

$$\begin{aligned} k_\varphi = {} & \frac{1}{4}\left(H_0 + H_{90^\circ}\right)\left(k_\sigma + k_\pi\right) \\ & - \frac{1}{2}\left(H_0 - H_{90^\circ}\right)\sqrt{k_\pi k_\sigma}\,\cos 2\varphi \\ & + \frac{1}{8}\left(k_1^2 - k_2^2\right)\left(k_\sigma - k_\pi\right)\sin 2\varphi \end{aligned} \tag{12}$$

which becomes for small angles φ, noting that $H_{90^\circ} << H_0$

$$k_\varphi = \left(H_{90^\circ} + H_0\,\varphi^2\right)\left(\frac{k_\pi + k_\sigma}{2}\right) + \frac{1}{2}H_0\,\varphi\left(k_\sigma - k_\pi\right) \tag{13}$$

Using the values of Δk_σ and Δk_π resulting from saturating the microwave resonance, given in Appendix A, one may compute the signal for the case of π optical pumping.

Dry ice temperatures are sufficient to reduce the dark current of an S-1 cathode(109) from 10^{-9} amp/cm^2 at room temperature of 10^{-16} amp/cm^2 and this would be needed for small angles φ, as a numerical analysis shows.

APPENDIX C ARTIFICIAL NARROWING OF A RESONANCE BY SEPARATED COHERENT PULSES

Although the phase distruction method of optical detection for the $0 \longleftrightarrow 0$ hyperfine resonance is well suited for narrowing the resonance beyond the limit ordinarily set by relaxation processes,

as discussed in the introduction, Section I A, the effect was not actually demonstrated experimentally because of some non-inherent experimental difficulties and limitations of time, as discussed in Sections III D and IV B. For this reason, a detailed analysis of the effect will not be given.

The proposal of Professor N.F. Ramsey[110] to narrow atomic and nuclear beam resonances by using spatially separated oscillatory field regions to perform transitions by two coherently phased pulses is well known and has been very successful for atomic beam frequency standards. Line narrowing could also be accomplished by having the oscillatory field act continuously for a longer time, but in atomic beams there are practical experimental difficulties with establishing a long region of uniform dc magnetic field and uniform phase of the oscillatory field.

When there is relaxation during the observation interval, for example atom-atom collisions, which badly perturb the phase of the wave-functions describing the two levels in question, or optical decay from the levels if they are excited states and such transitions are possible, the resonance line width is normally determined by the characteristic relaxation time. However, it was pointed out by Professor R.H. Dicke in unpublished work that resonances may be narrowed beyond the width set by the relaxation time by the use of coherent pulse excitation, at the sacrifice of signal strength. The demonstration by Romer and Dicke[111] that lines can narrowed by increasing the gain of an amplifier to compensate for the exponential decay in a signal following pulse excitation is closely related to this effect. Recently an analysis

for the case of optical decay in an atomic beam has been made by Professor Vernon Hughes.(112)

One may ask whether there is any improvement in the ability to locate the center of a line, for although it is made narrower, the signal to noise ratio becomes poorer. The net result, in an ideal situation, is indeed a loss as the following analysis shows, but it neglects certain things which will be mentioned below.

Let To be the characteristic relaxation time. Then the normal line width is

$$\Delta\nu \sim \frac{1}{T_o} \qquad (1)$$

The ability to locate the center of the line depends of the signal strength. If there are n_o electrons available during the observation time, and the noise is purely from fluctuations, an effective line width

$$\Delta\nu' \sim \frac{1}{\sqrt{n_o}} \frac{1}{T_o} \qquad (2)$$

is possible.

For the case of artificial narrowing by lengthening the interval of observation to T

$$\Delta\nu \sim \frac{1}{T} \qquad (3)$$

but the number of electrons available decreases exponentially

$$n = n_o\, e^{-T/T_o} \qquad (4)$$

so that the effective line width $\Delta\nu'$ becomes

$$\Delta\nu' \sim \frac{1}{\sqrt{n}}\frac{1}{T} = \frac{1}{\sqrt{n_0}}\frac{1}{T}\,e^{\frac{T}{2T_0}} \qquad (5)$$

It is apparent that the effective line width is greater if T is appreciably greater than T_0.

The point to be made, however, is that other experimental difficulties than purely statistical fluctuations determine the precision with which the line center can be measured in many cases and then it is often desirable to sacrifice a large signal in favor of a narrower line.

Another point to be emphasized for resonances detected in a bottle using the phase destruction technique is that it is not necessary to excite them with two pulses since the two 90° pulses define an active time interval for measurements. The difficulties encountered in atomic beam devices concerning field and phase uniformity mentioned above do not occur in the gas cell. A factor of approximately two can be gained by such double pulse excitation however.(110)

APPENDIX D TRANSITION PROBABILITIES; STOCHASTIC PUMPING AND RELAXATION MATRICES

In Section II A 3 the matrix elements of a vector operator which are required for the calculation of the transition probabilities between hyperfine magnetic substates used in computing optical pumping stochastic matrices are expressed in terms of the modern notation using Wigner 3-j and 6-j symbols.(113)

These are given explicit form here and their relation to the more usual notation of Condon and Shortley [114] is indicated.

The Wigner 3-j symbol is essentially the Wigner vector coupling coefficient, or Clebsch-Gordon coefficient, which serves to give the appropriate linear combination of the direct product wave functions of two definite angular momentum states in order that the linear combination have a definite angular momentum, angular momenta j_1 and j_2 giving rise to resultant momenta $|j_1 - j_2|, \cdots j_1 + j_2$. More symmetry is introduced by the definition

$$\left(F\, m,\ 1\, \sigma,\ F'\, m' \right) \equiv \frac{(-)^{F+F'-1}}{\sqrt{2F'+1}}\ S^{(F1)}_{F'm\sigma}\ \delta_{m',m+\sigma} \qquad (1)$$

where the symbol $S^{(F1)}_{F'm\sigma}$ is the one used by Wigner for the Clebsch-Gordon coefficient.

The 6-j symbol is closely related to the equations (8) of paragraph 11[3] of Condon and Shortley for the reduced matrix elements appearing in their equations (11) of paragraph 9[3] for matrix elements of a "class T" operator, which is essentially a vector operator. Among the important symmetries posessed by the 6-j symbols are these:

1) The value is unchanged by the interchange of any two columns

2) The value is unchanged by inverting any two columns simultaneously

These properties make it possible to reduce any of the 6-j symbols occuring in the calculation of the above matrix elements to one of

four standard forms which are given by Wigner[113] and reproduced here: ($J = j_1 + j_2 + j$ in these expressions)

$$\begin{Bmatrix} j_1 & 1 & j_1 \\ j_2 & j & j_2 \end{Bmatrix} = (-)^J \left[\frac{J(J+1)(J-2j_1-1)(J-2j_2)}{(2j_1-1)2j_1(2j_1+1)(2j_2-1)2j_2(2j_2+1)} \right]^{1/2}$$

$$\begin{Bmatrix} j_1 & 1 & j_1 \\ j_2 & j & j_2 \end{Bmatrix} = (-)^J \left[\frac{(J-2j_1)(J-2j_1+1)(J-2j_2)(J-2j_2+1)}{(2j_1-1)2j_1(2j_1+1)(2j_2-1)2j_2(2j_2+1)} \right]^{1/2}$$

$$\begin{Bmatrix} j_1 & 1 & j_1 \\ j_2 & j & j_2 \end{Bmatrix} = (-)^J \left[\frac{2(J+1)(J-2j)(J-2j_1)(J-2j_2+1)}{2j_1(2j_1+1)(2j_1+2)(2j_2-1)2j_2(2j_2+1)} \right]^{1/2}$$

$$\begin{Bmatrix} j_1 & 1 & j_1 \\ j_2 & j & j_2 \end{Bmatrix} = (-)^J \frac{j(j+1) - j_1(j_1+1) - j_2(j_2+1)}{\left[j_1(2j_1+1)(2j_1+2)j_2(2j_2+1)(2j_2+2) \right]^{1/2}}$$

The Wigner vector coupling coefficients $S^{(F1)}_{F'm\sigma}$ are given below:

F' \ σ	-1	0	1
$F-1$	$\sqrt{\frac{(F+m)(F+m-1)}{2F(2F+1)}}$	$-\sqrt{\frac{(F-m)(F+m)}{F(2F+1)}}$	$\sqrt{\frac{(F-m)(F-m-1)}{2F(2F+1)}}$
F	$\sqrt{\frac{(F+m)(F-m+1)}{2F(F+1)}}$	$\frac{m}{\sqrt{F(F+1)}}$	$-\sqrt{\frac{(F+m+1)(F-m)}{2F(F+1)}}$
$F+1$	$\sqrt{\frac{(F-m+1)(F-m+2)}{(2F+1)(2F+2)}}$	$\sqrt{\frac{(F-m+1)(F+m+1)}{(2F+1)(F+1)}}$	$\sqrt{\frac{(F+m+1)(F+m+2)}{(2F+1)(2F+2)}}$

The equations (11) in paragraph 9^3 of Condon and Shortley give only the numerators of the above table which differ by a factor $\sqrt{2}$ when account is taken of the use of the standard elements of the vector operator $p^{(\sigma)}$ as given in Section II A 3. The denominators of the above Table must be used with the 6-j symbols to obtain agreement with the Condon and Shortley formulation.

The sum rules given in Section II A 3 follow from the fact that the Clebsch-Gordon coefficients are the elements of a unitary matrix, which is actually an orthogonal matrix since they are real. This requires that

$$\sum_{m,\sigma} \left(S^{(F1)}_{F'm\sigma}\, \delta_{m', m+\sigma} \right)^2 = 1 \qquad (3)$$

or

$$\sum_{m,\sigma} \left(F\, m,\ 1\, \sigma,\ F'\, m' \right)^2 = \frac{1}{2F'+1} \qquad (4)$$

Some useful symmetries processed by the Wigner 3-j symbols are[113]

1) A cyclic permutation of entries (columns) does not change the value

2) A non-cyclic permutation introduces the factor $(-1)^{F + 1 + F'}$

3) a) Raising an index m changes the sign of m and introduced the factor $(-1)^{F-m}$

b) Lowering an index m changes the sign of m and introduces the factor $(-1)^{F + m}$

e.g. (a) $(F^m, 1^\tau, F'^{m'}) = (-1)^{F'-m'} (F^m, 1^\sigma, F'_{-m'})$

(b) $(F_m, 1^\sigma, F'_{m'}) = (-1)^{F+m} (F^{-m}, 1^\sigma, F'_{m'})$

The sum rule

$$\sum_{k,\tau} T_{ik}^{(\sigma)} = \text{const.} \tag{5}$$

requires the sum

$$\sum_{m',\sigma} (F^m, 1^\sigma, F'_{m'})^2 \tag{6}$$

This is easily put into the form in which the sum can be made over the first two indices, whose value is known from the orthogonality relations, by using the above symmetries, noting that the sign of the 3-j symbols do not matter since they appear squared and that the sign of an index which is summed over both positive and negative values also does not matter. Thus

$$\sum_{m',\sigma} (F^m, 1^\sigma, F'_{m'})^2 = \sum_{m'\sigma} (F'^{m'}, 1^\sigma, F_m)^2 = \frac{1}{2F+1} \tag{7}$$

A similar argument yields the second sum rule

$$\sum_{i,k} T_{ik}^{(\sigma)} \propto \sum_{m,m'} (F^m, 1^\sigma, F'_{m'})^2 = \frac{1}{2(1)+1} = \frac{1}{3} \tag{8}$$

These are the sums for the transitions between a state F and a state F'. If all accessible values of F' are included the sum rule which follows from the orthogonality of the 6-j symbol is needed[115]

$$\sum_{F'} (2F+1)(2F'+1) \begin{Bmatrix} F & 1 & F' \\ J' & I & J \end{Bmatrix}^2 = \frac{2F+1}{2J+1} \qquad (9)$$

The relative transition probabilities $T_{ik}^{(\sigma)}$ defined in Section II A 3 are displayed in the following tables (Table 5 and Table 6) for rubidium 87. The normalization chosen for these tables is conveniently expressed in terms of the sum rules of Section II A 3 as follows:

D_1 Transitions:

$$\sum_{i,k} T_{ik}^{(\sigma)} = 8 \quad \text{for each } \sigma = -1,\ 0,\ +1 \qquad (10)$$

$$\sum_{\sigma,k} T_{ik}^{(\sigma)} = 3 \quad \text{for each } i = 1,\ 2.....8 \qquad (11)$$

The second sum can be broken down in terms of the A_i introduced in Sections II A 6 and II B 3

$$\sum_{k} T_{ik}^{(+1)} = A_i \qquad (12)$$

$$\sum_{k} T_{ik}^{(0)} = 1 \qquad (13)$$

$$\sum_{k} T_{ik}^{(-1)} = 2-A_i \qquad (14)$$

D_2 Transitions:

$$\sum_{i,k} T_{ik}^{(\sigma)} = 16 \quad \text{for each } \sigma = -1,0,+1 \qquad (15)$$

$$\sum_{\sigma,k} T_{ik}^{(\sigma)} = 6 \quad \text{for each } i = 1,2,..8 \qquad (16)$$

This breaks down into

$$\sum_k T_{ik}^{(+1)} = 2\, A_i^{D2} \tag{17}$$

$$\sum_k T_{ik}^{(0)} = 2 \tag{18}$$

$$\sum_k T_{ik}^{(-1)} = 4 - 2\, A_i^{D2} \tag{19}$$

The stochastic matrices used to describe the optical pumping process, constructed from the transition probabilities as described in Section II A 3, are given in Tables 7 through 12 for σ^+, π, and σ^- pumping, along with the diagonal elements of the absorption matrix $\underset{\sim}{A}$ for σ^+ pumping.

Tables 13 and 14 give the stochastic relaxation matrices $\underset{\sim}{R}$ which result from the randomization of the electronic angular momentum leaving the nuclear spin unaffected. They may be computed by using the Wigner vector coupling coefficients (Clebsch-Gordon coefficients). The calculations were carried out by John McLeod at Princeton.

F,M_F / F,M_F	1,-1	1,0	1,1	2,-2	2,-1	2,0	2,1	2,2	$\sum_k T^{0}_{1k}$	$\sum_k T^{(+1)}_{1k}$	$\sum_k T^{(-1)}_{1k}$
1,-1	$\frac{1}{4}_{0}$	$\frac{1}{4}_{+}$	0	$\frac{3}{2}_{-}$	$\frac{3}{4}_{0}$	$\frac{1}{4}_{+}$	0	0	1	$\frac{1}{2}$	$\frac{3}{2}$
1,0	$\frac{1}{4}_{-}$	0	$\frac{1}{4}_{+}$	0	$\frac{3}{4}_{-}$	1_{0}	$\frac{3}{4}_{+}$	0	1	1	1
1,1	0	$\frac{1}{4}_{-}$	$\frac{1}{4}_{0}$	0	0	$\frac{1}{4}_{-}$	$\frac{3}{4}_{0}$	$\frac{3}{2}_{+}$	1	$\frac{3}{2}$	$\frac{1}{2}$
2,-2	$\frac{3}{2}_{+}$	0	0	1_{0}	$\frac{1}{2}_{+}$	0	0	0	1	2	0
2,-1	$\frac{3}{4}_{0}$	$\frac{3}{4}_{+}$	0	$\frac{1}{2}_{-}$	$\frac{1}{4}_{0}$	$\frac{3}{4}_{+}$	0	0	1	$\frac{3}{2}$	$\frac{1}{2}$
2,0	$\frac{1}{4}_{-}$	1_{0}	$\frac{1}{4}_{+}$	0	$\frac{3}{4}_{-}$	0	$\frac{3}{4}_{+}$	0	1	1	1
2,1	0	$\frac{3}{4}_{-}$	$\frac{3}{4}_{0}$	0	0	$\frac{3}{4}_{-}$	$\frac{1}{4}_{0}$	$\frac{1}{2}_{+}$	1	$\frac{1}{2}$	$\frac{3}{2}$
2,2	0	0	$\frac{3}{2}_{-}$	0	0	0	$\frac{1}{2}_{-}$	1_{0}	1	0	2

TABLE 5. TRANSITION PROBABILITIES TO $^2P_{1/2}$: $T^{(-1)}+T^{(0)}+T^{(+1)}$

F,M_F / F,M_F	0,0	1,-1	1,0	1,1	2,-2	2,-1	2,0	2,1	2,2	3,-3	3,-2	3,-1	3,0	3,1	3,2	3,3	$\sum_k T^{(0)}_{1k}$	$\sum_k T^{(+1)}_{1k}$	$\sum_k T^{(-1)}_{1k}$
1,-1	1_{+}	$\frac{5}{4}_{0}$	$\frac{5}{4}_{+}$	0	$\frac{3}{2}_{-}$	$\frac{3}{4}_{0}$	$\frac{1}{4}_{+}$	0	0	0	0	0	0	0	0	0	2	$\frac{5}{2}$	$\frac{3}{2}$
1,0	1_{0}	$\frac{5}{4}_{-}$	0	$\frac{5}{4}_{+}$	0	$\frac{3}{4}_{-}$	1_{0}	$\frac{3}{4}_{+}$	0	0	0	0	0	0	0	0	2	2	2
1,1	1_{-}	0	$\frac{5}{4}_{-}$	$\frac{5}{4}_{0}$	0	0	$\frac{1}{4}_{-}$	$\frac{3}{4}_{0}$	$\frac{3}{2}_{+}$	0	0	0	0	0	0	0	2	$\frac{3}{2}$	$\frac{5}{2}$
2,2	0	$\frac{3}{10}_{+}$	0	0	1_{0}	$\frac{1}{2}_{+}$	0	0	0	3_{-}	1_{0}	$\frac{1}{5}_{+}$	0	0	0	0	2	1	3
2,-1	0	$\frac{3}{20}_{0}$	$\frac{3}{20}_{+}$	0	$\frac{1}{2}_{-}$	$\frac{1}{4}_{0}$	$\frac{3}{4}_{+}$	0	0	0	2_{-}	$\frac{8}{5}_{0}$	$\frac{3}{5}_{+}$	0	0	0	2	$\frac{3}{2}$	$\frac{5}{2}$
2,0	0	$\frac{1}{20}_{-}$	$\frac{1}{5}_{0}$	$\frac{1}{20}_{+}$	0	$\frac{3}{4}_{-}$	0	$\frac{3}{4}_{+}$	0	0	0	$\frac{6}{5}_{-}$	$\frac{9}{5}_{0}$	$\frac{6}{5}_{+}$	0	0	2	2	2
2,1	0	0	$\frac{3}{20}_{-}$	$\frac{3}{20}_{0}$	0	0	$\frac{3}{4}_{-}$	$\frac{1}{4}_{0}$	$\frac{1}{2}_{+}$	0	0	0	$\frac{3}{5}_{-}$	$\frac{8}{5}_{0}$	2_{+}	0	2	$\frac{5}{2}$	$\frac{3}{2}$
2,2	0	0	0	$\frac{3}{10}_{-}$	0	0	0	$\frac{1}{2}_{-}$	1_{0}	0	0	0	0	$\frac{1}{5}_{-}$	1_{0}	3_{+}	2	3	1

TABLE 6. TRANSITION PROBABILITIES TO $^2P_{3/2}$: $T^{(-1)}+T^{(0)}+T^{(+1)}$

F,M_F \ F,M_F	1,-1	1,0	1,1	2,-2	2,-1	2,0	2,1	2,2
1,-1	$\frac{1}{12}$	$\frac{1}{6}$	$\frac{1}{12}$	0	$\frac{1}{4}$	$\frac{1}{6}$	$\frac{1}{4}$	0
1,0	0	$\frac{5}{24}$	$\frac{5}{24}$	0	0	$\frac{5}{24}$	$\frac{1}{8}$	$\frac{1}{4}$
1,1	0	0	$\frac{1}{2}$	0	0	0	$\frac{1}{6}$	$\frac{1}{3}$
2,-2	$\frac{1}{8}$	$\frac{1}{8}$	0	$\frac{5}{12}$	$\frac{5}{24}$	$\frac{1}{8}$	0	0
2,-1	$\frac{1}{12}$	$\frac{1}{6}$	$\frac{1}{12}$	0	$\frac{1}{4}$	$\frac{1}{6}$	$\frac{1}{4}$	0
2,0	0	$\frac{5}{24}$	$\frac{5}{24}$	0	0	$\frac{5}{24}$	$\frac{1}{8}$	$\frac{1}{4}$
2,1	0	0	$\frac{1}{2}$	0	0	0	$\frac{1}{6}$	$\frac{1}{3}$
2,2	0	0	0	0	0	0	0	1

$\underline{A} = \mathrm{diag}(\frac{1}{2}, 1, \frac{3}{2}, 2, \frac{3}{2}, 1, \frac{1}{2}, 0)$

TABLE 7. STOCHASTIC MATRIX FOR σ^+ PUMPING WITH D_1 RADIATION

F,M_F \ F,M_F	1,-1	1,0	1,1	2,-2	2,-1	2,0	2,1	2,2
1,-1	$\frac{7}{20}$	$\frac{1}{6}$	$\frac{7}{20}$	0	$\frac{1}{20}$	$\frac{1}{30}$	$\frac{1}{20}$	0
1,0	0	$\frac{17}{48}$	$\frac{17}{48}$	0	0	$\frac{5}{48}$	$\frac{1}{16}$	$\frac{1}{8}$
1,1	0	0	$\frac{1}{2}$	0	0	0	$\frac{1}{6}$	$\frac{1}{3}$
2,-2	$\frac{1}{4}$	$\frac{1}{4}$	0	$\frac{19}{150}$	$\frac{49}{300}$	$\frac{21}{100}$	0	0
2,-1	$\frac{1}{12}$	$\frac{1}{6}$	$\frac{1}{12}$	0	$\frac{21}{100}$	$\frac{111}{450}$	$\frac{21}{100}$	0
2,0	0	$\frac{5}{48}$	$\frac{5}{48}$	0	0	$\frac{401}{1200}$	$\frac{141}{400}$	$\frac{21}{200}$
2,1	0	0	$\frac{1}{10}$	0	0	0	$\frac{17}{30}$	$\frac{1}{3}$
2,2	0	0	0	0	0	0	0	1

$\underline{A} = \mathrm{diag}(\frac{5}{4}, 1, \frac{3}{4}, \frac{1}{2}, \frac{3}{4}, 1, \frac{5}{4}, \frac{3}{2})$

TABLE 8. STOCHASTIC MATRIX FOR σ^+ PUMPING WITH D_2 RADIATION

INITIAL \ FINAL	1,-1	1,0	1,1	2,-2	2,-1	2,0	2,1	2,2
1,-1	$\frac{5}{24}$	$\frac{5}{24}$	0	$\frac{1}{4}$	$\frac{1}{8}$	$\frac{5}{24}$	0	0
1,0	$\frac{1}{12}$	$\frac{1}{3}$	$\frac{1}{12}$	0	$\frac{1}{4}$	0	$\frac{1}{4}$	0
1,1	0	$\frac{5}{24}$	$\frac{5}{24}$	0	0	$\frac{5}{24}$	$\frac{1}{8}$	$\frac{1}{4}$
2,-2	$\frac{1}{2}$	0	0	$\frac{1}{3}$	$\frac{1}{6}$	0	0	0
2,-1	$\frac{1}{8}$	$\frac{1}{8}$	0	$\frac{5}{12}$	$\frac{5}{24}$	$\frac{1}{8}$	0	0
2,0	$\frac{1}{12}$	0	$\frac{1}{12}$	0	$\frac{1}{4}$	$\frac{1}{3}$	$\frac{1}{4}$	0
2,1	0	$\frac{1}{8}$	$\frac{1}{8}$	0	0	$\frac{1}{8}$	$\frac{5}{24}$	$\frac{5}{12}$
2,2	0	0	$\frac{1}{2}$	0	0	0	$\frac{1}{6}$	$\frac{1}{3}$

TABLE 9. STOCHASTIC MATRIX FOR π PUMPING WITH D_1 RADIATION.

INITIAL \ FINAL	1,-1	1,0	1,1	2,-2	2,-1	2,0	2,1	2,2
1,-1	$\frac{17}{48}$	$\frac{17}{48}$	0	$\frac{1}{8}$	$\frac{1}{16}$	$\frac{5}{48}$	0	0
1,0	$\frac{5}{24}$	$\frac{1}{3}$	$\frac{5}{24}$	0	$\frac{1}{8}$	0	$\frac{1}{8}$	0
1,1	0	$\frac{17}{48}$	$\frac{17}{48}$	0	0	$\frac{5}{48}$	$\frac{1}{16}$	$\frac{1}{8}$
2,-2	$\frac{1}{4}$	0	0	$\frac{1}{3}$	$\frac{5}{12}$	0	0	0
2,-1	$\frac{1}{16}$	$\frac{1}{16}$	0	$\frac{49}{600}$	$\frac{529}{1200}$	$\frac{473}{1200}$	0	0
2,0	$\frac{1}{24}$	0	$\frac{1}{24}$	0	$\frac{111}{600}$	$\frac{41}{75}$	$\frac{111}{600}$	0
2,1	0	$\frac{1}{16}$	$\frac{1}{16}$	0	0	$\frac{473}{1200}$	$\frac{529}{1200}$	$\frac{49}{600}$
2,2	0	0	$\frac{1}{4}$	0	0	0	$\frac{5}{12}$	$\frac{1}{3}$

TABLE 10. STOCHASTIC MATRIX FOR π PUMPING WITH D_2 RADIATION.

F,M_F / F,M_F	1,-1	1,0	1,1	2,-2	2,-1	2,0	2,1	2,2
1,-1	$\frac{19}{48}$	$\frac{1}{24}$	$\frac{1}{48}$	$\frac{1}{4}$	$\frac{9}{48}$	$\frac{1}{24}$	$\frac{1}{16}$	0
1,0	$\frac{5}{48}$	$\frac{5}{24}$	$\frac{5}{48}$	$\frac{1}{8}$	$\frac{1}{16}$	$\frac{5}{24}$	$\frac{1}{16}$	$\frac{1}{8}$
1,1	$\frac{1}{48}$	$\frac{1}{24}$	$\frac{19}{48}$	0	$\frac{1}{16}$	$\frac{1}{24}$	$\frac{9}{48}$	$\frac{1}{4}$
2,-2	$\frac{1}{8}$	$\frac{1}{8}$	0	$\frac{5}{12}$	$\frac{5}{24}$	$\frac{1}{8}$	0	0
2,-1	$\frac{9}{48}$	$\frac{1}{8}$	$\frac{1}{16}$	$\frac{1}{12}$	$\frac{11}{48}$	$\frac{1}{8}$	$\frac{9}{48}$	0
2,0	$\frac{5}{48}$	$\frac{5}{24}$	$\frac{5}{48}$	$\frac{1}{8}$	$\frac{1}{16}$	$\frac{5}{24}$	$\frac{1}{16}$	$\frac{1}{8}$
2,1	$\frac{1}{16}$	$\frac{1}{8}$	$\frac{9}{48}$	0	$\frac{9}{48}$	$\frac{1}{8}$	$\frac{11}{48}$	$\frac{1}{12}$
2,2	0	$\frac{1}{8}$	$\frac{1}{8}$	0	0	$\frac{1}{8}$	$\frac{5}{24}$	$\frac{5}{12}$

TABLE II. STOCHASTIC MATRIX FOR σ PUMPING WITH D_1 RADIATION

F,M_F / F,M_F	1,-1	1,0	1,1	2,-2	2,-1	2,0	2,1	2,2
1,-1	$\frac{13}{32}$	$\frac{5}{48}$	$\frac{7}{32}$	$\frac{1}{8}$	$\frac{3}{32}$	$\frac{1}{48}$	$\frac{1}{32}$	0
1,0	$\frac{17}{96}$	$\frac{17}{48}$	$\frac{17}{96}$	$\frac{1}{16}$	$\frac{1}{32}$	$\frac{5}{48}$	$\frac{1}{32}$	$\frac{1}{16}$
1,1	$\frac{7}{32}$	$\frac{5}{48}$	$\frac{13}{32}$	0	$\frac{1}{32}$	$\frac{1}{48}$	$\frac{3}{32}$	$\frac{1}{8}$
2,-2	$\frac{1}{16}$	$\frac{1}{16}$	0	$\frac{938}{1200}$	$\frac{49}{1200}$	$\frac{63}{1200}$	0	0
2,-1	$\frac{3}{32}$	$\frac{1}{16}$	$\frac{1}{32}$	$\frac{5}{24}$	$\frac{1039}{2400}$	$\frac{111}{1200}$	$\frac{189}{2400}$	0
2,0	$\frac{5}{96}$	$\frac{5}{48}$	$\frac{5}{96}$	$\frac{63}{1200}$	$\frac{423}{2400}$	$\frac{401}{1200}$	$\frac{423}{2400}$	$\frac{63}{1200}$
2,1	$\frac{1}{32}$	$\frac{1}{16}$	$\frac{3}{32}$	0	$\frac{189}{2400}$	$\frac{111}{1200}$	$\frac{1039}{2400}$	$\frac{5}{24}$
2,2	0	$\frac{1}{16}$	$\frac{1}{16}$	0	0	$\frac{63}{1200}$	$\frac{49}{1200}$	$\frac{938}{1200}$

TABLE 12. STOCHASTIC MATRIX FOR σ PUMPING WITH D_2 RADIATION

INITIAL \ FINAL	1,-1	1,0	1,1	2,-2	2,-3	2,0	2,1	2,2
1,-1	$\frac{5}{16}$	$\frac{1}{16}$	0	$\frac{3}{8}$	$\frac{3}{16}$	$\frac{1}{16}$	0	0
1,0	$\frac{1}{16}$	$\frac{1}{4}$	$\frac{1}{16}$	0	$\frac{3}{16}$	$\frac{1}{4}$	$\frac{3}{16}$	0
1,1	0	$\frac{1}{16}$	$\frac{5}{16}$	0	0	$\frac{1}{16}$	$\frac{3}{16}$	$\frac{3}{8}$
2,-2	$\frac{3}{8}$	0	0	$\frac{1}{2}$	$\frac{1}{8}$	0	0	0
2,-1	$\frac{3}{16}$	$\frac{3}{16}$	0	$\frac{1}{8}$	$\frac{5}{16}$	$\frac{3}{16}$	0	0
2,0	$\frac{1}{16}$	$\frac{1}{4}$	$\frac{1}{16}$	0	$\frac{3}{16}$	$\frac{1}{4}$	$\frac{3}{16}$	0
2,1	0	$\frac{3}{16}$	$\frac{3}{16}$	0	0	$\frac{3}{16}$	$\frac{5}{16}$	$\frac{1}{8}$
2,2	0	0	$\frac{3}{8}$	0	0	0	$\frac{1}{8}$	$\frac{1}{2}$

TABLE 13. RELAXATION STOCHASTIC MATRIX FOR $^2S_{1/2}$ AND $^2P_{1/2}$ STATES.

INITIAL \ FINAL	0,0	1,-1	1,0	1,1	2,-2	2,-1	2,0	2,1	2,2	3,-3	3,-2	3,-1	3,0	3,1	3,2	3,3
0,0	$\frac{1}{16}$	$\frac{1}{16}$	$\frac{1}{16}$	$\frac{1}{16}$	$\frac{1}{16}$	$\frac{1}{16}$	$\frac{1}{16}$	$\frac{1}{16}$	$\frac{1}{16}$	$\frac{1}{16}$	$\frac{1}{16}$	$\frac{1}{16}$	$\frac{1}{16}$	$\frac{1}{16}$	$\frac{1}{16}$	$\frac{1}{16}$
1,-1	$\frac{1}{16}$	$\frac{17}{200}$	$\frac{17}{400}$	$\frac{3}{50}$	$\frac{7}{80}$	$\frac{3}{40}$	$\frac{1}{16}$	$\frac{1}{20}$	$\frac{3}{80}$	$\frac{3}{40}$	$\frac{7}{80}$	$\frac{9}{100}$	$\frac{33}{400}$	$\frac{13}{200}$	$\frac{3}{80}$	0
1,0	$\frac{1}{16}$	$\frac{17}{400}$	$\frac{41}{400}$	$\frac{17}{400}$	$\frac{1}{16}$	$\frac{1}{16}$	$\frac{1}{16}$	$\frac{1}{16}$	$\frac{1}{16}$	$\frac{9}{80}$	$\frac{1}{16}$	$\frac{13}{400}$	$\frac{9}{400}$	$\frac{13}{400}$	$\frac{1}{16}$	$\frac{9}{80}$
1,1	$\frac{1}{16}$	$\frac{3}{80}$	$\frac{17}{400}$	$\frac{17}{200}$	$\frac{3}{80}$	$\frac{1}{20}$	$\frac{1}{16}$	$\frac{3}{40}$	$\frac{7}{80}$	0	$\frac{3}{80}$	$\frac{13}{200}$	$\frac{33}{400}$	$\frac{9}{100}$	$\frac{7}{80}$	$\frac{3}{40}$
2,-2	$\frac{1}{16}$	$\frac{7}{80}$	$\frac{1}{16}$	$\frac{3}{80}$	$\frac{1}{8}$	$\frac{1}{16}$	$\frac{1}{16}$	$\frac{1}{16}$	0	$\frac{1}{8}$	$\frac{1}{8}$	$\frac{1}{10}$	$\frac{1}{16}$	$\frac{1}{40}$	0	0
2,-1	$\frac{1}{16}$	$\frac{3}{40}$	$\frac{1}{16}$	$\frac{1}{20}$	$\frac{1}{16}$	$\frac{1}{8}$	$\frac{1}{16}$	0	$\frac{1}{16}$	$\frac{1}{8}$	$\frac{1}{16}$	$\frac{1}{20}$	$\frac{1}{16}$	$\frac{3}{40}$	$\frac{1}{16}$	0
2,0	$\frac{1}{16}$	$\frac{1}{16}$	$\frac{1}{16}$	$\frac{1}{16}$	$\frac{1}{16}$	$\frac{1}{16}$	$\frac{1}{16}$	$\frac{1}{16}$	$\frac{1}{16}$	$\frac{1}{16}$	$\frac{1}{16}$	$\frac{1}{16}$	$\frac{1}{16}$	$\frac{1}{16}$	$\frac{1}{16}$	$\frac{1}{16}$
2,1	$\frac{1}{16}$	$\frac{1}{20}$	$\frac{1}{16}$	$\frac{3}{40}$	$\frac{1}{16}$	0	$\frac{1}{16}$	$\frac{1}{8}$	$\frac{1}{16}$	0	$\frac{1}{16}$	$\frac{3}{40}$	$\frac{1}{16}$	$\frac{1}{20}$	$\frac{1}{16}$	$\frac{1}{8}$
2,2	$\frac{1}{16}$	$\frac{3}{80}$	$\frac{1}{16}$	$\frac{7}{80}$	0	$\frac{1}{16}$	$\frac{1}{16}$	$\frac{1}{16}$	$\frac{1}{8}$	0	0	$\frac{1}{40}$	$\frac{1}{16}$	$\frac{1}{10}$	$\frac{1}{8}$	$\frac{1}{8}$
3,-3	$\frac{1}{16}$	$\frac{3}{40}$	$\frac{9}{80}$	0	$\frac{1}{8}$	$\frac{1}{8}$	$\frac{1}{16}$	0	0	$\frac{1}{4}$	$\frac{1}{8}$	$\frac{1}{20}$	$\frac{1}{80}$	0	0	0
3,-2	$\frac{1}{16}$	$\frac{7}{80}$	$\frac{1}{16}$	$\frac{3}{80}$	$\frac{1}{8}$	$\frac{1}{16}$	$\frac{1}{16}$	$\frac{1}{16}$	0	$\frac{1}{8}$	$\frac{1}{8}$	$\frac{1}{10}$	$\frac{1}{16}$	$\frac{1}{40}$	0	0
3,-1	$\frac{1}{16}$	$\frac{9}{100}$	$\frac{13}{400}$	$\frac{13}{200}$	$\frac{1}{10}$	$\frac{1}{20}$	$\frac{1}{16}$	$\frac{3}{40}$	$\frac{1}{40}$	$\frac{1}{20}$	$\frac{1}{10}$	$\frac{1}{100}$	$\frac{37}{400}$	$\frac{3}{50}$	$\frac{1}{40}$	0
3,0	$\frac{1}{16}$	$\frac{33}{400}$	$\frac{9}{400}$	$\frac{33}{400}$	$\frac{1}{16}$	$\frac{1}{16}$	$\frac{1}{16}$	$\frac{1}{16}$	$\frac{1}{16}$	$\frac{1}{80}$	$\frac{1}{16}$	$\frac{37}{400}$	$\frac{41}{400}$	$\frac{37}{400}$	$\frac{1}{16}$	$\frac{1}{80}$
3,1	$\frac{1}{16}$	$\frac{13}{200}$	$\frac{13}{400}$	$\frac{9}{100}$	$\frac{1}{40}$	$\frac{3}{40}$	$\frac{1}{16}$	$\frac{1}{20}$	$\frac{1}{10}$	0	$\frac{1}{40}$	$\frac{3}{50}$	$\frac{37}{400}$	$\frac{11}{100}$	$\frac{1}{10}$	$\frac{1}{20}$
3,2	$\frac{1}{16}$	$\frac{3}{80}$	$\frac{1}{16}$	$\frac{7}{80}$	0	$\frac{1}{16}$	$\frac{1}{16}$	$\frac{1}{16}$	$\frac{1}{8}$	0	0	$\frac{1}{40}$	$\frac{1}{16}$	$\frac{1}{10}$	$\frac{1}{8}$	$\frac{1}{8}$
3,3	$\frac{1}{16}$	0	$\frac{9}{80}$	$\frac{3}{40}$	0	0	$\frac{1}{16}$	$\frac{1}{8}$	$\frac{1}{8}$	0	0	0	$\frac{1}{80}$	$\frac{1}{20}$	$\frac{1}{8}$	$\frac{1}{4}$

TABLE 14. RELAXATION STOCHASTIC MATRIX FOR $^2P_{3/2}$ STATES.

APPENDIX E OPTICAL PUMPING EQUATIONS; DIGITAL COMPUTER SOLUTIONS

The equations given in Section II A 6 are only approximate in that the excited state populations are neglected. Also they are written for the population vector $\underline{N}$ (i.e. the diagonal elements of the density matrix) rather than for the actual particle density vector $n\,\underline{N}$ where n is the number of atoms per cm^3 in the ground state. A set of two coupled equations are presented here for the vectors $n\,\underline{N}$ and $n'\underline{N}'$, where the primes denote the corresponding quantities in the excited state. The explicit conditions under which these reduce to equation (17) given in Section II A 6 are pointed out. That equation was derived by adding a rate to the basic transition probabilities resulting from treating the resonance fluorescence as a single process, as done by Hawkins and Dicke,[5] following Heitler,[25] when the interference terms in the excited state are neglected. The equations given here treat the resonance fluorescence as a process of absorption and subsequent emission, treating the absorption as an incoherent process.

The absorption, induced emission, and spontaneous decay terms will be separately included. For the ground state populations one obtains

$$\frac{d}{dt}(n N_j) = -\pi c r_0 \frac{2m\omega}{\hbar} \sum_k n N_j I_\nu^{jk} T_{jk}^{(\sigma)} \quad \text{Absorption}$$

$$+\pi c r_0 \frac{2m\omega}{\hbar} \sum_k n' N_k' I_{\nu_c}^{kj} T_{kj}^{(\sigma')} \quad \text{Induced Emission} \qquad (1)$$

$$+ \frac{1}{\eta} \sum_{k,\sigma'} \frac{n' N_k'}{\tau'} T_{kj}^{(\sigma')} \quad \text{Spontaneous Emission}$$

where $$\eta = \sum_{j,\sigma'} T_{kj}^{(\sigma')}$$

so that $$\eta^{-1} \sum_{\sigma'} T_{kj}^{(\sigma')} \qquad (2)$$

is a stochastic matrix. Except for the spontaneous decay time τ', which is defined below, the other notation is as given in Section II, except that $T_{ik}^{(\sigma)}$ is here taken as

$$T_{ik}^{(\sigma)} = |(i | r^{(\sigma)} | k)|^2$$

with $$r^{(-1)} = (x + iy)/\sqrt{2}$$

$$r^{(0)} = z$$

$$r^{(+1)} = -(x - iy)/\sqrt{2}$$

For the excited states populations the analogous equation is

$$\frac{d}{dt}(n'N_k') = \pi c r_0 \frac{2mc}{k} \sum_i n N_i I_{\nu_0}^{ik} T_{ik}^{(\sigma)} \quad \text{Pumping}$$

$$- \pi c r_0 \frac{2mc}{k} \sum_j n' N_k' I_{\nu_0}^{kj} T_{kj}^{(\sigma)} \quad \text{Induced Emission} \qquad (3)$$

$$- \frac{n' N_k'}{\tau'} \quad \text{Spontaneous Emission}$$

where

$$\frac{1}{\tau'} = \sum_{j,\sigma} A_{kj}^{(\sigma)}$$

The quantity $A_{kj}^{(\sigma)}$ is the Einstein A coefficient. As was first shown by Ladenburg,[116] the A coefficient is related to the oscillator strength by the equation

$$A_{kj}^{(\sigma)} = \gamma_0 f_{kj}^{(\sigma)} \tag{4}$$

where γ_0 is the decay constant for a radiation damped classical dipole oscillator

$$\gamma_0 = \frac{2}{3}\frac{e^2}{m}\frac{\omega^2}{c^3} \approx 10^8 \sec^{-1} \tag{5}$$

Since

$$f_{kj}^{(\sigma)} = \frac{2m\omega}{\hbar} T_{kj}^{(\sigma)} \tag{6}$$

we obtain

$$\begin{aligned} \frac{1}{\tau'} &= \frac{4}{3}\frac{e^2}{c^3}\frac{\omega^3}{\hbar}\sum_{j,\sigma'} T_{kj}^{(\sigma')} \\ &= \frac{4}{3}\frac{e^2}{c^3}\frac{\omega^3}{\hbar}\gamma_l \end{aligned} \tag{7}$$

The induced emission term will be negligible with respect to the other two terms under most excitation conditions, so that in the steady state

$$\pi c r_0 \frac{2mc}{\hbar}\sum_i n N_i I_{\nu_0}^{ik} T_{ik}^{(\sigma)} = \frac{n' N_k'}{\tau'} \tag{8}$$

One may substitute this into the spontaneous emission term in the equation for ground state populations to yield

$$\frac{1}{\gamma_l}\pi c r_0 \frac{2mc}{\hbar} n \sum_{i,k,\sigma'} N_i I_{\nu_0}^{ik} T_{ik}^{(\sigma)} T_{kj}^{(\sigma')} \tag{9}$$

This term is completely equivalent to

$$n \sum_i N_i \Gamma_i^{(\sigma)} P_{ij}^{(\sigma)} \tag{10}$$

where

$$\Gamma_i^{(\sigma)} = \pi c r_0 \frac{2m\omega}{\hbar} \sum_k I_{\nu_0}^{ik} T_{ik}^{(\sigma)} \tag{11}$$

and

$$P_{ij}^{(\sigma)} = \frac{1}{\tilde{A}_i^{(\sigma)} \Phi} \sum_{k,\sigma'} T_{ik}^{(\sigma)} T_{kj}^{(\sigma')} \tag{12}$$

with

$$\tilde{A}_i^{(\sigma)} = \sum_k T_{ik}^{(\sigma)} \tag{13}$$

This can be seen by summing each expression on j to yield

$$\sum_i n N_i \Gamma_i^{(\sigma)} = \pi c r_0 \frac{2m\omega}{\hbar} \sum_{i,k} n N_i I_{\nu_0}^{ik} T_{ik}^{(\sigma)} \tag{14}$$

It is convenient (and experimentally realistic) to let $I_{\nu_0}^{ik} = I_{\nu_0}^{(\sigma)}$ the same for all transitions of the (σ) type

then

$$\begin{aligned} \sum_i N_i \Gamma_i^{(\sigma)} &= \pi c r_0 \frac{2m\omega}{\hbar} I_{\nu_0}^{(\sigma)} \sum_{i,k} N_i T_{ik}^{(\sigma)} \\ &= \pi c r_0 \frac{2m\omega}{\hbar} I_{\nu_0}^{(\sigma)} \sum_i N_i \tilde{A}_i^{(\sigma)} \\ &= I_{\nu_0}^{(\sigma)} \pi c r_0 f_{eff}^{(\sigma)} \end{aligned} \tag{15}$$

where $$f_{eff}^{(\sigma)} = \frac{2 m_i \omega}{\hbar} \sum_i N_i \tilde{A}_i^{(\sigma)}$$

$$= \frac{2 m_i \omega}{\hbar} \sum_{i,k} N_i T_{ik}^{(\sigma)} \qquad (16)$$

$$= f_0 \sum_i N_i A_i^{(\sigma)}$$

where the definition

$$f_0 A_i^{(\sigma)} = \frac{2 m_i \omega}{\hbar} \tilde{A}_i^{(\sigma)} \qquad (17)$$

was used.

Then

$$\Gamma_i^{(\sigma)} = \pi c r_0 I_{\nu_0}^{(\sigma)} f_0 A_i^{(\sigma)} \qquad (18)$$

Using these last results and definitions, the absorption term in the ground state equation becomes

$$- \Gamma_j^{(\sigma)} n N_j$$

With neglect of the induced emission term involving n', the ground state equation becomes

$$\frac{d}{dt}(n N_j) = \sum_i n N_i \Gamma_i^{(\sigma)} P_{ij}^{(\sigma)} - \Gamma_j^{(\sigma)} n N_j \qquad (19)$$

as given in Section II A 6.

That n'/n is indeed small can be seen by summing equation (8) on k

$$\frac{n'}{\tau'} = \sum_i n N_i \Gamma_i^{(\sigma)} = n \Gamma^{(\sigma)} \frac{f_{eff}}{f_0} \qquad (20)$$

Where $\Gamma^{(\sigma)}$ is defined by

$$\Gamma_i^{(\sigma)} = \Gamma^{(\sigma)} A_i^{(\sigma)} \tag{21}$$

Thus

$$\Gamma^{(\sigma)} = \pi c r_0 I_{\nu_0}^{(\sigma)} f_0 \tag{22}$$

Since $\tau' << \left(\Gamma^{(\sigma)}\right)^{-1}$, one has $n'/n << 1$.

In vector form one may write equation (8) as

$$\frac{n'}{\tau'} \underline{N}' = n \Gamma^{(\sigma)} \underline{\underline{T}}^{(\sigma)\,T} \underline{N} \tag{23}$$

where $\underline{\underline{T}}^{(\sigma)}$ is the matrix with elements $T_{ik}^{(\sigma)}$.
Using equation (20) one has

$$f_{eff}^{(\sigma)} \underline{N}' = f_0 \underline{\underline{T}}^{(\sigma)\,T} \underline{N} \tag{24}$$

Relaxation terms could be included in the equations given here exactly as done in Section II A 6 by introducing relaxation stochastic matrices and characteristic times. For example, collisions in the excited state would require a term

$$\frac{1}{T'} \left[\sum_l N_l' R_{lk} - N_k' \right] \tag{25}$$

which should be retained along with the pumping term and the spontaneous emission term. Since R_{lk} is stochastic, the relation

between n and n' as expressed in equation (20) is not affected. The relation (23) between $\underline{N}$ and $\underline{N}'$ is changed and becomes

$$\frac{n'}{\tau'}\left(\frac{\tau'+T'}{T'}\right)\left[\underset{\sim}{I}-\left(\frac{\tau'}{\tau'+T'}\right)\underset{\sim}{R}^{T}\right]\underline{N}'=n\Gamma^{(\sigma)}\underset{\sim}{T}^{(\sigma)^{T}}\underline{N} \tag{26}$$

The spontaneous decay term in the ground state equation becomes in vector form

$$\frac{1}{\eta_1}\ \frac{n'}{\tau'}\ \underline{N}'^{T}\sum_{\sigma'}\underset{\sim}{T}^{(\sigma')} \tag{27}$$

which becomes, in terms of $\underline{N}$

$$\frac{1}{\eta}\ \Gamma^{(\sigma)}n\ \underline{N}^{T}\underset{\sim}{T}^{(\sigma)}\left(\frac{T'}{\tau'+T'}\right)\left[\underset{\sim}{I}-\left(\frac{\tau'}{\tau'+T'}\right)\underset{\sim}{R}\right]^{-1}\sum_{\sigma'}\underset{\sim}{T}^{(\sigma')} \tag{28}$$

If one defines

$$q=\frac{\tau'}{\tau'+T'} \tag{29}$$

then

$$1-q=\frac{T'}{\tau'+T'} \tag{30}$$

and one needs to consider the matrix

$$(1-q)\left[\underset{\sim}{I}-q\,\underset{\sim}{R}\right]^{-1} \tag{31}$$

If $\underset{\sim}{R}$ is the completely uniform stochastic relaxation matrix with elements R_{1k} = const. (const. = 1/8 for $^2P_{\frac{1}{2}}$ states and 1/16 for $^2P_{3/2}$ states)

Then

$$\left[\underline{\underline{1}} - q\,\underline{\underline{R}}\right]^{-1} = \underline{\underline{1}} + \frac{q}{1-q}\,\underline{\underline{R}} \tag{32}$$

since $\underline{\underline{R}}^2 = \underline{\underline{R}}$.

The spontaneous emission term now separates into a sum of two terms

$$\frac{1}{\eta}\,\Gamma^{(\sigma)}\,n\,\underline{N}^{\tau}\left\{(1-q)\,\underline{\underline{T}}^{(\sigma)}\sum_{\sigma'}\underline{\underline{T}}^{(\sigma')} + q\,\underline{\underline{T}}^{(\sigma)}\,\underline{\underline{R}}\sum_{\sigma'}\underline{\underline{T}}^{(\sigma')}\right\} \tag{33}$$

The matrices

$$\frac{1}{\eta}\,\underline{\underline{T}}^{(\sigma)}\sum_{\sigma'}\underline{\underline{T}}^{(\sigma')} = \underline{\underline{A}}^{(\sigma)}\,\underline{\underline{P}}^{(\sigma)} \tag{34}$$

and

$$\frac{1}{\eta}\,\underline{\underline{T}}^{(\sigma)}\,\underline{\underline{R}}\sum_{\sigma'}\underline{\underline{T}}^{(\sigma')} = \underline{\underline{A}}^{(\sigma)}\,\hat{\underline{\underline{P}}}^{(\sigma)} \tag{35}$$

are just those introduced in Section II A 4, to describe relaxation effects. If $\underline{\underline{R}}$ is not uniform, $\underline{\underline{R}}^2 \neq \underline{\underline{R}}$ and such a simple decomposition is not possible, but the rapid convergence of higher powers of $\underline{\underline{R}}$ can be utilized.

The density matrix describing the intensity and polarization of the emitted light as a function of angle can be readily obtained as a weighted sum of the density matrices $\hat{\rho}^{(\sigma)}$ given in Section II A 3. The number of photons per second emitted in a transition of the type (σ) is

$$n'\,\gamma_0\sum_{k,j} N_k'\,f_{kj}^{(\sigma)} \tag{36}$$

Each of these transitions gives rise to a photon described by the density matrix $\hat{\rho}^{(\sigma)}$. The resulting density matrix (times the intensity) is

$$\hat{\rho} = n' \gamma_0 \sum_{k,j,\sigma} N_k' f_{kj}^{(\sigma)} \hat{\rho}^{(\sigma)} \tag{37}$$

which may be simplified by defining an effective oscillator strength

$$f_{eff}^{'(\sigma)} = \sum_{k,j} N_k' f_{kj}^{(\sigma)}$$

then

$$\hat{\rho} = n' \gamma_0 \sum_{\sigma} f_{eff}^{'(\sigma)} \hat{\rho}^{(\sigma)}$$

As in the ground state, one can write

$$f_{eff}^{'(\sigma)} = f_0 \sum_{k} N_k' A_k^{'(\sigma)} \tag{39}$$

and express this in terms of a density matrix ρ' for the excited state and an operator $\underline{A}'^{(\sigma)}$

$$f_{eff}^{'(\sigma)} = f_0 \, Tr \, \rho' \underline{A}'^{(\sigma)} \tag{40}$$

$\underline{A}'^{(\sigma)}$ can be expressed in terms of the angular momentum F' and a change in the direction of the axis of quantization can be handled as described in Section II B 3. Excited state resonances could then be described conveniently as rotations of higher spin systems, which will lead to variations of $f_{eff}^{'(\sigma)}$ with time and a consequent modulation of the scattered light whose dependence on direction and polarization is given by equation (38). The experiments of Series[117] on "light beats" seem to be closely related to this effect.

Re-radiation of the light into a cone around the forward direction can contribute to the transmission detection signal if the acceptance angle of the optical arrangement following the gas cell is large. The foregoing analysis affords a means of calculating this effect, but no numerical estimates have been made for the geometries of the present experiment. Experimentally, the difference between a small and a large collecting cone can be seen by comparing the response to rf pulses in the two cases. Figure 18(a) was taken with a small acceptance angle and the top of the pulse is quite sharp. The response to pulses in Figures 21 through 23 were obtained with a large collecting cone and they display a rounded top. This is just what one expects from a qualitative analysis. It is possible that such effects contributed to the small signals obtained with pure D_2 pumping and detection mentioned in Section IV D 2, for the acceptance cone was large in those experiments.

Application of the foregoing analysis to an experiment in which light is collected in several directions and polarizations simultaneously to provide a number of signals could be expected to lead to a more detailed understanding of the dynamics of optical pumping. The analogy with the scattering experiments of nuclear physics is very suggestive for interesting investigations.

Digital Computer Solutions

A program for numerical integration of the eight simultaneous first order differential equations describing the time development of the ground state populations for rubidium 87 was prepared for an IBM 650 digital computer, by adapting an existing program to provide solutions for any set of values for the four parameters (x, ρ, q_1, q_2)

$$\alpha = \frac{\Gamma_1}{\Gamma_1 + \Gamma_2}$$ = fraction of D_1 pumping

$$\rho = \frac{1}{\Gamma T}$$ = ratio of characteristic pumping time to characteristic ground state relaxation time

$$q = \frac{\tau'}{\tau' + T'}$$ where τ' = excited state decay time

T'= excited state relaxation time

as defined in Section II A 8 for σ^+ pumping. A program for automatic plotting of the solutions was written for use with a digital plotting board at the Forrestal Research Center. Most of the programming was done by Mr. Robert Fuller. The solutions predicting crossing of the populations were obtained by Mr. Michael Menke.

Particular interest centered in pure D_2 σ^+ pumping under various relaxation conditions, partial mixing in the excited states, the effect of the non-uniform relaxation stochastic matrix obtained from randomizing electronic states, and combined D_1 and D_2 pumping.

The integral curves are presented in the following Figures 25 through 31. The numbering of states is that given in Section II A 2.

The curves for D_1 σ^+ pumping should be compared with those obtained by Franzen and Emslie.[14]

Attention should be called to:

1) The prediction of the crossing of populations of the (1,1) and (2,1) states for D_1 σ^+ pumping when the electron relaxation matrix is used. This could be checked by using pulse techniques to invert the populations for various delay times, observing whether the optical absorption signal changes sign.

2) The populating of state (1,1) above that of states (2,2) and (2,-2) for D_2 σ^+ pumping with $\tau' = T'$ is interesting. For $T' = \infty$ state (2,2) dominates while for $T' = 0$, state (2,-2) dominates.

3) The orientation with combined D_1 and D_2 σ^+ pumping with no excited state relaxation (wall coated bulb) is about the same as that for pure D_1 σ^+ pumping with no excited state relaxation although it is achieved more rapidly. This is shown by comparison with curves obtained by Franzen and Emslie (Second Quarterly Report under Contract No. DA-36-039 SC 73143 with the U.S. Army Signal Research and Development Laboratory, July, 1957) for the case $1/\Gamma' T = 1$. One difference is the computed populations is the two situations is that $N_7 > N_3$ for D_1 σ^+ pumping while $N_7 < N_3$ for combined D_1 and D_2 σ^+ pumping.

4) The orientation predicted for D_1 σ^+ pumping when electron relaxation is assumed (Fig. 25) is much larger than that predicted by Franzen and Emslie assuming uniform relaxation.

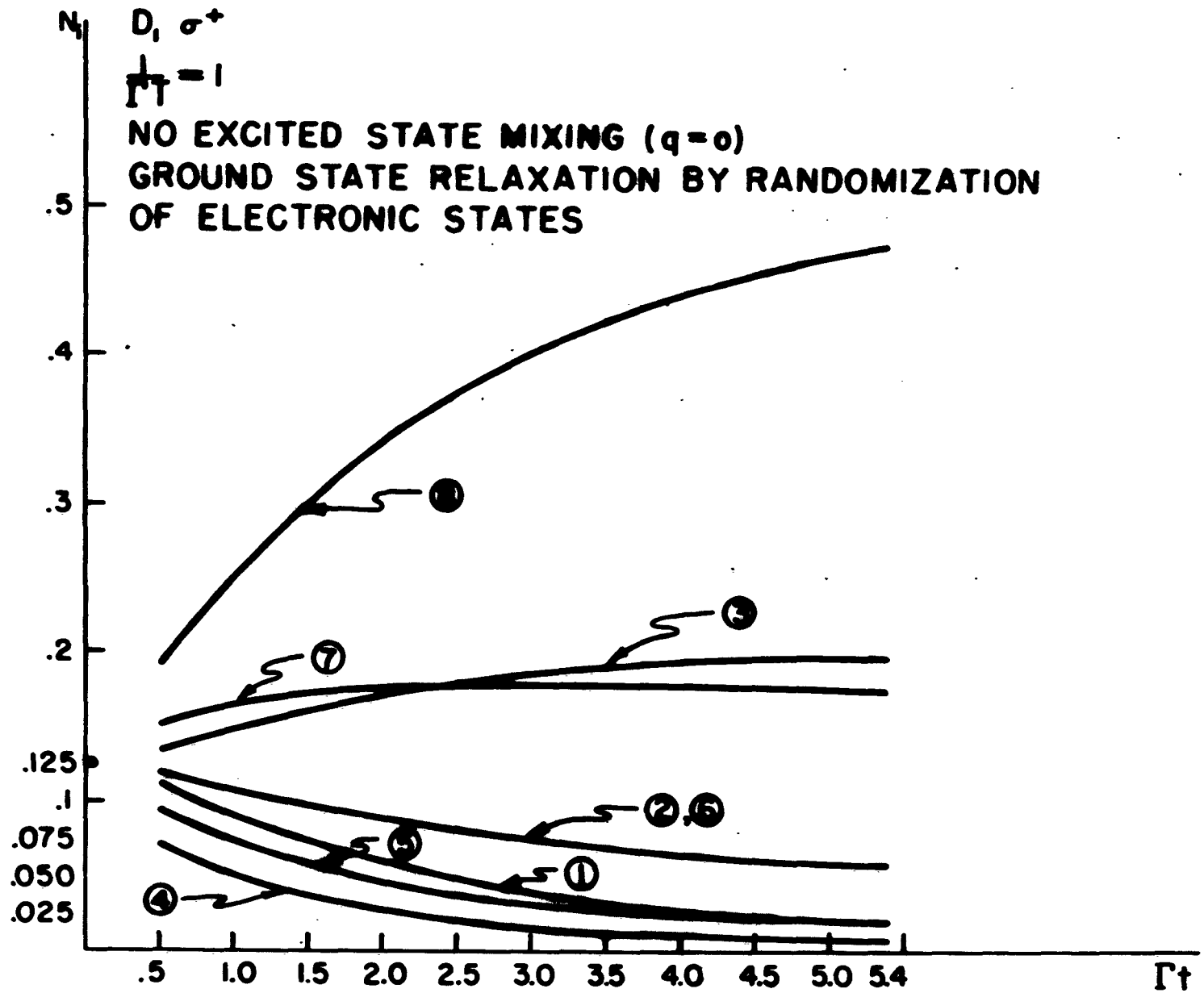
N_1
D_1 σ^+
$\frac{1}{\Gamma T} = 1$
NO EXCITED STATE MIXING (q=o)
GROUND STATE RELAXATION BY RANDOMIZATION
OF ELECTRONIC STATES
.5
.4
.3
.2
.125
.1
.075
.050
.025
.5
1.0
1.5
2.0
2.5
3.0
3.5
4.0
4.5
5.0
5.4
Γt
6
3
7
2,8
5
1
4

FIG. 25

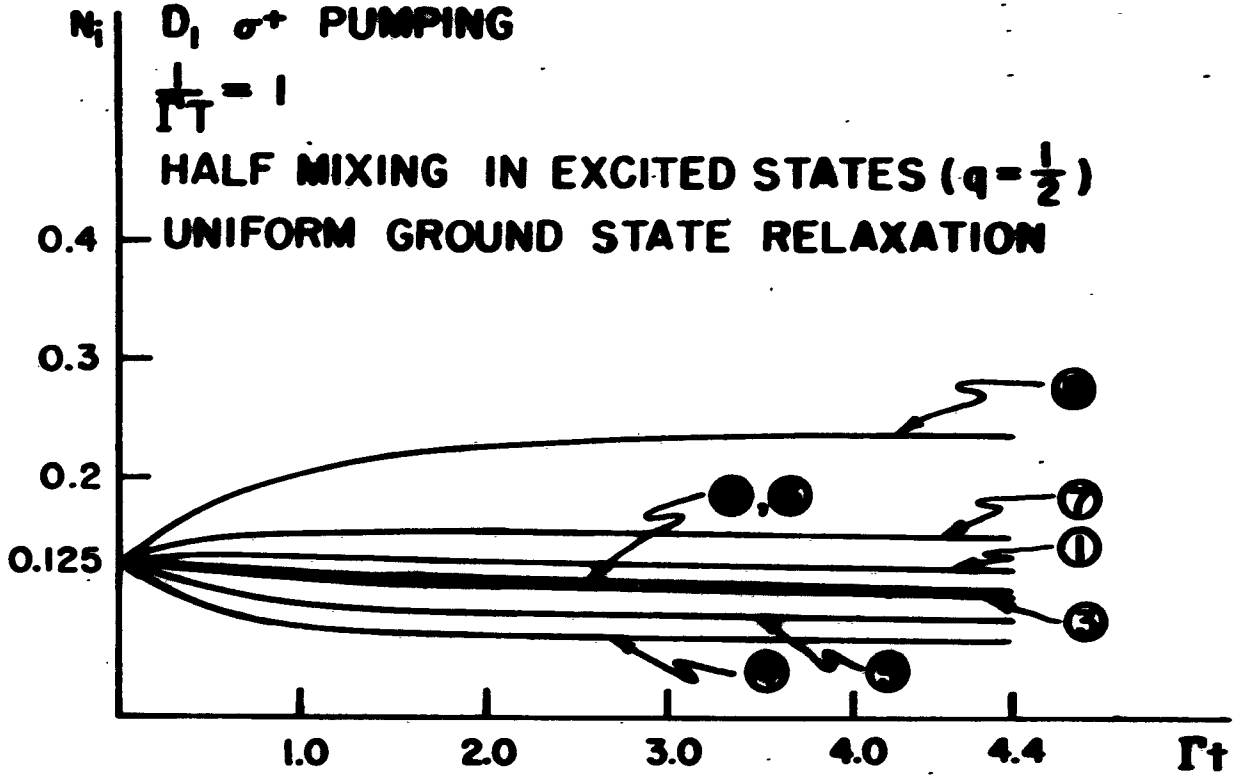
N_i
D_1 σ^+ PUMPING
$\frac{1}{\Gamma T} = 1$
HALF MIXING IN EXCITED STATES ($q = \frac{1}{2}$)
UNIFORM GROUND STATE RELAXATION
0.4
0.3
0.2
0.125
1.0
2.0
3.0
4.0
4.4
Γt

FIG. 26

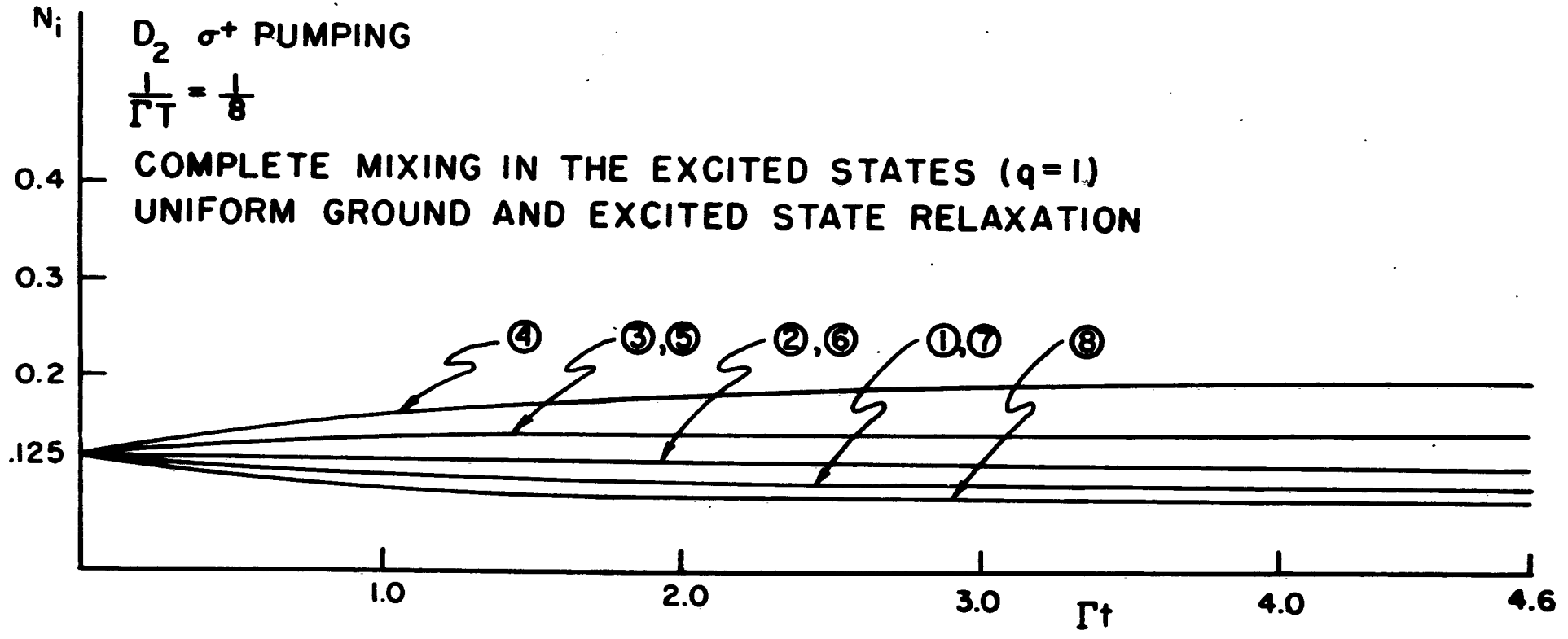
N_i
D_2 σ^+ PUMPING
$\frac{1}{\Gamma T} = \frac{1}{8}$
COMPLETE MIXING IN THE EXCITED STATES (q = 1)
UNIFORM GROUND AND EXCITED STATE RELAXATION
0.4
0.3
0.2
.125
④
③,⑤
②,⑥
①,⑦
⑧
1.0
2.0
3.0
Γt
4.0
4.6

FIG. 27

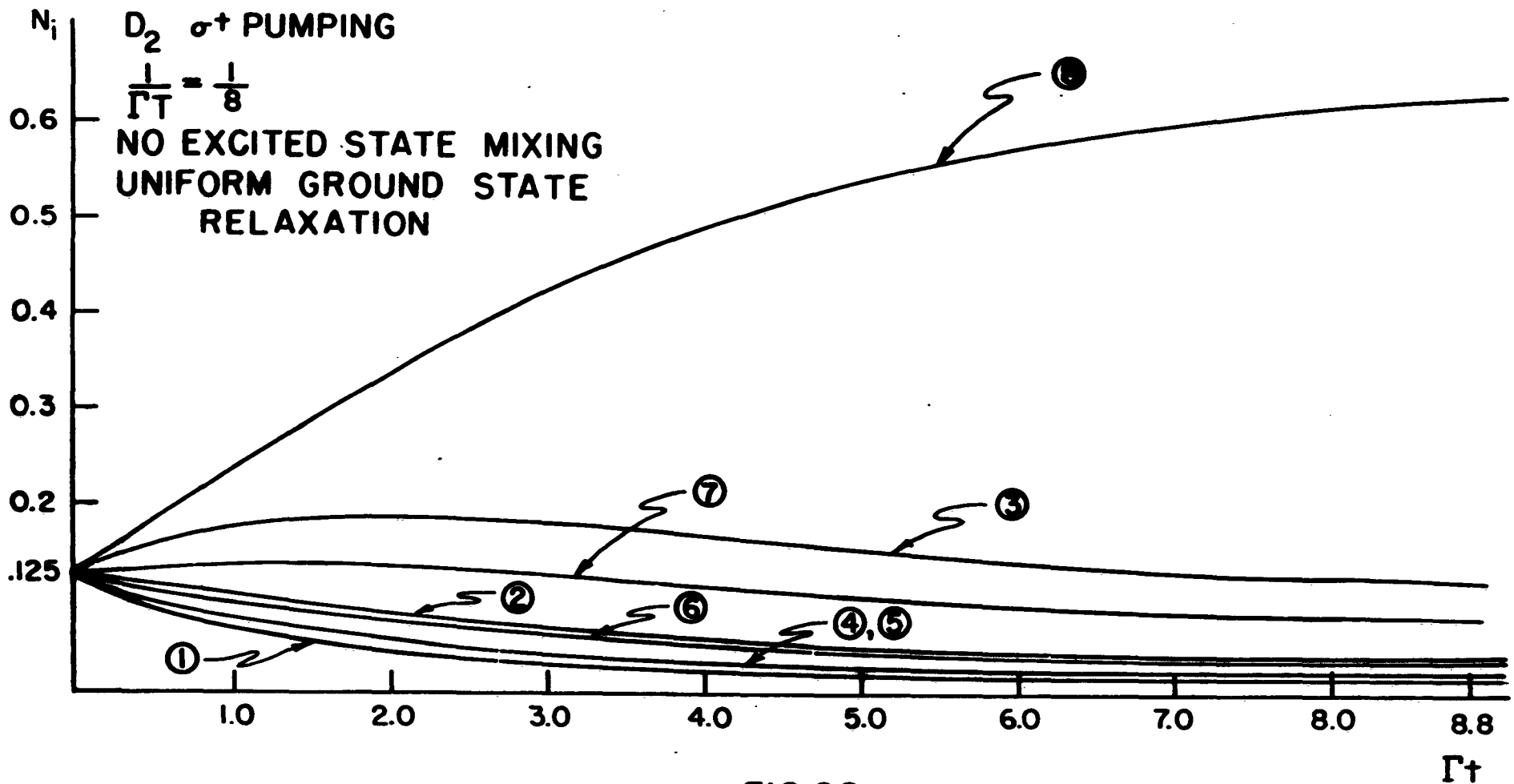
N_i
D_2 $\sigma+$ PUMPING
$\frac{1}{\Gamma T} = \frac{1}{8}$
NO EXCITED STATE MIXING
UNIFORM GROUND STATE
RELAXATION
0.6
0.5
0.4
0.3
0.2
.125
1.0
2.0
3.0
4.0
5.0
6.0
7.0
8.0
8.8
Γt
1
2
3
4,5
6
7

FIG.28

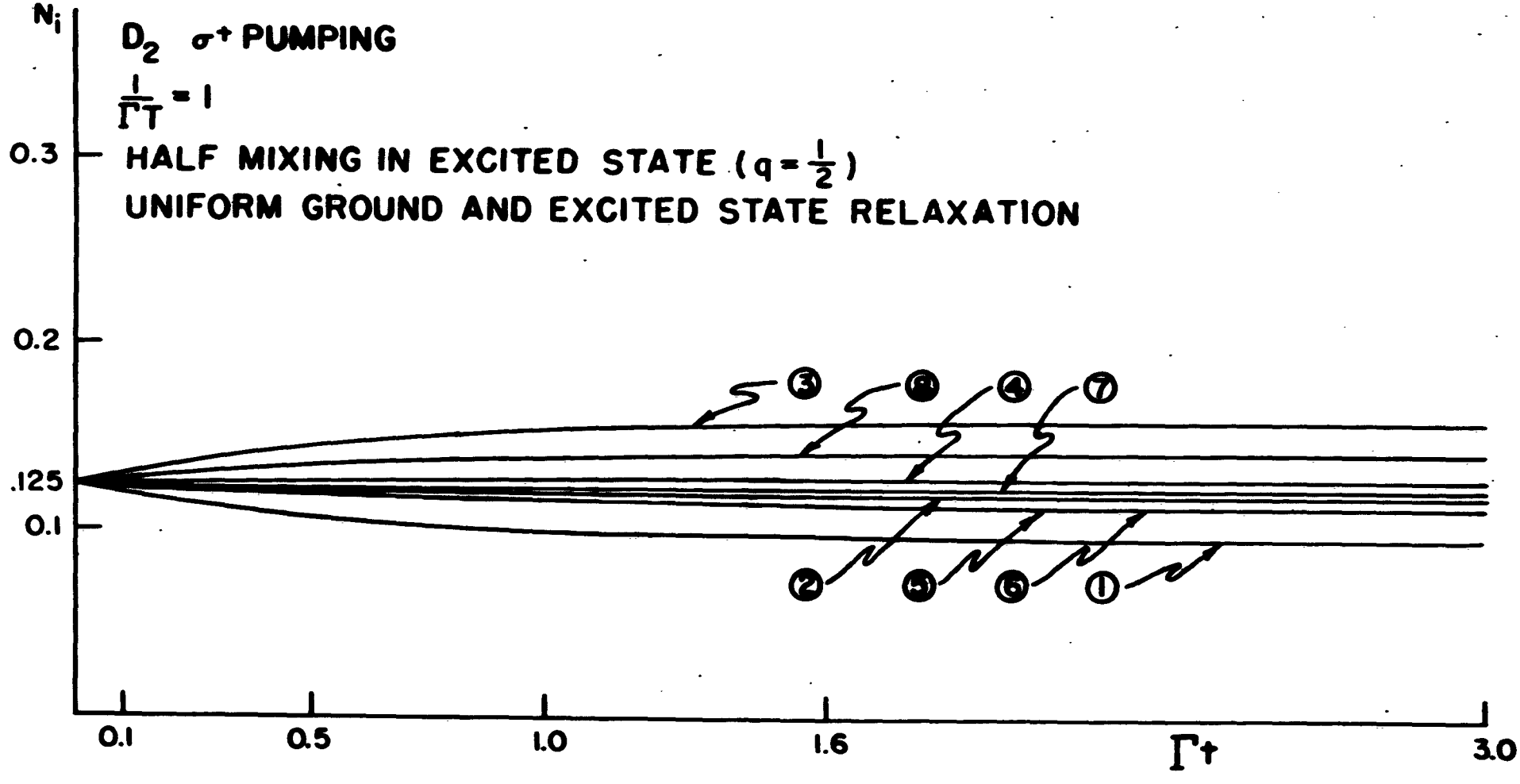
N_i
D_2 σ^+ PUMPING
$\frac{1}{\Gamma T} = 1$
HALF MIXING IN EXCITED STATE ($q = \frac{1}{2}$)
UNIFORM GROUND AND EXCITED STATE RELAXATION
0.3
0.2
.125
0.1
3
6
4
7
2
5
8
1
0.1
0.5
1.0
1.6
Γt
3.0

FIG. 29

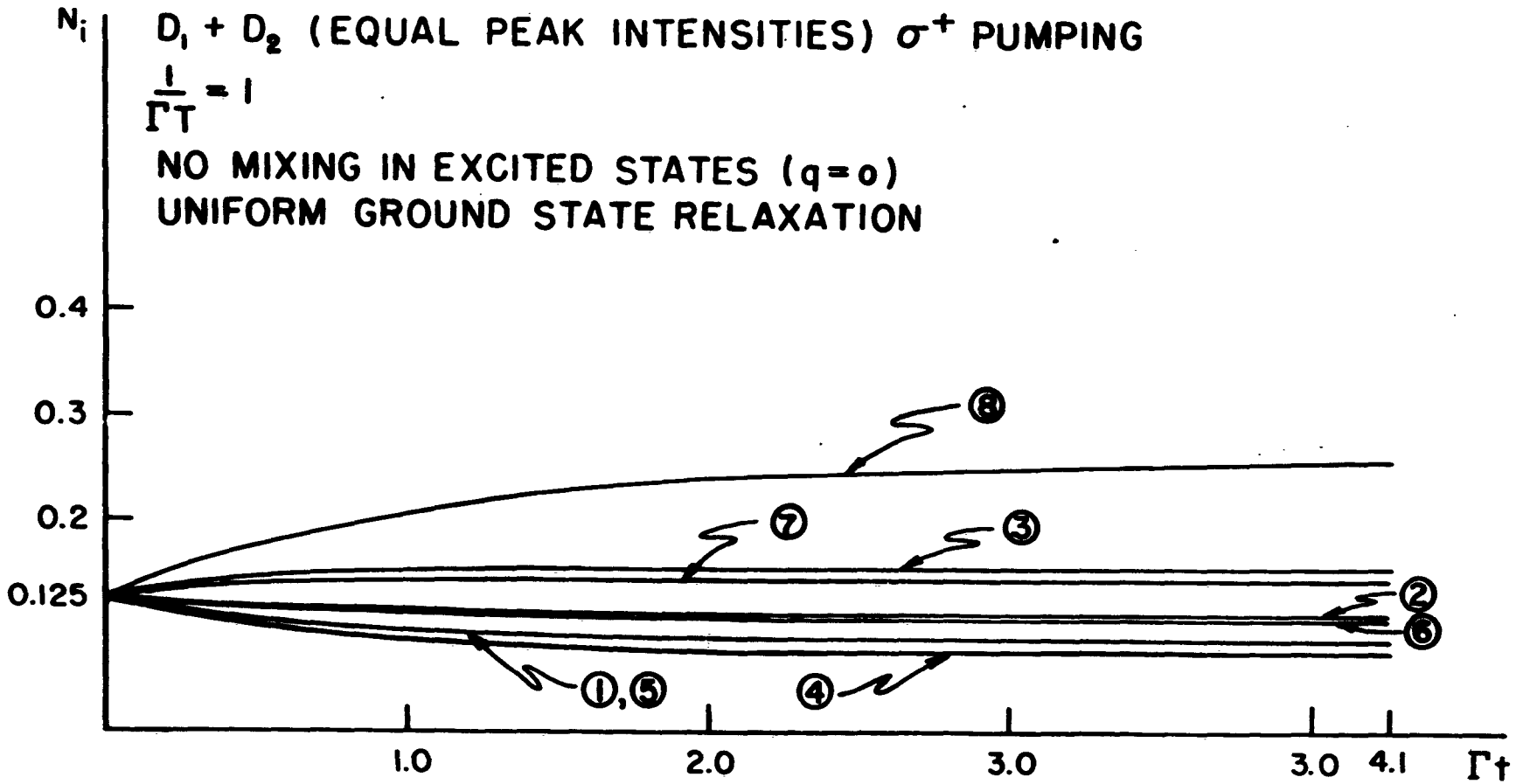
N_i
$D_1 + D_2$ (EQUAL PEAK INTENSITIES) σ^+ PUMPING
$\frac{1}{\Gamma T} = 1$
NO MIXING IN EXCITED STATES (q=o)
UNIFORM GROUND STATE RELAXATION
0.4
0.3
0.2
0.125
⑧
⑦
③
②
⑥
①,⑤
④
1.0
2.0
3.0
3.0
4.1
Γt

FIG. 30

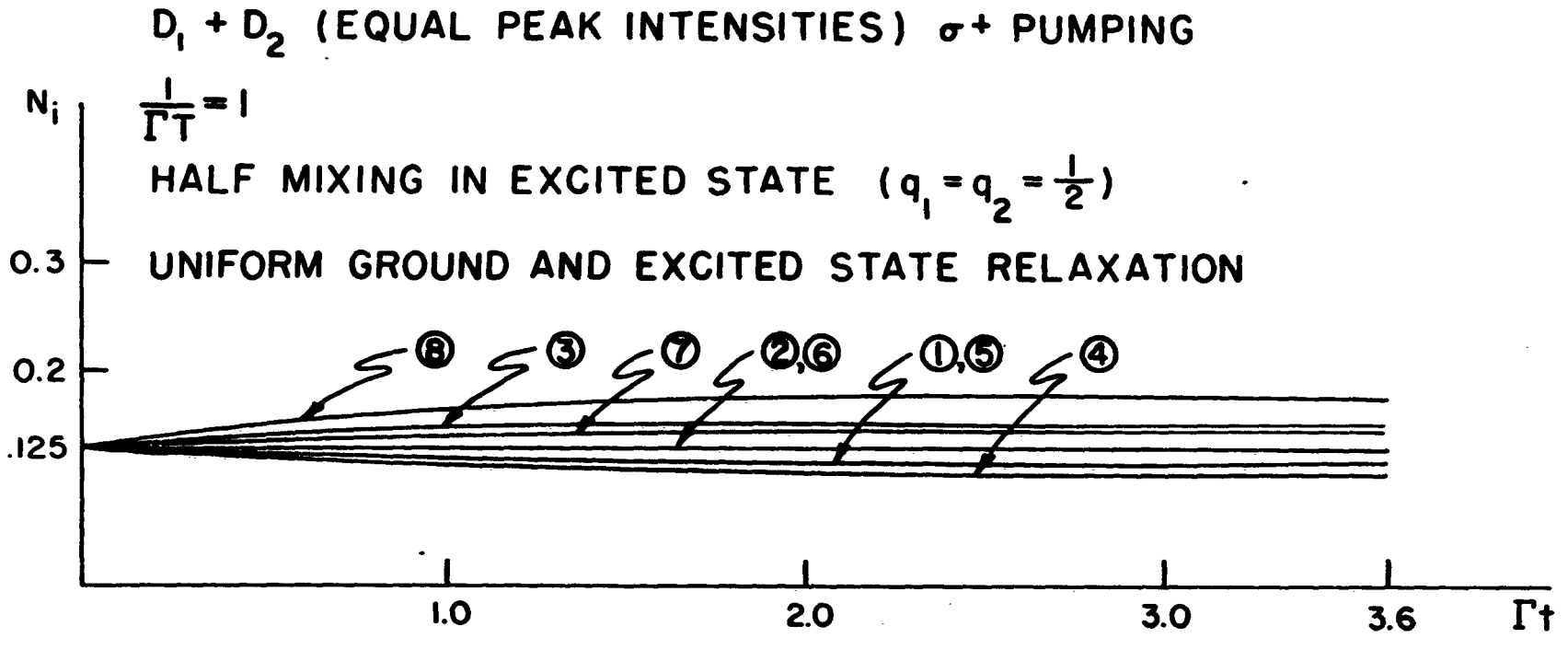
$D_1 + D_2$ (EQUAL PEAK INTENSITIES) $\sigma+$ PUMPING
N_i
$\frac{1}{\Gamma T} = 1$
HALF MIXING IN EXCITED STATE ($q_1 = q_2 = \frac{1}{2}$)
UNIFORM GROUND AND EXCITED STATE RELAXATION
0.3
0.2
.125
⑧
③
⑦
②,⑥
①,⑤
④
1.0
2.0
3.0
3.6
Γt

FIG. 31

REFERENCES

1. R.H. Dicke, T.R. Carver, C.O. Alley, and N.S. Vander Ven, Final Report on the Microwave Detection Phase of the Contract Entitled "Investigation of the Effect of Gas Collisions and Optical Pumping on the Breadth of Spectral Lines." This appeared in December, 1957, as Quarterly Report No. 8, Contract No. DA 36-039 SC 70147 placed with Princeton University by the U.S. Army Signal Research and Development Laboratory, Fort Monmouth, New Jersey.

   Other less complete references to this research are: T.R. Carver, Proceedings of the 11th Annual Symposium on Frequency Control of the U.S. Army Signal Research and Development Laboratory, May, 1957; Proceedings of the Ann Arbor Conference on Optical Pumping, June, 1959.

2. J.P. Wittke and R.H. Dicke, Phys. Rev. 103, o20 (1956).
   J.P. Wittke, Thesis, Princeton University, (1955).

3. R.H. Dicke, Phys. Rev. 89, 472 (1953).

4. R.H. Romer, Thesis, Princeton University, (1955).
   R.H. Dicke and R.H. Romer, Rev. Sci. Instr. 26, 915 (1955).
   R.H. Romer and R.H. Dicke, Phys. Rev. 99, 532 (1955).

5. W.B. Hawkins and R.H. Dicke, Phys. Rev. 91, 1008 (1953).
   W.B. Hawkins, Phys. Rev. 96, 532 (1954); Phys. Rev. 98, 478 (1955); Thesis, Princeton University, (1954).

6. P.L. Bender, Thesis, Princeton University, (1956).

7. R.H. Dicke, unpublished work (June, 1950).
Some information on this work is available in a review article on electron polarization: H.A. Tolhoek, Revs. Modern Phys. 28, 277 (1956).

8a. F.L. Bitter, Phys. Rev. 76, 833 (1949).

8b. J. Brossel and A. Kastler, Comptes rend. 229, 1213 (1949).

8c. A. Kastler, J. Phys. et Rad. 11, 255 (1950).

8d. F. Bitter and J. Brossel, Phys. Rev. 85, 1051 (1952).

9. J. Brossel, A. Kastler, and J. Winter, J. Phys. et Rad. 13, 668 (1952).
J. Brossel, B. Cagnac, and A. Kastler, Comptes rend. 237, 984-986 (1953).

10. C. Cohen-Tannoudji, J. Brossel and A. Kastler, Comptes rend. Sci. 244, 1027 (1957).
C. Cohen-Tannoudji, Thesis for Diplome d'Etudes Superieures, Ecole Normale Superieure (1956).
See also J. Brossel, J. Margerie and A. Kastler, Comptes rend. 241, 865 (1955).

11. A complete listing of the many publications of the Paris group will not be attempted. Reference should be made to the following review articles of A. Kastler: Proc. Phys. Soc. (London) A17, 853 (1954); Suppl. Nuovo Cimento 6, 1148 (1957); J. Opt.

Soc. Am. 47, 460 (1957). The review article by J. Brossel in Quantum Electronics, edited by C.H. Townes (Columbia University Press, New York, 1960) should also be consulted.

12. H.G. Dehmelt, Phys. Rev. 105, 1487 (1957).

13. W.B. Hawkins, Phys. Rev. 98, 478 (1955).

14. W. Franzen and A.G. Emslie, Phys. Rev. 108, 1453 (1957).

15 a. H.G. Dehmelt, Phys. Rev. 105, 1924 (1957).

15 b. W.E. Bell and A.L. Bloom, Phys. Rev. 107, 1559 (1957).

16. M. Arditi and T.R. Carver, Phys. Rev. 109, 1012 (1958).

17. W.E. Bell and A.L. Bloom, Phys. Rev. 109, 219 (1958).

18. M. Arditi and T.R. Carver, Phys. Rev. 112, 449 (1958).
E.C. Beaty and P.L. Bender, Bull. Am. Phys. Soc. 3, 185 (1958).

19. P.L. Bender, E.C. Beaty, and A.R. Chi, Phys. Rev. Letters 1, 311 (1958).

20. See, for example, papers in the Proceedings of the 13th Annual Symposium on Frequency Control sponsored by the U.S. Army Signal Research and Development Laboratory, May, 1959 by: J.M. Andres, D.J. Farmer and G.T. Inoye; R. Whitehorn; and M. Arditi.

21. E.C. Beaty, P.L. Bender, and A.R. Chi, Phys. Rev. 112, 450 (1958).

22. R.H. Dicke, unpublished work. See also papers in Quantum Electronics, edited by C.H. Townes (Columbia University Press, New York, 1960) by V.W. Hughes (p. 582) and C.O. Alley (p. 146).

23. E.L. Hahn, Phys. Rev. 76, 145 (1949); 77, 297 (1950); 80, 580 (1950); Phys. Today 6, No. 11, p.4 (1953).

24. H.Y. Carr and E.M. Purcell, Phys. Rev. 88, 415 (1952); 94, 630 (1954).

25. W. Heitler, The Quantum Theory of Radiation (Oxford University Press, London, 2nd Edition, 1944) pp. 137ff.

26. C. Cohen-Tannoudji, Thesis for Diplome d'Etudes Superieures, Ecole Normale Superieure (1956).

27. W. Franzen and A.G. Emslie, 2nd Quarterly Report under Contract No. DA-36-039 SC 73143, File No. 0071-PH-91 placed by the United States Army Signal Research and Development Laboratory with Arthur D. Little, Inc. (July, 1957).
See also reference 14 above.

28. Some useful introductions to the use of density matrix techniques are: U. Fano, Revs. Modern Phys. 29, 74 (1957).
R.H. Dicke and J.P. Wittke, Introduction to Quantum Mechanics (Reading: Addison-Wesley Publishing Co., 1960), Chapter 18.
R. Tolman, The Principles of Statistical Mechanics (Oxford University Press, London, 1938), Chapter IX.
D. Ter Haar, Reports on Progress in Physics, Vol. XXIV, p. 304 (1961).

29. C. Kittel, Elementary Statistical Physics (John Wiley and Sons, New York, 1958), pp. 169f.

30. Some studies along these lines are being pursued in Paris by J.P. Barrat and C. Cohen-Tannoudji (private communication).

31. E.U. Condon and G.H. Shortley, The Theory of Atomic Spectra (The University Press, Cambridge, 1935). The "Class T" operators of this type are defined in chapter III.

32. E.P. Wigner, Group Theory and Its Applications to the Quantum Mechanics of Atomic Spectra, translated by J.J. Griffin (Academic Press, New York, 1959), p. 245 and pp.303ff.

33. U. Fano, Revs. Modern Phys. 29, 74 (1957).

34. W. Feller, An Introduction to Probability Theory and Its Applications (John Wiley and Sons, New York, 1950), Chapter 15.

35. H.A. Bethe and E.E. Salpeter, Quantum Mechanics of One-and-Two Electron Atoms (Academic Press, New York, 1957), pp. 254ff. E.P. Wigner, reference 32 above, p. 268.

36. John McLeod, Princeton Thesis (1961) unpublished.

37. E. Merzbacher, Quantum Mechanics (John Wiley and Sons, New York, 1961), p. 453.

38. Solomon Lefschetz, Lectures on Differential Equations (Princeton University Press, Princeton, 1948), Chapter III.

39. A detailed application to optical pumping of some of the many theorems concerning Markov processes (see reference 34 above) would make an interesting exercise.

40. E.P. Wigner, Physik. Z. 32, 4501 (1931).

41. J.G. Kirkwood, Physik. Z. 33, 521 (1932).

42. A.C.G. Mitchell and M.W. Zemansky, Resonance Radiation and Excited Atoms (The University Press, Cambridge, 1934).

43. E.P. Wigner, reference 32 above, p. 243.

44. N.F. Ramsey, Molecular Beams (The Clarendon Press, Oxford, 1956) p. 52.

45. E.U. Condon and G.H. Shortley, reference 31 above, p. 427.

46. A complete discussion of the intermediate field case for sodium which applies also for rubidium 87 is given by J. Winter, Thesis, Ecole Normale Superieure (1956) pp. 26ff.

47. I.I. Rabi, N.F. Ramsey and J. Schwinger, Revs. Modern Phys. 26, 167 (1954).

48. E.P. Wigner, reference 32 above, p. 105

49. W. Pauli, "Die Allgemeinen Prinzipien der Wellenmechanik," Handbuch der Physik (Springer-Verlag, 1958), Band V, Teil 1, p. 100.

50. A.R. Edmonds. Angular Momentum in Quantum Mechanics (Princeton University Press, 1957), p. 55.

51. E.P. Wigner, reference 32 above.

V. Heine, Group Theory in Quantum Mechanics (Pergamon Press, London, England, 1960).

A.R. Edmonds, reference 50 above.

52. H. Weyl, The Theory of Groups and Quantum Mechanics, reprinted by Dover Publications, New York, (original translation, 1931).

J. Von Neumann, The Mathematical Foundations of Quantum Mechanics (The Princeton University Press, 1955), Chapter II.

53. E.L. Hahn, reference 23 above.

54. H.Y. Carr and E.M. Purcell, reference 24 above.

55. C.L. Cuccia, Harmonics, Sidebands, and Transients in Communication Engineering, (McGraw-Hill, New York, 1952), p. 39 and Appendix.

56. E. Fermi, Z. Physik. 60, 320 (1930).

57. N.F. Ramsey, reference 44 above, p. 74.

58. R.A. Ferrell, Am. J. Phys. 28, 484 (1960).

59. A.F. Stevenson, Phys. Rev. 58, 1061 (1941).

60. F. Bloch and A. Siegert, Phys. Rev. 57, 522 (1940).

61. R.H. Dicke, T.R. Carver, C.O. Alley, and N.S. Vander Ven, reference 1 above.

R.H. Dicke, reference 3 above.

R.H. Dicke and J.P. Wittke, reference 2 above.

62. M. Arditi and T.R. Carver, references 16 and 18 above.
E.C. Beaty, P.L. Bender, and A.R. Chi, reference 21 above.
P.L. Bender, E.C. Beaty, and A.R. Chi, reference 19 above.

63. V. Weisskopf and E.P. Wigner, Z. Physik. 63, 54 (1930); 65, 18 (1930).

64. W. Heitler, The Quantum Theory of Radiation (The Clarendon Press, Oxford England, 3rd Edition, 1954), p. 183, eq. (11).

65. J.P. Barrat and C. Cohen-Tannoudji, Comptes rend. 252, 93 (1961); 252, 255 (1961).
C. Cohen-Tannoudji, Comptes rend. 252, 394 (1961).

66. M. Arditi, Proceedings of the 15th Annual Symposium on Frequency Control sponsored by the U.S. Army Signal Research and Development Laboratory, June, 1961.

67. P.L. Bender (private communication).

68. R.H. Dicke and J.P. Wittke, reference 28 above.

69. N.F. Ramsey, reference 44 above, pp. 124ff.

70. B. Senitzky and I.I. Rabi, Phys. Rev. 103, 315 (1956).

71. This narrow a width from an alkali discharge has been observed by the Paris group (J. Brossel, private communication to T.R. Carver). This was also measured by J. Kinsey, Senior Thesis, Princeton University (1960).

72. W.F. Bell, A.L. Bloom, and J. Lynch, Rev. Sci Instr. 32, 688 (1961).

73. Private communication from manufacturer.

74. D.A. Jackson, Proc. Roy Soc. (London) 139, 673 (1933); 147, 501 (1934);148, 342 (1935); 165A, 303 (1938); 167A, 205 (1938).

75. J. Strong, Prodedures in Experimental Physics (Prentice Hall, New York, 1939), Chapter III.

76. W.B. Hawkins, Quarterly Reports Nos. 3 and 4, SCEL Project No. 142B, Yale (1957); 11th Annual Symposium on Frequency Control. May, 1957.

77. T.R. Carver (private communication).

78. H.G. Robinson, E.S. Ensberg, and H.G. Dehmelt, Bulletin of APS 3, 9 (1958); H.G. Dehmelt, 12th Annual Symposium on Frequency Control, May, 1958.

79. W. Franzen, 13th Annual Symposium on Frequency Control, May, 1959.

80. N.F. Ramsey, Rev. Sci. Instr. 28, 57 (1957).

81. H.M. Goldenberg, D. Kleppner, and N.F. Ramsey, Phys. Rev. 123, 530 (1961).

82. See e.g., D. Kleppner, Proceedings of the 2nd International Conference on Quantum Electronics, March 1961, to be published by Columbia University Press; M.A. Bouchiat, T.R. Carver and C.M. Varnum, Phys. Rev. Letters 5, 373 (1960); P.L. deZafra, Am. J. of Phys. 28, 646 (1960).

83. E.B.D. Lambe, Thesis, Princeton University, (1959).

84. F.J. Norton, General Electric Review 47, No. 8, 6 (August, 1944).

85. Such chemicals can be obtained from the Anderson Chemical Division of the Stauffer Chemical Company, Weston Michigan.

86. W.A. Weyl, "Some Practical Aspects of the Surface Chemistry of Glass," The Glass Industry 28, No. 5, 231 (1947).

87. K.L. Loewenstein, "A Survey of the Surface Treatments of Glass," J. Soc. Glass Technol., 42, 70N-84N (Oct. 1958).

88. This is a wax made by the firm Moore and Munger, 33 Rector St., New York 6, N.Y. by a Fischer-Tropsch synthesis for use in such things as floor waxes and shoe polishes.

89. The use of Vydax was suggested by R.M. Joyce of E.I. duPont de Nemours and Company. A sample was very kindly supplied by A.C. Haven of the Flourine Use Development Division of the same company.

90. R.H. Dicke, Rev. Sci, Instr. 19, 533 (1948).

91. E.B.D. Lambe, reference 83 above, pp. IV-4ff

92. J. Millman and H. Taub, Pulse and Digital Circuits (McGraw-Hill, New York, 1956) p.455ff ; J. Millman and T. H. Puckett, Proc. I.R.E. 43, 27 (1955).

93. C.L. Searle and D.D. McRae, MIT Research Laboratory of Electronics, Quarterly Report (April 15, 1956).

94. A.W. Warner and W.L. Smith, Proceedings of the 13th Annual Symposium on Frequency Control, May, 1959.

95. F. Reder, P. Brown, G. Winkler, and C. Bickart, Proceedings of the 15th Annual Symposium on Frequency Control, June, 1959.

96. H.M. Goldenberg, D. Kleppner, and N.F. Ramsey, Phys. Rev. Letters 5, 361 (1960).

97. These were supplied by the Bolsey Research and Development Corporation, 11 W. 57th Street, New York 19, N.Y. Their existance was very kindly pointed out by W.E. Bell.

98. Spectrolab, Inc. 7423 Varna Ave., North Hollywood, California.

99. N.F. Ramsey, reference 69 above.

100. See references 16 and 18 above.

101. See reference 21 above.

102. Precision atomic beam experiments carried out by S. Penselin, T. Moran, and V.W. Cohen of the Brookhaven National Laboratory and G. Winkler of the Signal Corps give the value 6835.682614$\pm$ 3 Mc/sec. See Bull. Am. Phys. Soc., Series II, Vol. 6, Dec. 27, 1961.

103. H.G. Dehmelt, (private communication).

104. R. Ladenberg and S. Levy, Z. Physik 65, 189 (1930), quoted in reference 42 above.

105. R.A. Smith, F.E. Jones, and R.P. Chasmur, The Detection and Measurement of Infra-Red Radiation (The Clarendon Press, Oxford, England, 1957).

106. H.Kopfermann and H. Krüger, Z. Physik. 103, 485 (1936).

107. H. Mueller, MIT notes, unpublished
R.C. Jones, J. Am. Opt. Soc. 37, 107 (1947).
E. Billings and E. Land, J. Am. Opt. Soc. 38, 819 (1948).
N.G. Parke, MIT Research Laboratory of Electronics, Publications No. 70, 95 and 119.

108. D.L. Falkoff and J.E. MacDonald, J. Am. Opt. Soc. 41, 861 (1951).
U. Fano, J. Am. Opt. Soc. 39, 859 (1949); Phys. Rev. 93, 121 (1954)
S. Chandrasekhar, Radiation Transfer (The Clarendon Press, Oxford, 1950) pp. 24ff.
P. Soleillet, Ann. de Physique 12, 23 (1929)
F. Perrin, J. Chem. Phys. 10, 415 (1942).
D.R. Hamilton, Astrophys. J. 106, 457 (1947).
J.M. Jauch and F. Rohrlich, The Theory of Protons and Electrons (Addison-Wesley Publishing Co., Cambridge, Mass., 1955) pp. 40ff.
M. Born and E. Wolf, Principles of Optics, (Pergamon Press, London, England, 1959) pp. 29ff. and pp. 550ff.

109. G.E. Kron, Astrophys. J. 115, 1 (1952).

110. N.F. Ramsey, Phys. Rev. 76, 996 (1949); 78, 695 (1950); 81, 278 (1951); 84, 506 (1951). See also reference 69 above.

111. See reference 4 above.

112. V.W. Hughes, Quantum Electronics, edited by C.H. Townes (Columbia University Press, New York, 1960) p. 582.

113. E.P. Wigner, reference 32 above, Chapter 24.

114. E.U. Condon and G.H. Shortley, reference 31 above.

115. A.R. Edmonds, reference 50 above, p. 120.

116. R. Ladenberg, Z. Physik. 4, 451 (1921); 48, 15 (1928).
R. Ladenberg and F. Reiche, Naturwissenschaften. 11, 584 (1923).
See also E.T. Whittaker, History of the Theories of Aether and Electricity (Thomas Nelson and Sons, London, England, 1953) Vol. II, pp. 200ff.
R. Becker, Theorie der Elektrizität, (B.G. Teubner, Stuttgart, Germany, 1959) Band II, 8th Edition, edited by F. Sauter, pp. 210ff.

117. G. Series, Proceedings of the 2nd International Conference on Quantum Electronics, March, 1961, to be published by Columbia University Press.
J.H. Dodd and G.W. Series, Proc. Roy. Soc. (London) A 263, 353 (1961).

VII. IDENTIFICATION OF TECHNICAL PERSONNEL

		Number of Hours Charged to Contract
R. H. Dicke	Project Leader Professor of Physics	None
C. O. Alley	Lecturer in Physics and Electrical Engineering and Research Assistant in Physics	6067
D. Curott	Graduate Assistant in Research	320
R. Fuller	Graduate Assistant in Research	320
J. Hardy	Graduate Assistant in Research	480

ERRATA

Page II-45, line 17: The word "lends" should be changed to "leads."

III-4, line 26: The word "on" should be changed to "as."

III-8, line 2: The word "dehydrogen" should be changed to "dihydrogen."

line 22: The words "a little" should be changed to "as little."

III-30, line 16: The word "presented" should be changed to "prevented."

III-45, line 7: The word "forused" should be changed to "focused."

IV-6, lines 4 & 11: The illegible symbol should be $\tilde{\sigma}$.

line ^0: The word "while" should be inserted between the words "resonance" and "using."

IV-11, line 27: The words "the under" should be transposed.

IV-12, line 23: The word "of" should be changed to "by" in the phrase "...light of an oriented..."

V-2, line 19: The word "by" should be deleted.

V-5, line 20: The word "spins" should be inserted between "nuclear" and "and."

line 24: The word "the" should be inserted between the words "of" and "integral."

V-6, line 25: The words "optical pumping" should be inserted before the word "lights."

A-6, line 11: The word "phtocathode" should be changed to "photocathode."

B-5, line 12: The words "of 10^{-16}" should be replaced by "to 10^{-16}."

C-1, line 25: The word "be" should be inserted before the word "narrowed."

D-4, line 19: A comma should be inserted after the word "included."

AD ____________________ Accession No. ____________________

Princeton University, Princeton, New Jersey

INVESTIGATIONS OF THE EFFECT OF GAS COLLISIONS AND OPTICAL PUMPING ON THE BREADTH OF SPECTRAL LINES - R. H. Dicke and C. O. Alley

Final Report on Optical Detection Phase, 1 October 1957 to 30 September 1960, 186 pages, 31 Figures, 13 Diagrams, 14 Tables. (Contract No. DA-36-039 SC-70147) File No. 229-PH-56-91 (3501). Unclassified Report.

A new method of optical detection of the $m_F = 0 \leftrightarrow m_F = 0$, $\Delta F = 1$ ground state magnetic hyperfine transition in alkali atoms, which is important for a atomic frequency standards because of its first order independence of an external magnetic field has been investigated theoretically and experimentally demonstrated for rubidium 87. After orientation by optical pumping a quantum mechanical superposition state is produced by a 90° rf pulse. A <u>phase change</u> between each $m_F = 0$ state and its partner states of the same F value is caused by a microwave field at ~ 6835 Mc/sec coupling the two $m_F = 0$ states. This phase change is converted into a <u>population change</u> by a second rf pulse to yield a large change in the resonance scattering of the optical pumping light on the order of that obtained by reversal of the orientation of the vapor.

Other methods of optical detection of this resonance were studied theoretically and are discussed: selective hyperfine absorption within the gas cell; a rubidium 85 gas cell hyperfine filter; and a polarization bridge.

Wall coatings for the inhibition of spin relaxation in confined oriented vapors were studied experimentally. It was demonstrated that treatment of glass surfaces with alkylchlorosilane vapors provides coatings at least as effective as long chain saturated hydrocarbon waxes with the added advantages of ease of application and the ability to withstand baking under vacuum at $\sim 350°$ C without deterioration. The $0 \leftrightarrow 0$ hyperfine resonance in such coated cells exhibited a reduced Doppler width (because of the confinement of the atoms) of the same order as that produced by a buffer gas and displayed a negative frequency shift of a few kc/sec.

Other subjects investigated included spin echo methods applied to oriented vapors; optical pumping with pulsed light sources; the general theory of optical pumping and detection; and digital computer solutions of the optical pumping equations for $\sigma^+ D_2$ light and partial excited state relaxation.

Unclassified

1. Gas Cell Atomic Frequency Standards
   Optical Pumping
2. Contract DA-36-039 SC-70147

AD ____________________ Accession No. ____________________

Princeton University, Princeton, New Jersey

INVESTIGATIONS OF THE EFFECT OF GAS COLLISIONS AND OPTICAL PUMPING ON THE BREADTH OF SPECTRAL LINES - R. H. Dicke and C. O. Alley

Final Report on Optical Detection Phase, 1 October 1957 to 30 September 1960, 186 pages, 31 Figures, 13 Diagrams, 14 Tables. (Contract No. DA-36-039 SC-70147) File No. 229-PH-56-91 (3501). Unclassified Report.

A new method of optical detection of the $m_F = 0 \leftrightarrow m_F = 0$, $\Delta F = 1$ ground state magnetic hyperfine transition in alkali atoms, which is important for a atomic frequency standards because of its first order independence of an external magnetic field has been investigated theoretically and experimentally demonstrated for rubidium 87. After orientation by optical pumping a quantum mechanical superposition state is produced by a 90° rf pulse. A <u>phase change</u> between each $m_F = 0$ state and its partner states of the same F value is caused by a microwave field at ~ 6835 Mc/sec coupling the two $m_F = 0$ states. This phase change is converted into a <u>population change</u> by a second rf pulse to yield a large change in the resonance scattering of the optical pumping light, on the order of that obtained by reversal of the orientation of the vapor.

Other methods of optical detection of this resonance were studied theoretically and are discussed: selective hyperfine absorption within the gas cell; a rubidium 85 gas cell hyperfine filter; and a polarization bridge.

Wall coatings for the inhibition of spin relaxation in confined oriented vapors were studied experimentally. It was demonstrated that treatment of glass surfaces with alkylchlorosilane vapors provides coatings at least as effective as long chain saturated hydrocarbon waxes with the added advantages of ease of application and the ability to withstand baking under vacuum at $\sim 350°$ C without deterioration. The $0 \leftrightarrow 0$ hyperfine resonance in such coated cells exhibited a reduced Doppler width (because of the confinement of the atoms) of the same order as that produced by a buffer gas and displayed a negative frequency shift of a few kc/sec.

Other subjects investigated included spin echo methods applied to oriented vapors; optical pumping with pulsed light sources; the general theory of optical pumping and detection; and digital computer solutions of the optical pumping equations for $\sigma^+ D_2$ light and partial excited state relaxation.

Unclassified

1. Gas Cell Atomic Frequency Standards
   Optical Pumping
2. Contract DA-36-039 SC-70147

AD ____________________ Accession No. ____________________

Princeton University, Princeton New Jersey

INVESTIGATIONS OF THE EFFECT OF GAS COLLISIONS AND OPTICAL PUMPING ON THE BREADTH OF SPECTRAL LINES - R. H. Dicke and C. O. Alley

Final Report on Optical Detection Phase, 1 October 1957 to 30 September 1960, 186 pages, 31 Figures, 13 Diagrams, 14 Tables. (Contract No. DA-36-039 SC-70147) File No 229-PH-56-91 (3501). Unclassified Report.

A new method of optical detection of the $m_F = 0 \leftrightarrow m_F = 0$. $\Delta F = 1$ ground state magnetic hyperfine transition in alkali atoms, which is important for atomic frequency standards because of its first order independence of an external magnetic field has been investigated theoretically and experimentally demonstrated for rubidium 87 After orientation by optical pumping a quantum mechanical superposition state is produced by a 90° rf pulse. A <u>phase change</u> between each $m_F = 0$ state and its partner states of the same F value is caused by a microwave field at ~ 6835 Mc/sec coupling the two $m_F = 0$ states. This phase change is converted into a <u>population change</u> by a second rf pulse to yield a large change in the resonance scattering of the optical pumping light, on the order of that obtained by reversal of the orientation of the vapor.

Other methods of optical detection of this resonance were studied theoretically and are discussed: selective hyperfine absorption within the gas cell; a rubidium 85 gas cell hyperfine filter; and a polarization bridge.

Wall coatings for the inhibition of spin relaxation in confined oriented vapors were studied experimentally. It was demonstrated that treatment of glass surfaces with alkylchlorosilane vapors provides coatings at least as effective as long chain saturated hydrocarbon waxes with the added advantages of ease of application and the ability to withstand baking under vacuum at $\sim 350°$ C without deterioration. The $0 \leftrightarrow 0$ hyperfine resonance in such coated cells exhibited a reduced Doppler width (because of the confinement of the atoms) of the same order as that produced by a buffer gas, and displayed a negative frequency shift of a few kc/sec.

Other subjects investigated included spin echo methods applied to oriented vapors; optical pumping with pulsed light sources; the general theory of optical pumping and detection; and digital computer solutions of the optical pumping equations for $\sigma^+ D_2$ light and partial excited state relaxation.

Unclassified

1. Gas Cell Atomic Frequency Standards
   Optical Pumping
2. Contract DA-36-039 SC-70147

AD ____________________ Accession No. ____________________

Princeton University, Princeton, New Jersey

INVESTIGATIONS OF THE EFFECT OF GAS COLLISIONS AND OPTICAL PUMPING ON THE BREADTH OF SPECTRAL LINES - R. H. Dicke and C. O. Alley

Final Report on Optical Detection Phase, 1 October 1957 to 30 September 1960, 186 pages, 31 Figures, 13 Diagrams, 14 Tables. (Contract No. DA-36-039 SC-70147) File No 229-PH-56-91 (3501). Unclassified Report.

A new method of optical detection of the $m_F = 0 \leftrightarrow m_F = 0$, $\Delta F = 1$ ground state magnetic hyperfine transition in alkali atoms, which is important for atomic frequency standards because of its first order independence of an external magnetic field, has been investigated theoretically and experimentally demonstrated for rubidium 87. After orientation by optical pumping a quantum mechanical superposition state is produced by a 90° rf pulse. A <u>phase change</u> between each $m_F = 0$ state and its partner states of the same F value is caused by a microwave field at ~ 6835 Mc/sec coupling the two $m_F = 0$ states. This phase change is converted into a <u>population change</u> by a second rf pulse to yield a large change in the resonance scattering of the optical pumping light. on the order of that obtained by reversal of the orientation of the vapor.

Other methods of optical detection of this resonance were studied theoretically and are discussed: selective hyperfine absorption within the gas cell; a rubidium 85 gas cell hyperfine filter; and a polarization bridge.

Wall coatings for the inhibition of spin relaxation in confined oriented vapors were studied experimentally. It was demonstrated that treatment of glass surfaces with alkylchlorosilane vapors provides coatings at least as effective as long chain saturated hydrocarbon waxes with the added advantages of ease of application and the ability to withstand baking under vacuum at $\sim 350°$ C without deterioration. The $0 \leftrightarrow 0$ hyperfine resonance in such coated cells exhibited a reduced Doppler width (because of the confinement of the atoms) of the same order as that produced by a buffer gas. and displayed a negative frequency shift of a few kc/sec.

Other subjects investigated included spin echo methods applied to oriented vapors; optical pumping with pulsed light sources; the general theory of optical pumping and detection; and digital computer solutions of the optical pumping equations for $\sigma^+ D_2$ light and partial excited state relaxation.

Unclassified

1. Gas Cell Atomic Frequency Standards
   Optical Pumping
2. Contract DA-36-039 SC-70147

AD_____ Accession No._____

Princeton University, Princeton, New Jersey

INVESTIGATIONS OF THE EFFECT OF GAS COLLISIONS AND OPTICAL PUMPING ON THE BREADTH OF SPECTRAL LINES - R. H. Dicke and C. O. Alley

Final Report on Optical Detection Phase, 1 October 1957 to 30 September 1960, 186 pages, 31 Figures, 13 Diagrams, 14 Tables. (Contract No. DA-36-039 SC-70147) File No. 229-FH-56-91 (3501). Unclassified Report.

A new method of optical detection of the $m_F = 0 \leftrightarrow m_F = 0$, $\Delta F = 1$ ground state magnetic hyperfine transition in alkali atoms, which is important for a atomic frequency standards because of its first order independence of an external magnetic field has been investigated theoretically and experimentally demonstrated for rubidium 87. After orientation by optical pumping a quantum mechanical superposition state is produced by a 90° rf pulse. A phase change between each $m_F = 0$ state and its partner states of the same F value is caused by a microwave field at ~6835 Mc/sec coupling the two $m_F = 0$ states. This phase change is converted into a population change by a second rf pulse to yield a large change in the resonance scattering of the optical pumping light on the order of that obtained by reversal of the orientation of the vapor.

Other methods of optical detection of this resonance were studied theoretically and are discussed: selective hyperfine absorption within the gas cell; a rubidium 85 gas cell hyperfine filter; and a polarization bridge.

Wall coatings for the inhibition of spin relaxation in confined oriented vapors were studied experimentally. It was demonstrated that treatment of glass surfaces with alkylchlorosilane vapors provides coatings at least as effective as long chain saturated hydrocarbon waxes with the added advantages of ease of application and the ability to withstand baking under vacuum at ~350° C without deterioration. The $0 \leftrightarrow 0$ hyperfine resonance in such coated cells exhibited a reduced Doppler width (because of the confinement of the atoms) of the same order as that produced by a buffer gas and displayed a negative frequency shift of a few kc/sec.

Other subjects investigated included spin echo methods applied to oriented vapors; optical pumping with pulsed light sources; the general theory of optical pumping and detection; and digital computer solutions of the optical pumping equations for Cs^{133} D_2 light and partial excited state relaxation.

Unclassified

1. Gas Cell Atomic Frequency Standards
   Optical Pumping
2. Contract DA-36-039 SC-70147

AD_____ Accession No._____

Princeton University, Princeton, New Jersey

INVESTIGATIONS OF THE EFFECT OF GAS COLLISIONS AND OPTICAL PUMPING ON THE BREADTH OF SPECTRAL LINES - R. H. Dicke and C. O. Alley

Final Report on Optical Detection Phase, 1 October 1957 to 30 September 1960, 186 pages, 31 Figures, 13 Diagrams, 14 Tables. (Contract No. DA-36-039 SC-70147) File No. 229-FH-56-91 (3501). Unclassified Report.

A new method of optical detection of the $m_F = 0 \leftrightarrow m_F = 0$, $\Delta F = 1$ ground state magnetic hyperfine transition in alkali atoms, which is important for a atomic frequency standards because of its first order independence of an external magnetic field has been investigated theoretically and experimentally demonstrated for rubidium 87. After orientation by optical pumping a quantum mechanical superposition state is produced by a 90° rf pulse. A phase change between each $m_F = 0$ state and its partner states of the same F value is caused by a microwave field at ~6835 Mc/sec coupling the two $m_F = 0$ states. This phase change is converted into a population change by a second rf pulse to yield a large change in the resonance scattering of the optical pumping light, on the order of that obtained by reversal of the orientation of the vapor.

Other methods of optical detection of this resonance were studied theoretically and are discussed: selective hyperfine absorption within the gas cell; a rubidium 85 gas cell hyperfine filter; and a polarization bridge.

Wall coatings for the inhibition of spin relaxation in confined oriented vapors were studied experimentally. It was demonstrated that treatment of glass surfaces with alkylchlorosilane vapors provides coatings at least as effective as long chain saturated hydrocarbon waxes with the added advantages of ease of application and the ability to withstand baking under vacuum at ~350° C without deterioration. The $0 \leftrightarrow 0$ hyperfine resonance in such coated cells exhibited a reduced Doppler width (because of the confinement of the atoms) of the same order as that produced by a buffer gas and displayed a negative frequency shift of a few kc/sec.

Other subjects investigated included spin echo methods applied to oriented vapors; optical pumping with pulsed light sources; the general theory of optical pumping and detection; and digital computer solutions of the optical pumping equations for Cs^{133} D_2 light and partial excited state relaxation.

Unclassified

1. Gas Cell Atomic Frequency Standards
   Optical Pumping
2. Contract DA-36-039 SC-70147

AD_____ Accession No._____

Princeton University, Princeton, New Jersey

INVESTIGATIONS OF THE EFFECT OF GAS COLLISIONS AND OPTICAL PUMPING ON THE BREADTH OF SPECTRAL LINES - R. H. Dicke and C. O. Alley

Final Report on Optical Detection Phase, 1 October 1957 to 30 September 1960, 186 pages, 31 Figures, 13 Diagrams, 14 Tables. (Contract No. DA-36-039 SC-70147) File No. 229-FH-56-91 (3501). Unclassified Report.

A new method of optical detection of the $m_F = 0 \leftrightarrow m_F = 0$, $\Delta F = 1$ ground state magnetic hyperfine transition in alkali atoms, which is important for atomic frequency standards because of its first order independence of an external magnetic field has been investigated theoretically and experimentally demonstrated for rubidium 87. After orientation by optical pumping a quantum mechanical superposition state is produced by a 90° rf pulse. A phase change between each $m_F = 0$ state and its partner states of the same F value is caused by a microwave field at ~6835 Mc/sec coupling the two $m_F = 0$ states. This phase change is converted into a population change by a second rf pulse to yield a large change in the resonance scattering of the optical pumping light, on the order of that obtained by reversal of the orientation of the vapor.

Other methods of optical detection of this resonance were studied theoretically and are discussed: selective hyperfine absorption within the gas cell; a rubidium 85 gas cell hyperfine filter; and a polarization bridge.

Wall coatings for the inhibition of spin relaxation in confined oriented vapors were studied experimentally. It was demonstrated that treatment of glass surfaces with alkylchlorosilane vapors provides coatings at least as effective as long chain saturated hydrocarbon waxes with the added advantages of ease of application and the ability to withstand baking under vacuum at ~350° C without deterioration. The $0 \leftrightarrow 0$ hyperfine resonance in such coated cells exhibited a reduced Doppler width (because of the confinement of the atoms) of the same order as that produced by a buffer gas and displayed a negative frequency shift of a few kc/sec.

Other subjects investigated included spin echo methods applied to oriented vapors; optical pumping with pulsed light sources; the general theory of optical pumping and detection; and digital computer solutions of the optical pumping equations for Cs^{133} D_2 light and partial excited state relaxation.

Unclassified

1. Gas Cell Atomic Frequency Standards
   Optical Pumping
2. Contract DA-36-039 SC-70147

DA36-039 sc-70147
Princeton University

Final Report
1 October 1947 - 30 September 1960

DISTRIBUTION LIST

	No. of Copies
Technical Library OASD (R and E) Rm 3E1065, The Pentagon Washington 25, D. C.	1
Chief of Research and Development OCS, Department of the Army Washington 25, D. C.	1
Continental Army Command Liaison Office U. S. Army Signal Research and Development Laboratory Fort Monmouth, New Jersey	1
Commanding Officer U. S. Army Signal Equipment Support Agency Fort Monmouth, New Jersey	1
Chief Signal Officer Department of the Army Washington 25, D. C. Attn: SIGRD	1
Armed Services Technical Information Agency Arlington Hall Station Arlington 12, Virginia	10
Commanding General Army Ballistic Missile Agency Huntsville, Alabama Attn: Technical Library	1
Chief, Bureau of Ships Department of the Navy Room 3348 Washington 25, D. C. Attn: Mr. R. B. McDowell, Code 817c	1
Director U. S. Naval Research Laboratory Code 2027 Washington 25, D. C.	1
Commanding Officer and Director U. S. Navy Electronics Laboratory San Diego 52, California	1

	No. of Copies
National Bureau of Standards Washington 25, D. C. Attn: Dr. Peter Bender	1
Commander Wright Air Development Division Wright-Patterson Air Force Base, Ohio Attn: WCLNE-1	1
Attn: WCLNK-2	1
Commander Wright Air Development Division Wright-Patterson Air Force Base, Ohio Attn: WCOSI-3	2
Commander Air Force Cambridge Research Center, CROTR L. G. Hanscom Field Bedford, Massachusetts	1
Commander Rome Air Development Center Griffiss Air Force Base, New York Attn: RCSST-3	1
Federal Telecommunications Laboratories Nutley, New Jersey Attn: Mr. M. Arditi	1
A. D. Little, Inc. 30 Memorial Drive Cambridge 42, Massachusetts	1
Radio Corporation of America David Sarnoff Research Center Princeton, New Jersey Attn: Mr. Thomas R. Rogers	1
Technical Research Group 17 Union Square West New York, New York Attn: Dr. R. T. Daly	1
Varian Associates 611 Hansen Way Palo Alto, California Attn: Dr. M. Packard	1

	No. of Copies
University of Washington Physics Department Seattle, Washington Attn: Dr. H. Dehmelt	1
Space Technology Laboratories P. O. Box 45564 Airport Station Los Angeles 45, California Attn: Dr. D. J. Farmer	1
Chief, U. S. Army Security Agency Arlington Hall Station Arlington 12, Virginia	2
Deputy President U. S. Army Security Agency Board Arlington Hall Station Arlington 12, Virginia	1
Commanding Officer U. S. Army Signal Research and Development Laboratory Fort Monmouth, New Jersey	
Attn: Director of Research	1
Attn: Technical Documents Center	1
Attn: Technical Information Division	3
Attn: Director, Solid State and Frequency Control Division	1
Attn: P. Brown, Solid State and Frequency Control Division	7
Total number of copies to be distributed	- 50

This contract is supervised by the Solid State and Frequency Control Division, Electronic Components Department, Fort Monmouth, New Jersey. For further technical information contact Mr. P. Brown, Project Advisor, Telephone 53-51770.